TUESDAY, JUNE 7, 1983

9:00–10:00 **Room 123**

Formal Opening and Plenary Session

WELCOME AND CALL TO ORDER: John A. Burdine, M.D., President, Society of Nuclear Medicine

REMARKS: B. Leonard Holman, M.D., Chairman, Scientific Program Committee 1983

REMARKS: Duffy Price, CNMT, President, Technologist Section

REMARKS: W. Mel Flowers, Jr., M.D., Chairman, Credentials and Membership Committee

RECEPTOR-SPECIFIC BINDING: William C. Eckelman, Ph.D., George Washington University Medical Center, Washington, DC

Opening of the 1983 SNM Exposition and Gala Ribbon Cutting Ceremony

10:30–12:00 **Room 123**

CARDIOVASCULAR CLINICAL I: CORONARY ARTERY THROMBOLYSIS

Moderator: Daniel S. Berman, M.D.
Co-moderator: George A. Beller, M.D.

IMMEDIATE ASSESSMENT OF VIABILITY AND NECROSIS OF REPERFUSED MYOCARDIUM FOLLOWING THROMBOLYSIS USING DUAL INTRACORONARY INJECTION OF THALLIUM-201 AND TECHNETIUM-99M-PYROPHOSPHATE. J Maddahi, I Geft, W Ganz, S Hulse, A Waxman, D Berman, Cedars-Sinai Medical Center, Los Angeles, CA

Although myocardial necrosis (NEC) is usually complete within 6 hrs of coronary artery (CA) occlusion, technetium-99m-PYP (Tc) uptake is rarely seen in the first 24 hrs of NEC potentially due to lack of its early access to the NEC myocardium. In 13 dogs, with 1.5 to 7 hrs of proximal CA occlusion, Tl-201 (Tl) (50 uCi) and Tc (350 uCi) were injected into the reopened CA. Tc was immediately taken up by the NEC myocardium in all dogs with NEC. In 10 with subendocardial NEC, intracoronary Tl was taken up by the reversibly ischemic (RIS) subepicardial myocardium. Subsequently post-REP dual intracoronary Tl/Tc imaging was applied to 12 pts in whom a total of 23 myocardial regions were successfully reperfused. Tc was immediately taken up by all 23 reperfused regions while concomitant Tl uptake varied and was marked in 13 (Group A), minimal in 4 (Group B), and absent in 6 (Group C). Lack of RIS in Group C regions was confirmed by continued a/dys-kinesis (kin) of the regions until 3-7 months followup (F/U) study. Presence of a mixture of RIS and NEC in Group A regions was confirmed in 11/13: by pre-discharge normo/mild hypo-kin in 9 and by normo-kin in an additional 2 on the F/U study. Three of 4 Group B regions remained a/dys-kin by F/U study while 1/4 normalized after severe hypo-kin. Thus, in successfully thrombolyzed pts uptake of both intracoronary Tl and Tc by the reperfused region is common, indicating presence of a mixture of reversibly ischemic and necrotic myocardium. This uptake pattern is usually associated with subsequent partial or complete wall motion recovery of the reperfused region.

TWO-DOSE INTRAVENOUS Tl-201 ADMINISTRATION AND QUANTITATIVE ANALYSIS IN THE IMMEDIATE ASSESSMENT OF INTRAVENOUS THROMBOLYSIS IN PATIENTS. T Weiss, J Maddahi, J Kropac, I Geft, W Ganz, D Berman, Cedars-Sinai Med Ctr, Los Angeles, CA

Successful reopening of the acutely occluded coronary artery and viability of the reperfused myocardium (myo) was evaluated by an objective 2-dose Tl-201 technique in 12 patients (pts) receiving intravenous (IV) streptokinase (SK) therapy. Nine pts (Group A) were judged to be successfully thrombolyzed using MB-CK release pattern (early peaking), clinical, and ECG criteria, and 3 pts (Group B) were unsuccessful. Two divided doses (1.5 mCi) of Tl were given IV, one before and the other after SK administration. The view with the largest initial Tl-201 defect was imaged for 10 minutes immediately before and 15 minutes after second Tl-201 dose without change in collimator position. Post-SK Tl-201 myo distribution image was obtained by computer subtraction of the first from the second dose Tl-201 image. After interpolative background subtraction on each image, Tl-201 defect intensity (DI) was quantitated as the area enclosed between the abnormal portion of the pts myo circumferential count profile and a previously established normal limit profile. Of 9 Group A pts, DI decreased in 8 from pre- to post-SK study and remained unchanged in 1 (650±471 to 460±351, mean±SD, $p<.05$). DI further decreased in all 6 of 9 Group A pts who had pre-discharge study (284±344). In 3 Group B pts, an insignificant increase in DI was observed from pre to post-SK and to pre-discharge study (918±460 to 1209±338 and 1129±248). Thus computer assisted 2-dose IV Tl-201 imaging and analysis provides a useful method for assessing noninvasively, quantitatively, and immediately the efficacy of intravenous streptokinase administration in evolving acute myocardial infarction.

FUNCTIONAL RECOVERY OF LVEF AND RVEF FOLLOWING STREPTOKINASE REPERFUSION: RELATION TO THE TIMING AND IMPACTS OF LAD/RCA REOPENING. T. Nishimura, T. Yasuda, H.K. Gold, R.C. Leinbach, K.A. McKusick, H.W. Strauss. Massachusetts General Hospital, Boston, MA.

To evaluate functional recovery of RVEF and LVEF after streptokinase reperfusion (Rp), 23 patients with anterior and inferior myocardial infarction (AMI, IMI) were investigated by gated blood pool scan at a mean of 4.9 hrs (range 2.5-8.0 hrs) after Rp and 10 days later. There were 18 patients with successful Rp and 5 patients with no Rp or reocclusion. Successful Rp cases were divided into two groups: Rp in less than 4 hrs from the onset of chest pain (Rp<4hrs, mean 3.2 hrs) (n=9, 4 AMI and 5 IMI) and Rp in more than 4 hrs (Rp>4hrs, mean 5.9 hrs) (n=9, 4 AMI and 5 IMI). As control group, gated blood pool scans were also performed in the early hours following infarction and 10 days in an additional 42 patients (18 AMI and 24 IMI) who received conventional treatments. The results of RVEF and LVEF at admission and 10 days were shown as follows (Data:Mean±SD, AD; time of admission,*$p<0.01$,**$p<0.05$):

	RVEF (%)		LVEF (%)	
AMI	AD	D10	AD	D10
Rp<4hrs(n=4)	54.0± 2.7	58.5± 6.8	39.5± 3.3	50.3± 3.1*
Rp>4hrs(n=4)	48.3± 2.1	51.5± 4.4	38.5± 3.9	42.3±10.3
Control(n=18)	47.6± 8.9	49.1± 9.6	38.6± 9.0	40.4±12.9
IMI				
Rp<4hrs(n=5)	44.0± 7.5	50.2± 5.3**	54.6± 4.3	61.4± 5.8*
Rp>4hrs(n=5)	43.4±14.8	49.8±14.0**	46.0± 5.8	48.0± 9.6
Control(n=24)	42.8±13.4	48.0± 9.0**	51.3± 8.2	53.4±10.8
No Rp(n=5)	35.8±11.8	41.4±12.1	38.6±21.5	37.0±15.6

1) Rp<4hrs demonstrated significant improvement in LVEF. 2) RVEF in AMI remained within normal range and did not show any changes. In IMI groups, whether reperfused or not, RVEF showed significant improvement. 3) In successful Rp, AMI had no collaterals, however, 5IMI who had adequate collaterals showed improvement of LVEF (from 52.4±6.3% to 58.6±8.6%*) than no collateral group. 4) No Rp group showed severe depressed ventricular function. In conclusion, these studies demonstrated important factor influencing functional recovery after streptokinase reperfusion; namely, the time of Rp, location of MI, and adequate collaterals may play a role after Rp.

POSITRON-CT FOR THE EVALUATION OF MYOCARDIAL METABOLISM AFTER REPERFUSION IN CHRONIC DOGS. M. Schwaiger, H.W. Hansen, R. Keen, J. Vinten-Johanson, D.J. Ellison, L.A. Yeatman, H.R. Schelbert, UCLA School of Medicine, Los Angeles, California.

The presence of viable tissue in myocardium reperfused after an ischemic insult cannot be determined reliably by regional myocardial function. Yet, clinical recognition of tissue viability is important because of increased clinical interest in reperfusion of "infarcted" myocardium. We hypothesized that tissue viability could be determined from residual metabolic activity evaluated in vivo by Positron-CT.

Therefore, chronically instrumented dogs were studied at control C, during a 3 hr LAD balloon occlusion (OC) and immediately, 24 hrs and 1 week after reperfusion (R). Myocardial perfusion was studied with microspheres and N-13 ammonia, glucose and free fatty acid (FFA) metabolism with F-18 deoxyglucose (FDG) and C-11 palmitic acid (CPA) and compared to regional shortening (RS) by ultrasonic crystals. During OC, MBF in the LAD territory was only 27±8% of C but improved to 62±43% at 1 week R. RS fell with OC to 4±13% of C, was 5.2±17.2% and 10.4±24% at 1 hr and 24 hrs and improved to 57±27% at 1 week. Regional metabolic alterations were characterized by a decrease in CPA uptake and in the fraction that became immediately oxidized and by longer tissue clearance halftimes consistent with a regional fall in FFA utilization and oxidation and absolute or relative increases in regional FDG uptake consistent with increased glucose utilization. These abnormalities were most prominent at 24 hrs but were still present at 1 week R. Even when RS indicated paradoxical wall motion at 1 hr and 24 hrs, increased FDG uptake at 24 hrs was followed by functional and metabolic improvement. Conversely, in 1 dog with hemorrhagic infarction which failed to recover regional function, there was no regional metabolic activity as evidenced by a lack of CPA and FDG uptake. Thus, the recovery of regional myocardial metabolism during R can be evaluated noninvasively by Positron-CT. Demonstration of metabolic activity early during R may reliably predict tissue viability and subsequent functional recovery.

ASSESSMENT OF RESTORATION OF MYOCARDIAL PERFUSION AND METABOLISM WITH POSITRON EMISSION TOMOGRAPHY AFTER CORONARY THROMBOLYSIS. S.R. Bergmann, K.A.A. Fox, A.L. Rand, M. J. Welch, M. M. Ter-Pogossian, and B. E. Sobel. Washington University School of Medicine, St. Louis, MO

Coronary thrombolysis is a potentially salutary intervention for restoration of myocardial perfusion and metabolism after myocardial infarction. However, non-invasive measurements are necessary for the assessment of the efficacy of therapy. We studied 26 closed-chest anesthetized dogs with induced coronary thrombosis with sequential positron emission tomography (PET). Regional myocardial perfusion was evaluated with a previously validated technique employing O-15 labeled H_2O (using a subsequent O-15 CO scan for correction of blood pool activity), and C-11 palmitate was used for assessment of myocardial metabolism. After initial PET was completed, thrombolysis was induced with intracoronary streptokinase. After thrombolysis, PET was repeated after a second administration of O-15 labeled H_2O and CO, and C-11 palmitate. Thrombolysis within 4 hours of the induction of ischemia resulted in flow restoration in the jeopardized zone to 72 ± 21% of flow in non-affected regions (quantitated in absolute terms with microspheres). Tomographically assessed myocardial metabolism recovered to 81% of normal. When thrombolysis was induced 6-12 hours after the onset of ischemia, myocardial perfusion averaged 65 ± 18% of normal, while myocardial metabolism recovered to only 27% of that seen in non-affected myocardium. Thus, metabolic salvage induced by thrombolysis is critically dependent on the time of reperfusion even though myocardial blood flow may be restored. Clinical studies using PET should be useful for characterizing in man the temporal constraints of this promising intervention.

FREE FATTY ACID SCINTIGRAPHY IN PATIENTS WITH SUCCESSFUL THROMBOLYSIS AFTER ACUTE MYOCARDIAL INFARCTION.F.C.Visser, G.Westera,E.E.van der Wall and J.P.Roos.Dept. of Cardiology Free University of Amsterdam,N.L.

Turnover rates of 123-I-heptadecanoic acid(I-HºA)-expressed in halftime values($T_{\frac{1}{2}}$)-distinguish between normal,reversible ischemic and irreversible ischemic myocardium:reversible tissue has higher $T_{\frac{1}{2}}$ than normal,irreversible ischemic myocardium a lower $T_{\frac{1}{2}}$.The purpose of this study was to evaluate the metabolic state of reperfused myocardium after successful thrombolysis.Successful thrombolysis was defined by restoration of antegrade flow in the acute stage of MI, and by patency of the vessel at reevaluation 6 weeks later. Scintigraphy was performed within 2 weeks after MI.After background correction for free 123-I-NaI,$T_{\frac{1}{2}}$ was calculated from the time-activity curves.$T_{\frac{1}{2}}$ from tracer defects were compared with normal zones.Contrast ventriculography was performed 6 weeks after MI.Ejection fractions and L.V. damage scores calculated:Fig I.

Results:catherisation data(table I)show a significant difference between L.V.damage scores of anterior and inferior infarctions:13 vs 10.2($P<0.05$).Ejection fractions are not different.Scintigraphic data(table II):$T_{\frac{1}{2}}$ were normal in 2 pts,5pts showed high $T_{\frac{1}{2}}$ and 16pts a lower $T_{\frac{1}{2}}$ than normal.If ejection fractions of patients with normal and high $T_{\frac{1}{2}}$ are compared with pts with a low $T_{\frac{1}{2}}$,a significant higher ejection fraction is present in the former: 70±6 vs 47±13($P<0.01$)Also L.V.damage score is significantly lower in patients with normal or high $T_{\frac{1}{2}}$:8.7 vs 12.($P<0.05$)

Conclusion:If,after successful thrombolysis a normal I-HºA scintigram is present or a tracer defect with high halftime values(suggesting reversible ischemia),it predicts a good left ventricular function.

10:30–12:00 **Room 130**

NEUROLOGY I: SPECT

Moderator: R. Edward Coleman, M.D.
Co-moderator: Thomas C. Hill, M.D.

SINGLE PHOTON EMISSION COMPUTERIZED TOMOGRAPHY (SPECT) EVALUATION OF THE BRAIN IMAGING AGENT, (I-123)HIPDM IN MAN WITH ROTATING GAMMA CAMERA. F.Fazio, P.Gerundini, M.C.Gilardi, G.L.Lenzi, G.Taddei, M.Piacentini, F.Colombo, R.Colombo, H.F.Kung and M.Blau. University and Politechnic of Milan and University of Rome, Italy; State University of New York at Buffalo, U.S.A.

A new brain imaging agent, (I-123)HIPDM (N,N,N'-trimethyl-N'-(2-hydroxy-3-methyl-5-(I-123)iodobenzyl)-1,3-propanediamine) has recently been developed. We studied a)the cynetic and organ distribution of this agent in humans, and b)the feasibility of using it for SPECT in man in combination with a commercial gamma camera. Thirteen normal volunteers were studied. Immediately after injection of 4 to 10 mCi of (I-123)HIPDM, brain, lung and liver activity were monitored with the γ camera on two alternate fixed positions (head and chest). Forty-five minutes after injection whole body counting was obtained. One, two, three and four hours after injection brain SPECT was performed. Main results were: 1)after i.v. injection in man, (I-123)HIPDM is rapidly extracted from the blood and can be found mainly in lungs and brain, not in liver; 2)lung and brain concentration is stable as from 30' after injection; 3)injection of 4 to 7 mCi of the tracer is enough to yield clinically useful tomograms. These functional tomograms reflect the blood flow distribution within brain structures (gray and white matter, basal ganglia, etc.), and can therefore be used for the location and evaluation of perfusion derangements in neurological disorders.

EVALUATION OF CEREBROVASCULAR DISORDERS USING THE BRAIN IMAGING AGENT, (I-123)HIPDM, AND SINGLE PHOTON EMISSION COMPUTERIZED TOMOGRAPHY (SPECT). F.Fazio, P.Gerundini, G.L.Lenzi, M.Collice, M.C.Gilardi, G.Taddei, M.Piacentini, F.Colombo, R.Colombo, H.F.Kung and M.Blau. University and Politechnic of Milan and University of Rome, Italy; State University of New York at Buffalo, U.S.A.

The association of new brain imaging agents and SPECT yields functional tomograms potentially useful for the evaluation of perfusion derangements in cerebrovascular disorders. We studied 20 patients with occlusion of a major cerebral artery; in 5 patients with occlusion of the internal carotid artery (ICA) the study was repeated within 2 weeks after ECA-ICA by-pass. Carotid angiography and CT were first performed. SPECT was then obtained with a commercial rotating γ camera 1 hour following i.v. injection of 4 to 7 mCi of (I-123)HIPDM. With this dose, 30 to 40 minutes of rotation yield 5 million total head counts. Stroke patients with hypodense areas on CT scans showed markedly reduced activity on emission tomograms, frequently extended to larger areas of the affected hemisphere. Asymptomatic patients with history of TIA or minor stroke (completely recovered),

and angiographic evidence of occlusion of ICA or MCA showed large cortical areas of reduced distribution of (I-123) HIPDM, usually in the presence of normal CT. Remote phenomena such as crossed cerebellar diaschisis were also observed. After ECA-ICA by-pass, normal perfusion was observed in previously ischaemic areas, whereas adjacent brain structures, previously normal, showed hyperperfusion.

THE PREDICTIVE VALUE OF SIZING OF PERFUSION DEFECTS USING N-ISOPROPYL I-123 P-IODOAMPHETAMINE BRAIN SCANS IN ACUTE STROKE. R.G.L. Lee, T.C. Hill, B.L. Holman, H.D. Royal, and M.E. Clouse. New England Deaconess Hospital, Brigham and Women's Hospital, Beth Israel Hospital and Harvard Medical School, Boston, MA.

N-isopropyl I-123 p-iodoamphetamine (IMP) studies in patients with acute stroke demonstrate areas of decreased uptake reflecting decreased blood flow and tissue ischemia or damage. In 17 patients with infarctions involving the distribution of the middle cerebral artery, we assessed the relationship of infarction size on the IMP scan to the degree of recovery. IMP scans were divided into those showing large defects involving greater than 50% of the hemisphere and small defects involving less than 50%. Recovery from neurological deficits was based on clinical assessment at time of discharge. In patients who did not show clinical improvement and did not die, follow-up averaged 7.5 months. Of the 17 patients, 9 patients had large defects on IMP study, all of whom initially showed severe neurological deficits. On follow-up, six of the eight patients had marked resolution of signs and symptoms. One patient had no improvement and two patients died. In 8 patients who had small deficits on IMP scan, 5 had marked neurological findings in the acute phase of the illness and 3 had minor neurological deficits. Follow-up showed that 5 of the 8 patients had marked improvement in their signs and symptoms while 3 patients showed no recovery. We conclude that size of the perfusion deficit seen on IMP scans has an erratic relationship to clinical progress and cannot predict the degree of recovery from neurological deficits.

A COMPARISON OF TWO CEREBRAL BLOOD FLOW TRACERS, N-ISOPROPYL I-123 p-IODOAMPHETAMINE AND I-123 HIPDM. B.L. Holman, R.G.L. Lee, T.C. Hill, R.D. Lovett and J. Lister-James. Brigham and Women's Hospital, New England Deaconess Hospital and Harvard Medical School, Boston, MA.

Both N-isopropyl I-123 p-iodoamphetamine (IMP) and N N'-trimethyl-N'-[2-hydroxyl-3-methyl-5-I-123-iodobenzyl]-1, 3-propanediamine (HIPDM) have been advocated as radiotracers for assessing regional cerebral perfusion. We compared the biodistribution of the two tracers in 17 patients without evidence of neurological or cerebrovascular disease using the Anger camera and the Harvard multidetector tomographic system. Following intravenous injection, both tracers accumulated initially in the lung. At 20 minutes after injection, brain activity was 91% of peak brain activity for both HIPDM and IMP. In two patients injected with both tracers, peak HIPDM brain activity/mCi averaged 62% of the peak IMP activity/mCi. In 3 HIPDM patients and 7 IMP patients studied with tomography, average peak activity/mCi injected dose of HIPDM was 57% of the peak IMP activity/mCi. There was slower washout of HIPDM from the lungs compared to IMP (at 20 min, lung activity was 70% of the initial peak activity for HIPDM and 55% for IMP) and 2-1/2 times greater accumulation of HIPDM in the liver than IMP. Tomographic images were similar in appearance for both tracers. No eye uptake greater in concentration than background activity was observed in any patient at 2, 24 and 48 hours with either tracer. In conclusion, although both IMP and HIPDM have similar organ distribution and kinetics, IMP has a higher brain uptake, lower liver uptake and faster lung clearance than HIPDM.

A COMPARISON OF REGIONAL CEREBRAL BLOOD FLOW MEASURED WITH I-123-LABELED DIAMINE OR AMPHETAMINE AND RADIOACTIVE TRACER MICROSPHERES. M.D. Devous, Sr., S.E. Lewis, P.V. Kulkarni, and F.J. Bonte. Nuclear Medicine Center, University of Texas Health Science Center at Dallas, Dallas, TX

In this study the distribution of I-123 isopropyliodoamphetamine (IMP) or the I-123 diamine HIPDM was compared to regional cerebral blood flow (rCBF) measured with 15±3 micron tracer microspheres (TM). IMP or HIPDM distributions, blood clearance, and lung uptake were studied 20 min after injection (6 dogs) or 6 hr after injection (6 dogs). In animals sacrificed 20 min postinjection, the distribution of IMP and HIPDM correlated linearly with rCBF (r=0.83 for HIPDM, r=0.87 for IMP), with a slope of approximately 0.7 for both agents. The modest slope indicates that gradations in I-123 uptake are not as significant as those in blood flow. Brain to lung uptake ratio at 20 min was 0.3 for HIPDM, and 0.8 for IMP. For animals sacrificed 6 hr postinjection the correlation between both agents and TM was poor. Iodine activity was distributed uniformly throughout the brain. In some dogs, tomographic images were acquired with a rotating gamma camera (GE 400T). Contrast between brain and surrounding tissue in tomographic images was similar with both agents and no difference in scatter contribution was observed with p,2n I-123 (IMP) or p,5n I-123 (HIPDM). Thus, both agents correlate with rCBF early after injection, but with a slope significantly less than 1. IMP has a better brain to lung uptake ratio which could affect tomographic imaging with certain systems.

EVALUATION OF Xe-133 DSPECT IN UNILATERAL CEREBROVASCULAR DISEASE. A COMPARATIVE STUDY TO TRANSMISSION CT AND X-RAY ANGIOGRAPHY. U. Buell, E. Moser, P. Schmiedek, E. Kleinhans, C.M. Kirsch, V. Olteanu, K. Einhäupl. Depts Nuclear Medicine Neurosurgery and Neurology, Univ. of Munich, FRGermany

To evaluate Xe-133 DSPECT as an investigative procedure for cerebrovascular disease (CVD), 28 patients (pts) with angiographically (AG) proved unilateral CVD and 12 normals were examined. All pts had TCT. A further subdivision was introduced by clinical presentation (completed stroke /CS/ n=15, PRIND n=7, TIA n=6). Inhalation of 133-Xe gas and a fast rotating, 64 crystal SPECT scanner for measurements of regional cerebral blood flow (rCBF, ml/100g/min) in 3 axial slices were used. Functional evaluation was done comparing rCBF in 12 areas per slice with normal values and computing right-to-left half-slice ratios (SR) and regional ratios (RR), expressed as the difference (D) to normal ratios. Topographically data were achieved by comparing the number of low density areas (LDA) in TCT with those of low flow (LFA) in SPECT. In normals, SR was .98±.06 and RR were between .95 and 1.0 pointing to the dominant left hemisphere. rCBF ranged from 50.4±11.5 ml (mean±SD, frontal poles) to 82.6±8.7 ml (motor areas). In pts, rCBF in the least LFA was 42.4±4.3 ml (mean±SEM) in CS, 52.0±5.3 ml in PRIND and 47.4±4.0 ml in TIA. However, SRD in CS were .23, in PRIND .17 and in TIA .04 ($p<0.01$). RRD for the least LFA were .40 in CS, .25 in PRIND and .13 in TIA ($p<0.02$). The number of LDA was smaller ($p<0.01$) than LFA (36 vs 61 in CS, 13 vs 28 in PRIND and TIA). Compared to AG (100%) RRD and rCBF revealed a sensitivity of 93% in CS, 100% in PRIND and 66% in TIA. We conclude that 133 Xe DSPECT is useful to detect unilateral CVD and to quantify rCBF. For detection, RRD is more sensitive than rCBF. Topographically, DSPECT is superior to TCT in describing the total area of low flow within a hemisphere.

10:30–12:00 **Room 120**

HEMATOLOGY I

Moderator: Gary F. Gates, M.D.
Co-moderator: Myron Pollycove, M.D.

RAPID DETECTION OF INTRA ABDOMINAL ABSCESSES USING INDIUM-111 TROPOLONATE LABELLED LEUCOCYTES. S.H. Saverymuttu, M.E. Crofton, A.M. Peters and J.P. Lavender

^{111}Indium leucocyte scanning is established as an accurate method for localising intra-abdominal abscesses. With the currently available cell labelling techniques, there is a variable and significant delay in localisation of abscesses which is its major disadvantage in comparison

to ultrasound or computer tomography. We have examined the speed and accuracy of localisation of leucocytes labelled in plasma with a new chelating agent indium-111 tropolonate in 80 patients with suspected intra-abdominal abscess. In 45 patients the accuracy compared to ultrasound was studied. Eighteen patients were shown to have abscesses. The sensitivity and specificity of indium-111 labelled leucocytes were 94% and 98% respectivlely. The sensitivity and specificity of ultrasound was 67% and 81% respectively. In 9 patients with abscesses, scanned sequentially from 40 min after return of the labelled cells; abnormal activity corresponding to the abscess was already visible in 8 patients on the 40 min scan. In all 8 patients, dynamic scanning over the abscess site demonstrated a rising count rate during the first 40 min indicating the image represented active accumulation of labelled leucocytes rather than blood pool. These results demonstrate that indium-111 plasma labelled leucocyte scanning is a rapid and accurate method of detecting abscesses.

RAPID IN VITRO LABELLING OF POLYMORPHONUCLEAR LEUKOCYTES WITH INDIUM-111-TROPOLONE. D. Bandyopadhyay, L.M. Levy, R. Schiff, S. Hoory, G. Moskowitz and D.K. Das. Long Island Jewish-Hillside Medical Center, New Hyde Park, N.Y.

The ability to form high lipid soluble complexes with trivalent metal cations and its water solubility has made tropolone preferable to oxine for leukocyte labelling. In the present study, we have isolated a pure population of polymorphonuclear leukocytes (PMNs) by a one step density centrifugation procedure employing the currently available "Mono-Poly Resolving Medium,"(Flow Laboratories), and the cells were subsequently labelled with In-111-tropolone. As opposed to other methods of leukocyte separation, this technic requires minimal manipulation allowing cells to be obtained in a shorter time with higher yield and viability. Fresh human venous blood (20ml) in ACD was layered on the above medium. A single centrifugation at 300xg for 30 min. separates monos,PMNs and erythrocytes in discrete bands. To form the In-111-tropolone complex, 100ul of In-111 chloride containing 10-15uCi/ml was mixed with different concentrations of tropolone in saline. To these complexes, $3x10^6$ cells of PMNs in Hanks Balanced Salt Solution containing Hepes buffer at pH 7.4 were added. Labelling was done both at 37°C and at room temperature for 20 min. Maximum labelling yield was obtained with a tropolone cencentration of $1x10^{-4}$(M) at 37°C. Cell viability and purity were found to be very high (>96%) both before and after labelling. Labelling yield was enhanced significantly with increase in cell concentration and temperature. Labelling efficiency in 90% plasma was found to be very poor (<10%). In summary, a very rapid and simple method for in vitro labelling of a pure population of PMNs with high yield and viability has been described. The method is presently being investigated for the detection of experimental abscesses in animals.

RECEPTOR MEDIATED SELECTIVE RADIOLABELING OF NEUTROPHILS R.C. Verma, L.R. Bennett, T. Kawada, J.I. Eisenman, UCLA & USC Schools of Medicine, Olive View Medical Center, Van Nuys, CA

This investigation was undertaken to explore the feasibility of a selective label for neutrophils. A synthetic hexapeptide, capable of eliciting chemotaxis at nanomolar concentrations was used. A human neutrophil possesses over 120,000 receptors for the peptide on its surface and after interaction with the peptide, the receptor-ligand complex is internalised. Human neutrophils labeled with the iodinated peptide (IHXP) were studied under various physico-chemical conditions.

Iodination was carried out by the modified chloramine T method and fractions with high concentration of IHXP eluted from a Biogel P-2 column were neutralized with NaH_2PO_4 & BSA and stored at -4°C. Neutrophils were isolated by dextran sedimentation and differential centrifugation in hypaque.

Iodination efficiency was 40-50%. Free iodine in the IHXP fractions was not more than 15%. Neutrophil viability was better than 94% in all experiments.

Maximum (50%) cell labeling efficiency was achieved when cells were labeled in a special buffer, IB (NaCl, NaH_2PO_4, $CaCl_2$ & BSA) with negligible elution in the subsequent washes with IB. Cell labeling in plasma was poorer than with IB. However if the proportion of buffer was increased in the medium, the labeling efficiency improved. Prolonged incubation in plasma of cells previously labeled and washed in the IB, did not result in any significant elution of the label.

The hexapeptide, labeled with the appropriate gamma emitter, offers great hope as a simple selective label for neutrophils for in vivo scintigraphic abscess localization.

Quantitative Measurement of Iron Storage in Patients with Iron Excess Using Diethylenetriamine Penta-acetic Acid (DTPA)

Authors: Chi-Kwan Yen, Myron Pollycove, Howard Parker, Mary Tono, Dilip Gohil

Despite the development of a simple measurement of body iron (Fe) stores by Barry et al. in 1970 using iron excretion following DTPA injection, the method has not been made widely available and there are no reports of confirmation by other investigators. We reviewed our experience using this method in 29 patients with suspected excessive iron storage. The method consists of intravenous injection of a solution containing 200 mg/ml DTPA and 0.4 uCi/ml Fe-59 calculated to administer a total DTPA dose of 16.7 mg/kg ideal body weight, followed by a 6 hours' urine collection. Urinary iron concentration and Fe-59 activity were measured and the total body DTPA chelatable iron calculated by the following formula: DTPA chelatable iron (mg) equals total iron excreted (mg) in urine multiplied by the ratio of total Fe-59 injected to the total Fe-59 excreted in the 6 hours' urine. In 18 patients with elevated body storage iron calculated by this method, venesections were then performed as rapidly as possible, i.e., up to 1 unit every week or every other week if tolerated, until the patient showed signs of mild iron deficiency anemia. The total body iron storage mobilized was calculated as 0.255 gm multiplied by the number of units of blood removed. Preliminary results in these phlebotomized patients indicate a close relationship between the excessive body iron predicted by the method and the actual amount removed by phlebotomy. Our studies confirm Barry's results, and the method has proved to be very useful in the diagnosis and management of patients with iron overload.

LYMPHOCYTE KINETIC STUDIES WITH INDIUM-111-OXINE LABELED LYMPHOCYTES IN MALIGNANT LYMPHOMA. T.Uchida, S.Matsuda, Y. Takagi, T.Yui, and S.Kariyone. Fukushima Medical College, Fukushima,Japan.

Lymphocyte kinetic studies were performed by using In-111-oxine labeled autologous lymphocytes in 3 normal subjects, 2 Hodgkin, and 11 non-Hodgkin lymphoma. Disappearance curves of the labeled lymphocytes showed two exponential components in all cases. In normal subjects, the half life of the first component was within 1 hr and the second one was 50.7 $\pm$ 6.4 hr for all lymphocytes, 52.0 $\pm$ 5.5 hr for T and 31.6 $\pm$ 4.9 hr for B lymphocytes. These data suggest all lymphocyte disappearance curve reflected T lymphocytes chiefly and the half life of B lymphocytes was shorter than that of T lymphocytes. In patients with malignant lymphoma, the half life of the second component was 60.2 $\pm$ 30.7 hr in T cell type and 63.7 $\pm$ 24.5 hr in B cell type. The half life of labeled lymphocytes became to be shorter and the recovery to be lower according to the progression of clinical stages from I to IV. There was significanf correlation between recovery (%) and clinical stages ($r= -0.86, p< 0.001$). These findings were assessed in a patient with follicular lymphoma in III A, with 32.6 hr of half life and 3.1 % of recovery. After the chemotherapy, the half life recovered to 51.7 hr and the recovery to 16.7%. Organ distribution of labeled lymphocytes in malignant lymphoma showed the difference in T and B cell type. Hepatic, splenic, cervical, axillary and inguinal lymph node accumulation was markedly noted 18 hr after the infusion in T cell type, however, no lymph node accumulation was seen in B cell type. In-111-oxine labeled lymphocyte technique might be useful to evaluate the pathophysiology of malignant lymphoma.

10:30-12:00 **Room 132**

GASTROINTESTINAL I: HEPATOBILIARY IMAGING

Moderator: Heidi S. Weissmann, M.D.
Co-moderator: Darlene M. Fink-Bennett, M.D.

HEPATOBILIARY SCINTIGRAPHY AND SCINTIANGIOGRAPHY IN TRAUMA. P. Colletti, M.E. Siegel, P.W. Ralls, J.M. Halls. USC School of Medicine, Los Angeles, CA.

The purpose of this paper is to evaluate the use of hepatobiliary scintigraphy and scintiangiography in a setting of acute abdominal trauma.

We obtained 41 studies in 38 patients with either blunt (16), stab (5) or gunshot wound (17). Ten mCi of disofenin was injected as a bolus and abdominal scintiangiography and hepatobiliary scintigraphy were performed. Routine and delayed views to at least 4 hours were obtained to look for biliary extravasation. Sulfur colloid images were obtained in 9 patients.

Abnormalities were found in 26/38 (68%). There were bilomas (4 with leak), 3 leaks without biloma, 4 liver hematomas, 3 liver infarcts, 3 renal injuries, 1 large hepatic artery aneurysm (traumatic) and 3 bowel injuries. The hepatic artery aneurysm and 2/3 renal injuries were seen only on scintiangiography. Three of 33 scintiangiograms gave unique information (9%). Sulfur colloid yielded no extra information in 9/9 patients (7 positives). Fifteen of 32 gallbladders were not visualized despite normal bowel transit and delayed views (47% false positive nonvisualization of gallbladder). Thirteen of 15 were normal at surgery (1 had stones), 1 was normal clinically.

We conclude that hepatobiliary scintigraphy is very useful to detect abnormalities in abdominal trauma. Scintiangiography yielded unique data in renal lesions that were not seen with routine images. Sulfur colloid has apparently no advantage over disofenin for liver injuries. We noted a high percentage of nonvisualized gallbladders (47%) in acutely traumatized patients and recommend caution in diagnosing cholecystitis in the face of trauma.

HEPATOBILIARY IMAGING IN PAPILLARY STENOSIS. A.M. Koroshetz, R.G.L. Lee, T.C. Hill, J. Gregg, and M.E. Clouse. New England Deaconess Hospital, Boston, MA.

Papillary stenosis, characterized by recurrent upper abdominal pain, frequently occurs after cholecystectomy and is relieved by surgical or endoscopic sphincterotomy. Biliary manometry is used for the definitive diagnosis of papillary stenosis. There has not, however, been a satisfactory noninvasive measure of papillary stenosis or the effects of sphincterotomy. Twenty-four patients with symptoms of papillary stenosis were studied by ERCP and Tc-99m cholescintigraphy to determine the role of radionuclide imaging. Endoscopic manometry was performed on most patients. The 16 patients with normal ^{99m}Tc-IDA cholescintigraphy had a mean basal sphincter pressure of 19.5 mm. Hg. (normal range being < 18 mm Hg.). Those patients with an abnormal hepatobiliary study based on our criteria of delayed biliary-enteric transit and abnormal ductal size and time-activity dynamics, had a mean pressure of 37.5 mm Hg. Sphincter pressures could not be measured in 4 patients with abnormal ^{99m}Tc-IDA studies because of inability to cannulate a tight sphincter. Eleven patients had hepatobiliary scans both before and after sphincterotomy. Those 5 patients with an abnormal pre-sphincterotomy study showed improvement on the repeat exam. Hepatobiliary imaging does not appear to be useful as a screening exam for patients with suspected papillary stenosis since many patients with elevated sphincter pressures and a positive response to sphincterotomy have normal preoperative ^{99m}Tc-IDA studies. In selected patients with severe stenosis, in whom manometry cannot be performed, hepatobiliary imaging appears useful for diagnosis and objective response to therapy.

THE INFLUENCE OF SCAN AND PATHOLOGICAL CRITERIA UPON THE SPECIFICITY OF CHOLESCINTIGRAPHY. R. E. Coleman, J. E. Freitas, C. E. Nagle, R. L. Bree, K. D. Krewer, and M. D. Gross. William Beaumont Hospital, Royal Oak MI.

The influence of scan and pathological criteria on the specificity of cholescintigraphy (CS) was assessed by a prospective study of 211 patients with suspected acute cholecystitis (AC) who underwent CS and had sufficient data available to confirm a final diagnosis. CS was performed in the standard fashion with delayed imaging using 5 mCi of Tc-99m Disofenin. Criteria for CS interpretation were: I) Normal - Gallbladder (GB) seen ≤1 hour; II) Abnormal - GB not seen ≤1 hour; III) Abnormal with delayed imaging - GB not seen ≤4 hours; and, IV) Obstructive - biliary tree and gut not seen. The pathological criteria for AC were: 1) Acute inflammatory infiltrates; 2) Hemorrhagic necrosis; 3) Criterion 2 or cystic duct obstruction and/or GB edema; and, 4) Criteria 2, 3, or relief of fever, pain, or leukocytosis post-cholecystectomy. The changes in sensitivity (Se), specificity (Sp), and predictive value of a + test (P+) induced by changes in scan or pathological criteria are shown below:

	STRICT<------PATH CRITERIA------>LIBERAL	
SCAN CRITERIA	CRITERION 1 Se%/ Sp%/ P+%	CRITERION 4 Se%/ Sp%/ P+%
II	100/85.1/68.4	98.4/92.1/85.1
III	98/90.9/77.8	95.3/98.6/96.8

The choice of scan criterion II, path criterion 1 favored by the ultrasonographer obscures the value of CS in the early detection of cystic duct obstruction, the functional step inducing AC. To understand the literature, an appreciation of the effect of scan and path criteria upon CS's specificity and predictive value is required. Path criterion 3 with delayed imaging is most appropriate.

THE ASSOCIATION OF BILIARY CHOLESTEROL CRYSTALS AND GALLBLADDER EJECTION FRACTION. W.R. Brugge, H.L. Atkins, SUNY at Stony Brook, NY 11794.

Decreased gallbladder motility following CCK or oral fat has been noted in patients with cholesterol gall stones and chronic cholecystitis. Less well documented is the lack of normal contraction following appropriate stimulation in patients with acalculous chronic cholecystitis. In the prairie dog model there is decreased emptying of the gall bladder when the bile contains cholesterol crystals.

In this study we attempted to determine if there was an association of poor gall bladder emptying with the presence of cholesterol crystals in symptomatic patients without evidence of gall stones by oral cholecystography and ultrasonography. Ten patients were intubated and sequentially imaged following the I.V. administration of 5m Ci (185 MBq) of Tc-99m DISIDA. After the liver activity had cleared and the gall bladder was well visualized an infusion of 20 ng/kg CCK-OP was given over 20 minutes while imaging was continued at 1 frame/min. for 30 minutes. At the same time bile was aspirated and examined for crystals. The gallbladder ejection fraction was determined at the end of the imaging session.

8/10 patients had cholesterol crystals present in the bile. The mean ejection fraction was 16.0% (SD 22.5) in these 8. In the other 2 patients the ejection fraction was 81.0% (SD 7.1). Of 5 subjects undergoing cholecystectomy, all had evidence of chronic cholecystitis. There appears to be a correlation among chronic cholecystitis, the presence of cholesterol crystals in bile and a reduced gall bladder ejection fraction.

ABNORMAL GALLBLADDER EMPTYING IN RESPONSE TO CHOLECYSTOKININ (OP-CCK) IN PATIENTS WITH ACALCULUS GALLBLADDER DISEASE. P. W. Doherty, P. Schlegel, M. A. King, J. K. Zawacki. University of Massachusetts Medical Center, Worcester, MA.

Fifty patients with longstanding symptoms suggestive of gallbladder disease who had normal ultrasounds, oral cholecystograms and upper GI series were selected for study. 60 minutes following the injection of 5 mCi of Tc-99m-IDA, 3 infusions of OP-CCK increasing from 10-30ng/Kg were given at 15 minute intervals. A continuous series of 3 minute images were collected on a computer and time activity curves generated over the gallbladder.

One group of 18 patients showed a smooth stepwise increase in gallbladder emptying at each dose level, achieving a total ejection fraction of 50-90%. 10 of these patients had reproduction of their symptoms. Abnormal

emptying occurred in the other group of 32 patients who had either no ejection response at any dose (n=15) or had total ejection fractions below 25% and did not respond on at least one dose level (n=17). In this group, 30 had reproduction of their symptoms, and 18 had surgery because of symptom severity. Pathologically, 8 had chronic cholecystitis, 3 diffuse fibrosis, 2 cystic duct syndrome, 2 cholestrolosis and 2 were normal. Relief of symptoms occurred in 16 with a mean follow-up of 14 months.

The combination of an absence of a uniform response to increasing doses of OP-CCK with reproduction of symptoms can be used to identify a sub-group of patients in whom surgery reveals a high incidence of gallbladder pathology and provides a symptomatic relief.

A COMPARISON OF CHOLESCINTIGRAPHY VERSUS SONOGRAPHIC MURPHY'S SIGN IN THE EVALUATION OF SUSPECTED ACUTE CHOLECYSTITIS. J. E. Freitas, R. L. Weinstein, and R. L. Bree. William Beaumont Hospital, Royal Oak MI.

To define the role of the sonographic Murphy's sign in evaluating acute right upper quadrant pain, a prospective study was performed on 34 patients having clinically suspected acute cholecystitis (AC) who were studied by cholescintigraphy (CS) and real-time ultrasound (RT) within 48 hours of each other. RT determination of cholecystitis (acute or chronic) was based on the presence of calculi, gallbladder wall edema, pericholecystic fluid and analysis of location of tenderness (sonographic Murphy's sign). CS with delayed imaging was performed following intravenous administration of Tc-99m Disofenin.

Pathological confirmation of AC was obtained in 18 patients, while 16 patients had other etiologies of abdominal pain. The results of CS and RT in these 34 patients is shown below.

	MURPHY'S SIGN		CHOLESCINTIGRAPHY		
	+	-	+	-	
ACUTE CHOLECYSTITIS	16	3	19	0	19
NOT ACUTE CHOLECYSTITIS	9	6	1	14	15
	25	9	20	14	34

The sensitivity of the sonographic Murphy's sign in acute cholecystitis was 84%, with a specificity of 40%, and an overall accuracy of 65%. By comparison, the sensitivity of CS in acute cholecystitis was 100%, with a specificity of 93% and overall accuracy of 97%. A positive Murphy's sign does not add significantly to the accuracy of ultrasound in the diagnosis of AC and is inferior to CS.

10:30-12:00 **Room 276**

RADIOPHARMACEUTICAL CHEMISTRY I: Tc-99m

Moderator: Edward A. Deutsch, Ph.D.
Co-moderator: Wynn A. Volkert, Ph.D.

Introduction. Edward A. Deutsch, Ph.D., University of Cincinnati, Cincinatti, OH

SYNTHESIS AND CHARACTERIZATION OF $[^{99m}Tc(dmpe)_3]^+$, A POTENTIAL MYOCARDIAL IMAGING AGENT. J-L. Vanderheyden, E. Deutsch, K. Libson, and A. R. Ketring. Departments of Chemistry and Radiology, University of Cincinnati, Cincinnati, OH.

As part of a larger effort to develop a practical Tc-99m myocardial agent, a series of cationic Tc-99 complexes of bis(1,2-dimethylphosphino)ethane (dmpe) has been prepared and characterized by the classical techniques of inorganic chemistry. This series includes the Tc(V), Tc(III) and Tc(I) species tr-$[Tc(O)_2(dmpe)_2]^+$, tr-$[TcCl_2(dmpe)_2]^+$ and $[Tc(dmpe)_3]^+$. The Tc-99 preparative chemistry has been extended to the "no carrier added" Tc-99m level using HPLC to monitor the course of the synthesis. Proper control of reaction conditions yields any one of the three cationic Tc-99m complexes in greater than 97% radiochemical purity.

"No carrier added" $[^{99m}Tc(O)_2(dmpe)_2]^+$ does not provide myocardial images. "No carrier added" $[^{99m}TcCl_2(dmpe)_2]^+$ satisfactorily images the heart of dogs and cats, but does not image the heart of pigs and provides only marginally useful myocardial images in monkeys and humans. "No carrier added" $[^{99m}Tc(dmpe)_3]^+$ successfully images the normal myocardium of several species including the dog, cat, pig and monkey. This agent can be simply prepared from generator eluted $^{99m}TcO_4^-$ in about 90 min using a "kit" formulation. The "kit" consists of an evacuated vial containing lyophilized dmpe·2HCl; reconstitution involves addition of aqueous NaOH. No chromatographic purification of the final $[^{99m}Tc(dmpe)_3]^+$ product is required. Quality control is effected by HPLC analysis on a reversed-phase C-8 column.

In sum, the chemistry and preparation of $[^{99m}Tc(dmpe)_3]^+$ is sufficiently well defined and developed to warrant evaluation of this myocardial imaging agent in man.

THE NOAH'S ARK EXPERIMENT. A SEARCH FOR A SUITABLE ANIMAL MODEL FOR THE EVALUATION OF CATIONIC Tc-99m MYOCARDIAL IMAGING AGENTS. A. R. Ketring, E. Deutsch, K. Libson and J-L. Vanderheyden, Departments of Chemistry and Radiology, University of Cincinnati, Cincinnati, OH. V. J. Sodd, H. Nishiyama and S. Lukes, Nuclear Medicine Laboratory, DEP, BRH, FDA, Cincinnati, OH.

$[^{99m}Tc(dmpe)_2Cl_2]^+$, where dmpe is bis(1,2-dimethylphosphino)ethane, successfully images the myocardium of dogs and baboons, and on this basis was evaluated as a potential myocardial imaging agent in humans (Deutsch, et al., JNM 23: P9 (1982)). However, in man the myocardial images produced by this agent are only of marginal utility because of a very high liver/heart uptake ratio that is not predictable from the dog and baboon models. This marked species difference in the biodistribution of $[^{99m}Tc(dmpe)_2Cl_2]^+$ led us to search for an animal species which might provide a predictive model for the development of cationic Tc-99m myocardial imaging agents.

The myocardial imaging efficacy of three cationic complexes $[^{99m}Tc(dmpe)_2(O)_2]^+$, $[^{99m}Tc(dmpe)_2Cl_2]^+$ and $[^{99m}Tc(dmpe)_3]^+$ has been evaluated in several animal species. Within a given species, the three complexes have markedly different imaging characteristics and for a given complex, images vary markedly from one species to the next. Because of this species variation, no single animal model appears to be suitably predictive of the myocardial images found in man. However, a judicious evaluation of new cationic Tc-99m agents in two or three complementary species (e.g. dog, cat and pig) should have predictive value.

On the basis of these studies, $[^{99m}Tc(dmpe)_3]^+$ appears likely to provide acceptable myocardial images in man.

SYNTHESIS, STRUCTURE AND BIODISTRIBUTION STUDIES OF A TECHNETIUM CATIONIC COMPLEX - $[Tc(dmpe)_3]^+$. V. Subramanyam, K.E. Linder, M.C. Sammartano, D.B. Pendleton, M. Delano, M. Liteplo and L.L. Camin. New England Nuclear Corporation, N. Billerica, MA 01862

Recent works from the laboratories of Deutsch[1] and Davison[2] have demonstrated that cationic complexes derived from lower oxidation states of technetium are useful in imaging the myocardium of experimental animals. We have synthesized a new cationic technetium complex, determined its structure by physical methods and evaluated its distribution in mice and rats. The technetium-99 sample is prepared by refluxing $NH_4^{99}TcO_4$ with excess 1:2-bis(dimethylphosphino)ethane (dmpe) in aqueous ethanolic sodium hydroxide. The diamagnetic complex has been isolated from the reaction mixture either as the chloride or as the tetraphenylborate salt. Results of elemental analysis (C,H and P) of the tetraphenylborate salt agree (±0.4%) with the formulation $[Tc(dmpe)_3][B(C_6H_5)_4]$. A molecular ion ($M^+$) peak at 549 for the cation $[Tc(dmpe)_3]^+$ is the most dominant peak in the Fast Atom Bombardment mass spectrum of the chloride salt. Single crystal X-ray studies on the tetraphenylborate salt show that the technetium atom is octahedrally coodinated by six phosphorus atoms from three dmpe molecules. The technetium complex ion moves toward the cathode in electrophoretic studies. The $[^{99m}Tc(dmpe)_3]^+$ complex for pharmacological studies was prepared by the procedure described above. HPLC shows the radiochemical purity to be greater than 95%. In vivo distribution of the ^{99m}Tc-complex intravenously injected in mice is characterized by rapid blood clearance and concentration in the liver, kidneys, intestines and heart. Very good images of the rabbit heart have been obtained using $^{99m}Tc(dmpe)_3^+$ administered intravenously.

A TETRADENTATE AMINE OXIME COMPLEX OF Tc-99m.
D.E. Troutner, W.A. Volkert, T.J. Hoffman, and R.A. Holmes, University of Missouri and Harry S. Truman Memorial Veterans Hospital, Columbia, MO.

A neutral, lipophilic complex of Tc-99m with a multidentate amine oxime has been synthesized and characterized radiochemically. The oxime, 2,2'-(1,3-diaminopropane)bis (2-methyl-3-butanone)dioxime, commonly called propylene amine oxime (PnAO), is known to form complexes of the general formula $M\text{-PnAO}^{+1}$ with M^{+2} cations. The complexes are macrocyclic due to the formation of a hydrogen bond between the oxime oxygens. Previous work(1) showed that macrocyclic amine complexes of Tc include the TcO_2^{+1} core, suggesting that a Tc-PnAO complex should be neutral.

The complex was prepared in aqueous solution using "no-carrier-added" Tc-99m and Tc-99 concentrations up to 10^{-4}M. Analysis by HPLC showed a single complex peak and yields of greater than 98% at pH 5-9. Electrophoresis resulted in a peak near the origin. The octanol/water ratio was 13±4 and the $CHCl_3$/water ratio was 29±5. The complex migrated with the solvent front in both acetone and butanol ascending paper chromatography. These properties are very different from those of the previously reported cationic Tc-amine complexes, and indicate that Tc-PnAO is neutral and lipophilic. It is stable in air 20 hrs or longer after preparation.

Preliminary biodistribution studies suggest that the Tc-PnAO complex can penetrate the intact BBB and it will be used in the formulation of new radiopharmaceuticals for brain imaging.

(1) Zuckman et al., Inorg. Chem. 20, 2386 (1981).

SYNTHESIS AND CHARACTERIZATION OF A NEUTRAL OXOTECHNETIUM-(V)DIAMINODITHIOL COMPLEX. L.A. Epps, A.V. Kramer, H.D. Burns, S.E. Zemyan, R.F. Dannals, H. Goldfarb, and H.T. Ravert. Johns Hopkins Medical Institutions, Baltimore, MD.

Diaminodithiol ligands have been reported to form stable neutral complexes with technetium-99m (Tc-99m), and it has been suggested that these complexes may be capable of diffusing through cell membranes and the blood:brain barrier. We have investigated the technetium-99 (Tc-99) chemistry of this class of ligands to evaluate its suitability for use in the development of Tc-99m radiopharmaceuticals. One of the most promising candidates, N,N'-bis(2-methyl-2-mercaptopropyl)ethylenediamine (I) or its HCl salt, reacts with Tc-99m or Tc-99 pertechnetate in the presence of any of a variety of reducing agents to form in high yield the stable, neutral and lipid soluble technetium (V) complex (II), where Cl, OH or OR, depending upon solvent and reaction conditions. In solution the Tc-99 complex is yellow-brown, but isolation of the pure product yields the corresponding five coordinate N-deprotonated complex (III) as brick red needles.

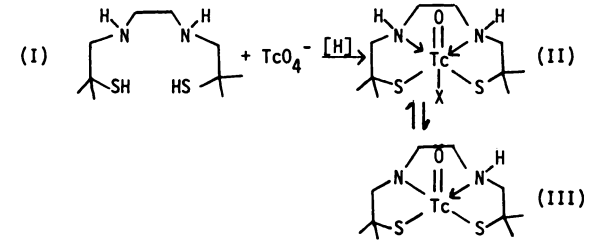

SYNTHESIS OF NEUTRAL, LIPID SOLUBLE TECHNETIUM COMPLEXES OF BIS(2-MERCAPTOETHYL)AMINES. H.T. Ravert*#, H.D. Burns*, N.D. Heindel#, A.V. Kramer*, and L.A. Epps. *The Johns Hopkins Medical Institutions, Baltimore, MD, and #Department of Chemistry, Lehigh University, Bethlehem, PA.

A major goal in Tc-radiopharmaceutical research in recent years has been the development of lipid soluble Tc-99m complexes capable of diffusing through cell membranes and the blood:brain barrier. In an attempt to develop such a Tc-99m complex, we have examined the chemistry of mercaptoamine complexes of Tc-99m and Tc-99. A series of bis(2-hydroxyethyl)amines were reacted with thionyl chloride to give the corresponding nitrogen mustards which were treated with thiourea. Hydrolysis of the resulting isothiouronium salts yielded the desired bis(2-mercaptoethyl)amine ligands. These ligands formed stable, neutral, lipid soluble complexes with Tc-99m when pertechnetate ion was reduced with either sodium dithionite or sodium borohydride in an aqueous ethanol solution of the ligand. For example, the octanol:saline partition coefficients of the Tc-99m complexes were 0.97 (R = ethyl) and 2.89 (R = butyl). Similar reactions with Tc-99 yielded brown crystalline solids which were shown by HPLC and TLC and octanol:saline partition coefficients to be identical to those formed with no-carrier added Tc-99m. The Tc-99 complexes were analyzed by IR, NMR (H and C-13), elemental analyses and field desorption mass spectrometry. The infrared spectra possessed strong Tc = O stretches at 925 and 895 cm^{-1}. Although the exact chemical structure is not yet known, all data indicate that the stoichiometry of the complexes is $Tc_2O_2[RN(CH_2CH_2S)_2]_3$.

COMPARATIVE EVALUATION OF Tc-99m MEBROFENIN AND Tc-99m PYRIDOXYL-5-METHYLTRYPTOPHAN IN RATS. A.R. Fritzberg, D.C. Bloedow, D. Eshima, D. L. Johnson, and W.C. Klingensmith III. University of Colorado Health Sciences Center, Denver, CO.

Recent reports have indicated Tc-99m mebrofenin (N-(3-bromo-2,4,6-trimethyl)acetanilideiminodiacetate) (JNM 22: P51, 1981) and Tc-99m N-pyridoxyl-5-methyltryptophan (PHMT)(JNM 23:517, 1982) to be superior hepatobiliary radiopharmaceuticals with respect to specificity, kinetics, and ability to compete with bilirubin or other transport pathway analogs. This study compared their specificity, rates of blood disappearance, biliary appearance, hepatic clearance, and volumes of distribution in normal and BSP treated rats. The specificity of Tc-99m mebrofenin was higher with 93.9% in the bile at 90 min compared to 91.4% for Tc-99m PHMT. Correspondingly urine excretion at 90 min was 1.9% for Tc-99m PHMT and 0.3% for Tc-99m mebrofenin in normal rats. In BSP treated rats the urine excretion was slightly increased at 0.5% for Tc-99m mebrofenin and 3.0% for Tc-99m PHMT. The blood disappearance of both agents was similar, but Tc-99m PHMT appeared faster in bile. BSP slowed the blood disappearance and biliary appearance of both, but to a lesser extent with Tc-99m PHMT. Clearance of Tc-99m PHMT was 70 ml/min/kg in normal rats and 47 in BSP treated rats; that of Tc-99m mebrofenin was 51 ml/min/kg in normal and 30 in treated rats. Volumes of distribution were larger for Tc-99m PHMT with 1695 ml/kg in normal rats and 1042 ml/kg in BSP rats and 743 ml/kg in normal and 546 ml/kg in treated rats for Tc-99m mebrofenin. Tc-99m PHMT was kinetically superior with higher clearance and lower hepatocyte transit time, but slightly inferior in specificity.

10:30–12:00 **Room 275**

INSTRUMENTATION I: POSITRON EMISSION TOMOGRAPHY

Moderator: Nathaniel M. Alpert, Ph.D.
Co-moderator: David A. Weber, Ph.D.

EVALUATION OF THE ACCURACY OF THE MEASURED ATTENUATION CORRECTION IN POSITRON TOMOGRAPHY. E.J. Hoffman, L.M.A.M. van der Stee, A.R. Ricci. UCLA School of Medicine, Los Angeles, CA.

An apparent advantage of Positron Computed Tomography (PCT) over SPECT is the ease of performing attenuation correctons in PCT. This work was undertaken to evaluate the accuracy of that correction in PCT.

Attenuation of 511 keV annihilation radiation was measured in water phantoms of various diameters (6 to 20 cm) in a PCT system. Computer simulations of these measurements were performed assuming an attenuation coefficient of 0.095 (1/cm). Simulations were also made of emission scans, assuming 0% or 10% scatter. Attenuation by phantom was included in simulations. Simulated emission data were corrected by measured attenuaton correction factors (ACFs). A method of correcting for errors in measured

ACFs was developed and all measurements were reevaluated after correction was applied to ACFs.

Measured attenuation coefficients ranged from .084 to .090 (1/cm) with higher values observed for smaller diameters and lowest values observed in centers of largest diameter phantoms. Measured ACFs produce 15 percent error at center of 20 cm diameter emission scans. The proposed correction scheme gave values of measured attenuation coefficients of 0.0951 +/- .0006 (1/cm) for 6 to 20 cm diameter scattering media. Emission data were in excellent agreement with correct values after the additional correction was applied.

Measured ACFs in PCT have significant errors due to scattered photons, resulting in underestimation of ACFs. However, relatively simple correction procedures can compensate for these errors.

AN EXPERIMENTAL EVALUATION OF THE SIGNAL AMPLIFICATION TECHNIQUE (SAT) IN POSITRON TOMOGRAPHY. E.J. Hoffman, A.R. Ricci, L.M.A.M. van der Stee, M.E. Phelps. UCLA School of Medicine, Los Angeles, CA.

We have recently reported on a theoretical analysis of the effect of very narrow detectors on the signal to noise ratio in positron tomography. In this work, we undertake an experimental evaluation of the use of very high resolution detectors in positron tomography.

Line sources, the Derenzo phantom, a 16 cm diameter uniform cylinder and a brain phantom were imaged with a pair of 4.5 mm wide BGO detectors on the UCLA tomographic simulator. These images allowed evaluation of resolution, resolution in a complex extended object, signal to noise ratio and image quality in a typical clinical study, respectively. The images were reconstructed with the Shepp filter and Shepp filter with 1/2, 1/3 or 1/4 the standard cutoff frequency followed by 0, 1, 2 or 3 three point smoothings of the image. The standard deviations of the mean pixel value was evaluated in a 12 cm diameter region of interest in a 500K count uniform cylinder under all these conditions.

It was found that the percent standard deviation in the uniform cylinder ranged from 26 to 8 for image resolutions ranging from 4.4 to 8.5 mm FWHM. All of the patterns in the Derenzo phantom were clearly resolved even in those cases in which smoothing had removed all obvious statistical mottle. In comparisons of brain phantom image quality to images taken on the NeuroECAT, SAT images of 500K are clearly superior to NeuroECAT images of 5 million counts.

THE ORBITING ROD SOURCE: IMPROVING PERFORMANCE IN PET TRANSMISSION CORRECTION SCANS. L.R. Carroll, P. Kretz, G. Orcutt. The Cyclotron Corporation, Berkeley, CA.

Accurate attenuation correction is essential in obtaining quantitative measurements in Positron Emission Tomography studies. The correction is usually derived from a transmission scan, employing a hoop source of annihilation radiation external to the object under study.

We have dispensed with the hoop source in favor of a moving rod source, oriented parallel to the axis of the tomograph and orbiting just outside the field of view within the detector aperture.

Among the advantages provided by this approach we observe: 1) A compact physical implementation; simple automatic insertion and retraction from a shielded vessel. 2) Knowledge of the position of the source at any moment can be exploited to reject random coincidence events which do not intersect the source.

The latter is of particular interest. Normally one obtains an estimate of randoms using delayed coincidence or similar techniques, and substracts that estimate from the total observed counts. Unfortunately, one is still left with the variance, or fluctuating component, which at high count rates will be comparable to the fluctuating component in the measurement of "true" counts.

We have developed a technique called "Rod Source Masking" wherein we are able not just to subtract an estimate of the mean random contribution, but to actually reject most randoms on a count-by-count basis. This allows us to employ a much "hotter" transmission source without suffering a penalty from the fluctuation due to simple background subtraction.

EFFECT OF RESOLUTION IMPROVEMENT ON REQUIRED COUNT DENSITY IN EMISSION COMPUTED TOMOGRAPHY. G. Muehllehner, Hospital of the University of Pennsylvania, Philadelphia, PA.

An investigation was undertaken to determine the trade-off between spatial resolution and number of counts in the images for emission computed tomography systems.

A variety of high-contrast phantoms were generated in a computer simulation so that the spatial resolution, number of counts in the image, and reconstruction filter could be changed easily and over a wide range. System spatial resolution was varied from 4 mm to 14 mm, and the total counts in the image were varied from 50,000 counts to 6.4 million. These images were ranked for visual image quality. Furthermore, the change of contrast was measured and the results were compared to theoretical formulations.

As spatial resolution is improved, significantly fewer counts are needed to give images of comparable quality. Over a wide range of parameters, it was found that the number of counts could be reduced by a factor of 4 for a 2-mm improvement in spatial resolution for 100% object contrast. This is due to the fact that image contrast increases rapidly with spatial resolution in high-contrast objects such as those used in this simulation and typically encountered in brain and cardiac ECT studies.

A HEXAGONAL BAR POSITRON CAMERA. G. Muehllehner and A. Guvenis, Hospital of the University of Pennsylvania, Philadelphia, PA.

A positron camera has been designed and constructed which consists of six position-sensitive detectors arranged in a hexagon to form a single image plane. Each detector consists of a 500-mm long bar of NaI(Tl) to which ten photomultipliers are coupled; position of a scintillation event along the bar is determined through an Anger-type processing electronics.

This arrangement has a number of desirable features. Use of continuous, position-sensitive detectors obviates the need for detector motion such as wobbling or rotating as is necessary with discrete detector designs. This is particularly useful in cardiac imaging. Furthermore, high spatial resolution can be achieved without resorting to ever smaller crystals which increase complexity and thereby cost.

Several problems had to be overcome in implementing this design. Each detector has to be able to handle input counting rates up to 700,000 counts per second which was achieved by pulse clipping and the use of fast electronics throughout the system. At the corners between detectors, gaps occur which result in missing projection data. These small angular gaps have to be compensated for in the reconstruction algorithm.

To date, a spatial resolution of 6.5 mm FWHM measured in the projection data data has been achieved. It is expected that this will result in a final image resolution near 8 mm FWHM.

PRELIMINARY RESULTS OBTAINED WITH TOFPET I: A WHOLE BODY TIME OF FLIGHT POSITRON EMISSION TOMOGRAPH. N.A. Mullani, W.H. Wong, R.K. Hartz, F.A. Philippe, K. Yerian, J. Gaeta and K.L. Gould, Division of Cardiology, University of Texas Medical School, Houston, TX.

We have designed and built a high resolution (9 mm FWHM) 9 slices time-of-flight positron camera for imaging the whole body. The camera uses 720 fast cesium fluoride detectors arranged in five rings of 144 detector each. The detectors measure the difference in the time of flight between the two detected annihilation gamma photons to an accuracy of 600 picosecond (9 cm) FWHM for an estimated improvement in the image S/N ratios of a factor of 2 (for a 35 cm uniform object). A new method of utilizing all the interplane cross coincidences is incorporated in the design of TOFPET to improve the sensitivity of the inner slices by using the time of flight information for positioning an annihilation event in a particular slice. The detectors are made to wobble 19.6 mm in diameter for improved spatial sampling and can translate 20 mm in the axial direction for sampling in between the nine slices. A tilt capability of ±45° for the mechanical gantry, patient couch rotation ±30° and a large patient opening of 58 cm diameter with a slim camera design allow a fair amount of flexibility in scanning any part of the human body.

The camera is completed and preliminary images have been obtained from phantoms and animal studies. The measured sensitivity for an outer slice is 10,000 cts/sec for a 20 cm object filled with uniform activity of 1μCi/cc, while the sensitivity of the inner five slices is in excess of 26,000 cts/sec each. The coincidence timing window for a 20 cm source can be software selected to be less than 4 nanoseconds for fast dynamic imaging.

1:30-3:00 **Room 123**

CARDIOVASCULAR CLINICAL II: METABOLISM

Moderator: Heinrich R. Schelbert, M.D.
Co-moderator: R. Edward Coleman, M.D.

NONINVASIVE EVALUATION OF REGIONAL MYOCARDIAL FATTY ACID METABOLISM IN MAN WITH C-11 PALMITIC ACID AND POSITRON-CT. H.R. Schelbert, E. Henze, P.M. Guzy, Toni A. Don-Michael, M. Schwaiger and J.R. Barrio, UCLA School of Medicine, Los Angeles, CA

The possibility of evaluating regional myocardial free fatty acid (FFA) metabolism noninvasively with C-11 palmitic acid (CPA) and Positron-CT has been demonstrated in animals. In this study we examined this possibility in man for evaluating changes in regional FFA metabolism due to altered cardiac workload. Seven pts with rate programmable pacemakers were studied with CPA and Positron-CT first at control (C) when heart rate averaged 57±6 (SD) bpm and again after heart rate was increased to 104±8 bpm (P). Myocardial C-11 time activity curves derived by serial Positron-CT revealed the typical biexponential clearance where the early rapid clearance phase is related to oxidation of CPA. The relative size of the early phase as an index of the CPA fraction that is immediately oxidized averaged 43.7±12.1% at C and increased to 61.6±7.1 with P ($p<0.01$). The clearance half-time OF 22.6±5.6 min at C decreased to 14.1±4.4 min with P. Initial CPA uptake and clearance at control were homogeneous in all 7 pts and both remained homogeneous with P in 5 pts but became heterogeneous in the 2 pts with angiographic coronary disease. Ischemic myocardium was characterized by a regional delay in CPA clearance on the serial images. Initial CPA uptake was 20.8% less and clearance halftimes were 36% longer than in the normal segments. Thus, the known increase in FFA utilization with increased heart rate was characterized in normal myocardium by the size of the fraction of CPA entering the oxidative pool and its faster turnover rate. In acutely ischemic tissue - consistent with impaired β-oxidation - disproportionately less CPA entered this pool and turned over more slowly.

ON THE RATE-LIMITING STEP IN MYOCARDIAL CLEARANCE OF LABEL FROM 16-IODOHEXADECANOIC ACID (IHDA). S.J. Gatley, J.R. Halama, J.E. Holden, T. DeGrado, A.L. Shug, Dept. of Medical Physics, University of Wisconsin, 1300 University Avenue, Madison, WI 53706.

It has been hoped that dynamic studies with radioiodinated long chain fatty acids would give information about regional rates of metabolism by β-oxidation. The end-product of oxidation of IHDA should be iodoacetylcoenzyme A. High blood levels of iodide are observed 20 min after administration of this agent, but it has not been demonstrated that iodide is the species which actually exits the heart. Iodoacetate formed from iodoacetyl CoA would be expected to cross membranes faster than iodide but is also rather unstable. This might make even-chain acids like IHDA more sensitive to impairment of β-oxidation than odd-chain acids, where iodide is the final catabolite. We presented 0.5 mCi of ^{125}I-IHDA (in Tween 80) to isolated rat hearts. The extracted fraction was 70% and the half-clearance time was 21 min. Samples of perfusate were analysed immediately with a SAX column eluted with 22.5 mM KH_2PO_4, pH 2.35. Iodide was the sole labeled species (99%: Retention volume = 11 ml). No iodoacetate (RV = 6 ml) was observed. Hearts were homogenized in chloroform/methanol after 30 min. An amino column with heptane/ethylacetate/acetic acid (88:10:2) was used to analyze for lipid soluble compounds. Components with RV = 3.3 ml (triglyceride), 4.9 ml (IHDA), 6.5 ml and 8.0 ml were found. Iodobutanoic and iodoacetic acids elute at about 9 ml and 15 ml respectively. Aqueous fractions of homogenates contained only iodide. Clearance of IHDA from hearts is thus limited, like that of iodoheptadecanoic acid, by transport of iodide.

TRACER KINETIC MODEL OF C-11 PALMITATE (CPA) FOR ESTIMATING REGIONAL FREE FATTY ACID (FFA) UTILIZATION IN MYOCARDIUM. S.C. Huang, M. Schwaiger, C. Selin, M.E. Phelps, H.R. Schelbert, UCLA School of Medicine, Los Angeles, California

We developed a tracer kinetic model of CPA for interpreting CPA kinetic data in terms of myocardial FFA utilization. The model consists of separate compartments for CPA, for triglycerides (TG), and for C-11 carbon dioxide (CD). The C-11 label can be transferred from CPA to TG through esterification or to CD through oxidation. The model was tested with experimental data obtained after intracoronary bolus or IV injections of CPA in dogs. Tissue activity kinetics from intracoronary injections were monitored with scintillation detectors and those of IV injections with serial Positron-CT. Myocardial FFA utilization was calculated by the Fick method from microsphere blood flow and the AV difference of plasma FFA. The model fitted very well the kinetic data of both CPA injection types. Turnover halftimes of 114±22 and 4.1±1.3 min were found for TG and CD, respectively. FFA utilization rates estimated from the model ranged from 0.055 to 0.112 mEq/min/g and were consistently 50% higher than the Fick measurements. Utilization rates disproportionately greater for palmitic acid than other FFA in plasma, or TG as an additional source for myocardial utilization FFA could account for the differences between predicted and measured FFA utilization rates. Correction for this overestimation is possible with lumped constants as is the case for the measurement of glucose utilization using the FDG method. While further investigation (with possible modifications) of the model is needed, the results indicate that noninvasive estimation of regional myocardial FFA utilization is possible from CPA tissue kinetics with Positron-CT and an appropriate tracer kinetic model.

QUANTITATIVE TOMOGRAPHIC IMAGING EVALUATION OF MYOCARDIAL CLEARANCE OF I-123 PHENYL PENTADECANOIC ACID IN ACUTE MYOCARDIAL INFARCTION. J.S. Rellas, C.G. Morgan, J.R. Corbett, P.V. Kulkarni, L. Bush, M.D. Devous, R.W. Parkey, J.T. Willerson, and S.E. Lewis, University of Texas Health Science Center, Dallas, TX.

In order to evaluate segmental myocardial clearance of I-123 phenyl-pentadecanoic acid (PPA), a fatty acid tracer whose metabolities retain the iodine label, we performed serial tomographic imaging in 5 control dogs and in 14 dogs with acute (range 90-150 min.) occlusion of the LAD. Tomographic images were acquired at 5 and 25 minutes after IV injection of 2-5 mCi I-123 PPA. Dogs were positioned so that reconstructed coronal sections corresponded to LV short axis views. Sixteen 1 cm thick coronal slices were analyzed for each dog. Slices were matched from the base and grouped to give apical, mid-LV, and basal sections. Early (set 1 to set 2) clearance data were calculated for 15 24-degree sectors per slice and expressed as percentage change from initial values. Control dogs showed a uniform early washout of PPA activity (apex = +39.8%±5.0; mid-LV = +44.1%±0.2; base = +40.9%±2.4; mean±S.D.). In LAD dogs, infarcts were identified by a computer algorithm which showed good agreement with microsphere flow determinations and pathology. Infarcts showed a mean washin of PPA activity = 6.4%. Sectors adjacent to the infarcts showed a mean washout = 7.4% and normal sectors distant from the infarcts showed a mean washout = 17.8%. All values were significantly different from control values at the $p<0.01$ level. Within slices containing infarct, infarct sectors were significantly different from adjacent and normal sectors ($p<0.01$) but there was not a significant difference between adjacent and normal sectors. We conclude that tomographic analysis of I-123 PPA permits accurate characterization of global and regional myocardial fatty acid metabolism during evolving MI and may be of value in predicting viability before and after intervention.

FLOW-DEPENDENCE OF UPTAKE OF (I-123-PHENYL)-PENTADECANOIC ACID(IP) IN THE CANINE HEART.
S.N.Reske,S.Schön,W.Eichelkraut*,N.Hahn*,H.-J.Machulla**.
Inst.Clin.Exp.Nucl.Med.,*Dept.Exp.Chir.,Univ.Bonn,
**Inst.Rad.Phys.Biol.,Univ.Essen, FRG

In this study flow-dependence of IP-uptake in the heart was investigated in 6 pentobarbital (25mg/kg)-unaesthesized mongrel dogs. In 3 animals acute ischemia was pro-

duced by ligation of LAD 15 min. before tracer application. Regional myocardial blood flow (MF) was determined with arterial reference technique after left atrial injection of Ru-103-labeled microspheres (M). IP was injected into left atrium 5 min. after M-application. The hearts were excised, ischemic and non-ischemic tissue was cut into multiple samples, weighed and assayed for Ru-103 and I-123 radioactivity. In hearts with LAD-occlusion autoradiographs of myocardial slices were performed. MF was in the range of 80-110 ml/min. x 100 gm in non-ischemic tissue and 10-50 ml/min. x 100 gm in ischemic tissue. Ischemic cardiac regions were characterized by a sharply demarcated reduction of IP-uptake in tissue autoradiographs. Total cardiac IP-uptake ranged from 4.6-4.9 % of injected dose. Regional myocardial IP-uptake showed a close correlation with MF ($r=0.997$, $N=285$, $p<0.01$). In conclusion, initial cardiac uptake of IP is closely related to it's arterial input and might be used for non-invasive assessment of relative regional perfusion of heart muscle.

CLEARANCE-PATTERNS OF 15(p-I-123 PHENYL-)PENTADECANOIC ACID (IP) IN PATIENTS WITH CAD AFTER BICYCLE EXERCISE. S.N.RESKE, R.KNOPP,H.J.MACHULLA*,H.J.BIERSACK,C.WINKLER.Inst.Clin.Exp. Nucl.Med.Univ.Bonn,*Inst.Rad.Biol.Phys.Univ.Essen,FRG

Regional cardiac IP-metabolism was studied in 7 patients with CAD after symptom-limited bicycle exercise.After IP-injection i.v. at maximal work-load,sequential scintigraphy (Δt=.5 min,T=60 min) of the heart was performed in 20° RAO and 40° LAO projection simultaneously by means of a γ-camera equipped with a bilateral collimator.Background-corrected time-activity curves obtained over normal perfused segments were characterized by a rapid tracer accumulation (T-max~3 min) and biexponential cardiac tracer clearance(1.T-1/2=6.3 ±1.3 min,2.T-1/2=83.7±40.1 min,$\bar{x}$±SD,N=9).All segments in the distribution of significantly obstructed coronary arteries (>75%) showed a different clearance pattern:in 3 patients without stress-induced ECG-changes,markedly prolonged monocomponent tracer clearance in the distribution of obstructed coronary arteries was observed,when compared to normal perfused segments.4 patients with exercise-induced ST-depression showed an initial delay of myocardial tracer clearance until 15-20 min p.i. in the distribution of the most severely affected segments.With relief of ECG-changes,biexponential tracer clearance was restored.Parametric images of IP-clearance half times depicted typical patterns of IP-uptake/turnover mismatches in areas of compromised myocardium. These findings suggest that ischemia-assotiated alterations of cardiac IP-metabolism might be indicative of jeopardized myocardium.

1:30–3:00 **Room 132**

PULMONARY I

Moderator: Barry A. Siegel, M.D.
Co-moderator: Stephen C. Scharf, M.D.

Tc-99m SULFUR COLLOID (Tc-SC) AND Tc-99m RED BLOOD CELLS (Tc-RBC) FOR DETECTING PULMONARY BLEEDING: CORRELATION WITH CLINICAL, SURGICAL AND RADIOGRAPHIC FINDINGS. G.G. Winzelberg, M.H. Wholey, C. Jarmolowski, M. Sachs, and J. Weinberg. Shadyside Hospital, Pittsburgh, PA.

Over a 30 month period, 24 patients (pts) with hemoptysis of 50 ml/24 hr period or greater were studied to determine if Tc-SC or Tc-RBC could accurately detect sites of hemorrhage. In 24 pts, 30 Tc-SC and 18 Tc-RBC scans were performed. 13 pts were studied sequentially with Tc-SC followed by Tc-RBC over a 24 hour period. 40 control pts were also studied. Upright Tc-SC scans were done after bolus injection of 6 mC Tc-SC; a posterior flow study at 2 frames/second followed by 500,000 count posterior views of the chest was obtained at 2 minute (min) intervals for 20 min; anterior and lateral views were then obtained. 500,000 count anterior, posterior and lateral chest Tc-RBC scans were obtained after in vivo labeling with 20 mC Tc-pertechnetate. Tc-RBC scans were obtained immediately after Tc-SC studies and follow-up views over 24 hours were obtained. Scan results were correlated with chest x-ray, bronchoscopy, bronchial angiography and surgical findings. Of 30 Tc-SC studies, the static scans demonstrated 7 true positives (pos) studies which accurately correlated with the site of bleeding determined from bronchoscopy or bronchial angiography. The scans usually became positive after the first 6 minutes of imaging. There was one false pos. Only one flow study was abnormal. Of 18 Tc-RBC scans, there were 6 true pos and 12 neg. 4 of the pos scans were on delayed scans at 4-24 hours.

We conclude that Tc-SC and Tc-RBC can accurately detect pulmonary bleeding with bleeding rates as low as 50 ml/24 hrs. Tc-RBC has the advantage of detecting pulmonary bleeding that may be intermittent in nature.

VENTILATION-PERFUSION (V/Q) LUNG STUDIES: UTILIZATION BY REFERRING CLINICIANS. N. Frankel, R.E. Coleman, D.B. Pryor, and C.E. Ravin. Duke University Medical Center, Durham, NC.

To determine if the results of V/Q studies influence patient management, physicians ordering 349 V/Q studies were asked the probability (low, medium, high) of pulmonary embolism (PE) before the scan was performed. The ventilation (Xe-133) and perfusion (Tc-99m MAA) study was performed and reported; 2-3 days later the ordering physician was contacted to determine how the patient (pt) was managed. Of the 119 with low pretest probability (prob), 104 had low prob (3 angio, all negative) and 15 moderate (mod) prob (5 angio, 2 positive) by V/Q, and 2 were treated for PE. Of the 168 with medium pretest prob, 126 had low prob (4 angio, all neg) and 27 had mod prob (4 angio, 1 pos), and 4 were treated for PE; the other 15 pts had high prob V/Q and 13 were treated. Of the 62 with high pretest prob, 32 had low prob (3 angio, all neg) and were not treated; 12 had mod prob (5 angio, 3 pos) and 7 were treated; 18 were high prob (3 angio, all pos) and were treated.

In summary, 261 of 262 pts with low prob scans were not treated and 31 of 33 pts with high prob scans were treated. In the group with the discordant result of high pretest and low V/Q prob, 29 of 32 pts had no angio and no treatment. In the group with medium pretest and mod V/Q prob - thus not necessarily altering the pretest prob - 21 of 27 pts had neither angio nor treatment. Of the 40 pts with mod prob V/Q scans and no angio, 34 were not treated. These data demonstrate the following: 1) the V/Q scan is being used as a final arbiter in pt management; 2) the pretest prob generally does not influence pt management; 3) a mod prob V/Q reading is used as a reason to not treat.

VENTILATION-PERFUSION LUNG SCANNING IN PULMONARY HYPERTENSION. D.G. Johnson, S.R. Mills, and R.E. Coleman. Duke University Medical Center, Durham, NC.

Ventilation-perfusion lung scans in 16 patients with pulmonary hypertension were reviewed to determine if lung scanning could differentiate patients with primary pulmonary hypertension (PPH) from patients with pulmonary hypertension secondary to chronic pulmonary thromboembolism. Six patients had PPH. All of these patients underwent right heart catherization which documented pulmonary hypertension and ruled out intra-cardiac shunt as the etiology. Four patients had pulmonary angiography which excluded chronic pulmonary embolism; the remaining two patients were young females with a family history of PPH. Ten patients had chronic pulmonary embolism proven by pulmonary angiography. Ventilation scans were performed with Xe-133 and perfusion scans with Tc-99m MAA.

In all six patients with PPH, lung scans demonstrated a low probability for pulmonary embolism (PE) pattern. Each patient demonstrated prominent non-segmental central perfusion defects related to dilated pulmonary arteries. All ten patients with chronic PE had a high probability lung scan pattern with normal or nearly normal ventilation scans and multiple segmental and/or lobar defects on perfusion scans.

These results suggest that ventilation-perfusion lung scanning is useful in ruling out chronic PE as the cause of pulmonary hypertension and may eliminate the need for pulmonary angiography.

PATTERNS OF REGIONAL VENTILATION IN LIFE LONG SMOKERS AND NON-SMOKERS USING KRYPTON-81m : COMPARISON WITH TESTS OF TOTAL LUNG FUNCTION. S.J. Barter, J.P. Lavender, F. Gibellino and N.B. Pride. Hammersmith Hospital, London, UK.

This study was undertaken to see if there was a difference between patterns of regional ventilation using Krypton-81m in the asymptomatic smoker and non-smoker. We have also compared sensitive tests of overall lung function with differences in regional ventilation detected between smokers and non-smokers. Ventilation scans using Krypton-81m were carried out on 50 asymptomatic smokers and 44 life long non-smokers. Multiple images of ventilation during tidal breathing using a large field of view gamma camera (GE MAXI) with a low energy collimator were obtained. All those studied also had the following lung function tests, FEV1, MEFV curve and single breath N2 washout tests performed. Scans were graded as normal, Focal abnormality, Grade I abnormal or Grade II abnormal, the latter 2 representing multiple symmetrical ill-defined defects.

RESULTS	NORMAL	FOCAL	I	II	TOTAL
Smokers	24	7	12	7	50
Non-smokers	41	3	-	-	44

All tests of respiratory function show an overlap between the smoker, and non-smoker, the best discriminant being the N2 washout test. Images demonstrating focal defects of ventilation occur in both groups, but Grade I or Grade II widespread changes occur in smokers only. This would appear to represent early lung damage occurring in this group.

INCREASE IN PULMONARY EPITHELIAL PORE DIMENSIONS AMONG SMOKERS DOCUMENTED BY DIFFUSION SCINTISCAN. GR Mason, RM Effros, and I. Mena. Harbor-UCLA Med. Ctr., Torrance, CA

The disappearance from the lungs of inhaled aerosols of Tc-99m-DTPA has been used to detect increased pulmonary epithelial permeability in smokers and patients with pulmonary fibrosis or adult respiratory distress syndrome. These increases in permeability can be attributed either to the appearance of additional diffusional pathways or enlargement of these "pores". To determine whether the pore dimensions are increased in smokers, we have compared the clearance of 2 radionuclides from the lungs: Tc-99m-DTPA (m.w.492) and Tc-99m-pertechnetate (m.w.163). Five normal non-smoking subjects and five otherwise normal smokers inhaled aerosols containing each of these indicators on subsequent days and regional activity over the posterior chest was monitored with a scintillation camera. Clearance rates were calculated over 7 minute intervals following 2 minutes of loading. The clearance of labeled DTPA and pertechnetate averaged .66 ± .11(SE) and 5.62 ± .55 in normal subjects. These values were increased to 4.20 ± 1.02 and 7.52 ± .29 in the smokers. The ratio of pertechnetate to labeled DTPA fell from 6.84 ± .98 in normals to 2.29 ± .53 in smokers, indicating that the ability of the epithelium to resist the diffusion of the diffusion of the larger molecule relative to the smaller molecule had been lost. The concentration of each of the radionuclides in the blood reached a plateau value within 10 to 15 minutes and labeled DTPA activity rapidly appeared over the kidneys and in the urine. This observation and the difference in clearance rates related to molecular size argue for diffusional rather than mucociliary clearance in both populations. This study suggests that smoking causes enlargement of the epithelial pores.

GA-67 LUNG SCANNING IN THE EVALUATION OF PULMONARY SARCOID ALVEOLAR ACTIVITY. G.J. Duffy, K. Thirumurthi, M. Casey, F. Barker, N. Brennan and M.X. Fitzgerald, St. Vincent's Hospital, Dublin, Ireland.

Pulmonary sarcoidosis, in approximately 20% of patients is a progressive destructive disorder. It is important to identify these patients so that treatment may be instituted before irreversible damage occurs. The percentage of lymphocytes in alveolar lavage fluid has been shown to separate those patients with a high incidence of progressive disease (>28% lymphocytes) from those with a high rate of spontaneous remission (≤ 28% lymphocytes). We have investigated Ga-67 lung scanning to see if it also could be used to identify those high risk patients.

Fifteen patients with biopsy evidence of sarcoidosis obtained both 48hr. Ga-67 lung scans, using a gamma camera and a mini-computer and cell counts on alveolar lavage fluid. Three semi-quantitative methods were used to measure Ga-67 uptake in the parenchyma of the lungs: a) lung/liver activity per unit area b) lung/background (abdomen) activity per unit area c) lung/medial thigh activity per unit area. We like others found an insignificant relationship between the percentage of lymphocytes in alveolar lavage fluid and Ga-67 lung uptake as measured by methods (a) or (b), but we found a highly significant relationship using method (c) ($p = 0.0001$, $r = 0.632$). All six patients with >28% lymphocytes in alveolar lavage fluid had lung/thigh activity ratios ≥ 4 and all 9 patients with ≤ 28% in alveolar lavage fluid had lung/thigh ratios < 4.

These results suggest that Ga-67 lung/thigh activity ratios may be used to identify those patients with a high risk of progressive pulmonary sarcoid.

1:30–3:00 **Room 130**

ONCOLOGY I: CLINICAL ANTIBODY IMAGING

Moderator: Frank H. DeLand, M.D.
Co-moderator: Samuel E. Halpern, M.D.

Introduction: Antibody Labelling
Gordon Philpott, M.D., Washington University and Jewish Hospital, St. Louis, MO

LOCALIZATION AND THERAPY OF MELANOMA WITH I-131 (ANTI-P97) FAB. J.A. Carrasquillo, S.M. Larson, K.A. Krohn, R.W. McGuffin, J.P. Brown, J.M. Ferens, P.L. Beaumier, W.B. Nelp, K.E. Hellstrom, I. Hellstrom. Seattle VAMC, University of Washington and Fred Hutchinson Cancer Center, Seattle, WA.

We have identified 2 major problems with the use of whole mouse monoclonal IgG for tumor localization: (1) prolonged circulation in blood pool causing low tumor to background ratios and (2) development of human antimouse antibodies which effectively neutralize the injected antibody. For this reason we have investigated the use of Fab.

We have utilized 2 I-131 anti-p97 Fab's (1-20 mg with 5-342 mCi) directed against different epitopes of p97 a melanoma associated antigen.

Twenty seven patients were studied on 41 occasions. Uptake was visualized in 21 patients. In eight patients injected with both specific and non specific radiolabeled Fab the ratio of specific to non-specific uptake was 3.4 and 3.7 (48 and 72 hour) in tumor biopsies.

In selected patients with good tumor uptake, dosimetry estimates utilizing the MIRD schema were 1000 Rads to tumor with 23 Rads to bone marrow and 205 Rads to liver per 70 mCi I-131 Fab. A phase 1 trial with individual doses from 34 to 342 mCi and cummulative doses of 132-871 mCi is underway. 7 patients have been studied. Because of massive tumor burden 5 patients died of progressive disease having received only 132 to 207 mCi. One patient developed human anti-mouse antibodies which precluded further therapy and died of progressive liver metastases. One patient had stabilization of metastatic liver disease. In therapy patients, mild bone marrow toxicity was observed with the exception of one patient who received a total dose of 842 mCi and developed significant marrow toxicity and required 7 units of platelets, but no clinical sequelae were noted. Marrow suppression improved by 47 days post treatment. Two patients had skin rashes and one had a hypotensive episode.

In summary we conclude that (1) Fab fragments show tumor specific uptake (2) toxicity is mild and (3) their use for therapy warrants further investigation.

IS IMMUNOSCINTIGRAPHY USING RADIOIODINATED MONOCLONAL ANTIBODIES USEFUL TO CANCER DIAGNOSIS ?
J.F. Chatal, J.C. Saccavini, P. Fumoleau, J.Y. Douillard, C. Curtet, M. Kremer. U.211 INSERM, 44035 NANTES CEDEX, and Office des Rayonnements Ionisants, SACLAY, FRANCE.

Two monoclonal antibodies (Mabs) specific in cell cultures for gastrointestinal carcinomas and recognizing 2 different epitopes were kindly provided by H. Koprowski, Wistar Institute, Philadelphia, and radioiodinated for immunoscintigraphic application. With the intact 17-1A Mab, 21 out of 35 colorectal cancer sites (60%) were visualized but none of the 21 noncolonic cancer sites (J. Nucl. Med. 23:P8, 1982). With the 19-9 Mab injected as F(ab')2 fragments, there were 17 out of 25 positive colorectal cancer sites (68%). Regardless of antibody, image interpretation was easier late (>4 days) when tumor to tissues ratios were maximal and non-specific radioactive spots tended to disappear. In 1 prospective study case only immunoscintigraphy confirmed clinical and biological suspicion of recurrence of rectum carcinoma. In 16 patients a quite satisfactory correlation was found between results of immunoscintigraphy with 19-9 and those of immunoperoxidase staining with 19-9 performed on

resected specimens. With the immunohistochemical method, 3 cases were negative with 19-9 (scans also negative) but positive with an anti-CEA monoclonal antibody (VII 23) kindly provided by J.P. Mach, Lausanne, Switzerland, thus indicating the potential value of associating 2 antibodies. In a prospective study case, after injection of this radioiodinated anti-CEA, the scan permitted detection of a primary utero-ovarian cancer in a patient with multiple lung metastases. In 9 patients injected with 2 antibodies (17-1A + 19-9 or 19-9 + anti-CEA), 8 out of 10 colorectal cancer sites were positive. It is hoped that these promising results will be confirmed for an improved detection of early recurrences.

OVARIAN CANCER:DIAGNOSIS USING I-123 MONOCLONAL ANTIBODY IN COMPARISON WITH SURGICAL FINDINGS. M. Granowska, J. Shepherd, K.E. Britton, B. Waird, S. Mather, J. Taylor-Papadimitriou, A.A. Epenetos, M.J. Carroll, C.C. Nimmon, L.A. Hawkins, and W. Bodmer. St Bartholomew's Hospital, London U.K.

The aim of this study was to evaluate the non-invasive diagnosis of the presence and extent of ovarian cancer using I-123 labelled monoclonal antibodies by comparison with the surgical findings. The monoclonal antibody, MA, is an IgG1 against epithelial surface antigen of human breast duct, also present in normal ovarian tubules. Normally a duct lining antigen is not exposed to blood and only with the architectural disorganisation of malignant change does it become so. The antibody is labelled with dry I-123 using the iodogen technique (Lancet, ii, 999, 1982). 2 mCi I-123 MA is injected and dynamic studies are made for the first 10 minutes using a computer linked gamma camera over the anterior pelvis. Anterior and Posterior static images are obtained, at 10 min, 4 h and 2 h together with marker images to aid repositioning. Enhancement of specific primary and secondary ovarian uptake, made by subtracting the early 'blood pool' image from the later images, was often unnecessary.

24 patients underwent laparotomy shortly after the 22 h image. Primary ovarian cancer uptake was correctly diagnosed in 20/22 and correctly not diagnosed in 2/2. The extent of positive uptake correlated well with the extent of spread at surgery particularly in the pelvis and mid-abdomen but less well so for subdiaphragmatic disease. In conclusion I-123 monoclonal antibody against an ovarian tumour associated antigen shows considerable promise as a diagnostic tool.

THE CLINICAL EVALUATION OF 111 INDIUM LABELED MONOCLONAL ANTI-MELANOMA ANTIBODIES (111 IN-ANTI MEL) FOR TUMOR SCANNING. S.E. Halpern, R.O. Dillman, P.L. Hagan, J.D. Dillman, I. Royston, and R.E. Sobel, VA Medical Center, and University of California, San Diego; and J.M. Frincke, R.M. Bartholomew, G.S. David, and D.J. Carlo, Hybritech, Inc., San Diego, CA.

Larson, et, al, have successfully imaged metastatic malignant melanoma using 131 I labeled monoclonal anti-melanoma antibodies (MoAb; types P-96.5 or P-8.2). Animal data from our own laboratory has indicated that greater tumor (T) incorporation of the P-96.5 MoAb could be obtained if it were 111 In labeled due to dehalogenation of the 131 I moiety. Accordingly, the purpose of this report is to detail our results using 111 In-anti mel in 4 patients (pts) with metastatic T.

The P-96.5 MoAb was labeled with 111 In using a bifunctional chelation technique. Labeling efficiency ranged to 85 percent (%) and immunoreactivity was approximately 50%. Three of the pts studied received a 2 hr infusion of 3-5 mCi of P-96.5 111 In-anti mel associated with 5 mg of MoAb. One pt received a 30 minute administration of 3 mCi of P-96.5 anti-mel associated with 1.2 mg of MoAb. Blood (B) was taken at multiple intervals post injection.

Approximately 15, 21, 23 and 32% of the Tr (respectively) remained in the pts B 72 hrs from the time of peak Tr levels. About 3% was excreted in the urine in 24 hrs. The liver, kidneys and spleen acquired 111 In-anti mel as part of the normal Tr distribution. Tumor sites were observed without the necessity of subtraction techniques.

We conclude that 111 In-anti mel shows promise as a T scanning radiopharmaceutical and should be evaluated further for this purpose.

THE OPTIMIZATION OF DUAL ISOTOPE IMAGING TECHNIQUES IN IMMUNOSCINTIGRAPHY. A.C. Perkins, J.G. Hardy, and J.D. Hardcastle. Queen's Medical Centre, Nottingham, U.K.

With monoclonal antibodies to human tumor associated antigens the target-to-non-target uptake (T:NT ratio) is relatively low (about 2:1) and background subtraction is necessary. Good separation of photopeaks is a principal consideration for simultaneous dual isotope imaging. However, when the photopeak separation is great, as in the case of I-131 and Tc-99m, there is a large difference in gamma ray attenuation and scatter. This prevents a perfect subtraction and the resulting images can be misleading.

Experiments have been undertaken to optimize the background subtraction techniques. A phantom was constructed to represent a variable blood pool activity with a target positioned at different depths. Combinations of radionuclides were assessed. Subtraction images both of the phantom and clinical studies were viewed for artifacts and the changes in T:NT ratios were measured.

Results show that subtraction artifacts can be reduced considerably using a combination of radionuclides with comparatively similar photopeak energies. For example, the use of In-113m rather than Tc-99m subtraction from I-131 images results in a reduction of artifacts. A better choice of labels for subtraction immunoscintigraphy is Ga-67 and In-111. These radionuclides have similar photopeak energies and physical half lives but they can be imaged simultaneously. Labeling antibody with one radionuclide and normal IgG with the other provides an optimum combination for subtraction. The two proteins will distribute in the non-target tissues with a similar time-activity profile which will lead to better image correction.

1:30–3:00 **Room 120**

RENAL/ELECTROLYTE/HYPERTENSION I

Moderator: Andrew T. Taylor, M.D.
Co-moderator: Thomas A. Powers, M.D.

NON-INVASIVE RADIONUCLIDE SCINTIPHOTOGRAPHIC TECHNIQUE FOR THE ASSESSMENT OF PRESERVED RENAL ALLOGRAFT VIABILITY. D. Anaise, H. Atkins, Z. Oster, H. Asari, W. Waltzer, R.J. Bachvaroff, W. Pollack, and F.T. Rapaport. SUNY at Stony Brook, Stony Brook, NY 11794.

Renal microcirulation studies utilizing microspheres provide a highly reliable index of viability of preserved kidneys, but require sectioning for tissue analysis. This report describes a non-invasive approach for a similar assessment, which permits subsequent transplantation of the tested kidney. During this study, 43 fresh canine kidneys were treated as follows: Group A - perfused with Collins' solution (C^2) and stored at 4°C; Group B - perfused with the same solution to which 5 mg% of trifluoperazine (TFP) was added. Both groups (A and B) were subdivided into 4 subsections, with kidney preservation at 4-8°C for 5, 24, 48, and 72 hours, respectively. At the indicated interval, each kidney was perfused with 50,000 Tc-labeled microspheres (mean diameter 15u) from a standard height of 100 cm, and radioscintiphotography and computer analysis of the distribution of the microspheres were performed. Kidneys preserved for 5 hours had uniform cortical activity; there was a decrease in cortical activity and increase in hilar activity at 48 hr. By 72 hrs there was very poor cortical uptake in Group A; however, addition of TFP resulted in increases in cortical activity at 48 and 72 hrs. There was a clear correlation between the results and the capacity of such kidneys to sustain life after retransplantation.

We have also perfused the kidneys with Tl-201 and the distribution correlates well with the microsphere distribution.

MEASUREMENT OF DIFFERENTIAL RENAL FUNCTION USING TC-99M GLUCOHEPTONATE. T.A. Powers, W.J. Stone, W.S. Witt, L.T. Killion, J.A. Patton and R.D. Bowen. VA Medical Center and Vanderbilt Medical Center, Nashville, TN.

Determination of the percent of total renal function supplied by each kidney is important in many renal diseases. We have previously validated Tc-99m DTPA and DMSA studies for this purpose and recently undertook the evaluation of Tc-99m glucoheptonate (GH). 11 adult mongrel dogs received partial ureteral obstruction (5), unilateral renal infarction (4) or an ipsilateral combination of both (2). Seven to ten days following these procedures the dogs were anesthetized with pentobarbital and a bolus injection of 10 mCi Tc-99m GH was administered. Studies were acquired in the posterior projection on a minicomputer at 2 seconds/frame for 3 minutes. Static images were obtained anteriorly and posteriorly between three and five hours postinjection. The next day iothalamate and creatinine clearances were measured by ureteral catheterization. There was good correlation between differential function calculated from the 1-3 minute portion of the bolus study and that determined by the ureteral catheter studies, $r \geq .99$. Correlations based on the static images were less satisfactory due to pelvic retention in the obstructed animals, r=.73. We conclude that Tc-99m GH may be used to determine differential renal function.

Tc-99m DTPA TRANSIT TIME AS AN INDEX OF PROXIMAL TUBULAR FUNCTION. G. Vivian, and I. Gordon. The Hospital for Sick Children, Great Ormond Street, London WC1.

The application of fractional clearance techniques to unilateral renal disease has been limited by the need for ureteric catheterization. The mean transit time (MTT) of a non-reabsorbable tracer (Tc-99m DTPA) through the kidney is influenced by the prevailing rate of salt and water excretion; the present study was undertaken to investigate the relationship between the MTT and tubular function as determined by clearance during Hypotonic Volume Expansion (HVE).

10 children (2-16 years) with a solitary kidney were studied; HVE was established according to the protocol of Soriano and a 20 minute dynamic renal study with 0.5-2.0 mCi Tc-99m DTPA performed once a stationary urine flow rate was maintained. Renal parenchyme was identified by a mean time image and whole kidney MTT (WKMTT) and parenchymal MTT (PTT) derived by deconvolutional analysis with Diffy algarithm. Fractional urine volume (V') and the proportion of the load reabsorbed distally ($C_{H_2O} / C_{H_2O} + C_{Na}$ were determined at maximum urine flow rate and factored by GFR. A correlation was shown between PTT and V' (r = -0.81) and WKPTT and V' (r = -0.66). There was no relationship $C_{H_2O} / C_{H_2O} + C_{Na}$ and WKMTT (r = 0.3) or PTT (r = 0.19).

The PTT may be considered an index of proximal rather than distal tubular function when measured during HVE, and the technique may be used to assess proximal tubular function in unilateral renal disease.

OBSTRUCTIVE NEPHROPATHY:A COMPARISON OF THE PARENCHYMAL TRANSIT TIME INDEX AND FRUSEMIDE DIURESIS. M.K. Nawaz, C.C. Nimmon, K.E. Britton, M.J. Carroll, M. Granowska, E. Mlodkowska, and H.N. Whitfield. St Bartholomew's Hospital, London, U.K.

This study assesses two methods of determining whether a kidney's outflow is or is not obstructed. Dilation of the outflow tract is insufficient to diagnose obstruction. The increased resistance to outflow, if trivial, may be overcome by frusemide diuresis, FD, if there are sufficient nephrons. Failure to do so indicates obstruction. The slight rise in pressure from glomerular filter to the site of resistance due to the presence of true outflow obstruction causes increased salt and water reabsorption and therefore prolongs the transit time of a non reabsorbable solute such as Tc-99m DTPA through the nephrons. The parenchymal transit time index, PTTI, is given by subtracting the minimum transit time from the mean parenchymal transit time obtained by deconvolution analysis of the left ventricular and renal parenchymal activity time curves (Lancet, ii, 900, 1981) taken from a computer linked gamma camera posteriorly placed, after 10 mCi intravenous Tc-99m DTPA. Patients with 63 kidneys with X-ray evidence of a dilated outflow tract were studied both with PTTI and with FD. Final clinical outcome, frusemide urography and/or antegrade perfusion pressure measurements were used as the criteria of obstruction. In 36 obstructed kidneys PTTI was correct in 35, FD in 30. In 25 non-obstructed kidneys PTTI was correct in 24, FD in 25. In 2 outcome was uncertain. In conclusion the study and these highly significant results indicated that, although FD is easier to perform, PTTI is more sensitive than FD to the presence of outflow obstruction and can be used with poor renal function than FD.

RENAL UPTAKE OF TECHNITIUM 99m DIMERCAPTOSUCCINIC ACID (Tc 99m DMSA) TO ASSESS RENAL ISCHEMIA AND PRETREATMENT DRUG EFFECTS. D. Chopin, J.L. Moretti, C. Abbou. Henri Mondor Hospital 94000 Creteil, France.

Warm ischemia during urological surgery is not always controllable and is known to have an adverse effect upon the recovery of normal renal function. Effects of drug pretreatment remain controversial, since an evaluation of renal function after an ischemic insult is limited by practical considerations. This study investigated the Tc 99m DMSA* renal uptake in the Sprague Dowley rat (N=150) after complete unilateral occlusion of the renal artery. Variation of renal uptake and/or modification induced by pharmacological pretreatment was studied using 2 protocols.

First, Tc 99m DMSA renal uptake (% of injected dose: 14.8MBq/rat) was related to 131I orthoidohippurate (131I-OIH:3.4 MBq/rat) clearance on the same rats for 2 periods of ischemia (60 min and 90 min), by using a gamma camera (mounted with a pinhole collimator) linked to a computer§. Secondly, Tc 99m DMSA relative renal uptake (RRU) was related to several periods of ischemia from 30 to 120 min with and without pretreatment of the following drugs: Furosemide (3mg/kg), Inosine (150 mg/kg), Mannitol (2.5 mg/kg) and Phenoxybenzamine (5mg/kg). The RRU was calculated as the ratio of ischemic versus contralateral renal uptake. In this case renal activity was obtained by a direct count (gamma camera§) on each harversted kidney.

There was a significant correlation between Tc 99m DMSA renal uptake and 131 OIH clearance of both ischemic and normal kidneys. According to the data obtained with the ischemic group, a significant increase of RRU was obtained with Furosemide, Mannitol, and Inosine, but not with Phenoxybenzamine. Inosine seems to have the most predominant effect. *C.E.A. Saclay §C.G.R., France

DELAYED RENAL LOCALIZATION OF GA-67. D. S. Lin, J. A. Sanders, and B. R. Patel, University of Mississippi Medical Center and V. A. Medical Center, Jackson, MS.

This investigation was done to evaluate the incidence of delayed Ga-67 renal localization and the clinical significance of different degrees of uptake in 500 consecutive scans performed in the years of 1981 and 1982. The scans were requested either for detection or follow-up of inflammatory or neoplastic disease. In adults, 4-5 mCi Ga-67 citrate was given by I.V. and for children doses proportional to weight were used. Renal uptake on 48 or 72 hr total body LFOV gamma camera images were graded as follows: 0 = background activity; 1+ = greater than background but less than spine; 2+ = close to spine but less than liver; 3+ = to liver; 4+ = greater than liver.

In the 500 scans, 996 kidneys were evaluated and among them 600 (60%) had 0 uptake, 340 (34%) had 1+ uptake, and 56 (6%) had 2+ or more uptake. Since 1+ uptake was usually bilateral, GU asymptomatic and not related to any specific underlying group of disease, it was considered to be normal. Among the possible causes of the 56 kidneys (35 cases) having 2+ or more uptake were: infection (27, 48%), drug-induced renal damage (10, 18%), urine stasis or slow excretion (7, 12%), collagen vascular disease (6, 11%), renal failure (4, 7%), acute tubular necrosis (1, 2%), and indeterminate (1, 2%). Cases of renal infection or failure tended to show more or less 4+ uptake while drug damage or urine stasis tended to have 2+ uptake.

Faint visualization (1+) of kidneys on a delayed scan occurred often and should be considered normal. Higher than 1+ uptake was clinically significant, having a total incidence of about 6%.

1:30-3:00 Room 275

COMPUTER I: CARDIAC

Moderator: Michael L. Goris, M.D., Ph.D.
Co-moderator: Mark W. Groch, M.S.

Regional Quantitation and Fourier Analysis.

Michael L. Goris, M.D., PH.D, Stanford
University Medical Center, Stanford, CA

OPTIMUM ORDER HARMONICS OF FOURIER ANALYSIS IN MULTIGATED BLOOD-POOL STUDIES. T. Mukai. The Johns Hopkins Medical Institutions, Baltimore, MD. and N. Tamaki, Y. Yonekura, K. Minato, R. Morita, and K. Torizuka. Kyoto University Medical School, Kyoto. and Y.Ishii. Fukui Med. School, Fukui, Japan.

Phase analysis by fundamental Fourier transform in Tc-99m RBC multigated blood-pool studies is in widespread, but it contains significant inaccuracies in curve fitting. To solve this, higher-order harmonics have been investigated. This study is undertaken to determine the optimum order harmonics by using a simulation model. Statistical noise from Poisson random derived from end-diastolic counts (EDC) and temporal noise from Gaussian random of R-R interval variation as standard deviation (σ) were added to an ideal curve to simulate various volume curves. The first through 4th-order harmonics of Fourier transform was performed to obtain the fitted curves. The systolic parameters (time to end-systole:TES; peak ejection rate:PER; and time to PER:TPE), the early diastolic parameters (peak filling rate:PFR; and time to PFR:TPF), and the late diastolic parameters (atrial kick:AK; and time to AK:TAK) were analysed from each fitted curve. The first harmonics did not yield them accurately. The 4th-order harmonics were unsatisfactory, because high frequency noise can not be excluded under small EDC. In the 2nd and the 3rd-order harmonics, the systolic parameters were reliable even under large noises. Although the values of early diastolic parameters fluctuated under modelate temporal noise (σ=15%), they were less than 10% or 50msec different from the ideal values. On the other hand, the late diastolic parameters were not reliable. This study indicates that the 2nd-order (in small EDC) and the 3rd-order (in large EDC) harmonics of Fourier transform is optimum for curve fitting which can accurately assess systolic and diastolic functions separately in gated blood-pool studies.

OPTIMUM NUMBER OF HARMONICS FOR FITTING CARDIAC VOLUME CURVES. S.L. Bacharach, M.V. Green, D. Vitale, G. White, M.A. Douglas, R.O. Bonow and A.E. Jones. NIH, Bethesda, MD

Statistical fluctuations limit the accuracy of quantities derived from global or regional cardiac time-activity curves (TACs). Thus many workers have fit their TACs with a truncated Fourier series giving rise to two sources of error: (1) The truncated Fourier series may not adequately describe the TAC shape, causing errors in parameters calculated from the fit, and (2) TACs acquired from the same subject under identical circumstances will fluctuate due to counting statistics, causing the Fourier fits (and parameters derived from them) to fluctuate. These two errors respectively decrease and increase as harmonic number increases, suggesting the existence of a minimum in total error. This "minimum error" harmonic number(MEHN) was calculated for each of six parameters descriptive of LV TACs: time-to-end-systole (TES), ejection fraction (EF), peak ejection rate (PER), peak filling rate (PFR), and their times of occurrence (TPER,TPFR). The "true" value of each parameter was determined from TACs of very high statistical precision (82 subjects: 16 @ $.65*10^6$ counts/10 msec point & 66 @ $.2*10^5$ /10msec point). Poisson noise was added to simulate lower count rates. For these parameters MEHN was not a strong function of detailed TAC shape. MEHN could be predicted using a crude signal to noise(S/N)ratio = 1st harmonic amplitude/(avg. counts)**.5 The MEHN for a TAC is predicted for each parameter @ various S/N. Using either fewer or more harmonics than MEHN increases the total error. MEHN is dependent on the parameter chosen. We find that at S/N=1.7, typical of single pixel TACs used in functional maps, 2 harmonics are optimum for all parameters except PFR, which requires 3.

THE EFFECT OF STOCHASTIC PIXEL NOISE ON THE DISTRIBUTIONS OF MAGNITUDE AND PHASE VALUES IN THE FOURIER ANALYSIS OF GATED STUDIES. J.R. Halama, J.E. Holden. Medical Physics Dept., University of Wisconsin, Madison, WI 53706.

In Fourier methods of analyzing gated equilibrium blood pool studies of ventricular function, regions of uniform phase would still yield a finite distribution of calculated phase values due to the propagation of stochastic pixel noise into the calculated Fourier phases and magnitudes. We have studied this noise component of phase distributions using phantom studies and computer simulation. In both approaches, several thousand one-pixel 'ventriculograms' were generated, all identical to each other except for stochastic noise. Fourier magnitudes and phases at the first harmonic were calculated and histograms generated. In the phantom experiments, higher frequencies were also investigated. A theoretical prediction of the distributions of magnitude and phase was developed and observed to fit the experimental results exactly. In the limit of high signal/noise, the Fourier magnitude and phase distributions at each frequency are completely determined by the signal-to-noise measure $M\sqrt{N}/A$, when M is the actual magnitude in pixel counts, N is the number of frames/cycle, and A is the average pixel count over the cycle. Our formalism can be used to determine study count requirements, or for fixed study counts, to assess the significance of stochastic noise in the interpretation of the measured magnitude and phase distributions.

A METHOD FOR IMPROVING THE SPECIFICITY OF PHASE ANALYSIS FOR REGIONAL DEFECTS IN THE PRESENCE OF DEPRESSED GLOBAL LEFT VENTRICULAR FUNCTION. M.V. Green, S.L. Bacharach, B.A. Jones-Collins, S.L. Findley, and R.E. Patterson. National Institutes of Health, Bethesda, MD.

An increase in the standard deviation (STD) of regional left ventricular (LV) Fourier phase about the mean phase has been associated with regional wall motion abnormalities (RWMAs). However, STD will also increase as LV ejection fraction (EF) and/or total LV counts decrease, even if no RWMAs are present. We have devised a measurement parameter (% area mismatch (AM) between superimposed model and observed LV phase distribution functions) that is largely independent of these effects and, thus, should be specific for RWMAs over a wide range of EFs. Specificity of the STD and AM measurements was compared in 5 normal gated blood pool studies manipulated to yield 20 image sequences with EF artificially reduced (.8,.6,.4,.2 x normal EF) holding mean LV counts constant. Even though wall motion was normal, STD identified 15/20 of these studies as abnormal; AM identified 0/20 as abnormal. Comparative sensitivity was tested in 16 additional studies, each with RMWAs and reduced EFs. STD identified 15/16 of these studies as abnormal, AM 13/16. We conclude that an increase in STD is not a reliable indicator of RWMAs when EF is reduced. In contrast, AM, while of comparable sensitivity to STD, is far more specific for RWMAs when EF is depressed. Thus, AM may be useful in discriminating global from regional dysfunction in patients with poor LV function.

LIMITATIONS OF COUNT-BASED REGIONAL EJECTION FRACTION AS A MEANS OF ASSESSING REGIONAL LEFT VENTRICULAR FUNCTION IN TRANSMURAL MYOCARDIAL INFARCTION. Harvey J. Berger, Michael Plankey, Jay L. Meizlish, Barry L. Zaret. Yale University, New Haven, Connecticut.

Regional ejection fraction (REF) obtained in the left anterior oblique (LAO) position was compared to regional wall motion (RWM) analysis based on visual interpretation of 4-view gated equilibrium blood pool imaging in 26 studies of patients (pts) with acute transmural myocardial infarction (MI). By ECG, 14 had AMI and 12 inferior (I) MI. For the semiquantitative technique, the left ventricle (LV) was scored by 2 blinded observers on a 5-point scale from dyskinetic (dys,-1) to normal (nl,+3). All pts had $\geq$ 1 abnl segment. The steep lateral views were essential in IMI and demonstrated the consistent involvement of the posterobasal region. REF was calculated using a fixed end-diastolic center of mass and 8 sectors. After eliminating the 2 basal sectors, there were 2 each for septum (S), apex (AP), and posterolateral (PL) wall. The S usually is associated with AMI, the PL wall with IMI, and the AP with both. REF averaged ($\pm$SE) 60$\pm$2% in nl LAO segments (N=79), 42$\pm$4% in hypokinetic segments (N=21, $p < 0.05$ vs nl), and 15$\pm$4% in akinetic or dys segments (N=30, $p < 0.01$ vs nl). REF only differed significantly between AMI and IMI in the S segments and the medial AP segment ($p < 0.01$). In AMI, 22/28 (79%) S segments had REF $\leq$40% vs 1/28 (4%)

in IMI ($p < 0.001$). S REF was preserved ($\geq 50\%$) in 20/24 (83%) IMI pts. PL REF was $\leq 50\%$ only infrequently in IMI (7/24 [29%]), which was similar to AMI (15/28 [54%]).

Thus, although REF relates well to visual assessment of RWM, it is a poor technique for quantifying I RWM. The PL segments usually are nl in IMI. These findings justify the need for multiview blood pool studies to assess RWM.

1:30-3:00 **Exhibit Hall**

POSTER SESSION I

More than 200 poster presentations of scientific papers will be on display Tuesday through Friday and approximately half of the authors will be present to answer questions during this time period. For a complete listing of posters, authors, and times see POSTER PRESENTATIONS, which immediately follow the Scientific Papers on Friday.

WEDNESDAY, JUNE 8, 1983

10:30-12:00 **Room 123**

CARDIOVASCULAR CLINICAL III: SPECT, COMPUTER & BASIC

Moderator: John W. Keyes, Jr., M.D.
Co-moderator: Ron J. Jaszczak, Ph.D.

VALUES AND LIMITATIONS OF SEGMENTAL ANALYSIS OF STRESS AND REDISTRIBUTION TL ECT FOR LOCATION OF CORONARY ARTERY DISEASE. N. Tamaki, Y. Yonekura, T. Mukai, K. Minato, R. Nohara, K. Kadota, H. Kambara, C. Kawai, Y. Ishii, and K. Torizuka. Kyoto University Medical School, Kyoto, Japan.

To predict lesions in individual coronary arteries, segmental analysis was performed in Tl-201 emission computed tomography (ECT) using a rotating gamma camera. Stress and redistribution ECT images were obtained in 38 cases with coronary artery disease (CAD) and 13 with normal coronary artery. The reconstructed images of contiguous transaxial, short-axis, and long-axis sections were divided into 9 segments. Perfusion defects located in anterosuperior or septal wall were defined as LAD lesion, inferior or posterobasal wall as RCA lesion, and posterolateral wall as LCX lesion. Sensitivity (Sn) and specificity (Sp) in the diagnosis of disease in individual coronary arteries were:

	overall	RCA	LAD	LCX
Sn	35/38(92%)	15/19(79%)	29/34(85%)	14/22(64%)
Sp	12/13(92%)	28/32(87%)	16/17(94%)	26/26(100%)

In the study of LAD, perfusion defect in anterosuperior wall is sensitive (83%) and specific (88%) for the proximal disease of LAD. Accurate diagnosis was made in 71% of single vessel disease (1VD) and 91% of 2VD, while only 38% of 3VD were correctly predicted. The segmental perfusion defect was comparatively evaluated with regional wall motion abnormality (RWMA) in contrast ventriculography. Severe RWMA (dys- or akinesis) was seen in 51% of the segments showing persistent defect, while normal or mild RWMA was seen in 80% of redistribution positive segments. Thus, stress and redistribution ECT imaging permits prediction of disease in individual arteries with high specificity and evaluation of viability of the myocardium, but it still contains difficulties identifying 3VD.

EVALUATION OF NONTRANSMURAL MYOCARDIAL INFARCTION BY TL SINGLE-PHOTON EMISSION CT. N. Tamaki, Y. Yonekura, K. Minato, H. Itoh, T. Mukai, H. Kambara, K. Kadota, C. Kawai, and K. Torizuka. Kyoto University Medical School, Kyoto, and D. Hamanaka, and Y. Ishii. Fukui Medical School, Fukui, Japan

The sensitivity of Tl planar scintigraphy for nontransmural myocardial infarction (MI) is limited. This study was undertaken to determine whether single-photon emission CT (SPECT) of Tl permits detection and characterization of nontransmural MI. A series of contiguous transaxial, the short-axis, and the long-axis sections were reconstructed from 32 different views over 180° (from LPO to RAO) following the planar Tl imaging in 13 with nontransmural MI and 21 with transmural MI. Decreased activity in SPECT images was qualitatively and quantitatively evaluated. In contrast to the high sensitivity of both SPECT (100%) and the planar imaging (90%) in the study of transmural MI, SPECT yielded significantly higher sensitivity (85%) in the detection of nontransmural MI than the planar imaging (54%, $p<0.05$). Tomographically estimated infarct size was smaller in nontransmural MI (9.2 ± 5.2 ECT-g-Eq) than that in transmural MI (38.3 ± 22.8 ECT-g-Eq, $p<0.001$). Residual radioactivity in infarct zone expressed as % of maximum myocardial activity was higher in nontransmural MI (74.5 ± 7.8%) than that in transmural MI (47.6 ± 12.1%, $p<0.001$). In each nontransmural MI, SPECT did not delineate subendocardial perfusion defect, probably due to relatively poor resolution and ungated images. Inverse correlation was seen between infarct size and residual radioactivity in transmural MI ($r=-0.79$). In nontransmural MI, on the contrary, residual activity was higher as compared to its infarct size, suggesting heterogenous distribution of Tl in infarct zone. Thus, Tl SPECT is a useful method in detecting and characterizing nontransmural and transmural MI.

COMPARISON OF ROTATIONAL TOMOGRAPHY WITH PLANAR IMAGING FOR THALLIUM-201 STRESS MYOCARDIAL SCINTIGRAPHY. F Prigent, J Friedman, J Maddahi, J Bietendorf, E Garcia, J Areeda, K Van Train, A Waxman, D Berman, Cedars-Sinai Medical Center, Los Angeles, CA

To evaluate the relative diagnostic potential of rotational tomography (tomo) for Tl-201 stress myocardial scintigraphy, tomo and standard planar imaging were performed immediately and 4 hours after stress Tl injection in 33 pts: 13 normals (<1% likelihood of coronary artery disease [CAD]) and 20 undergoing coronary angiography (cath). Imaging was performed using a camera with a 1/4" NaI crystal and 75 photomultiplier tubes (Siemens Orbiter). Planar imaging employed 3 10-min views and tomo used 32 30-sec images spaced by 5.6°. For tomo, backprojected transaxial tomograms were reconstructed into sagittal and oblique planes and were visually assessed by 3 blinded observers. In oblique views, slices containing the LV cavity were assessed, and with 3 o'clock=0, defects from 120° to 355° were assigned to the anterior (ant) and the remaining to the posterior (post) coronary circulation. In sagittal views, only apical regions were assessed, and defects were not assigned to ant or post unless they involved only the upper or lower portion respectively. Of the 13 nl pts, 11 were normal by planar and 10 were normal by tomo. Among the cath pts, tomo was positive in 16/19 with CAD and planar in 17/19; both were positive in the 1 pt without CAD. Regarding extent of disease, tomo correctly identified 10/11 and planar 7/11 pts with both ant and post CAD. Tomo incorrectly called ant and post disease in only 1/8 pts with single-region CAD compared to 4/8 incorrect by planar. These results suggest that planar and tomo techniques have similar accuracy in the detection of CAD but that tomo is more accurate in the assessment of extent of disease.

SINGLE PHOTON EMMISSION COMPUTED TOMOGRAPHY (SPECT) COMPARED TO PLANAR Tc-99m PYROPHOSPHATE INFARCT-AVID SCINTIGRAPHY. R. Pettigrew, E. Atwood, R. Webb, M. Johnson, G. Perkins, R. Burks, S. Halpern, J. Verba, K. Witztum. VA Medical Center, San Diego, CA.

This study was undertaken to evaluate SPECT in comparison to 4-view planar imaging (PLANAR) in detecting acute myocardial infarction (MI) with Tc-99m-pyrophosphate (PYP). We assessed PLANAR and SPECT for ability to diagnose MI, and for interobserver agreement in diagnosing and localizing MI. 20 chest pain syndrome and/or perioperative patients suspected of MI were studied 2 to 3 days post onset of symptoms. PLANAR was done with 25 mCi PYP at 6 hrs and was immediately followed by SPECT. A GE 400T-STAR system acquired data in 32 views over 180° at 45 sec per view. Images were read double blind by 4 independent observers without knowledge of patient or clinical data. An interpretation of no MI, an MI, and of MI location each required a consensus of

3 of 4 observers. There was standard diagnostic clinical evidence of MI in 14 patients, of which 10 had nontransmural MI. 6 patients had no MI. RESULTS:

	PLANAR	SPECT	INTEROBSERVER AGREEMENT 4 of 4 AGREE	
			No MI	MI
SENS	64%	100%		
SPEC	100%	83%	PLANAR in 50% of TN	in 66% of TP*
ACC	70%	95%	SPECT in 80% of TN	in 86% of TP

(*TP = True Pos; TN = True Neg)

78% of SPECT vs. 44% of PLANAR positive MI had 4 of 4 observer agreement on MI location. WE CONCLUDE: SPECT is 1)significantly more sensitive than PLANAR for detecting MI; 2)less observer variable for presence and location of MI; 3)may be a simple, accurate method for MI diagnosis when ECG, CPK/LDH, and patient history are non-diagnostic.

SCINTIGRAPHIC QUANTITATION OF MYOCARDIAL ISCHEMIA. B. Massie, J. Wisneski, M. Hollenberg, E. Gertz, M. Go, S. Henderson. VAMC and Univ. of CA., San Francisco.

While both exercise (EX) TL-201 scintigraphy and the EX electrocardiogram (ECG) can diagnose coronary disease (CAD), a quantification of the resulting ischemia would be valuable. To attempt this, we studied 61 patients: 11, 6, 12 and 32 with 0, 1, 2 and 3 vessel CAD. EX and 3 hr redistribution imaging were performed by 7 pinhole tomography, generating circumferential profiles of the initial and 3 hr distribution of TL-201 and of the 3 hr clearance for each of 3 slices. A scintigraphic ischemic score (SIS) was derived by summing the area between the EX and 3 hr profiles and the area in which clearance fell below normal. This summed area was normalized for the level of stress by dividing by the product of by EX duration (in min) times the fraction of predicted heart rate achieved. The ability of the SIS to quantitate ischemia was assessed by relating it to the EX ECG and the coronary anatomy. The treadmill ECG Score (TES) was derived from the algebraic sum of the area of J point deflection and ST segment slope in 2 leads during EX and recovery, which was then normalized by the same factor as the SIS. An angiographic ischemic score (AIS) was derived by rating 8 major branches on a 10 point scale, including only vessels perfusing viable regions and accounting for collateral circulation. The sensitivity and specificity of scintigraphy for CAD were 96% and 80%. For 0, 1, 2 and 3 vessel disease, SIS was 52±19, 233±110, 427±98 and 879±138 units. Not suprisingly, overlap was considerable, though intergroup differences were significant. More importantly, SIS correlated significantly with both AIS (R=0.78) and with TES (R=-.68). Thus, a continuous quantitative measurement of ischemia, the validity of which is supported by ECG and anatomic data, can be derived from the quantitative analysis of myocardial TL-201 distribution and clearance.

A THRESHOLD METHOD OF VOLUME DETERMINATION FROM TOMOGRAPHIC RECONSTRUCTIONS. J.A. Malko, R.L. Eisner, J.C. Engdahl, G.T. Gullberg, D.J. Nowak, E.M. Woronowicz, General Electric Medical Systems Division, Milwaukee, WI; R.L. Van Heertum, W.P. Kowalsky, St. Vincent's Hospital and Medical Center, New York, NY; B.D. Collier, R.S. Hellman, Medical College of Wisconsin, Milwaukee, WI; J. Thrall, M. Tuscan, University of Michigan Medical Center, Ann Arbor, MI.

A computerized method for approximating volumes of phantom and clinical data from their tomographic reconstructions has been developed. The main characteristic of the method is the use of a count-threshold to select slice-pixels to be counted in the computed volume. This threshold is applied to each slice of the tomographic reconstruction; pixels with count-values above the threshold are defined to be in the desired volume. The sum of these selected pixels for each slice define the slice-area, which, when multiplied by the slice thickness, results in a slice-volume. The totality of the slice-volumes makes up the 3-dimensional volume of interest. The key to the method is the appropriate threshold definition. For sufficiently large and simple shapes, a threshold defined as a fixed percent of the slice average or maximum count gives reasonable volume estimates. As the size of the volume decreases or as its shape becomes less regular the simple threshold technique becomes less accurate.

10:30–12:00 **Room 132**

CARDIOVASCULAR BASIC I: MYOCARDIAL METABOLISM

Moderator: Heinrich R. Schelbert, M.D.
Co-moderator: James H. Thrall, M.D.

EXTERNAL DETECTION OF INCREASES IN β-ADRENOCEPTOR DENSITY IN ISOLATED PERFUSED HEARTS WITH I-125 HYDROXYBENZYLPINDOLOL B. Hughes, S.R. Bergmann, P.B. Corr and B.E. Sobel Washington University School of Medicine, St. Louis, MO

Alterations in cardiac β-receptor number have been associated with a variety of cardiac pathologies. We previously demonstrated that specific binding of the β-receptor ligand I-125 hydroxybenzylpindolol (I-125 HYP) can be detected externally in isolated hearts. The present study was conducted to determine whether increases in β-receptor number can be detected with this ligand. Since there is species variation in the response to thyroxine (T4) and tri-iodothyronine (T3), both rats and cats were treated with T4 or T3 to increase β-receptor density. Isolated, paced, isovolumically beating hearts from treated and untreated animals were perfused retrogradely at constant flow at 37°C with modified Krebs-Henseleit buffer. I-125 HYP (6-8μCi) was recirculated for 40 min, and uptake and release were monitored with a gamma probe. Hearts from animals treated with T4 or T3 exhibited increased uptake of I-125 HYP detectable externally and a 60% increase in receptor number by Scatchard analysis of ventricular membrane preparations. Specificity of binding was assessed by measuring the turnover rate of I-125 HYP during perfusion of the hearts with specific (β-receptor agonists/antagonists) and non-specific (Krebs-Henseleit buffer) displacers. In control and treated rat hearts a significant portion of the binding was displaceable with HYP. In cat hearts efflux of I-125 HYP was greater with l-compared with d-isoprenaline (-.011±.001 vs .006 ±.001min^{-1}, P<.05). Thus, increases in β-receptor number can be detected externally in an isolated perfused heart preparation. Further development of this technique should enable in vivo detection of alterations in β-adrenoceptor number in intact animals and ultimately in patients.

EFFECTS OF INSULIN, INCREASED WORK, AND ANOXIA ON FLUORODEOXYGLUCOSE DERIVED RATE CONSTANTS AND FICK METABOLIC RATES. J. Krivokapich, S.C. Huang, M.E. Phelps, C. Watanabe, C. Selin, K.I. Shine. UCLA School of Medicine, Los Angeles, Ca.

The glucose (Glc) analog F-18-fluorodeoxyglucose (FDG) was used with a mathematical tracer kinetic model to determine the effects of insulin, increased work, and anoxia on the rate constants for FDG forward and reverse transport (k1*,k2*), phosphorylation of FDG (k3*), dephosphorylation of FDG-6-P (k4*) and on Fick derived myocardial metabolic rates for Glc utilization (MMRGlc). FDG was constantly perfused into isolated rabbit interventricular septa and tissue F-18 radioactivity was measured by coincidence counting. Control conditions were flow 1.5 ml/min, 72 beats/min with 5.6mM Glc and 5 units/L insulin. Five changes from control were studied: no insulin; 5 times control insulin; 96 paired stimulations (PS)/min; anoxia with insulin; and anoxia without insulin. Transport k*'s were greater than k3* or k4* under all conditions. The absence of or increase in insulin under control conditions resulted in no significant# change in the Fick MMRGlc or rate constants. The Fick MMRGlc was significantly increased by 96 PS, and anoxia with or without insulin. k1* increased over 30% with 96 PS and anoxia with insulin as compared to control k1*, but did not increase during anoxia without insulin. k3* significantly increased during anoxia with or without insulin, but k4* increased only with anoxia without insulin. Thus, phosphorylation is rate limiting compared to transport even in the absence of insulin; 96 PS accelerates forward transport; anoxia increases forward transport only if insulin is present; and anoxia accelerates hexokinase. #p<0.05.

EXTERNAL MEASUREMENT OF MYOCARDIAL OXYGEN EXTRACTION WITH O-15-LABELED OXYGEN. K.A.A. Fox, S.R. Bergmann, A.L. Rand, H.D. Ambos, and B.E. Sobel. Washington University School of Medicine, St. Louis, MO

To determine whether myocardial extraction of oxygen (O_2) can be quantified externally, open-chest dogs were evaluated after injection of O-15-labeled O_2 ($t_{½}$=2.1 min) as a bolus into the circumflex coronary artery. Myocardial time-activity curves were characterized with a ß-probe, permitting precise determination of myocardial activity from selected, subepicardial regions without contamination from activity in extracardiac sources. Myocardial blood flow and oxygen utilization were altered by infusion of 1 mg/kg of dipyridamole (n=5) and subsequently by ligation of a marginal coronary artery (n=3). Myocardial blood flow (MBF) and oxygen utilization were analyzed after equilibration under each set of conditions. Extraction fraction of O-15 was determined by back extrapolation of the monoexpoential portion of the myocardial time-activity curve. Epicardial veins were cannulated for direct determination of oxygen utilization. MBF, calculated by analysis of the time-activity curve after bolus injection of O-15-labeled H_2O, varied between 0.14 and 3.41 ml/g/min. Oxygen utilization (calculated from direct measurements of arterio-venous differences x MBF) varied from 0.014 to .213 ml O_2/g/min. Correlation between oxygen utilization measured directly, and utilization assessed externally was close (r = .83, n = 36 determinations). Thus, assessment of myocardial oxygen utilization can be accomplished with O-15-labeled oxygen, a method potentially applicable to patients with the use of positron emission tomography.

KINETICS OF CELLULAR UPTAKE OF (N-13)-AMMONIA,A MARKER USED IN MYOCARDIAL SCINTIGRAPHY. B.Rauch, M.Grunze,F.Helus,A.Wieland,E.Braunwell,W.Hassel= bach,and W.Kübler.Department of Cardiology, Uni= versity of Heidelberg,Federal Republic of Germany.

To study kinetics and principles of cellular up= take of (N-13)-ammonia (N-13),heart muscle cells of adult rats were isolated by perfusion with collagenase and hyaluronidase.Net uptake of N-13 was measured by flow dialysis.Extracellular con= centration of N-13 at the begin of the reaction was 100µM.N-13 was produced in the cyclotron by the O-16(p,∝)N-13 reaction.The following results could be obtained:1)In the presence of bicarbo= nate and carbon dioxide (medium I),a rapid initial extraction of N-13 with a rate constant k=0,125 $sec^{-1}$was measured (pH7,4;37°C).Total extraction of N-13 nitrogen (U),60 seconds after the reaction start,was 820±70µMol/l cell volume. 2)Replacing medium I by a buffer solution without bicarbonate and carbon dioxide (medium II),k was reduced to 0,01sec^{-1},whereas U was 35±5% of the control value.A similar reduction of N-13 uptake was ob= tained by preincubation of 50µM 4,4'diisothio2,2' stilbene disulfonic acid (DIDS),an inhibitor of anion exchange systems,in medium I. 3)Inhibition of glutamine synthetase by 100µg/ml l-methionine sulfoximine also significantly reduced cellular uptake of N-13 (k=0,02sec^{-1};U=40±7% of the control value). 4) No N-13 extraction was observed when cells, destroyed by calcium overload,were used in the experiment.The results indicate that,in addi= tion to metabolic trapping,N-13 uptake in myocytes may be controlled by an anion exchange system.

C-11 LIGAND BINDING TO ADRENERGIC AND MUSCARINIC RECEPTORS OF THE HUMAN HEART STUDIED IN VIVO BY PET. A. Syrota, D. Dormont, G. Berger, M. Mazière, C. Prenant, J. Sastre, J.M. Davy, M.C. Aumont, G. Motté and R. Gourgon. S.H.F.J. Commissariat à l'Energie Atomique, Département de Biologie Orsay and Services de Cardiologie, Hôpital Antoine Béclère, Clamart, Hôpital Beaujon, Clichy, France.

Beta adrenergic and muscarinic cholinergic receptors have been characterized in man using antagonists, respectively, C-11 Practolol (PRAC) and C-11 methyl quinuclidinyl benzilate (MQNB). C-11 PRAC was obtained by the reaction of C-11 acetone on N-deisopropyl-practolol. C-11 MQNB was obtained after methylation of QNB. About 20 mCi of C-11 PRAC and C-11 MQNB were intravenously injected in 4 and 18 patients respectively. A single axial transverse tomographic image of the heart was obtained 25 to 30 times as a function of time for 50-70 minutes. Twenty minutes following tracer injection, 0.2 mg/kg Propranolol or 3-20 µg/kg Atropine were i.v. injected as a bolus to study the competitive inhibition of binding. A small region-of-interest was automatically outlined on the septum. Concentration values were corrected for the loss in count recovery due to the small thickness of the septum and were expressed as % of the injected dose per cm^3. C-11 PRAC concentration in the septum was 16.61 ± 4.34 x 10^{-3} (m ± SD) and C-11 MQNB concentration was 19.48 ± 2.29 x 10^{-3}.
Kinetics of C-11 PRAC and C-11 MQNB were slightly different. However both ligands could be displaced from their binding sites after injection of unlabeled propranolol or atropine. These preliminary results are the first demonstration of the visualization of beta-adrenergic and cholinergic receptors in the human heart using PET. They suggest that these ligands could be used to monitor changes in kinetics as a function of disease.

MYOCARDIAL METABOLIC STUDIES IN PATIENTS WITH CARDIO-MYOPATHY (CM). R.Dudczak, R.Homan, A.Zanganeh, R.Schmoliner P.Angelberger, K.Kletter, H.Frischauf.
1st Med.Clin., Univ.Vienna, Austria

Recently we introduced a modified investigation procedure in studies with I-123 heptadecanoic acid (HDA) which improved data analysis. This report gives our findings in 15 pts with CM (CCM/HCM: congestive/9; hypertroph/6) and 9 controls. Patients were studied fasted in the LAO view. After iv HDA data were recorded for 70 min. Regional myocardial time activity curves were analyzed by a biexponential fit: elimination half times (T) of the initial and second phase, and the ratio of the relative size of each phase (C) were evaluated. Uptake (U) was estimated from the myocardium to background (V.cava) ratio. Repeated studies were done in 3 pts with CCM during dobutamine (D) infusion, and 60 min following 100g glucose (oG) orally. Blood glucose (BG), lactate (L), and C-peptid (CP) were monitored.

Compared to controls T was prolonged and C decreased ($p<0.01$). The reduction in U was more pronounced in CCM than in HCM ($p<0.05$). Regional myocardial findings were erratic in CCM, but not in HCM. Changes in T,C, and U following oG were dependent on BG and L, but also on the increment in CP. D-infusion enhanced in 2/3 T and increased C, whereas in 1 patient T increased.

Our findings show, that in CM alterations in HDA utilization relate not only to their T but also to their compartmentalisation. When interpretating influences of an glucose load on myocardial fatty acid utilization also the pancreatic ß cell response is of importance. Possibly sympathomimetic drugs may offer an estimate on the myocardial reserve for fatty acid utilization.

10:30–12:00 **Room 130**

NEUROLOGY II: CLINICAL PETT

Moderator: Abass Alavi, M.D.
Co-moderator: Martin Reivich, M.D.

PATTERNS OF LOCAL CEREBRAL GLUCOSE UTILIZATION IN DEPRESSION, MULTIPLE INFARCT DEMENTIA, AND ALZHEIMER'S DISEASE. D.E. Kuhl, E.J. Metter, W.H. Riege, R.A. Hawkins, J.C. Mazziotta, M.E. Phelps, A.S. Kling. UCLA School of Medicine, Los Angeles, CA.

The ^{18}F-fluorodeoxyglucose method with positron emission tomography (spatial resolution 12mm) was used to determine patterns of local cerebral glucose utilization ($LCMR_{glc}$) in 5 patients with unipolar depression (D), 6 patients with multiple infarct dementia (MID), 6 patients with Alzheimer's Disease (AD), and 5 age-matched normal controls. Ages ranged from 54 to 73 years. On the average, global CMR_{glc} was normal in D, was reduced 17% in MID and 33% in AD, and was lowest in the most severely demented patients. Patterns of $LCMR_{glc}$ differed among patient groups. The posterior part of the lower left frontal cortex (Brocas's area) was less metabolic than on the opposite side in all D patients (L/R = 0. 91 ± 0.08, mean ± SD), but in only one normal subject (L/R = 1.00 ± 0.05, mean ± SD). All MID

patients had CT evidence of small old infarcts and scattered metabolic defects in cortex, caudate, thalamus, white matter, and cerebellum. A total of 39 leasions were detected by combined CT and FDG scans. Lesions missed by FDG scan (5) were small lacunar infarcts and white matter lesions. Those missed by CT scan (24) were often large and the average $LCMR_{glc}$ decrease was 17%. In lesions detected by both CT and FDG scan, average $LCMR_{glc}$ decrease was 48%. In AD, the average decrease in zonal metabolism was 47% in parietal and external occipital cortex, 28% in frontal, temporal, and medial occipital cortex, and only 12% in caudate and thalamus. Values of the ratio of parietal cortex to caudate-thalamus CMR_{glc} clearly separated AD patients (0.44 ± 0.13, mean ± SD) from normal, D, and MID subjects (0.74 ± 0.04,0.70 ± 0.13, 0.79 ± 0.09, respectively).
The findings support the premise that cerebral metabolic patterns can be distinctive among normal, depressed, and demented persons.

LOCAL CEREBRAL GLUCOSE UTILIZATION IN PARKINSON'S DISEASE Kuhl, D.E., Metter, E.J., Riege, W.H., Phelps, M.E., Winter, J. UCLA School of Medicine, Los Angeles, CA.

^{18}F-fluorodeoxyglucose (FDG) scans were performed on 9 patients who had Parkinson's disease (PD) in order to learn if there were characteristic alterations of local cerebral glucose utilization ($LCMR_{glc}$). All patients were studied when they were receiving levodopa medication. In addition, 2 patients were also studied when they were receiving no medications. Results were compared with those from an age-matched normal control group (N = 14). The average global CMR_{glc} for PD patients was 19.6 ± 4.4 mol $100g^{-1}min^{-1}$ and for controls was 25.1 ± 5.0 mol $100\ g^{-1}min^{-1}$ (mean ± SD). Except for a single patient, PD values for relative distribution of $LCMR_{glc}$ could not be distinguished from age-matched control values. None of the metabolic measures correlated with disease stage, duration, severity, dementia, tremor, or dystonia. The FDG scan did not differ in the levodopa medicated and unmedicated states. These results obtained in human PD patients agree with those obtained by others who have studied the rat model of hemiparkinsonism using ^{14}C-DG autoradiography. They support the conclusion that alterations of the nigrostriatal pathway in Parkinson's disease have no major selective effect on regional cerebral metabolism. Our results do not reinforce the postulate that dementia of PD may be explained by the simultaneous presence of Alzheimer's disease. We did not find in these demented parkinsonian patients the marked reductions in overall glucose utilization, especially in parietal cortex, which are typical of the demented patient with Alzheimer's disease.

LOCAL CEREBRAL GLUCOSE METABOLISM IN PATIENTS WITH AFFECTIVE PSYCHIATRIC DISORDERS: DRUG-FREE STATES AND EFFECTS OF METHYLPHENIDATE. M.E. Phelps, J.C. Mazziotta, R. Gerner, L. Baxter, D. Kuhl. UCLA School of Medicine, Los Angeles, CA

Unipolar (depressed, N=8) and bipolar (manic-depressed, N=7) patients were studied with F-18 fluorodeoxyglucose and positron CT to determine local cerebral glucose metabolism (LCMRGlc) in drug-free states and acute drug trials of methylphenidate (N=4). Patients were clinically evaluated (Beck Depression Inventory, Brief Psychiatric Rating Scale) before and after each study. Results demonstrate reduced global LCMRGlc in both depressed and manic patients (-42%) compared to controls (N=6). Depressed patients had reduced LCMRGlc when measured as a % of hemispheric mean LCMRGlc for frontal (8%, normals=24%), inferior parietal (9%, normals=15%) and superior temporal (17%, normals=30%) cortex. While normal subjects had left-right metabolic symmetry (L/R=1.01 ± 0.03) for all cortical zones, depressed patients had left < right asymmetries (7%) of frontal, inferior parietal and superior temporal cortex. Manic patients had frontal symmetry but left < right inferior parietal asymmetries. Treatment of depressed patients with methylphenidate results in exaggeration of asymmetries with clinical worsening, amelioration of asymmetries with clinical improvement and no changes in LCMRGlc with no changes in symptoms. Depressed patients with spontaneous recovery also returned to normal symmetric LCMRGlc distribution. Increase in cingulate to frontal cortical LCMRGlc correlated with drug-induced improvement. These data indicate that affective disorder patients have metabolically distinct subgroups and that spontaneous recovery and drug effects can be monitored with positron CT.

LOCAL CEREBRAL GLUCOSE CONSUMPTION DURING COGNITIVE ACTIVITY. M. Reivich, R.C. Gur, A. Alavi, J. Greenberg, A.D. Rosen, A. Wolf. University of Pennsylvania, Philadelphia, PA and Brookhaven National Laboratories, Upton, New York.

The effects of cognitive tasks on local cerebral glucose metabolism (LCMRgl) were studied in 8 young right-handed males. Stimuli were either verbal analogies taken from Miller Analogies Test or a spatial stimulus adopted from Benton's Line-Orientation Test. LCMRgl was calculated for 7 cortical regions: frontal pole (FP), inferior frontal (IF), frontal eye fields (FEF), inferior temporal (IT), superior temporal (ST), auditory (AUD), inferior parietal (IP) and visual association (VA). ST, IP and FEF were chosen because of evidence suggesting their activation during verbal and spatial tasks. The other regions were selected as control regions. Analysis of variance revealed a significantly higher right-hemispheric metabolism across groups ($F(1,6)=23.25$, $p<.01$). This may be due to predominence of right hemispheric involvement in attentional processes. There was also a significant effect of the two tasks on hemispheric metabolism ($F(1,6)=24.75$, $p=.0025$). The regions also differed significantly in their metabolism ($F(7,42)=12.97$, $p<.0001$) and there was a significant laterality of metabolic activity as a function of brain region ($F(7,42)=3.84$, $p<.005$). The two groups differed in laterality of metabolism in regions ST ($p<.05$, 1-tailed), IP ($p<.001$, 1-tailed) and FEF ($p<.025$, 1-tailed) with greater right hemispheric metabolism during the spatial and greater left hemispheric metabolism during the verbal task. The differences between the two groups were not significant in any of the control regions. These results provide an experimental confirmation of hypotheses based upon clinical observations.

EVALUATION OF CEREBRAL GLUCOSE METABOLISM IN PATIENTS WITH AMYOTROPHIC LATERAL SCLEROSIS (ALS) BY [F-18]-FLUORODEOXY-GLUCOSE (FDG) AND POSITRON EMISSION TOMOGRAPHY (PET). L. Mansi, M.C Dalakas, G. Di Chiro, J.L. Sever, N. Patronas, D. Bairamian, R.A. Brooks, and A. Eric Jones.
National Institutes of Health, Bethesda, MD.

Regional cerebral glucose metabolic rates (rCMR-Glc) of five patients with ALS were measured by FDG-PET scanning.At the time of the study the patients were bed-ridden with quadriparesis and bulbar involvement. Five normal subjects were used as controls with measurement of rCMR-Glc in corresponding areas of the cortex.

All five ALS patients exhibited a localized region of low glucose metabolism in the motor-sensory areas of the lateral cortex that was unilateral in four cases and bilateral in one. The degree of deficit was 19-32% as compared with the contalateral or, in the bilateral case, surrounding cortex. On the contrary, in all five normal subjects there was no significant localized deficit on either side (<15%). In 3 of the 4 unilateral ALS cases there was clinical correspondence with the side of primary involvement.

The relatively large areas of cortical suppression in the ALS patients, with inclusion of sensory areas in addition to the motor cortex, may appear unexpected. This finding, however, is in agreement with recent autoradiographic obsevations in monkeys, which showed a marked increment in glucose utilization in cerebral tissues concerned with sensory monitoring during motor activity. Finally, considering the profound degree of motor weakness in these patients,the relatively modest disturbance of cortical metabolism is of some note. An explanation is that weakness in ALS is the combined result of upper and lower motor neuron pathology.

CEREBRAL GLUCOSE UTILIZATION PATTERNS IN WILSON'S DISEASE. R.A. Hawkins, M.E. Phelps, J.C. Mazziotta, D.E. Kuhl, UCLA School of Medicine, Los Angeles, CA.

Wilson's disease is a disorder characterized by excessive copper deposition and low levels of serum ceruloplasmin. We studied 4 subjects with Wilson's disease (3 with significant neurologic symptoms and one with minimal CNS involvement with the "hepatic" form) with F-18

fluorodeoxyglucose (FDG). All subjects (ages 20-35) were injected with 10 mCi FDG and were scanned with a NeuroECAT positron tomograph. We calculated the rates of local cerebral glucose metabolism (LCMRglc) in mg/100gm/min in selected structures of the brain and compared these values to an age matched control group of four neurologically normal volunteers. (See table)

Region	Wilson's 1 (Hepatic form)	Wilson's 2-4 (CNS symptoms)	Control
Global	3.78(0.29)	2.78(0.97)	5.44(1.16)
Cort.Gray	4.60(0.64)	3.44(1.29)	7.21(1.56)
Sub Cort.Gray	4.80(0.12)	3.04(0.72)	5.80(1.53)
Caudate	4.70(0.16)	3.06(0.79)	6.39(1.20)
Lentiform Nuc	4.84(0 10)	2.96(0.75)	6.64(1.51)
Thalamus	4.88(0.04)	3.09(0.75)	4.37(0.67)
White	2.43(0.34)	1.78(0.56)	3.94(1.12)

All of the values for Wilson's 2-4 are significantly less than both controls ($p<0.02$) and Wilson's 1 ($p<0.05$) while all values for Wilson's 1 are significantly less than controls ($p<0.05$) with the exception of the thalamus, which is comparable in both Wilson's 1 and controls. These results suggest that all regions of the brain are significantly affected in the "CNS" form of Wilson's disease and that even with minimal CNS symptoms ("hepatic" form) there is significant hypometabolism in most regions of the brain.

10:30-12:00 **Room 120**

PEDIATRIC I

Moderator: Massoud Majd, M.D.
Co-moderator: H. Theodore Harcke, Jr., M.D.

THE ASSESSMENT OF REGIONAL CEREBRAL BLOOD FLOW IN THE NEWBORN WITH POSITRON EMISSION TOMOGRAPHY. P. Herscovitch, J.M. Perlman, J.J. Volpe, and M.E. Raichle. Washington University School of Medicine, St. Louis, MO.

The pathogenesis and nature of the brain injury in the newborn with major intraventricular hemorrhage (IVH) and intraparenchymal hematoma (IPH) is obscure. To study this critical issue, we are using positron emission tomography to determine regional cerebral blood flow (rCBF) in premature infants with IVH-IPH. To date, seven studies have been performed in six infants (birth weights 920-1200 g). All exhibited severe IVH as well as unilateral IPH delineated by ultrasound scans. Flow studies were performed 5 to 17 days after birth. Scans were obtained with the PETT VI tomograph following the bolus intravenous injection of O-15 water. An autoradiographic approach was used to obtain regional flow information (Raichle et al, J Cereb Blood Flow Metab 1:S19, 1981). In the hemispheres containing the IPH, there was a decrease in flow which was much more widespread than the anatomical extent of the localized hematoma, involving both gray and white matter. A follow-up study of one infant, three months later, showed a persistence of decreased hemispheric flow. In the three autopsies obtained, the involved hemisphere showed extensive infarction, in accord with the rCBF findings. These observations represent the first use of PET to define rCBF in the human newborn. They demonstrate extensive impairment in flow in a hemisphere containing a restricted IPH. The hematoma may be secondary to this ischemic process, or may be the cause of a more generalized flow disturbance. PET clearly holds great promise in the study of these problems.

THE SCINTIGRAPHIC EVALUATION OF LACRIMAL DRAINAGE IN CHILDREN. S. Heyman, M.D., B. Smoger, M.D., J. Katowitz, M.D., Children's Hospital of Philadelphia, Philadelphia, Pa.

Children presenting with epiphora may be evaluated by the dye disappearance test, the meniscus level, irrigation and probing, and dacryocystography. Dacryoscintigraphy (DS) has been found to be a useful, noninvasive adjunctive study. Twenty patients aged 22 months to 20 years have been studied. Patients are premedicated with potassium perchlorate, 6 mg/Kg given orally. Four infants required sedation with chloral hydrate. Sequential analogue images are obtained every minute for 20 minutes with computer acquisition at 4 frames/minute, following the instillation of 100 uCi technetium 99m pertechnetate in 10 ul into each eye. With normal transit activity is seen in the nasolacrimal sac by 1 minute, and there is flow down the duct by 2 - 3 minutes.

Of 40 eyes studied there was agreement with other tests in 35 cases, 21 being abnormal and 14 normal. The dacryoscintigram determined the extent of further surgery in 3 patients, while surgery in 1 infant was cancelled. Drainage following trauma in 1 case was normal, though the nasolacrimal duct was tortuous.

DS has successfully delineated the level of anatomical blockage. When drainage is prolonged, maneuvres such as forceful blinking, massaging over the sac, or deep nasal inspiration have distinguished an anatomical block from a physiological delay in drainage.

DS in children has been found to be useful, highly physiological and easy to perform. It is less invase than probing and dacryocystography, and does not require a general anesthetic. The radiation dose to the lense is about 4 mrads, less than the 370 mrads from a radiograph of the skull or 3 rads from dacrycystography.

PARTIAL URETEROPELVIC JUNCTION OBSTRUCTION: COMPARISON OF PERCUTANEOUS ANTEGRADE PYELOGRAPHY AND DIURETIC RENAL SCINTIGRAPHY. M.J. Gelfand, R.B. Towbin, J.L. Strife, J. Wacksman, Radioisotope Laboratory and Division of Pediatric Radiology, Department of Radiology, and Division of Urology Univ. of Cincinnati and Children's Hospital, Cincinnati, OH.

Percutaneous antegrade pyelography with antegrade perfusion (PAP) and diuretic renal scintigraphy (DR) were used to assess the severity of ureteropelvic junction obstruction in 9 kidneys. All 9 children were unoperated and had normal renal function. PAP was performed using increasing perfusion rates from 2 to 10 cc/min. Moderate high flow rate partial obstruction was present if opening pressure in the renal pelvis (P) was less than 15 cm H2O and rose more than 5 cm H2O only at perfusion rates greater than 4-5 cc/min. Patients with more severe abnormalities were considered to have high-grade partial obstruction. DR was performed using Tc-99m-DTPA followed by 0.3-0.5 mg/kg of intravenous furosemide. DR was called normal if $t_{\frac{1}{2}}$ of the washout of activity after diuretic was <10 min; probably normal if $t_{\frac{1}{2}}$=11-15 min; borderline if $t_{\frac{1}{2}}$=16-20 min; and abnormal if $t_{\frac{1}{2}}$>20 min.

One child was normal by PAP; DR $t_{\frac{1}{2}}$ was in the probably normal range. Of 4 children with high flow rate partial obstruction by PAP, one had normal DR, 2 had probably normal DR and one had borderline DR. Of 4 children with high-grade partial obstruction by PAP, 3 were abnormal by DR and one was probably normal by DR.

DR does not appear to identify children with moderate high flow rate partial obstruction, who have abnormal P only at very high urine flow rates. At a mean age of 7.5 yr, these children continue to have normal renal function; it is not known if they are at risk for future loss of renal function.

THE EFFICACY OF Tc-99m DTPA AND Tc-99m DMSA RENOGRAPHY IN THE SCREENING OF PEDIATRIC PATIENTS FOR RENAL ETIOLOGIES OF HYPERTENSION. P.R. Rosen, Wilford Hall USAF Medical Center, Lackland AFB, TX; S. Treves, Children's Hospital and Medical Center, Boston, MA.

Eighty-one Tc-99m DTPA and DMSA renal studies (RS) of 80 patients being evaluated for hypertension were reviewed. Patients were 5 days to 19 years of age. The etiology of the hypertension was established on the basis of additional diagnostic procedures and clinic course. RS were interpreted in the absence of clinical information. Both DTPA and DMSA studies were recorded digitally. Differential flow, transit time and concentration were quantitatively analyzed, and considered abnormal, if either DTPA perfusion transit, or DMSA morphology/distribution was asymmetric. 12/13 DMSA studies and 6/13 DTPA studies were abnormal in the patients with renal pathology. 3/13 neonates were positive for renal thromboembolic events. 5/48 adolescents (greater than 12 years) were positive (3 chronic pyelonephritis). All patients (4) with renovascular abnormalities were between 2-8 years of age.

	Renal Abnormality	No Renal Abnormality
DTPA+	6	1
DTPA-	7	67
DMSA+	12	2
DMSA-	1	66

DTPA Sens. = 6/13 = 46%
DTPA Spec. =67/68 = 98%
Accuracy = 73/81 = 90%
DMSA Sens. =12/13 = 92%
DMSA Spec. =66/68 = 97%
Accuracy = 78/81 = 96%

We conclude that RS are specific and sensitive in detecting renal etiologies of hypertension. DMSA is clearly superior to DTPA in detecting renal abnormalities. Renal evaluation is least productive in the adolescent hypertensive (5/48). The highest yield occurs in the neonate with a history of umbilical artery catheterization (3/8).

EFFECT OF CAPTOPRIL ON EFFICACY OF RENAL SCINTIGRAPHY IN DETECTION OF RENAL ARTERY STENOSIS. M. Majd, B.M. Potter, P.C. Guzzetta, and E.J. Ruley. Children's Hospital National Medical Center, Washington, DC.

Captopril is an angiotensin converting enzyme inhibitor which is especially effective in the treatment of renin mediated hypertension. Three hypertensive boys, ages 3, 10, and 11, with angiographically demonstrated severe renal artery stenosis were treated with captopril during the interval between diagnosis and angioplasty. Renal scans were performed as part of their original hypertensive work-up and again immediately before angioplasty. Following normalization of blood pressure by captopril, marked diminution of renal function occurred on the affected side. This was reversible following revascularization.

A fourth boy, age 2, was persistently hypertensive following repair of aortic coarctation. On captopril therapy, unilateral decrease in renal function was observed by renal scan prospectively suggesting renal artery stenosis. This was proved subsequently by angiography.

Unilateral renal functional impairment in hypertensive patients on captopril is suggestive of renal artery stenosis and is an indication for angiography. Because captopril impairs renal function in patients with renal artery stenosis, pretreatment may increase the efficacy of renal scanning for detecting these patients.

THE ACCURACY OF THE INDIRECT (INTRAVENOUS) RADIONUCLIDE CYSTOGRAM IN CHILDREN. M. Majd, E.J. Kass, and A.B. Belman. Children's Hospital National Medical Center, Washington, DC

One hundred twenty children with documented vesicoureteral reflux underwent both direct (retrograde) and indirect (intravenous) radionuclide cystography in order to determine the efficacy of indirect method to detect known vesicoureteral reflux. The interval between direct and indirect cystograms was less than 2 weeks in 80 patients and longer in 40 patients. The direct cystograms showed reflux in 100 patients (44 bilateral and 56 unilateral). In the remaining 20 patients, no reflux was demonstrated. The indirect cystograms failed to demonstrate the presence of reflux in 51% of the kidneys with Grade I to III reflux and in 12% of the kidneys with Grades IV and V reflux. In 13 patients (with 20 refluxing units), the indirect cystograms were suboptimal due to inability of the patients to void on command or inadequate drainage of the tracer from the urinary tracts. None of the 20 patients who had a negative direct cystogram showed reflux on the indirect study.

Indirect radionuclide cystography is not as reliable as direct cystography in detecting vesicoureteral reflux and should be considered accurate only if a positive study is obtained.

10:30-12:00 **Room 276**

RADIOPHARMACEUTICAL CHEMISTRY II: GENERAL

Moderator: Alun G. Jones, Ph.D.
Co-moderator: Gopal Subramanian, Ph.D.

Introduction. Alun G. Jones, Ph.D., Harvard Medical School, Boston, MA.

PREPARATIVE CONTROL, HPLC ANALYSIS, AND IN VIVO EVALUATION OF COMPONENTS OF A TECHNETIUM-MDP RADIOPHARMACEUTICAL MIXTURE. K. Libson, E. Deutsch, W. R. Heineman, S. Tanabe and J. P. Zodda, Departments of Chemistry and Radiology, University of Cincinnati, Cincinnati, OH.

This study was undertaken in order to better understand and control the complicated chemistry and biological properties of Tc-99m diphosphonate (DiP) bone imaging agents.

High performance liquid chromatographic (HPLC) analysis has shown that Tc-99m-DiP skeletal imaging agents are not single chemical entities, but rather are complex mixtures of several components which can exhibit distinct biological distributions (Pinkerton, et al., IJARI 33: 907 (1982)). To determine if the generation of individual Tc-99m-DiP components can be controlled, 99m-Tc($NaBH_4$)-MDP mixtures were prepared as a function of pH, presence or absence of Tc-99 carrier, and presence or absence of air. These mixtures were then analyzed by anion exchange HPLC to determine the resulting distribution of products. The formulation pH proved to be most effective in controlling the generation of specific components, and thus allowing preparation of specific components in quantities suitable for biological evaluation. Several HPLC isolated components were evaluated as skeletal imaging agents in rats, and thus shown to exhibit markedly different bone uptakes and soft tissue localizations.

In sum, the distribution of component complexes in 99m-Tc-($NaBH_4$)-MDP mixtures can be controlled, and the yield of selected components maximized, by variation of the formulation conditions. Since the biodistributions of the individual 99m-Tc-MDP components are significantly different, control of formulation conditions thus allows control of the ultimate biodistribution of the entire radiopharmaceutical mixture.

THE ALPHA HELIX AND PROTEIN BINDING OF Tc-99m. D. Lanteigne and D. J. Hnatowich, University of Massachusetts Medical School, Worcester, MA.

The avidity with which reduced Tc-99m binds to protein is such that even DTPA, a strong chelator, often cannot compete at reasonable concentrations. It has been shown that mercuric ion can interfere with this binding to suggest that the sulfhydryl groups on proteins may participate.[1] However, we have found that myoglobin, a protein without sulfhydryl groups, and albumin in which the sulfhydryl groups have been blocked with Ellman's reagent, both bind reduced Tc-99m despite the presence of DTPA. This avidity of Tc-99m for proteins suggested to us that the alpha-helical structure of proteins may be an important binding site. This possibility was investigated by determining the binding of Tc-99m to poly-L-glutamic acid and poly-L-lysine. The former polypeptide undergoes a conformational change from the alpha helix at pH 5 to the random conformation at pH 7, whereas the latter polypeptide changes from the random conformation at pH 9 to the alpha helix at pH 11. Reduced Tc-99m was found to bind to both these polypeptides only in their alpha-helical form. We have also found that the degree of Tc-99m binding to poly lysine in its alpha-helical form is decreased in the presence of mercuric ions. These results suggest that the alpha helix plays an important role in the binding of Tc-99m to proteins and that certain metal ions may compete for these sites.

1. J. Steigman et al. "The Importance of the Protein Sulfhydryl Group in HSA Labeling with Technetium-99m." J. Nucl. Med. 16 (1975) 573, Abstract.

SYNTHESIS AND BIODISTRIBUTION OF NEUTRAL LIPID-SOLUBLE TC-99M COMPLEXES WHICH CROSS THE BLOOD-BRAIN BARRIER HF Kung, M Molnar, J Billings and M Blau, SUNY at Buffalo and V.A. Medical Center, Buffalo, New York.

We have previously reported a pH-shift brain imaging agent, I-123 HIPDM, which has a fixed brain distribution pattern reflecting regional perfusion. The first requirement of a Tc-99m complex having similar properties is the ability to cross the blood brain barrier.

A series of Tc-99m labeled neutral chelates was prepared and evaluated. A ten member ring N_2S_2 heterocycle (1,2-dithia-5,8-diazacyclodecane) was chosen as the backbone of the ligand system for chelating reduced Tc. The ligands were synthesized by condensing 2,2'-dithio-

bis-ethanal with 1,2-ethanediamine and reducing the imine adduct with sodium borohydride. Labeling of the ligands was achieved by reducing Tc-99m pertechnetate with Sn(II) or sodium borohydride. The lipid-soluble Tc-99m complexes were extracted with hexane and were >95% pure (HPLC). Electrophoresis studies indicated that the Tc-99m compounds were neutral. Biodistribution in rats showed a significant brain uptake (1-3%/whole brain) at 2 minutes (i.v.). At 15 min the brain uptake dropped to about a tenth of the original level indicating free passage in both directions across the BBB. Autoradiography of frozen brain sections at 2 min after injection showed the typical regional perfusion pattern (high in gray and low in white matter). As expected, at 15 min the regional distribution of the radioactivity became homogeneous.

This group of Tc-99m compounds clearly exhibited in vivo stability and the ability to cross the BBB after an i.v. injection. Derivatives containing pH-shift tertiary amine groups might have prolonged brain retention and should be suitable for SPECT brain perfusion studies.

Tc-99m-GALACTOSYL-NEOGLYCOALBUMIN (Tc-NGA): IN VITRO AND IN VIVO RECEPTOR PROPERTIES. K.A. Krohn, D.R. Vera, R.C. Stadalnik, and P.O. Scheibe. University of California, Davis Medical Center, Sacramento, CA; ADAC Laboratories, Sunnyvale, CA.

Tc-99m-galactosyl-neoglycoalbumin (Tc-NGA), a synthetic ligand to hepatic binding protein (HBP), exhibits receptor binding properties of high tissue specificity, and affinity and dose dependent-uptake.

In vitro binding of NGA was similar to native HBP ligands. When bound to hepatic membranes the radioligand could be displaced by galactose, N-acetylgalactosamine, or unlabeled ligand, but not by D-glucose; thus, exhibiting similar substrate specificity as native HBP ligands (asialoglycoproteins). Monophasic Scatchard plots indicated low nonspecific binding. The forward binding rate constant (k_b), calulated using in vitro equilibrium constants and binding displacement rates, depended upon the number of galactose units attached to each albumin. Varying the molar ratio of galactose to HSA from 5 to 44 caused k_b to range from $0.3x10^{-3}$ to $2.7x10^{-3}$ $M^{-1}sec^{-1}$.

In vivo binding of NGA followed the known molecular bio-logy of HBP ligands. The liver was the only site of NGA uptake (>80%ID). The lack of hepatic uptake in chickens corresponded the known diminished HBP concentration in avian species. In mammals the maximum and peak-times for hepatic uptake curves depended upon the carbohydrate density and injected amount of NGA. This indicates an in vivo sensi-tivity to receptor affinity and concentration. Because HBP is not involed in hepatic detoxification, NGA uptake is not sensitive to serum bilirubin; coinjection of Tc-NGA and ICG, a bilirubin analog, at a molar ratio of 1:100 did not alter hepatic time-activity curves or ICG clearance in pigs.

BONE UPTAKE OF CHEMICALLY DIVERSE LIGANDS LABELED WITH TIN-117m IN 2+ AND 4+ OXIDATION STATES. S.C. Srivastava, P. Richards, G.E. Meinken, P. Som, Z.H. Oster, F.F. Knapp, Jr., and T.A. Butler. Medical Department, Brookhaven National Laboratory, Upton, NY; Oak Ridge National Laboratory, Oak Ridge, TN.

Tin is an essential ingredient of Tc-99m radiopharmaceuticals but its in-vivo fate is not well understood. Tin-117m ($t_{½}$ 14 d; γ 159 keV, 87%) is an ideal tracer for the study of biological behavior of tin compounds as well as for developing clinically useful radiopharmaceuticals. This work describes the preparation and in-vivo distribution in mice of: Sn(2+)chloride, pH 2 and 7 (A,B); Sn(4+)chloride, pH 2 (C); and Sn(2+ and 4+)-labeled MDP (D,E), DTPA (F,G), EHDP (H,I), and PYP (J,K). High and unexpected bone uptake of Sn-DTPA and of all above compounds (except B and C) indicates a high specific affinity of tin for bone despite the chemically diverse ligands. The various compounds however, show significant differences in blood clearance, excretion, and soft tissue uptake. Differences among Sn(2+) and Sn (4+) compounds with the same ligand are particularly noteworthy, e.g., higher uptake of Sn(4+) compounds in bone and of Sn(2+) compounds in RBC. The localization of E and G is almost exclusively in bone (bone to blood and bone to muscle ratios: 1135, 460 (D) and 1903, 863 (G), at 24 hr). B and C show high liver uptake, as expected. It appears that binding of these compounds to bone is through the tin ion and their in-vivo distribution depends upon factors such as charge, oxidation state of tin, and kinetic and thermodynamic stabilities of the complexes. Because of the favorable half-life and decay characteristics of tin-117m, Sn(4+)-labeled DTPA and MDP may be potentially useful for diagnosis and therapy of bone tumors and other bone disorders.

IODINE-123 YIELDS FROM 800-MeV PROTON IRRADIATION OF CsCl TARGET. J. W. Barnes, M. A. Ott, P. M. Wanek, G. E. Bentley, K. E. Thomas, F. J. Steinkruger, and H. A. O'Brien, Jr. Los Alamos National Laboratory, Los Alamos, NM.

A study designed to determine the optimum parameters for batch production of I-123 using the 800-MeV proton beam at LAMPF is in progress. The technique employed is to form 2.1-hr Xe-123 in a CsCl target, isolate the radioxenon rapidly after the end-of-bombardment (EOB), allow Xe-123 to decay to I-123, transfer remaining xenon from the growth chamber, and recover I-123. The major interference arises from the simultaneous production of 16.8-hr Xe-125, which decays to 60-d I-125. To maximize the I-123 yield but minimize the I-125 contamination, the appropriate combination of irradiation and growth periods is being determined.

In previous experiments with 11 CsCl targets irradiated in small cylinders for 2- and 4-hr periods, the average I-123 yield was observed to increase by 23% by increasing the growth periods from 2 to 4 hours. An increase in the irradiation time from 2 hr to 4 hr results in a 55% increase in the I-123 yield. A larger target was constructed to increase the amount of CsCl in beam by a factor of 5. A 2-hr irradiation of this target followed by a 4-hr growth period yielded about 600 mCi of I-123 with an I-125 content of 0.4%.

A study of radioiodine oxidation states in the recovered solution demonstrated two iodine species and two unidentified species. In all cases, more than 90% of the observed species was I^-. Anion chromatography is being studied to allow separation of the I^- from all of the species, both radioactive and stable.

10:30-12:00 **Room 275**

INSTRUMENTATION II: NEW SYSTEMS AND DEVICES

Moderator: James C. Ehrhardt, Ph.D.
Co-moderator: Ronald R. Price, Ph.D.

New Instrumentation for Dynamic and Quantitative Imaging. Thomas F. Budinger, M.D., Ph.D., University of California, Berkeley, CA

MULTIWIRE PROPORTIONAL COUNTER GAMMA CAMERA AND TANTALUM-178 RADIONUCLIDE--NEW IMAGING TECHNOLOGY. J.L. Lacy, A.D. LeBlanc, J.W. Babich, M.W. Bungo, P.C. Johnson. Johnson Space Center, Baylor College of Medicine, Methodist Hospital, Houston, TX

A pressurized Xenon multiwire proportional counter (MWPC) specifically designed for nuclear medicine applications has been developed. The device employs a high speed readout system which provides very high count rates (>800,000 cps), excellent image resolution (2.5mm FWHM), and distortion free performance at the highest rates. The device is a light weight compact unit which is well suited to portable operation. It has a high sensitivity for x-ray energies up to 80 KeV. It can be employed effectively with Xe-133 and Tl-201 radionuclides. A newly developed radionuclide, Ta-178, is an excellent imaging agent for use with the camera having both optimal energy (60 KeV) and a short half life (9.3 min). High quality first pass cardiac studies employing 20 mCi Ta-178 have been performed in five volunteer subjects. Studies have been analyzed to obtain right and left heart images, ventricular wall location determinations, ejection fraction values, and region of interest histograms. These results demonstrate the feasibility of performing first pass studies with higher spatial resolution and image statistics and with far less radiation exposure than is currently possible employing Tc-99m and current imaging technology.

HIGH ACTIVITY Kr-81m GENERATOR-DELIVERY SYSTEM FOR DYNAMIC PULMONARY CINESCINTIGRAMS. G. Gergans, E. Kaplan, A. Friedman, S. Pinsky. Hines VA Hospital, Hines, IL.

In order to produce a dynamic scan of the pulmonary respiratory cycle, a high activity Kr-81m generator delivery system has been developed. Previous systems suffered from decay of radioactivity prior to entry into the respiratory system. One major loss was because of slow gaseous elution from the generator with subsequent decay of the 13 second half-life isotope. The second main loss of activity was due to not collecting Kr-81m during patient exhalation, accounting for an approximately 50% loss of radioactive gas. To overcome these difficulties, a system was designed consisting of loosely packed Dowex 200-400 ion exchange resin containing 30 mCi of Rb-81. Humidified compressed air eluted the Kr-81m gas at 3 liters per minute and was transferred to an inflatable reservoir. The subject breathed from this reservoir through a low dead space valve. With this technique, over 3 million counts were obtained in 5 minutes. Thus, 16 frames of a dynamic ventilation study, each statistically significant, were obtained and replayed in the cine mode demonstrating dynamic regional ventilation.

DEVELOPMENT OF SMALL γ-RAY IMAGING PROBES FOR IN-VIVO USE. H.B. Barber, H.H. Barrett, W.J. Wild and J.M. Woolfenden. University of Arizona Health Sciences Center, Tucson, AZ.

A common problem in Nuclear Medicine is to detect small tumors marked with radiotracers using large external imaging systems. An alternative is to use small radiation detectors as in-vivo probes to locate such radiolabeled tumors at endoscopy or during surgery. A recurrent problem with such probes is the inability of uncollimated detectors to discriminate between distant tumors and small variations in tissue background activity. Simple forms of collimation such as pinholes or single slits are possible with probes but angular scanning greatly lengthens the procedure. To solve this problem we have constructed a prototype γ-ray imaging system just 2.08 cm in diameter and 1.34 cm long. Interchangeable cylindrical coded apertures with uniformly redundant binary codes of 15 or 31 elements are used with an axial fiberoptic-coupled NaI(Tl) detector. Axial resolution is provided by parallel slat collimators with the detector. A time-coded image is formed by monitoring the detector during rotation of the coded aperture followed by axial translation. Image reconstruction is done on a digital computer using correlation decoding with a bipolar form of the original aperture function. Bench tests of both apertures using 122 KeV γ-ray sources show that azimuthal angular resolution is nearly optimum corresponding to the angle subtended by one aperture element at the detector. Clear images of complex extended sources have been obtained. Water phantom tests verify that this imaging system has a considerable advantage in sensitivity over alternative single slit designs. A miniature imaging system of this type can be used in sites such as the gastrointestinal tract, with the potential for detecting and imaging small tumors deep within the body.

A MODULAR IMAGING SYSTEM FOR USE IN NUCLEAR MEDICINE. T.D. Milster, L.A. Selberg, R.L. Easton, H.H. Barrett, G.R. Rossi. University of Arizona, Tucson, AZ.

The performance of imaging systems currently used in nuclear medicine is limited by low count rates, coarse spatial resolution and poor photon utilization. State-of-the-art Anger Cameras have one large scintillation crystal 10-18" in diameter and typically 37 PMT's. Signals from all 37 PMT's must be processed simultaneously to provide position information from one incident gamma photon. By using a modular design, the detector area can be divided into 4" square modules that act as independent units. Parallel processing of module signals increases the count rate. Prototype geometries consist of PMT's and a scintillation crystal coupled by a light guide. Finer spatial resolution is achieved by using shadow casting optics in the light guide of each module to encode the positional information on the PMT's. High-reflection coatings on the light guide enable improved energy resolution. Current goals for the modular camera are a spatial resolution of < 3.0 mm, dead time < 2 μsec and energy resolution < 10% at 140 keV. Prototypes include the two-dimensional camera mentioned above and a one-dimensional camera capable of giving positional information along one detector axis only. Applicatcns for the 1-D camera include coded-aperture imaging, ECT and whole body scanners. Using analog electronics, resolutions of 4 mm for the 1-D camera and 5 mm for the 2-D camera have been measured. Energy resolution was typically 11-15%. An all-digital system has also been developed that utilizes a lookup table which isomorphically maps PMT responses to scintillation position in each module. The digital electronics provide complete pulse processing, including dead time, in 3 μsec.

COMPARATIVE TOMOGRAPHIC IMAGING PERFORMANCE OF A HYBRID CODED-APERTURE/PARALLEL-PLATE STATIONARY COLLIMATOR AND A ROTATING CAMERA. D.R. Neumann, M.J. Flynn, S. Gottschalk, S.N. Wiener. The Mt. Sinai Medical Center, Cleveland, OH; The University of Michigan, Ann Arbor, MI; and Technicare Corporation, Solon, OH.

A stationary collimator has been built which provides fine angular and spatial sampling for tomographic myocardial imaging. It uses parallel plates to collimate in the X direction and a pseudorandom sequence of slits to collimate in the Y direction. The noise and resolution characteristics of parallel ray views have been previously reported (JNM 23: P59, 1982). Its performance for myocardial tomographic imaging has now been measured and compared against rotating camera tomograms. Measurements were performed with a phantom consisting of two concentric cylinders 6.5 and 8.0 cm in diameter. The outer ring contained a region subtending 36 degrees to emulate a myocardial wall with a defect. With water in all the chambers and 600 microcuries of Tc-99m in the larger outer chamber, the phantom was put in the cardiac region of an Alderson human thorax phantom. Reconstruction with a fast backprojection algorithm using attenuation correction was performed from a 24 minute rotating camera study. Reconstruction with a SIRT algorithm without attenuation correction was performed from two 12 minute stationary collimator studies encompassing a total of 120 degrees of sampling. A plane thickness of 4 mm was the same for both techniques. Relative image noise in the region of the phantom wall (SD/mean), the wall thickness at the 50% level, and the ratio of mean defect intensity to mean wall intensity was .174, 18 mm, and .02% for the stationary collimator tomograms and .059,18mm and 7% for the rotating camera tomograms. The stationary collimator appears to have potential clinical use for tomographic myocardial imaging.

10:30-12:00 **Room 270**

VETERINARY NUCLEAR MEDICINE

Moderator: Dan Hightower, D.V.M.
Co-moderator: Francis A. Kallfelz, Ph.D.

Scintigraphic Anatomy in Animals - Pitfalls for the Unwary. Dan Hightower, D.V.M., Texas A&M University, College Station, TX

TOXIC NODULAR GOITER IN CATS: EVALUATION BY NUCLEAR MEDICINE (NM), COMPUTERIZED TOMOGRAPHY (CT), AND NUCLEAR MAGNETIC RESONANCE (NMR)
M.E. Peterson, J.B. Kneeland, R.J.R. Knowles, P.T. Cahill New York Hospital-Cornell Medical Center, The Animal Medical Center, and Polytechnic Institute of New York

Hyperthyroidism occurs frequently in cats and offers a potentially useful model for toxic nodular goiter in humans. A seven-compartment model has been developed for 131-I tracer kinetics in cats. It was found that in general hyperthyroid cats do not have significant storage pools and that most thyroid hormones in fact originate from a fast pool. For 22 hyperthyroid cats, 131-I tracer kinetics were correlated with serum T3 and T4 values (cat normals: T3 = 25-100 ng/dl and T4 = 0.8-3.5 ug/dl). Two distinct clusterings were observed: a rapid turnover group (average T3 = 168 ng/dl and average T4 = 11 ug/dl) and a ultrarapid turnover group (average T3 = 529 ng/dl and average T4 = 25 ug/dl).

Thyroid dosimetry for tracer and therapeutic doses of 131-I have been calculated for ten cats. These calculations indicate considerable disagreement between intended and delivered doses. One source of this disagreement may be the volume estimates for cat thyroids. To improve this

estimate, cat thyroids were imaged with a GE CT/T 9800 CT scanner and with Technicare 0.3 T and 0.5 T superconducting NMR units in addition to standard imaging in multiple projections with a pinhole collimator mounted on a scintillation camera. Three-dimensional volume determinations from CT and NMR agreed well with each other but agreed less well with volume estimates from the two-dimensional nuclear medicine images. Preliminary results indicate that CT and NMR thyroid volumes improve the accuracy of 131-I therapy.

EXPERIMENTAL MODEL OF LV ANEURYSM FOR VALIDATION OF PHASE ANALYSIS IN DOG AND BABOON. D. Pavel, R. Fang, F. Eckner, K. Roper, N. Silverman, S. Karesh, K. Markwell, P. Briandet, S. Levitsky. University of Illinois Hospital, Chicago, IL.

The need for experimental validation is due to the fact that standard functional diagnostic techniques are usually not yielding the type of quantitative information and topographic mapping that is generated by phase analysis. Method: technique was aimed at generating a predetermined size infarction by subdividing the heart projection (viewed along the long axis) into imaginary slices of equal width. The epicardial colaterals over the predetermined area are ligated and subsequently the circumflex artery (1-2 cm from the aorta) and the major LAD branches supplying the area. Gated studies were performed in 12 dogs and followed up to 4 months, and in 6 baboons followed up to 6 months p.op. Phase analysis performed by technique previously published. Results: 1) Dogs: extreme variation of baseline phase pattern between dogs and between supine or prone positions. Variability of maximum phase abnormality found due to extensive but unpredictable amount of sclerotic adhesions connecting the heart to thoracic wall. Overall the maximum stable effect appeared after 1 mo. 2) Baboons: very reproducible baseline study, minimal amount of adhesions p. op., average time for maximum effect after 2 months. Good correlation between size of abnormal area detected by phase and pathologic findings. The normalized amplitude images proved essential in ascertaining the quality of remaining portion of LV. Conclusion: for phase analysis purpose the dog appears unsuitable for practical and hypothetical reasons. The baboon model enabled a detailed evaluation and validation of the technique as applied in clinical practice, and emphasized the importance of combining phase quantification with amplitude normalization.

QUANTIFICATION OF PLATELET TURNOVER IN NORMAL ANIMALS WITH IN-111-LABELED PLATELETS. M.K. Dewanjee, P. Didisheim, S. Chowdhury, D. Kluge, P.E. Zollman, Mayo Clinic and Mayo Foundation, Rochester, MN.

Although In-111-labeled platelets are currently used in multiple thrombosis models in several species of animals, no platelet survival lifetime (PSLT) values are available for normal healthy animals. Platelets from Foxhound dogs, Sinclair S-1 miniature pigs, and Holstein calves were labeled with In-111 tropolone in ACD-saline (pH 6.5) and ACD-plasma (pH 7.4) media. 200-300 microcuries of In-111-labeled autologous platelets were administered intravenously. 4-5 ml blood samples were collected in preweighed heparinized tubes at 10 min, 4, 24, 48, 72, 96, 120, and 144 hours post-injection. Free In-111 in plasma was also determined simultaneously. Labeling efficiency, platelet survival lifetime and recovery values determined by exponential least square curve fitting program were tabulated below:

	Foxhounds (n=16)	Pigs (n=18)	Calves (n = 7)
Labeling Efficiency	85 ± 14	81 ± 6	--
ACD-Saline $T_{1/2}$(hr)	56 ± 12	39 ± 8	--
Recovery(%)	69 ± 11	89 ± 10	--
Labeling Efficiency	75 ± 10	--	40 ± 13
ACD-Plasma $T_{1/2}$(hr)	56 ± 7	--	48 ± 9
Recovery(%)	72 ± 10	--	74 ± 8

Platelet survival lifetime in ACD-saline and plasma is similar. Platelet survival lifetimes in these animals appear shorter than that of 28 human volunteers: 85 ± 10 hours in ACD-saline and 92 ± 9 hours in ACD-plasma. Platelet pool as obtained by biodistribution in pigs and calves is similar but different from that of the dog.

AN OPTIMIZED METHOD OF RBC LABELING FOR USE IN GATED CARDIAC STUDIES IN DOGS AND BABOONS. S. Karesh, D. Pavel, R. Fang, K. Markwell, University of Illinois Hospital, Chicago, IL.

In vivo RBC labeling has often been disappointing in animals in our experience. We have evaluated a modified procedure for consistently high labeling yields for high quality gated cardiac studies in dogs and baboons. This is especially important since ventricular size in these animals is considerably smaller than in humans and elevated background counts seriously degrade image quality and increase computer processing difficulties. The labeling procedure involved an I.V. injection of stannous pyrophosphate (PYP) followed by a 20 min waiting period. Five ml of heparinized blood were then withdrawn, diluted with 5 ml of 0.9% saline solution in a vacutainer, mixed and centrifuged in an inverted position for 5 min at approximately 1500 x g. Then 1.5 ml of packed RBC's were withdrawn and injected into the vial containing $^{99m}TcO_4$. After a 10 min incubation period on a 12 rpm rotator, tag efficiency was measured by the microhematocrit method, then the required dose was drawn. For a total of 146 studies performed over a period of 1 year the tag efficiency was consistently excellent. In only 9 studies out of 146 performed was tag efficiency < 90%. The very high tag efficiency measured correlated very well with image quality. The quality of the blood pool and gated images was unaffected by up to 4-5 hours delay p. injection and was strikingly changed in the case of poor labeling by the in vivo technique. Conclusion: this is a very effective, relatively simple, rapid method which can be performed with materials and kits available in any laboratory, and has been extremely reliable in studies on dogs and baboons.

INTRACELLULAR DISTRIBUTION OF RADIONUCLIDES AND TURNOVER OF Cr-51, In-111, and Tc-99m-LABELED RED BLOOD CELLS IN DOGS. S.T. Mackey, S. Chowdhury, P. Didisheim, and M.K. Dewanjee, Mayo Clinic and Mayo Foundation, Rochester, MN.

The effect of intracellular distribution of Cr-51, In-111, and Tc-99m radionuclides on turnover measurements of labeled red cells was studied in five mongrel dogs. Saline washed red cells from citrated dog blood were labeled with Cr-51-chromate (50 μCi), In-111-tropolone (100 μCi), and Tc-99m pertechnetate in vitro (10 mCi) and administered intravenously. The distribution of radionuclides was measured by hypotonic lysis of red blood cell in 0.015 M phosphate buffer. The membrane was separated by ultracentrifugation at 100,000 G for two hours at 4°C and membrane filtration. Blood clearances of in vivo labeled Tc-99m red blood cells (20 μg Sn^{2+}/kg) and in vitro labeled Tc-99m, Cr-51, and In-111 red blood cells were determined. The red blood cell distribution (%) of the radionuclides and mean exponential red blood cell survival time (ERBCST) in days (D) and the major blood clearance component (%) were tabulated:

	Membrane	Hemoglobin	ERBCST(D)	Comp.
Tc-99m (in vitro)	58 ± 9	40 ± 7	2.7	66
Tc-99m (in vivo)	29 ± 5	64 ± 7	6.7	51
In-111	60 ± 6	40 ± 3	16.3	77
Cr-51	9 ± 3	91 ± 4	28.8	85

Red blood cells labeled with Tc-99m are most unstable. In-labeled red blood cells have a faster blood clearance than Cr-red blood cells. This change in blood clearance of Tc-99m, In-111, and Cr-51 labeled red blood cell may be due to the change in the distribution of radionuclides on the membrane and hemoglobin. More membrane binding may lead to faster turnover rate.

1:30-3:00 **Room 123**

CARDIOVASCULAR CLINICAL IV: PHASE ANALYSIS & VENTRICULAR VOLUMES

Moderator: Elias Botvinick, M.D.
Co-moderator: Ismael G. Mena, M.D.

LEFT VENTRICULAR VOLUMES FROM GATED RADIONUCLIDE VENTRICULOGRAMS: ATTENUATION CORRECTION IN FEMALES AND MALE PATIENTS. JR Corbett, JS Rellas, JT Willerson, R Huxley, PH Nicod, B Firth, SE Lewis. Univ. Texas Health Science Center, Dallas, TX

We tested the hypothesis that measurement of left ventricular (LV) volumes based upon detected ventricular activity during radionuclide ventriculography (RVG) is more accurate with attenuation correction (AC) in females. An "individualized" geometric correction technique was utilized in 17 females and 13 males. Following acquisition of the "best" septal view RVG (20-70° LAO), a radioactive point source was placed over the center of the LV. Images were acquired at ± 20° or 30° so that the LV perimeter remained visible. Average depth of the LV was determined from the average distance of the point source to the LV center/sine (x degrees). LV attenuation was calculated using the attenuation coefficient for water at 140 keV (0.15 cm^{-1}). In 9 females, a second "best" septal RVG and attenuation determination was made with the left arm abducted and left breast taped away from the precordium. Contrast ventriculograms were obtained within 3 weeks in all patients. LV end-diastolic volume ranged from 93-539 ml (mean 175 ± 100). LV attenuation varied from 0.089-0.391 (mean 0.26 ± 0.07). Correlation of scintigraphic and angiographic volumes was improved significantly ($p<0.05$) by AC (y=.29X-8.43, r=0.86 without, and y=.89X+3.57, r=0.96 with AC). In females, minimizing interposed breast tissue resulted in a significant reduction in LV attenuation (0.293 ± 0.83 vs 0.240 ± 0.097, $p<0.01$). AC significantly improved the correlation of scintigraphic and angiographic volumes in females (y=.26X-3.97, r=0.751 without correction; y=.90X+1.18, r=0.930 with AC). Uncorrected scintigraphic volumes correlated less well in females than in males (r=0.751 vs r=0.896, $p<0.05$). We conclude that attenuation correction of radionuclide LV volumes using an adaptive geometric technique improves the accuracy significantly, especially in females.

RELIABILITY OF RADIONUCLIDE ABSOLUTE LEFT VENTRICULAR VOLUME MEASUREMENTS. W. Wijns, J.H.C. Reiber, S.P. Lie, K. van Duyvendijk, M.L. Simoons. Thoraxcenter, Erasmus University, Rotterdam, the Netherlands.

Total reproducibility and inter- and intra-observer variability of radionuclide left ventricular end-diastolic volume (LV EDV) measurements from gated blood pool studies were evaluated in 19 patients (pts). A fully automated computer program was used for LV contour detection and optimal background selection. Counts within the LV contour were corrected for decay and attenuation ($e^{-\mu d}$); μ was 0.15 cm^{-1} and d the depth of the LV center. The activity of a blood sample was used to calculate LVV (ml).

Two independent studies were repeated in 8 pts after a mean interval of 16 min. Results (mean ± sd) :

		study 1	study 2
EF	%	33 ± 15	33 ± 16
LV EDV	ml	196 ± 73	196 ± 68

LV EDV sd of difference 18 ml

In 11 pts, the standard study (6 min.) was compared with a 3 min. acquisition obtained before supine exercise :

		6 min.	3 min.
EF	%	33 ± 9	33 ± 10
LV EDV	ml	212 ± 88	222 ± 85

LV EDV sd of difference 14 ml

Finally, inter- and intra-observer variabilities (two observers, two months interval) were calculated in all independent 6 min. studies (n = 27). The sd of differences between LV EDV values were 11 and 13 ml respectively. Correlation coefficients were 0.99 in both cases.

Thus, reliable LVV can be obtained using a non geometric method with attenuation correction. The variability of the measurements is less than 20 ml, provided automated processing of the data is available.

MITRAL STENOSIS: RIGHT AND LEFT VENTRICULAR VOLUME ASSESSED BY RADIONUCLIDE VENTRICULOGRAPHY. D. L. Johnston, V. Gebhardt, D.R. Boughner, A. Patel, P. Purves, W.J. Kostuk. University Hospital, London, Ontario, Canada.

Rest (Rs) and exercise (Ex) ventricular volume changes have not been described in patients (pts) with mitral stenosis (MS). Using equilibrium radionuclide ventriculography (RNV), we developed a rapid, non-geometric method to assess left and right ventricular (LV,RV) volume. Correlation of the combined scintigraphic end-diastolic and end-systolic volume (EDV, ESV) with cardiac catheterization was excellent. (LV r = 1, n = 25, RV r = .92, n = 10). Using this method, 15 pts with isolated, moderate to severe MS (mitral valve area ≤ 1.4 cm^2) and 10 pts with mild MS (> 1.4 cm^2; underwent RNV at Rs and during symptom-limited supine bicycle Ex.

Moderate - Severe MS, n = 15

	Rs	Ex		Rs	Ex
LVEF(%)	62±15	69±16**	RVEF(%)	47±15	45±14
LVESV (ml/m^2)	35±19	25±17**	RVESV (ml/m^2)	71±32	79±37*
LVEDV (ml/m^2)	90±27	78±24**	RVEDV (ml/m^2)	124±40	132±42

(*p = $<.05$, **p = $<.02$ Rs to Ex, EF = ejection fraction, values = mean + SD)

In ten pts with mild MS showed similar but less significant changes in ventricular volumes. Cardiac index rose with Ex from 4.4 to 6.3 $l/min/m^2$ due to an increase in heart rate not stroke volume. Values for pts in atrial fibrillation were similar to pts in sinus rhythm. Thus, in MS, both ventricles respond abnormally to Ex but by different mechanisms. LV size decreased suggesting a disorder in LV diastolic filling while RV size increased consistent with a disorder in RV systolic function.

FOURIER VENTRICULAR AMPLITUDE RATIO TO ASSESS VALVULAR REGURGITATION BY GATED BLOOD POOL SCAN. P.T. Makler, Jr., D.M. McCarthy, J.P. Kleaveland, J.U. Doherty, H.A. Goldstein, M.G. Velchik, and A. Alavi. Hospital of the University of Pennsylvania, Philadelphia, PA.

In the amplitude (AMP) image obtained from first harmonic Fourier analysis of the gated blood pool scan there is clear separation of the four cardiac chambers. Since a pixel's AMP value is a function of its stroke counts, the ratio of AMP values of the left and right ventricles - the ventricular AMP ratio (VAR) - should reflect the ratio of ventricular stroke counts.

We investigated the utility of the VAR in evaluating valvular regurgitation in 47 patients (pts). There were 14 normals (N), 16 pts with coronary artery disease (CAD) with wall motion abnormalities and 17 pts with valvular insufficiency (9 aortic, 7 mitral, 1 mixed). The VAR (±sd) was 2.31±77 (range 1.49-4.17) in pts with valvular insufficiency vs 1.14±.11 in N and 1.22±.18 in CAD ($p<.001$). The degree of intra- and interobserver agreement was high (r= 0.94, 0.95), reflecting the ease with which ventricular boundaries can be defined on the AMP image.

To assess whether the VAR is an accurate estimate of the stroke volume ratio (SVR) obtained during cardiac catheterization, we studied 13 additional pts who had SVR's ranging from 1.16 to 3.70 (mean 2.00). The VAR and SVR were calculated by different observers in a double blind manner. There was a close correlation between VAR and SVR (r=0.89, slope=1.06, SEE=0.30).

In conclusion, the VAR is a reproducible and accurate method for determining the presence and magnitude of valvular insufficiency by gated blood pool scan.

PHASE ANALYSIS IN PATIENTS WITH WOLFF-PARKINSON-WHITE SYNDROME WITH SURGICALLY PROVED ACCESSORY CONDUCTION PATHWAYS. K. Nakajima, H. Bunko, A. Tada, J. Taki, N. Tonami, K. Hisada, T. Misaki, and T. Iwa. School of Medicine, Kanazawa University, Kanazawa, Japan.

The correlation between the site of an accessory conduction pathway(ACP) in Wolff-Parkinson-White syndrome(WPW) and the abnormalities of the phase image was studied. Twenty patients with WPW who underwent surgical division of the ACP were studied by ECG-gated blood pool scintigraphy(GBPS). The localization of ACP was determined by electrophysiologic study using catheter and was confirmed by epicardial mapping and surgery. Based on the surgically confirmed localization of ACPs, patients with WPW were classified into 9 right cardiac type(R-type), and 10 left cardiac type(L-type) and 1 R-type with two ACPs in the right ventricle. In GBPS, the patient was imaged at 35-45° LAO, 10°RAO and/or 70°LAO projections; slant hole collimator (35° caudal tilt) was generally used. In each case, a functional image of the phase using the fundamental wave of the Fourier transform was generated. All of R-type were correctly diagnosed. In L-type, 6 patients were correctly diagnosed, however, the other 4 patients who had ACPs on the anterior or lateral wall of the left ventricle were not detected. Sensitivities to detect the ACPs were 80%(16/20); 100% for R-type and 60% for L-type. These observations indicate that the abnormal wall motion is

associated with the pre-excitation. In conclusion, the phase analysis can provide interesting informations and was useful for the evaluation of contraction patterns before and after surgery of WPW. However, as a method of pre-operative study, it seems difficult to point out the exact site of the ACP by phase analysis alone.

THE CONTRIBUTION OF ATRIAL CONTRACTION TO LEFT VENTRICULAR FILLING IN PATIENTS WITH CORONARY ARTERY DISEASE. Y.Ishida, M.Inoue, M.Matsumoto, M.Fukushima, BH.Kim, T.Tsuneoka, K.Kimura, H.Abe. Osaka Univ. School of Med., Osaka, Japan

To assess the effect of atrial contraction(AC) on left ventricular(LV) filling in patients(pts) with coronary artery disease(CAD), LV volume(LVV) changes during rapid filling(RF) and AC phases were studied by equilibrium radionuclide ventriculography in 10 normals(N) and 17 pts with CAD, 8 pts without(CAD-1) and 9 pts with(CAD-2) prior myocardial infarction(MI). The data was acquired in a list-mode fashion as a series of X,Y coordinates, time markers and ECG R wave(R) plus second heart sound(S2) markers. LVV curves were obtained from three types of multi-gated images by (1) R-synchronized forward reformatting for analysis of systolic phase(ejection fraction:EF), (2) S2-synchronized forward reformatting for analysis of RF phase(peak filling rate:PFR-RF and filling fraction:FF) and (3) R-synchronized backward reformatting for analysis of AC phase(peak filling rate:PFR-AC and LVV increment with atrial contraction/stroke volume:AC/SV). The results are :

	EF (%)	PFR-RF (EDV/sec)	FF (%)	PFR-AC (EDV/sec)	AC/SV
N	58.2±5.8	2.3±0.4	37.0±8.2	0.8±0.3	0.13±0.07
CAD-1	52.7±6.4	1.5±0.4*	23.0±0.7*	1.3±0.3*	0.30±0.06*
CAD-2	36.0±8.1*	1.3±0.4*	19.0±8.0*	0.6±0.4	0.18±0.09

*p<0.01 vs N , mean±SD

Although PFR-RF and FF were reduced both in CAD-1 and -2, the mean PFR-AC and AC/SV were significantly greater in CAD-1 than N or CAD-2. These results indicate that in pts with CAD but without prior MI, AC could compensate the impaired rapid filling, wheras in pts with prior MI this compensatory mechanism is absent presumably because of the elevated LV end-diastolic pressure.

1:30–3:00 **Room 132**

CARDIOVASCULAR BASIC II: MYOCARDIAL PERFUSION

Moderator: Denny D. Watson, Ph.D.
Co-moderator: Michael L. Goris, M.D., Ph.D.

A STATISTICAL INTERPRETATION OF QUANTITATIVE THALLIUM-201 MYOCARDIAL PERFUSION SCINTIGRAPHY. M.L. Goris and E. Gordon, Stanford University Medical Center, Stanford, CA

The size and distribution of perfusion abnormalities are used to determine the likelihood and localization of coronary artery disease.

The method is based on circumferential analysis of planar scintigraphies. Additionally, for each of three views the profile is subdivided in three segments (e.g., apical, septal, posterior) and the sum of the differences between the test profile and the expected profile is computed for each segment. The nine resulting segmental values represent the degree by which the test case differs from "normal".

By permutation and combination of two degrees of lesions in three vascular domains, 30 "diseases" are defined, including D(1) for "no lesions" or normal and D(30) for "any lesion". An updatable statistical file is produced, in which the nine average segmental values are stored, with their standard deviation, for the 30 diseases, using arteriographically verified cases.

Using a probability function h(t) assumed to be Gaussian Bayes' theorem is sequentially applied to 30 diseases and nine symptoms. In this way $P(h_i(x)/DJ)$ represents the sensitivity of a value x in segment i for the detection of disease j.

The results confirm the impression that single vessel disease is easier to detect and identify and that detection is generally easier than identification. Surprisingly, the system yields nearly binary results which support the usual negative-positive approach.

OPTIMAL COUNT RATES FOR RELIABLE ASSESSMENT OF THALLIUM-201 MYOCARDIAL WASHOUT. F. J. Wackers, R. C. Fetterman, J. Mattera, J. Clements. Univ. of Vermont, Burlington, VT.

Quantitative analysis of Tl-201 stress images involves calculation of percent Tl-201 washout (WO). Tl-201 images typically are low in counts (cnts). On background subtracted circumferential profiles, total cnts per 10° segment (128x128 matrix) range from 500-2000. Statistical error is inversely proportional to cnts. We evaluated the effect of various cnt densities on accuracy of WO values by quantitative analysis of two-dimensional phantoms. Four paintings with Tc-99m solution representing imitations of typical LAO Tl-201 images (normal, fixed defect, and 2 transient defects) were each imaged 7x, acquiring 25k, 50k, 100k, 150k, 300k, 500k, 750k, cnts in whole field of view. Then, the transient defects were "filled in".The phantoms were imaged 3 hrs later for identical times. Thus, myocardial WO was mimicked by decay of Tc-99m. After interpolative background subtraction, circumferential cnts and WO profiles were generated. The 32 studies were randomly coded and in 16 segments per study WO was graded as abnormal or normal on probability scale 1-5 to construct modified receiver operating characteristics (ROC) curves. Low cnt rate studies resulted in random and abnormal values for WO in both normal and abnormal segments. The frequency of false positive (FP) results at any diagnostic criterion level (DCL) was inversely related to cnts in profiles.At strict and moderately strict DCL, no FP results occurred when total cnts in 10° segments were 900 or higher. Statistical error was inversely proportional to absolute value of WO. Thus, 1. Low cnts tend to create FP WO results. 2. For reliable analysis of WO, total cnts in 10° segments should be 900 or more. 3. Because of low cnt rate, WO in peri-infarction areas should be interpreted cautiously.

COMPARISON OF THE TRANSPORT OF $^{42}K^+$, $^{22}Na^+$, $^{201}Tl^+$ & ^{99m}Tc-DMPE USING HUMAN RED BLOOD CELLS.

H. Sands, M. L. Delano, P. Shaw, K. Linder, L. L. Camin, B. M. Gallagher
New England Nuclear Corp., N. Billerica, MA 01862

Accumulation of monovalent cations by an active Na^+/K^+ ATPase system is thought to be essential for myocardial imaging. We have used the ability of isolated RBC's (human red blood cells) to exchange Na^+ for K^+ to study the characteristics and interactions of the transport of several monovalent cations. Both efflux and influx studies were done. Efflux of $^{22}Na^+$ from RBC's loaded in Ringers·SO_4 buffer was stimulated by the addition of K^+, and inhibited by the addition of ouabain. The addition of $[^{99}Tc(DMPE)_2 \cdot Cl_2]^+$ complex [DMPE= 1, 2-bis (dimethyl phosphino)ethane] at 5 mM had no effect on $^{22}Na^+$ eflux, whereas K^+ and Tl^+ at 10 mM stimulated ^{22}Na efflux. Influx of $^{42}K^+$ was shown to be inhibited by the addition of ouabain, unlabelled K^+, or Tl^+. ^{99}Tc-DMPE had no effect on ^{42}K uptake. $^{201}Tl^+$ influx was more rapid and of a greater magnitude than $^{42}K^+$. Influx of $^{201}Tl^+$ was shown to be unaffected by ouabain, and inhibited by the addition of unlabelled Tl^+. Addition of ^{99}Tc-DMPE at 5 mM resulted in an inhibition of ^{201}Tl influx. ^{99m}Tc-DMPE influx resembled that of $^{42}K^+$ with respect to rate and magnitude. Influx of ^{99m}Tc-DMPE was shown to be unaffected by ouabain or unlabelled K^+ or Tl^+. Addition of 5 mM ^{99}Tc-DMPE initially had no effect on ^{99m}Tc-DMPE influx, however, with time a stimulation in the influx of the ^{99m}Tc-DMPE was observed. We conclude that the influx into RBC of the monovalent cations is mediated by different mechanisms. Most clearly the influx of ^{99m}Tc-DMPE is not by a mechanism similar to that of K^+ or Tl^+.

QUANTIFICATION OF REGIONAL MYOCARDIAL FLOW WITH Rb-82 DESPITE PHARMACOLOGIC INTERVENTION. R.A. Goldstein, N.A. Mullani, D.J. Fisher, S.K. Marani, H.A. O'Brien, and K.L. Gould. Department of Medicine University of Texas Health Science Center. Houston, TX.

We have previously developed a two compartment model that allows the accurate measurement of regional myocardial flow with Rb-82, a generator produced positron emittor. However, since extraction of Rb-82 may be altered by pharmacologic interventions independent of flow, we determined whether cardiac drugs would invalidate the accuracy of flow measurement using our model. Anesthetized open-chested dogs (n=9) were injected simultaneously with intravenous Rb-82 and left atrial microspheres after the administration of intravenous digoxin (10μg/kg), propranolol (1.5 mg/kg), or glucose-insulin (2 units insulin/glucose). Flow was increased by intravenous dipyridamole with phenylephrine being added as required to maintain control arterial pressure and heart rate. Flow was decreased by graded occlusion. Myocardial positron counts (corrected for gammas) were monitored on the anterior left ventricular wall at 0.5 second intervals using a beta probe. The range of positrons in tissue is ~4 mm which excludes counts from the posterior left ventricular wall and blood pool. An arterial reference sample was also monitored. First pass extraction was measured using a simple two compartment model. Myocardial flow determined by the model for Rb-82 correlated linearly with flow by microspheres in the same sample volume after digoxin (r=.97, n=16, slope=.92), propranolol (r=.95, n=20, slope=.90), and glucose-insulin (r=.99, n=10, slope=.95), over a range of flow from 0.1 to 7.8 ml/min/g. Regional myocardial blood flow may be accurately determined using our model despite the presence of cardiac pharmaceuticals.

THALLIUM MYOCARDIAL UPTAKE DURING ACUTE CARDIAC ALLOGRAFT REJECTION. J.G. Losman, I. Kim, U.Y. Ryo, E. Byrom, J. Lee, R.L. Replogle, S. Pinsky. Michael Reese Hospital, The University of Chicago, Chicago, IL.

This study investigates changes of distribution and extraction of Thallium-201 (Tl) during cardiac allograft (CG) tolerance & rejection (r) in 14 mongrel dogs. Ectopic CGs were grafted to the recipient neck vessels. Immunosuppression included azathioprine 3 mg/kg and prednisolone 5 mg/kg, both tapered down and discontinued by day 25. CGs survival ranged from 8 to 37 days (mean 19 ± 8). CGs ECG voltage was recorded twice daily (epicardial electrodes). Twice or 3 times weekly both Tl scans of recipient heart (RH) and the CG, and full thickness left ventricular biopsies were done and compared with the ECG evidence of graft tolerance changes. Acute r was diagnosed by a 20% or greater drop in ECG voltage, confirmed by histologic evidence. CGs' Tl uptake, corrected for unspecific variation by comparing CG and RH uptake, dropped significantly during r ($p<0.005$) but did only correlate moderately with serial ECG changes (coefficient = 0.663). However, in 9 r episodes, this Tl uptake drop was preceded by a significant rise from 1.07 to 1.44 ($p<0.05$), while the ECG voltage fell from 8.08 to 4.55 mV ($p<0.005$). Only 3 CGs did not increase at all their Tl uptake. This finding may reflect an early change in CG capillary permeability or in rate of ion exchange, and following technical refinements and dynamic uptake/washout studies, could become a clinical noninvasive test to confirm the suspicion of acute r based on ECG or clinical evidences, reducing the need for transvenous endomyocardial biopsy.

QUANTITATION OF THALLIUM 201 MYOCARDIAL PERFUSION DEFECT SIZE BY SINGLE PHOTON EMISSION COMPUTED TOMOGRAPHY (SPECT). J.H. Caldwell, J.L. Ritchie, G.D. Harp, D.L. Williams, and J.R. Stratton. VA Medical Center and Univ. of Washington, Seattle, WA.

To determine if Tl-201 myocardial perfusion defect size (PDS) in SPECT images accurately reflects the anatomic PDS, the following study was performed. After IV injection of 1 mCi Tl-201 in 4 dogs, the animals were placed in the SPECT system (GE 400T) and 64 projection images acquired over the anterior 180°. One week later, a snare was placed around a coronary artery, the chest closed, the artery occluded, and 1 mCi Tl-201 injected IV. SPECT images were recorded and reconstructed using a standard filtered backprojection algorithm without attenuation correction. The animal was sacrificed, the heart excised, RV and atria removed and the LV cut into 4 cross section slices each 1.8 cm thick. Each slice was cut into 32 transmural samples equally spaced around the circumference of the slice, weighed, and counted in a well counter. Myocardial PDS in the anatomic slices was defined by identifying those samples whose counts/gram were more than 2 SD below the mean value for 10 adjacent samples in the normal zone of the respective slice. The tomographic images were reoriented into a series of short axis images similar to the anatomic slices and analyzed using a computer algorithm developed at this institution.

Anatomic PDS was 33.6 ± 13.49 gm (mean ± SD). This was 32.69 ± 10.37% of LV myocardial weight. SPECT PDS was 36.00 ± 5.68 cm^3 which represented 32.84 ± 13.06% of LV volume. The correlation between anatomic (gm) and tomographic (cm^3) PDS was fair (r = 0.60; SEE = 5.54; y = 0.25X + 27.46). The correlation between anatomic PDS as % LV weight and tomographic PDS as % LV volume was excellent (r = 0.91; SEE = 6.52; y = 1.15X - 4.78).

We conclude that PDS measured by SPECT accurately reflects anatomic defect size. As such, this technique could potentially be used to quantitate myocardial infarct size in the clinical setting.

1:30–3:00 **Room 130**

GASTROINTESTINAL II: SPECT & QUANTITATIVE HEPATOBILIARY ANALYSIS

Moderator: Dennis G. Patton, M.D.
Co-moderator: Manuel L. Brown, M.D.

IMPROVEMENT OF SCINTIGRAPHIC LIVER IMAGING BY SPECT - A REVIEW OF 797 CASES. H.J. Biersack, K. Reichmann, S.N. Reske, R. Knopp, C. Winkler. Institute of Nuclear Medicine, University of Bonn, FRG

This study was undertaken to evaluate the diagnostic usefulness of SPECT in combination with conventional liver scintigraphy. A total of 797 patients (focal liver lesions: 96, cirrhosis/fibrosis: 203, no liver disease: 498) was investigated. Diagnosis was confirmed by CT, sonography, laparascopy, laparatomy, and autopsy. The conventional study (3 projections) was performed after injection of Tc-99m sulphur colloid by means of a LFOV camera. For SPECT, a rotating gamma camera system was used. During one 360° rotation 64 frames were acquired (15 min). On hand of an array processor transverse, sagittal, and coronal slices were rapidly obtained. The respective results are as follows: In liver metastases (n=68) sensitivity could be improved from 79% up to 90% by combination of SPECT with conventional scintigraphy. The respective values in primary liver tumors (n=26) were 77% and 92%. Right negative findings were obtained in 80% by SPECT and in 84% by conventional scintigraphy. When both methods were combined the specificity could be improved up to 88% in 498 patients. In liver cirrhosis (n=169), SPECT did not yield additional information due to image degradation (poor statistics). In conclusion, it can be stated that SPECT improves sensitivity as well as specificity of liver scintigraphy.

CLINICAL EVALUATION OF SINGLE-PHOTON EMISSION COMPUTED TOMOGRAPHY ON SCREENING OF SMALL HEPATOCELLULAR CARCINOMA. M.Kudo, Y.Ibuki, K.Fujimi, S.Tomita, H.Komori, Y.Okimoto, A.Todo, Y.Kitaura and K.Ikekubo. Kobe General Hospital, Kobe, Japan; N.Tamaki and K.Torizuka. Kyoto University, School of Medicine, Kyoto, Japan.

This investigation was undertaken to evaluate the clinical usefulness of single-photon emission computed tomography (SPECT) using a GE Maxi Camera 400T with Tc-99m phytate on screening of small hepatocellular carcinoma (HCC), defined as solitary tumors less than 5 cm in diameter.

SPECT was performed in 342 patients with chronic liver diseases (187 liver cirrhosis and 155 chronic hepatitis) following conventional liver scanning. Ultrasound (US) and AFP assay were performed on all cases, too. The detectability of small HCC with these 4 modalities was compared.

The results were as follows: (A) We could diagnose 15 small HCC in 342 patients. (B) We could detect 4/15 (27%) by AFP, 8/15 (53%) by conventional liver scanning, 11/15 (73%) by US and 12/15 (80%) by SPECT. (C) Three of 4 lesions that could not be detected by US were located in the subdiaphragmatic region of the right lobe, where lesions are

often overlooked by US. These 3 lesions were correctly detected by SPECT. (D)The 3 lesions that could not be detected by SPECT were correctly detected by US. (E)All 15 lesions were detected by the combination of SPECT and US.

In conclusion,the combination of SPECT and US is very useful as a screening procedure for small HCC.

VASCULAR INTRAHEPATIC DEFECTS IN SINGLE PHOTON EMISSION COMPUTED TOMOGRAPHY (SPECT) OF THE NORMAL LIVER AS DEFINED BY Tc-99m RBCs AND SULFUR COLLOID. R. Pettigrew, K. Witztum, S. Halpern, J. Verba, G. Perkins, M. Johnson, R. Burks, VA Medical Center, San Diego, CA.

Because of the high target-to-background contrast obtained with (SPECT), normal intrahepatic vessels ~ 2 cm in diameter may appear as distinct focal "defects" in tomographic sections throughout the liver, though normal vessels rarely cause such "defects" on planar images. To assess this problem, 5 subjects without evidence of liver disease underwent tomography (tomo) of the liver with 5 mCi of Tc-99m sulfur colloid (TSC), and 2 days later tomo of the intrahepatic blood pool with 25 mCi of Tc-99m autologous red blood cells (RBC). A GE 400T-STAR tomo system with a high resolution collimator was used. The acquisition protocol was 64 views in 360° at 30 seconds per view. In each TSC study, well demarcated "defects" were seen in contiguous tomo slices in each of 3 orthogonal planes. Direct comparison with RBC tomo slices showed that each TSC "defect" corresponded to intrahepatic vessels; typically the right portal vein, its anterior and posterior branches and the left portal vein. For tomographic planes in which these veins are oriented end-on, the "defects" are circular, appear in several contiguous sections, and therefore may be very easily misinterpreted as pathologic lesions. Examination of these "defects" in the remaining orthogonal planes usually shows linear photopenic areas extending from the porta hepatis. We conclude, to avoid high false positive rates, interpretation of TSC tomograms requires: 1) Knowledge of intrahepatic vascular anatomy in various tomographic planes; 2) Examination of each defect in multiple orthogonal planes; and 3) In some cases, a tomographic study with RBCs.

DIFFERENTIATION OF OBSTRUCTIVE FROM NON-OBSTRUCTIVE JAUNDICE BY DECONVOLUTIONAL ANALYSIS OF HEPATOBILIARY SCANS J.E. Juni, J.W. Keyes, Jr., W. Carter, R. Bowers, M.D. Gross, D. Smock, C. Samosik-Mast; University of Michigan Medical Center, Ann Arbor, MI.

The differential diagnosis of jaundice is a difficult clinical problem. We have developed a radionuclide technique for quantitating hepatocyte function by deconvolutional analysis. Deconvolution corrects the liver time-activity curve (TAC) for systemic tracer recirculation, simulating a tracer injection directly into the hepatic blood supply.

We studied 27 pts: 7 with biliary obstruction (bili 2.5-5.8, mean = 4.5), 8 with hepatocyte dysfunction (HD) (bili 2.0-11.7, mean = 5.6) and 11 normals (bili 0.2-0.8, mean = 0.5). Final diagnosis was determined by surgery (11 pts), operative cholangiogram (10), ultrasound (12), CT (6), and clinical follow-up and enzymes in all. Thirty-two 1-min. images of the heart and liver were obtained, beginning one min. prior to injection of 5-15 mCi of Tc-99m-disofenin. TAC's of liver and blood pool (heart) were deconvolved by a Fourier transform technique. The initial peak of the resulting curve represents total tracer activity presented to the liver. The remainder of the curve represents hepatocyte retention and excretion. We calculated the hepatocyte dysfunction index (HDI) as the ratio of this initial peak to the initial hepatocyte retention. All normals had an HDI of 1-1.01 (SD=0), pts with biliary obstruction had HDI mean of 1.3 (SD=0.25), while pts with HD had a mean mean HDI of 5.0 (SD=3.16 p<.001).

Deconvolutional analysis eliminates the effects of recirculation on the hepatic TAC, thus permitting separation of vascular and hepatocyte activity. The hepatocyte dysfunction index appears to be a reliable means of detecting hepatocyte dysfunction and distinquishing obstructive from non-obstructive jaundice.

QUANTITATIVE ANALYSIS OF LIVER FUNCTION IN PERCUTANEOUS TRANSHEPATIC DRAINAGE PATIENTS. M.G. Velchik, W. Schwartz, J.W. London, P.T. Makler, Jr., and A. Alavi. Hospital of the University of Pennsylvania, Philadelphia, PA.

This investigation was undertaken to evaluate the diagnostic usefulness of cholescintigraphy with Tc-99m DISIDA in patients who have undergone a percutaneous transhepatic drainage (PTD) procedure for extrahepatic biliary obstruction. 29 cholescintigrams were performed in 14 patients. The exams were divided into 2 groups: Group A (N=17) in which the patient's clinical status deteriorated (febrile, septic) within 2 to 3 days of the examination; Group B (N=12) in which the patients did well clinically. No significant difference between the 2 groups was demonstrated by visual analysis of the analog images utilizing a weighted grading system which incorporated blood pool activity, biliary to bowel transit time, and renal activity. Similarly, no correlation with serum bilirubin level was demonstrated. We have developed a computer program that quantitates several parameters of hepatic function based on compartmental analysis. After drawing regions of interest around the heart and liver, time activity curves are constructed and the transport constants K1 (blood pool clearance) and K2 (hepatic clearance) are derived by a non-linear regression algorithm. There was a significant difference ($p<.001$) between the mean clearance constants for the 2 groups (Group A: K1 2.94±1.47, K2 0.040±0.018; Group B: K1 5.20±2.03, K2 0.091±0.020). Better separation of the 2 groups was obtained with K2 than with K1. Serum bilirubin levels and visual inspection of analog images are inadequate indicators of hepatic function in patients post PTD. The clearance constants K1 and K2 are quantitative parameters of hepatic function and may be of prognostic value in patients post PTD.

RETENTION RATIO IMAGE: A USEFUL PARAMETRIC IMAGE FOR DETECTING INTRAHEPATIC LITHIASIS. S.H. Yeh, L.C. Wu, and R.S. Liu. Veterans General Hospital, Taipei, Taiwan.

This study was undertaken to develop a parametric image, HIDA retention ratio image, useful for detecting intrahepatic lithiasis.

Data were acquired in the hepatic region for one min at 5 and 40 min after i.v. injection of Tc-99m HIDA with the patient in the same position. The retention ratio at 40 min was calculated on pixel-by-pixel basis, the ratio distribution histogram was analyzed, and the two-color retention ratio image was created. The retention ratio image was masked with hepatic ROI exclusive of the gallbladder and common duct. All values are presented as mean ± standard deviation (SD).

The study was based on 32 normal subjects (N) and 32 lobes of 20 proved patients (pts) with intrahepatic lithiasis (unilobar in 8 and bilobate in 12). The mean retention ratio was greatly increased in pts with liver stones (1.33 ± 0.42 vs 0.56 ± 0.16 in N, $p < 0.001$), indicative of intrahepatic retention. Pts markedly increased the spread of the mean SD of ratio standard deviations (0.17 ± 0.11 vs 0.04 ± 0.02 in N, $p < 0.001$). For generating two-color ratio images, the optimal decision threshold as determined by ROC analysis was the normal mean retention ratio + 1.5 SD, i.e., 0.8, with resultant sensitivity and specificity of 93% and 96%, respectively. Such ratio images showed: (a) green in the normal parenchyma and (b) red in the abnormal parenchyma with retention due to intrahepatic stones.

In summary, retention ratio images can provide an objective and highly sensitive and specific means for detecting intrahepatic lithiasis in a clear and concise manner.

1:30-3:00 **Room 276**

RADIOPHARMACEUTICAL CHEMISTRY III: ONCOLOGY

Moderator: Suresh C. Srivastava, Ph.D.
Co-moderator: Alan R. Fritzberg, Ph.D.

Introduction. Suresh C. Srivastava, Ph.D., Brookhaven National Laboratory, Upton, NY

DEVELOPMENT OF COPPER-67 CHELATE CONJUGATED MONOCLONAL ANTIBODIES FOR RADIOIMMUNOTHERAPY. W. Cole, S. DeNardo, C. Meares, G. DeNardo, H. O'Brien. Nuclear Medicine and Department of Chemistry, UCD and Los Alamos National Laboratory. Supported by DOE, CRCC and ACS #PDI-94D.

In order to develop an effective approach for radioimmunotherapy, we have evaluated the pharmacokinetics of monoclonal antibodies and their fragments. These studies demonstrated that the effective tumor membrane residence time for these antibodies was between 1 and 4 days, and a cellular heterogeneous uptake required energy to be deposited over several cells for homogeneous dosimetry. The copper-67, with a 62 hour T1/2 and beta particle energy from 395-577 keV, demonstrated significant advantages as a therapeutic radionuclide to be carried on these molecules.

Therefore, we have developed a radiolabeling method utilizing CITC (isothiocyanobenzyl-EDTA) as a conjugant for the copper to the antibody molecule. CITC was conjugated to monoclonal IgG1 with protein concentrations ranging from 1mg/ml to 10mg/ml. CITC:protein reaction ratios were evaluated at levels from 3:1 to 100:1. The apparent number of CITC molecules binding to the immunoglobulin was demonstrated by the number of metal atoms chelated, and varied from 1:2 to 2.5:1.

Copper-67-CITC-IgG1 labeled at a 1:1 molar ratio of copper to antibody was evaluated for stability by cellulose acetate electrophoresis over 24 hours and biodistribution in nontumor bearing BALB-C mice. Comparisons were made to I-125 labeled antibodies. Whole body retention studies showed comparable curves over 48 hours. Blood clearance curves had an average T1/2 accelerated compared to the iodinated IgG, with preliminary organ distributions suggesting increased hepatic uptake.

COMPARISON OF THREE METHODS FOR DTPA CONJUGATION TO ANTIBODY. C.H. Paik, P.R. Murphy, M.A. Ebbert, C.R. Lassman, R.C. Reba, W.C. Eckelman. The George Washington University Medical Center, Washington, D.C.

We have compared three methods (DTPA carboxycarbonyl anhydride, cyclic DTPA anhydride and carbodiimide method) of conjugating DTPA to antibody in our attempt to optimize the balance between the number of DTPA groups conjugated to the antibody and the antibody-binding activity. We used a practical concentration (300 µg in 1 ml medium) anti HSA antibody (Ab). The DTPA carboxycarbonyl anhydride and cyclic DTPA anhydride methods are two step synthetic methods using DTPA as a starting compound. The carbodiimide method is, however, a one step synthesis using carbodiimide as a coupling agent to conjugate DTPA to amino groups of Ab. DTPA carboxycarbonyl anhydride is very unstable and requires that the reaction be carried out below 4°C. An optimum conjugation giving 3 indium atoms incorporated per Ab with 65% retention of antibody-binding activity was obtained when an anhydride to antibody ratio of 1173 was used. For cyclic DTPA anhydride method, DTPA conjugation was dependent on the pH of the reaction medium. Four buffer solutions were compared: Hepes buffer at pH 7, phosphate buffer at pH 7, borate buffer at pH 8.6 and bicarbonate buffer at pH 8.2. The bicarbonate buffer was the best in terms of pH stability and indium atoms (11) incorporated per Ab (50% retention of the binding activity occurred). The carbodiimide method was the simplest we have studied and enabled us to incorporate up to 18 indium atoms per Ab with a retention of 40% activity when the reaction was carried out at pH 6.2. The systematic variation of the parameters of these classical reactions using dilute antibody solutions has allowed us to choose the optimal labeling conditions for a particular situation.

CHANGES IN UPTAKE OF Ga-67 AND I-125-TRANSFERRIN BY MALIGNANT TRANSFORMATION OF HAMSTER EMBRYO CELLS. J. Saito, A. Muranaka, K. Nagai and Y. Ito. Kawasaki Medical School, Kurashiki and Fukushima Medical School, Fukushima, Japan.

In order to reevaluate the role of transferrin (Tf) and Tf receptors on tumor accumulation of Ga-67, changes in uptake of Ga and I-125-Tf by transformation of hamster embryo (HE) cells were investigated in vitro. The results in HE cells were also compared with those in HeLa S3 and Yoshida sarcoma (YS) cells. HE cells were prepared by trypsinization of mincing 13-day-old whole golden hamster embryos. Transformed HE (HEA-3) cells were obtained in cultures treated with 4NQO and produced malignant transplantable tumors in adult hamsters. Cells were incubated with 1µCi/ml Ga or 0.5µCi/ml I-Tf at 37°C in MEM containing various concentrations of human Tf. Usually 6 hrs later, uptakes per 10^6 cells were measured. When 50-100µg/ml Tf was added to MEM, Ga uptake by HEA-3 increased 3-7 times that in MEM only, showing a tendency similar to HeLa S3. On the other hand, Ga uptake by normal HE showed no marked increase. However, I-Tf uptake by HEA-3 was not greater than that by normal HE and was 1/4-1/3 as much as that by HeLa S3 in MEM only. The number of Tf receptor sites per cell (R:$\times 10^5$) and equilibrium association constant (K:$\times 10^7$ liters/mol) obtained from analysis by Scatchard plot of binding of I-Tf and cells were: normal HE:R=1.6, K=2.5, HEA-3:R=1.1, K=2.2, HeLa S3:R=3.1, K=5.0. When YS cells were rendered nonviable by heating, Ga uptake decreased markedly compared with viable cells in MEM containing 100µg/ml Tf, while I-Tf uptake increased slightly. In conclusion, changes in Ga uptake by transformation of HE cells are presumably affected by the activation of internalization process into cells followed by the binding of Ga-Tf to Tf receptor rather than the changes of Tf receptor per se.

COMPARISON OF In-111 AND I-125 AS LABELS FOR MONOCLONAL ANTIBODY (MoAb) TO A HUMAN HIGH MOLECULAR WEIGHT MELANOMA ASSOCIATED ANTIGEN (HMW-MAA). S.C. Srivastava, R.A. Fawwaz, T.S.T. Wang, J. Elmor, P. Giacomini, S. Ferrone, P. Richards, M.A. Hardy, P.O. Alderson. Brookhaven National Laboratory, Upton, NY and Columbia University, New York, NY.

The properties of In-111 and I-125 as radiolabels for anti-HMW-MAA MoAb were compared in tissue culture and in vivo. The iodogen method was used for radiolabeling with I-125, and DTPA served as a bifunctional chelate for the attachment of In-111. Anti-HMW-MAA MoAb was labeled with either In-111 or I-125 or doubly labeled with both In-111 and I-125. The mean labeling efficiency with In-111 alone was 25% vs 30% with I-125 alone; the efficiencies were 25% and 40%, respectively, in the double labeled preparation. In the in vitro experiments, 10^7 cultured melanoma cells were incubated for 30 min with 1 ug of either In-111 MoAb or I-125 MoAb. The binding of the former was over twice that of the latter (50 vs 23%; $p<0.001$). In the in vivo experiments, nude mice (n=12) bearing subcutaneous human melanoma received 1 to 5 uCi of one of the 3 agents i.v. Biodistribution was compared 4 days post-injection. With In-111 MoAb the mean tumor uptake was 16.1±4.1%ID/g, the mean tumor:blood ratio was 3.9:1 (SD± 0.3) and the kidney and liver were other major sites of activity. With I-125 MoAb the tumor uptake was significantly ($p<0.01$) lower (2.3±0.1%ID/g). With the double labeled MoAb, there was relatively poor tumor uptake of both In-111 and I-125 (2.6±0.2% and 1.4±0.1%, respectively). These differences in tumor cell affinity in vitro and in vivo suggest that In-111 MoAb may be superior to I-125 MoAb for localizing melanoma in patients.

USE OF SPECIFIC ANTIBODY FOR RAPID CLEARANCE OF CIRCULATING BLOOD BACKGROUND FROM RADIOLABELED TUMOR IMAGING PROTEINS. D.A. Goodwin, C.F. Meares, C.I. Diamanti, M.J. McCall, C.D. Lai, F.M. Torti, and B.C. Martin. VA Medical Center, Stanford University Medical Center, Palo Alto, CA, and University of California, Davis, CA.

A major problem when radiolabeled serum proteins, including antitumor antibodies, are used for tumor imaging is a large amount of blood background (Bkg) for several days. Human transferrin (HTrf) and human immunoglobulin (HIgG) were alkylated with the bifunctional chelate reagent 1-(p-bromoacetamidobenzyl)-EDTA. Lyophilized goat anti-HTrf; titer 1:8 total protein 195mg and goat anti-HIgG; titer 1:16, total protein 109.4 mg, were reconstituted in 2ml DI H_2O. The mouse model used BALB/c mice with KHJJ adenocarcinoma in the flank. In 6 mice, In-111 HTrf IV was followed in 18 hrs by 0.2ml (19.5 mg) of anti-HTrf IV in 3, and sacrifice of all 6 at 20 hrs. A similar experiment was performed with In-111 HIgG and anti-HIgG. Anti-HTrf reduced the Bkg to 1/3 with no decrease in tumor concentration (=13%/gm); the Tu/Bl ratio increased from 1.2:1 to 3.4:1. Blood activity was removed by liver with no increase in bone marrow. A high uptake of nonspecific In-111 HIgG was in tumor at 20 hrs; but tumor concentration was less than blood. Anti-HIgG IV reduced blood to 1/50 with no decrease in tumor. Tu/Bl increased from 0.6:1 to 27:1 with the liver picking up the activity. Plasma $Tb_{\frac{1}{2}}$ of In-111 HTrf in the dog was 32 hrs and the y-intercept at 0 time was 56% of injected dose; 90% was cleared 15 min after 60mg anti-HTrf IV. In-111 HTrf (1mCi) dog images after anti-HTrf showed a rapid decrease in Bkg in heart and large vessels in 11 min and an increase in liver. Abdominal images showed a similar rapid drop in Bkg over the gut and kidney areas. Digitized ROI's showed heart fell to 1/6 and liver increased 2.4 times. This technique may be an alternative to Fab fragments, or injection of 2nd radiopharmaceutical for computerized Bkg subtraction. It has the advantage

of allowing a high circulating concentration of tracer until just minutes before imaging (unlike Fab fragments) but it has the disadvantage of producing high liver activity which may preclude tumor localization in this organ.

INDIUM-111 CHELATE CONJUGATES OF TRANSFERRIN FOR TUMOR IMAGING. D.A. Goodwin, C.F. Meares, C.I. Diamanti, M.J. McCall, H.H. Sussman, C.D. Lai, and C.H. Song. VA Medical Center, Stanford University Medical Center, Palo Alto, CA, and University of California, Davis, CA.

Evidence has been accumulating for several years that at least one of the major pathways of tumor uptake of the commonly used tumor scanning agent gallium-67 citrate is via the transferrin receptor. This suggests the use of stably radiolabeled transferrin for tumor imaging. Human apo-transferrin (HTrf) was reacted with BABE (1-p-bromoacetamidobenzyl)-EDTA to yield ≈ 1 chelating group per HTrf molecule. The mouse tumor model employed BALB/c mice with subcutaneously implanted KHJJ adenocarcinoma in the flank. 3 mice were used for each time point at 2 hrs, 4 hrs, 1,2,3 & 7 days following injection. In-111 HTrf concentration in tumor at 24 hrs (≈13%/gm) was greater than any other organ. The bone + bone marrow concentrations were low: (2%/gm). The blood and tumor kinetics of In-111 HTrf and I-125 HTrf were markedly different. In-111 HTrf blood $Tb_{\frac{1}{2}}$ was 33 hrs (r=0.97) and the tumor washout $Tb_{\frac{1}{2}}$ was 72 hrs (r=0.99). The maximum tumor concentration (≈13%/gm) plateaued at 24 and 48 hrs. The tumor-to-blood (Tu/Bl) ratio was >1 at 24 hrs and continued to rise to ≈4:1 at 3 days. A figure of merit: $M=Tu-Bl/\sqrt{Tu+Bl}$, reached a maximum at 72 hrs. I-125 HTrf blood and tumor $Tb_{\frac{1}{2}}$'s were not significantly different (≈18 hrs) and the tumor-to-blood ratios were <1 at all times. This suggests that the former is more stable in vivo and that the more rapid disappearance of I-125 HTrf is possibly due to deiodination. In-111 chelate labeled HTrf has favorable tumor and organ concentrations as well as blood and tumor kinetics that produce high tumor-to-blood ratios. These characteristics suggest a possible future application for imaging a wide spectrum of human tumors.

1:30–3:00 **Room 120**

PEDIATRICS II

Moderator: John R. Sty, M.D.
Co-moderator: Peggy A. Gainey, M.D.

PINHOLE RADIONUCLIDE VENTRICULOGRAPHY IN SMALL INFANTS. D.W. Hannon, M.J. Gelfand, J. Hall, W.W. Bailey S. Kaplan. Radioisotope Laboratory, Department of Radiology, University of Cincinnati and Divisions of Pediatric Cardiology and Cardiothoracic Surgery, Children's Hospital, Cincinnati, OH.

25 pinhole (PH) radionuclide ventriculograms (RNV) were performed in 17 infants to evaluate PH RNV and compare it with RNV performed with general purpose collimation (GP). Infants (ages 3 da-15 mo, mean 6.8; weighing 2.4-8.6 kg, mean 5.4) were studied by Tc-99m in vivo red cell labelling (RBCL) before and/or after cardiac surgery. RBCL failed in a 26th RNV.

PH left ventricular (LV) ejection fraction (EF) was calculated in all 25 studies and ranged from 0.18-0.80. Right atrium (RA) and right ventricle (RV) were at least moderately well separated in 21/25, allowing calculation of RVEF (range 0.24-0.56). In 1/25 RA-RV separation was poor (RVEF =0.20), and in 3/25 the RV was hypoplastic.

In 20 studies both PH and GP were performed. RV-LV separation was adequate in 16/20 GP and 20/20 PH studies. PH and GP LVEF correlated with r=0.70; this was expected as LV edge identification was difficult on GP images.

In only 5 studies both RA-RV and RV-LV separation was achieved by GP. Improved PH magnification and resolution aided in area of interest selection and/or cine interpretation in 19/20 studies.

PH studies were performed in 7 infants with transposition of the great vessels (TGV). RV (systemic ventricle) EF was calculated in all 7 (range 0.26-0.56). However, RVEF could not be calculated in any of the 6 GP studies in TGV infants.

PH RNV is valuable in infants because it provides improved magnification and resolution, allowing calculation of RVEF and LVEF in almost all cases.

EXERCISE RADIONUCLIDE ANGIOGRAPHY WITH PHASE ANALYSIS IN CHILDREN WITH FAMILIAL HYPERCHOLESTEROLEMIA. M.S. Schaffer, D.L. Gilday, M. deSouza, V. Rose, E. Regelink, and R.D. Rwoe, The Hospital for Sick Children, Toronto, Canada.

Hypercholesterolemia and atherosclerosis are identifiable in childhood. Using radionuclide exercise studies and deriving phase statistics, we undertook a study to attempt to detect markers of early coronary and myocardial involvement in young patients with hypercholesterolemia. In twenty-two pediatric patients (14.25 ± 3.11) with familial hypercholesterolemia, normal left ventricular ejection fractions at rest (63.5 ± 4.9) and exercise (80.4 ± 7.2) were obtained. Heart rate and blood pressure at rest and exercise were normal in these patients.

Phase histograms were obtained after a temporal Fourier analysis at the fundamental frequency on a pixel by pixel basis was computed on the filtered multigated studies. Left ventricular phase statistics were derived by masking the ventricle with its respective region of interest. Fifteen patients showed no change or a decrease (13.14 ± 3.09 vs. 9.69 ± 2.42) in phase standard deviation (Group I). Seven patients (Group II) had a significant increase in standard deviation in response to exercise (10.26 ± 1.94 vs. 14.11 ± 1.94). Group II patients were older, had higher mean values for cholesterol, low density lipoprotein cholesterol, and triglycerides, and lower high density lipoprotein cholesterol than Group I patients.

The standard deviation of the phase histogram may be a marker of ventricular asynchrony implying coronary and myocardial involvement in the atherosclerotic process.

VENTRICULAR FUNCTION, MITRAL REGURGITATION AND EARLY PROGNOSIS IN INFANTS AND CHILDREN WITH CARDIOMYOPATHY: A RADIONUCLIDE STUDY. R.A. Hurwitz, A. Siddiqui, D.A. Girod, R.L. Caldwell, Indiana University School of Medicine Indianapolis, IN.

Equilibrium ventriculography was performed on 15 symptomatic patients (ages 10 mos-15 yrs) during initial hospitalization for myocardial disease from July, 1981-Dec, 1982. Seven had primary congestive cardiomyopathy, one had a form of idiopathic hypertrophic subaortic stenosis and 7 had non-rheumatic myopericarditis. Cardiac catheterization (8) and two-dimensional echocardiocardiography (15) disclosed no significant additional morphological abnormalities. Left ventricular ejection fraction (LVEF) was severely depressed in 7/8 cardiomyopathy patients; LVEF was borderline in 3/7 patients with presumed myopericarditis. Left ventricular: right ventricular stroke volume ratio (SVR) was estimated in 14, and ranged from 1.2-2.1 (our normal, < 1.5). No patient had a SVR suggesting more than mild-moderate mitral regurgitation. Of the 7 patients with an initial LVEF <0.30, the clinical course was one of early death in 3 and continued symptoms and gross cardiomegaly in the other four. Those with myopericarditis were all improved and essentially normal. These data suggest: 1) an ominous prognosis for patients with symptomatic cardiomyopathy and markedly abnormal LVEF: 2) a good outlook for children with myopericarditis and borderline LVEF; and 3) only mild mitral regurgitation to be present in children in the early stage of primary myocardial disease. Thus, radionuclide angiocardiography should provide a non-invasive method to evaluate the course and prognosis of children with cardiomyopathic disease.

THE VALUE OF INDIUM-111 WBC SCANNING IN INFLAMMATORY BOWEL DISEASE IN CHILDHOOD. G.C. Vivian, P.J. Milla, and I. Gordon. Hospital for Sick Children, London WC1.

Indium-111 White Blood Cells (In-111 WBC) have been used in the assessment of Inflammatory Bowel Disease (IBD) in adults. We have undertaken a prospective study of In-111 WBC scanning in 10 children with suspected IBD.

Mixed autologous WBC harvested from 10-50mls. blood were labelled with In-111 oxine ($250\mu Ci/1.73m^2$) and reinfused. Anterior and posterior abdominal images were collected at 1, 4 and 24 hours with an LFOV Gamma Camera linked to an Informatek computer. Total colonoscopy, including multiple biopsies, was performed under sedation in all the children. Scans and colonoscopies were

assessed independently in a double blind manner.

The In-111 WBC scan was positive in 7 patients with IBD; 3 of these children were noted to have small bowel involvement in addition to the abnormal colon. 3 In-111 WBC scans were negative. One was associated with a non-specific pancolitis, one with Crohn's disease and one child had a normal colonoscopy and biopsy. The extent of disease as assessed by colonoscopy correlated well with that shown by the In-111 WBC scan.

We conclude that In-111 WBC scanning has a high degree of specificity (100%), sensitivity (77%) and accuracy (90%) in the investigation of IBD in childhood.

ANALYSIS OF GASTRIC EMPTYING STUDIES IN A PEDIATRIC POPULATION. P.R. Rosen, Wilford Hall USAF Medical Center, and S. Treves, Children's Hospital and Medical Center, Boston, MA.

The radionuclide studies of gastroesophageal reflux (GER) and gastric emptying (G-EMP) of 126 pediatric patients (0-16 yrs) were reviewed. Most studies were to evaluate GER in relation to respiratory symptoms or emesis.

Patients received 5% dextrose and water containing a maximum of 1 mCi of Tc-99m Sulfur Colloid after fasting. A gamma camera with a high-sensitivity collimator was positioned posteriorly, with the patient supine. Data was collected in 30 second frames for 60 minutes, with computer acquisition and 2 minute analog images. Visual and computer processing assessed GER. G-EMP was expressed as % residual at 60 minutes determined by the ratio of counts in a ROI corresponding to the gastric image.

The results of these studies were analyzed to assess the relation of G-EMP to age, GER, and symptoms:
(1) When G-EMP is evaluated versus age, there is a significant difference between those less than 2 yrs.,(mean % residual (MPR=54) and those 2-16 yrs., (MPR=30).
(2) There were no significant differences in G-EMP between those with (46) and without (80) GER. The lack of correlation between G-EMP and GER persisted in all age groups.
(3) 9 patients evaluated for apnea and another 9 for abdominal pain had MPR appropriate for age.
(4) The lack of an identified normal population, as well as the wide standard deviation, prevents our establishing normal age related values for G-EMP.

SCROTAL SCINTIGRAPHY FOR THE EVALUATION OF TESTICULAR-EPIDIDYMAL PATHOLOGY. G.N. Sfakianakis, L. Maggiolo, C. Smuclovisky, J. Lockhart, C. Lynne, M. Hourani, V. Politano and A. Serafini. University of Miami School of Medicine, Miami, Florida.

In the patient with acute scrotal edema and pain, torsion of the spermatic cord should be considered; the clinical differentiation from torsion of the appendix testis or epididymitis is often not certain and scrotal exploration is performed to avoid progression of a potentially reversible testicular ischemia. Tc-99m pertechnetate scintigraphy is a reliable diagnostic method helpful in the differential diagnosis.
Of 120 studies, we performed the last 7 years, 82 (equal number of children and young adults) had records with a surgical (S) diagnosis (43) or sufficient follow up information for a clinical (C) diagnosis (39). All patients had an iv injection of 200 μCi/kg Tc-99m-pertechnetate, a flow study (5 sec for 1 min) and 3-4 static images (400K) after appropriate positioning under a regular or small field of view camera with a regular or converging collimator.
Of 18 torsions of the spermatic cord (17S, 1C) 17 showed typical ischemic scintigraphic patterns; the one missed was in a newborn with bilateral necrosis. The 10 torsions of the appendix (S) showed hyperemia (8), ischemia (1) or normal activity (1). The 29 epididymites (3S, 26C) showed hyperemia. The 4 tumors (S) showed a well circumscribed local hyperemia, the 3 hematomas/hydrocele (S) showed focal defects. The 15 scintigrams showing no ischemia or slight hyperemia corresponded to normal or detorsed cases (6S,9C). An absent testis and 2 cases after orcheopexis gave the expected images. This analysis indicates the accuracy of scrotal imaging in the diagnosis of testicular ischemia, and the usefulness of the technique in the differential diagnosis of testicular-epididymal pathology.

1:30-3:00 **Room 275**

COMPUTERS AND DATA ANALYSIS II: MODELS

Moderator: Andrew E. Todd-Pokropek, Ph.D.
Co-moderator: Ronald R. Price, Ph.D.

IDENTIFIABILITY OF A RECEPTOR-BINDING RADIOPHARMACOKINETIC MODEL. D.R. Vera, P.O. Scheibe, K.A. Krohn, and R.C. Stadalnik, University of California, Davis Medical Center, Sacramento, CA; and ADAC Laboratories, Sunnyvale, CA.

The ability to calculate a unique set of physiochemical parameters from radiopharmaceutical uptake data depends upon the validity and identifiability of the kinetic model. Identifiability is a measure of a model's ability to provide precise estimates of the parameters which govern the output of a kinetic system. We have studied the identifiability of a kinetic model for the receptor-mediated binding of Tc-99m-galactosyl-neoglycoalbumin (Tc-NGA), and have found four principle means by which the precision of the parameter estimates may be enhanced: *i*) chemical control of the forward rate constant of binding (k_b), *ii*) molar dose of injected ligand, *iii*) number and positioning of the detectors and, *iv*) independent knowledge of specific parameters.

By simulating the kinetic model under differing conditions we obtained an indentifiability index for the simultaneous estimation of hepatic blood flow (Q), receptor concentration [R], and k_b. Assuming Poisson statistics for the detector data, singular value analysis of the system sensitivity matrix yields coefficients of variation (CVs) for each parameter.

All three parameters could be simultaneously estimated (CV < 10%) if the injected dose contained an amount of NGA capable of occupying at least 10% of the receptor sites, and if the binding rate constant permitted moderate hepatic extraction ($k_b[R] \equiv Q$). At lower injected doses simultaneous estimation of two parameters, Q and [R], can be achieved only if the actual value of the rate constant is known. Lower CVs can be achieved if a set of blood samples or a precordial detector is included in the data.

A METHOD FOR MEASUREMENT OF REGIONAL CEREBRAL BLOOD FLOW USING SHORT-LIVED TRACERS AND EMISSION COMPUTED TOMOGRAPHY. N.M. Alpert, L. Eriksson*, J. Chang, M. Bergstrom+, J.A. Correia, R.H. Ackerman, G.L. Brownell, J.M. Taveras. Massachusetts General Hospital, Boston, MA; *University of Stockholm and +Karolinska Institute, Stockholm, Sweden.

This paper describes a new strategy for measurement of rCBF which rigorously accounts for differing tracer partition coefficients and recirculation, but is convenient for use with PET. Based on the Kety model, the measured tissue concentration, C, can be expressed in terms of the arterial concentration, C_A, the rate constant K and the blood flow f. The local partition coefficient may be computed as p=f/K. In our approach K and f are estimated by the equations:

$$\frac{\alpha\int C(t)dt}{\int t\,C(t)dt} = \frac{\alpha\int\int C_A(u)e^{K(u-t)}du\,dt}{\int t\int C_A(u)e^{K(u-t)}du\,dt}$$

$$f = \frac{\alpha\int C(t)dt}{\int\int C_A(u)e^{K(u-t)}du\,dt} \quad \text{where T = observation period.}$$

Integrals of the form $\int t^n C(t)dt$ can be evaluated by a single reconstruction when the projection data are first weighted by t^n and then summed. For a given input function, C_A, the right side of Eq 1 and the denominator of Eq 2 may be tabulated as a function of K. Eq 1 and 2 permit rapid generation of quantitative K and f images by means of two reconstructions and a table look-up procedure.

Theoretical studies of noise propagation in the estmates were carried out as a function of tomographic count rate, total measurement time and tracer half-life for varying input functions. These studies predict that statistical errors in f of between 5 and 10% at a resolution of 1cm FWHM can be obtained with existing tomographs following IV injection.

To compare theory and experiment, a series of flow studies were carried out in phantoms using the Scandatronix PC-384 tomograph at the Karolinska Institute. These studies demonstrate close agreement among flow and noise estimates in a controlled situation.

The close agreement between theory and experiment as well as the low statistical errors observed suggest this approach may be useful in clinical investigation.

CONTINUOUS INFUSION METHOD FOR DETERMINING LOCAL CEREBRAL METABOLIC RATE IN MAN. M.H. Selikson and R.J. Frost. George Washington University Medical Center, Washington, DC and The Johns Hopkins Medical Institutions, Baltimore, MD.

Recently several methods for measuring cerebral metabolism by evaluating glucose metabolic rate using computed tomography and C-11 or F-18 deoxy-glucose (DG) have been developed. C-11 glucose has also been proposed but does not result in static distribution of tracers suitable for tomographic imaging. DG does result in a static distribution but the method is prone to error due to approximations about the rate constants and the lump constant which cannot be evaluated independently from a single scan. In this paper a continuous infusion method for measuring glucose metabolic rate is presented. The advantage of this approach is that the distributions of tracer are static or pseudo static. In addition, several measurements, each at a different infusion rate, produce enough information to evaluate all the rate constants individually. Blood clearance curves and average values of the rate constants are used to calculate the tissue time curves for C-11 DG. The time required to reach equilibrium in the tissue, the concentration of activity in the tissue at equilibrium and the total amount of activity injected are determined for different rates of infusion. Additional advantages of this alternative approach versus the FDG method are: better counting statistics, shorter procedure duration, measurement repeatability, and increased accuracy.

A GENERAL MODEL FOR THE MEASUREMENT OF METABOLISM WITH ANALOG TRACERS. R.B. Buxton, N.M. Alpert. Massachusetts General Hospital, Boston, MA.

Deoxyglucose (DG) is the prototype analog tracer of metabolism, but the restrictive assumptions of the Sokoloff model of DG kinetics lead to theoretical difficulties when the model is applied to other analogs, such as highly extracted modified fatty acids in the myocardium. We have developed a more general model of analog tracer kinetics which applies to an arbitrary capillary bed, makes no assumptions about the details of capillary-tissue exchange, and is valid for substances with arbitrary extraction fractions. The model expresses the analog tissue concentration (C_T) as a function of time (t) in terms of blood flow (F), arterial analog concentration (C_A), net and one-way extraction fractions (E_n and E) and a single model dependent transfer function (M):

$$(1)\quad C_T(t)=F[E_n+(E-E_n)M(t)]*C_A(t)$$

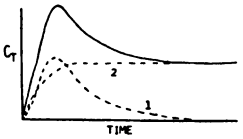

where * indicates convolution.The form of M(t) depends on the details of uptake and metabolism (e.g.,in the DG model M(t) is represented as a single decaying exponential).If C_A decreases rapidly to zero, C_T will have the general form sketched as the solid curve in the figure. C_T is the sum of two terms: a transient, model dependent function [$F(E-E_n)M(t)*C_A$, curve 1] and a model independent function [FE_n*C_A, curve 2]. If F, C_A and C_T are measured, Eq (1) can be used to determine E_n and E.The plateau level, $C_T(\infty)$,can be used to determine $FE_n=C_T(\infty)/\int C_A(s)ds$, independent of the form of M. For the analog to be useful in measuring the metabolism of the native substance the ratio of net extraction fractions of the analog and the native substance (the lumped constant in the DG model) must be known. This work indicates that analogs with high tissue extraction may be used in conjunction with emission tomography to measure regional metabolism.

A COMPREHENSIVE METHOD FOR THE 4-DIMENSIONAL QUANTIFICATION OF ROTATIONAL THALLIUM-201 MYOCARDIAL TOMOGRAMS. E Garcia, K Van Train, J Maddahi, J Areeda, J Friedman, J Bietendorf, A Waxman, D Berman, Cedars-Sinai Med Ctr, Los Angeles, CA; N Clinthorne, University of Michigan Med Ctr, Ann Arbor, MI

Visual interpretation of Tl-201 rotational tomograms is cumbersome and subject to observer variability. Thus we have developed a new computer method to express the relative 4-dimensional (x, y, z and time) myocardial distribution of Tl. At 6 min and 4 hrs after exercise Tl injection, 32 projections were acquired for 30 seconds each over a 180° arc in 11 normals pts (nls) and 13 with CAD (≥50% stenosis). Transaxial cuts were reconstructed using filtered backprojections. Sagittal (sag) and oblique (obl) cuts were obtained along the long and short axis of the left ventricle (LV) using angular transformations of the frame of reference, averaged along the perpendicular axis. Circumferential profiles (CP) of maximum counts were obtained at stress and 4 hrs for each sag cut lying between the endocardial borders of the septal and posterolateral walls and for each obl cut between the endocardial border of the apex and the base of the LV. Washout (W) CPs were calculated as %W from stress for each cut. Five regional lower limits of nl (LLN) for the sag and 5 for the obl cuts were calculated as the mean -2.5 SD from each CP and WCP of the pooled nls. The computer compared each pt's CP and WCP to its corresponding LLN. Analysis considered the entire 360° of each obl cut and the arc between 60° to 120° of each sag cut. Criteria for perfusion defect or slow W abnormality were developed which best separated nls from CAD pts and resulted in the correct identification of all CAD pts and 10/11 nls. This new method of quantifying the 4-dimensional distribution of myocardial Tl-201 appears to provide accurate, objective assessment of CAD.

CINEMATIC DISPLAY OF ORGAN MOTION DURING RESPIRATION WITH IMPEDANCE PLETHYSMOGRAPHY.
SL Heller, SC Scharf, R Hardoff, and MD Blaufox,
Albert Einstein College of Medicine & Montefiore Medical Center, Bronx, New York

Respiratory (RE) motion limits image resolution of mobile organs. A single static image may consist of 10-60 RE cycles. Previous technics to reduce motion artifact either 1) reposition data and ignore organ rotation and plasticity, 2) require face mask (gas leakage, 02 consumption) and patient cooperation, 3) gate on a single respiratory volume, or 4) are limited to ventilation studies.

A technic was developed for obtaining isovolume (iso V) images. Transthoracic impedance (IM), measured using electrodes placed in the anterior axillary line, is monotonically related to lung V. IM is converted to an FM signal with frequency proportional to lung V, simulating a 'Z' signal. Simulated X and Y signals locate 'Z' at the periphery of a computer field-of-view. Studies are recorded in dynamic mode at 3 fr/s for 500s in 64x64 byte mode. Thus, each frame contains a 'Z' count representing a particular phase of respiration. Dividing the 'Z' count range into 10 equal levels permitted creation of 10 iso V images which can be displayed in cine mode.

Forty-seven studies have employed this technic to generate images which illustrate lung or liver motion. Motion-free static images (400K) of the liver clearly improve resolution while lower density studies (100-200k/iso V image) require use of cine display. For all studies, cine improves resolution by moving count profiles across computer pixel borders and by the observer's ability to recognize patterned motion (borders) and differentiate from noise. This new technic offers a potential for improved image resolution in many organ studies.

1:30-3:00 **Room 270**

RADIOASSAY I

Moderator: Arthur Carmen, M.D.
Co-moderator: Benjamin Rothfeld, M.D.

Berson-Yalow Award Abstract

RADIOIMMUNOASSAY OF HUMAN LEUKOCYTE INTERFERON. J.Bernier, A.Reuter, Y. Gevaert, P.Franchimont. Laboratoire de Radioimmunologie, University of Liege, Belgium.

By developing a specific and sensitive radioimmunoassay for human leukocyte interferon, our purpose was to make available, for investigators and clinicians, a simple and direct assay since biological methods are known to be influenced by a great number of factors.

P-IF (Public Health Laboratory,Helsinki) was used for immunizing rabbits. Antisera immunological titers, ranging from 1/10.000 to 1/30.000 at a thirty percent binding level, were

obtained after three monthly intradermal injections. Recombinant leukocyte A interferon (Hoffman - Laroche, Basel) was labelled with I-125. Specific radioactivity was 100 microCi/microgr protein. Specificity studies showed partial cross-reactivity of antisera with lymphoblastoid interferon. Fibroblastic and immune types did not inhibit binding reactions. Sensitivity was inferior to 5 M.R.C. Units/ml when the sequential saturation technique was carried out. Sera of patients with viral infections were assayed: their leukocyte interferon levels were significantly higher than those from a control group ($P < 0.0001$).

Because of the good reproducibility of its results, radioimmunoassay should be a reliable routine method for assaying human leukocyte interferon in several biological fluids or tissues.

CREATINE KINASE-MB IMMUNORADIOMETRIC ASSAY TO DIAGNOSE MYOCARDIAL INFARCTION FOLLOWING AORTO-CORONARY BYPASS SURGERY. E.G. DePuey, A.E. Aessopos, L.R. Monroe, W.L. Thompson, R.J. Hall, and J.A. Burdine. Baylor College of Medicine and St. Luke's Episcopal Hospital, Houston,TX.

Perioperative myocardial infarction (POMI) is difficult to accurately diagnose following open heart surgery due to ECG abnormalities and nonspecific elevations of standard "cardiac" enzymes which routinely occur. Following aortocoronary bypass creatine kinase (CK)-MB was measured serially in 144 non-randomly selected patients (pts) at 0, 8, 16, 24, 48, and 72 hrs using a new two-site immunoradiometric assay (MB-IRMA) (EMBRIA®). SGOT, LDH, total CK, and CK-MB by electrophoresis (MB-elect) were also measured serially. POMI was diagnosed in 24 pts (17%) by new ECG Q waves and/or new wall motion abnormalities detected by gated radionuclide ventriculography.

In pts without POMI, MB-IRMA (mean ± 1 standard deviation) was elevated to 6.4 ± 4.9 equivalent units/liter (EU/L) at 0-8 hrs but decreased to 3.4 ± 1.3 EU/L by 16 hrs. In pts with POMI peak values occurred at 16-24 hrs (21.0 ± 19.8 EU/L), allowing optimal discrimination from pts without POMI at that time ($p<.00001$). By increasing the threshold value of 5.0 EU/L used for non-operative pts to 8.5 EU/L for post-bypass pts, 97% of those with POMI were correctly identified at 16-24 hrs (sensitivity = 88%, specificity = 99%). Discriminant analysis demonstrated that MB-IRMA was superior to each of the other assays or combinations thereof using previously empirically determined threshold values for this institution (MB-elect = 50 IU/L; total CK = 1000 IU/L; SGOT = 200 U/L; LDH = 500 U/L) (all p's <.06). Using threshold values retrospectively optimized for this study population (MB-elect = 85 IU/L; total CK = 1328 IU/L; SGOT = 154 U/L; LDH = 456 U/L), MB-IRMA accuracy was also greater (p's <.05 for all but MB-elect, for which p was not significant). We conclude that MB-IRMA is a valuable adjunct in the diagnosis of POMI.

COMPARISON OF METHODS FOR CK-MB DETECTION IN SUSPECTED ACUTE MYOCARDIAL INFARCTION (MI). J. E. Freitas, E. Epstein, J.D. Ferry, A. M. Hauser, R. E. Karcher and G.T. Timmis. William Beaumont Hospital, Royal Oak MI.

Since prompt, accurate determination of serum CK-MB is essential for MI detection, we compared two new methods for determination of CK-MB in 60 patients admitted for suspected acute infarction. Serum samples were obtained on admission and at six hour intervals thereafter for one-two days. The new methods evaluated were two-site sandwich immunoradiometric assay (Embria-CK), and enzymatic 2-step immunoinhibition, immunoprecipitation assay (Isomune-CK).

The diagnosis of myocardial infarction was based on electrocardiographic findings, presence of CK-MB by gel electrophoresis, and other clinical findings of the attending cardiologist.

Assay results in the 60 patients (33 MI, 27 non-MI) are shown below:

	Embria-CK (>4 EU/ml)		Isomune-CK (>10 U/l)		Electrophoresis (Present)	
	+	-	+	-	+	-
MI (33)	33[5]	0	31[1]	2	32	1
Non-MI (27)	1	26	0	27	0	27

There is no significant difference in sensitivities or specificities of the three methods in this small study population. Five patients by Embria-CK and one patient by Isomune-CK (shown in brackets) remained + for a longer time than the other methods. Of these three methods for CK-MB determination, Embria-CK may be preferable because of sensitivity, longer detectability and ability to quantitate infarct size.

MEASUREMENT OF PLASMA P-97 LEVELS IN MELANOMA PATIENTS USING A NEW RADIOASSAY. J.C. Reynolds, B. Mestvedt, S.M. Larson, P. Beaumier, J.A. Carrasquillo, I. Hellstrom, K.E. Hellstrom. Seattle VAMC, University of Washington and Fred Hutchinson Cancer Center, Seattle, WA.

A sandwich radioimmunoassay (RIA) using two monoclonal antibodies (McAb) has been developed to measure the melanoma associated antigen P-97 in plasma. The F(ab) fragment of McAb 96.5 which is specific for epitope P-97A was labeled with I-125 using chloroglycouril. Whole McAb 8.2 specific for epitope P-97C was coupled to polyacrylamide beads with carbodiimide. A plasma membrane lysate of culture melanoma 1477 served as standard. In the assay, precipitable counts were linearly proportional to antigen concentration from 0.1 to 5 ng.. Dilution of normal sera gave linear dose response values in the assay.

In patients with widely metastatic melanoma (n=6) plasma P-97 levels were 10.1±4.0 ng/ml whereas in hospitalized controls (n=11) and normal adults (n=4), the plasma levels were 5.7±1.7 ng/ml and 5.1±1.3 ng/ml, respectively. The values for the six melanoma patients were 9.8, 4.0, 6.4, 11.8, 14.6, 13.7, ng/ml.. The new radioimmunoassay thus measures P-97 levels in normal and melanoma patients. There is a trend to higher P-97 values in patients with large tumor burden and we are therefore evaluating the possibility that this assay will be helpful in monitoring tumor progression.

CLINICAL EVALUATION OF A NEW SOLID PHASE SEQUENTIAL RADIOIMMUNOASSAY FOR FREE T_4. A.V. Heal, F.S. Ashkar, H. Khan. University of Miami School of Medicine, Miami, FL

Free T_4 (FT_4) is the active portion of thyroid hormone in contact with the target organs. It is unaffected by alterations in binding protein levels, and the measurement of FT_4 should reflect true thyroid function or dysfunction. While most of the present radioassay methodologies provided satisfactory screening information, they failed to perform satisfactorily in some clinical situations. The purpose of this study was to clinically evaluate this new FT_4 in the absence and presence of other clinical problems and compare it to other thyroid function tests.

The FT_4 test evaluated was a solid phase sequential radioimmunoassay requiring approximately 2.5 hrs for completion. A total of 370 patients were studied and consisted of the following groups: euthyroid, hyperthyroid, hypothyroid, pregnancy (1st and 3rd trimester), non-thyroidal illness (NTI) varying triglyceride and cholesterol levels and dilantin medication.

The FT_4 correlated well in all groups except NTI with other thyroid function tests and the patients clinical diagnosis . In NTI the FT_4 results were decreased with only 80% correlation with the diagnosis. This correlation however was equivalent to the FTI and only the normalized T_4 had a better correlation (94%). The intra-assay CV's for 30 samples were 12.5%, 8.6% and 9.2% ($\bar{x}$ = 0.3, 1.35 and 2.57 ng/dl respectively).

This FT_4 procedure was found to be useful as a screening test and also as a primary thyroid function test, but still suffered from lack of correlation in certain clinical situations. When compared to other thyroid function tests it was equivalent to FTI, but not as good as the normalized T_4.

A MODIFIED RADIOIMMUNOASSAY FOR THE DIFFERENTIAL DETECTION OF IgM-ANTI-HBc. Y.F. Liaw, C.M. Chu, M.J. Huang, L.H. Lin. Chang-Gung Memorial Hospital, Taipei, Taiwan, R.O.C.

The standard radioimmunoassay for anti-HBc (CORAB) was modified for the differential detection of IgM-anti-HBc by incorporation of a step in which IgG-anti-HBc was preferentially absorbed by Staphylococcus aureus cells (Protein A). The ratio (R) of IgM-anti-HBc to total

anti-HBc is evaluated by computing the ratio of sample cpm's after and before protein A absorption. The R values of acute B hepatitis ranged from 0.9 to 2.1 (mean 1.32 ± 0.3) while those of chronic HBsAg carriers ranged from 3.1 to 11.6 (mean 5.72 ± 1.87). Adopting 2.1 as the upper limit of R value for acute B infection, this modified CORAB was shown to be capable of differentiating acute from past HBV infection in HBsAg positive patients, and discriminating acute B hepatitis from non-A, non-B hepatitis in HBsAg negative but anti-HBc positive acute hepatitis.

3:30-5:00 **Room 123**

CARDIOVASCULAR CLINICAL V: TI-201 IMAGING

Moderator: B. Leonard Holman, M.D.
Co-moderator: Robert S. Gibson, M.D.

COMPARISON OF PREDISCHARGE EXERCISE TESTING, THALLIUM-201 SCINTIGRAPHY AND CORONARY ANGIOGRAPHY FOR IDENTIFYING POST-INFARCTION PATIENTS AT RISK FOR FUTURE CARDIAC EVENTS.
R.S.Gibson,D.D.Watson,R.S.Crampton,M.J.Denny and G.A.Beller. University of Virginia, Charlottesville, Virginia

To determine if patients(pts)at risk for future cardiac events(CE)can be identified after acute MI, 140 consecutive pts underwent submaximal exercise testing(SMTX),quantitative Tl-201 scintigraphy(SCINT)and coronary angiography(CA)before hospital discharge. Pts were considered at high risk(HR)if: SMTX=S-T seg depression(ST ↓)or angina;SCINT=redistribution (Rd),defects in > 1 specific vascular region or increased lung uptake(↑ LU);CA=2 or 3 vessel disease(VD)(stenosis ≥ 50%). Low risk(LR) was designated if:SMTX=no ST ↓ or angina;SCINT=single region defect, no Rd or ↑ LU; CA=1VD. By 16 ± 11 months, 50 pts had a CE including 7 deaths, 9 reinfarctions and 34 pts with unstable angina. The predictive accuracy (table) for identifying HR pts were comparable using the 3 techniques, but SCINT was a better indicator of LR compared to SMTX or CA ($p < .01$).

	SMTX		SCINT		CA	
	HR	LR	HR	LR	HR	LR
Total CE Rate(pts)	28/57	22/83	47/91	3/49	37/82	13/58
(%pts)	(49)	(26)	(52)	(06)	(45)	(22)

Of 13 pts with 1VD by CA who had a CE, 12(92%) had Rd on SCINT. HR markers by SCINT detected 47 of 50 pts(94%) experiencing a CE compared to only 28 pts with SMTX(56%; $p < .0001$)and 37 pts with CA(71%; $p < .006$).

Thus, (1)SCINT markers of high risk were more sensitive than either SMTX or CA for identifying future CE;(2)SCINT was useful in detecting 1VD pts at high risk for a future CE; and (3)a group of low risk pts having only a 6% CE rate (2% mortality) can be identified by demonstrating a single region SCINT defect, no Rd or ↑ LU.

DETECTION AND LOCALISATION OF SINGLE VESSEL CORONARY DISEASE: BIPLANAR EXERCISE RADIONUCLIDE VENTRICULOGRAPHY OR TL-201 MYOCARDIAL IMAGING?
P.J. Currie, M.J. Kelly, V. Kalff, Y.L. Lim, and A. Pitt. Alfred Hospital, Melbourne, Australia.

The ability of biplanar (BIP) radionuclide ventriculography (RVG) and 4 view Tl-201 myocardial perfusion imaging to detect and localise myocardial ischemia with maximal graded supine and erect bicycle exercise respectively was compared in 45 patients (pts) with angina, single vessel coronary disease (SVD) of ≥50% stenosis and no prior myocardial infarction. Anti-anginal medications were ceased before exercise. A BIP collimator was used for RAO gated first-pass imaging at rest and maximal exercise and LAO equilibrium imaging at rest and at graded workloads. RVG wall motion abnormalities and Tl-201 perfusion defects were assigned to left anterior descending (LAD), circumflex (LCX) or right coronary artery (RCA) by agreement of 2/3 independent blinded observers. All studies were read concurrently with those from control subjects with chest pain and normal coronary angiograms. The specificities were 90% (38/42) for RVG and 93% (13/14) for Tl-201. Of the 45 pts with SVD, 32 had ≥ 1mm ECG ST depression with RVG and 15 with Tl-201 ($p < 0.001$). Abnormalities correctly assigned/total detected were:

Stenosed Vessel		Tl-201	LAO RVG	BIP RVG
LAD	n=28	17/17	17/22	20/24
LCX	n=6	3/3	3/4	3/5
RCA	n=11	3/3	0*/3	5/6
Total	n=45	23/23*	20/29	28/35

* = $p < 0.05$ versus BIP RVG.

BIP RVG is more sensitive than Tl-201 in detecting exercise induced myocardial ischemia in pts with SVD. Although BIP imaging improved RVG localisation for RCA, Tl-201 still localised abnormalities better. The ECG results suggest that the greater sensitivity of BIP RVG may be due to greater ischemia produced by exercise in the supine posture.

BAYESIAN ANALYSIS USING FOURIER TRANSFORMS OF Tl-201-SCINTISCANS TO PREDICT THE PRESENCE OF CORONARY ARTERY DISEASE.
W.R. Tzall, R.R. Sciacca, D.K. Blood, D.M. McCarthy, J.C. Feder, P.O. Alderson and P.J. Cannon. Columbia University, New York, NY and Univ. of Penna., PA.

A non-visual, objective method for interpretation of Tl-201 myocardial perfusion scans was previously developed using 2 dimensional Fourier transforms of 30° LAO exercise and redistribution scans. A discriminant function was created using Fourier amplitude coefficients obtained from the transforms to detect the presence of coronary artery disease (>70% luminal narrowing of at least one major coronary artery). The discriminant function was developed using a population consisting of 110 patients with coronary artery disease (CAD) and 64 controls. In the present study, the discriminant function was applied prospectively to 100 consecutive patients who had exercise Tl-201 myocardial perfusion and redistribution scans between January 1980 and July 1981 and who also had coronary angiography within 6 months of the scans. There were 83 patients with CAD and 17 controls. For each patient an a priori probability of CAD was determined from the patient's age, sex, and anginal symptoms. These probability estimates were combined with the discriminant function predictions using Bayes theorem. The presence of CAD was predicted with 88% accuracy; 74 of 83 CAD patients and 14 of 17 controls were correctly classified. Furthermore, 48% of the CAD patients were predicted to have CAD with a probability exceeding 99%. In summary, Bayesian analysis using a discriminant function incorporating Fourier transforms of Tl-201 scans provided an objective technique for scan interpretation which had an 88% accuracy in a prospective series of patients evaluated for CAD.

DETECTION AND QUANTITATION OF REMOTE MYOCARDIAL INFARCTION BY TOMOGRAPHIC EXERCISE-REDISTRIBUTION TL-201 SCINTIGRAPHY.
B. Massie, J. Wisneski, I. K. Inouye, M. Hollenberg, E. Gertz, S. Henderson. VAMC and University of California, San Francisco.

The ability of exercise redistribution TL-201 scintigraphy to diagnose and quantitate old myocardial infarction (MI) has not been studied. Therefore we, performed exercise and 3 hour redistribution scintigrams by 7 pinhole tomography in 60 patients undergoing coronary and right anterior oblique left ventricular angiography. Fifty had significant coronary disease (CAD); 27 had old MI by history ECG, or angiography. Circumferential profiles were generated from 3 left ventricular slices. Normal limits were derived from 15 volunteers deemed free of CAD by noninvasive testing. Ischemia was quantitated from the area between exercise and redistribution profiles. MI was diagnosed if the redistribution profile fell below the normal limits over a 30 arc except in the regions with near complete (>80%) redistribution. MI was quantitated from the area between the redistribution profile and the normal limits for redistribution.

MI was detected in 22/27 patients (81% sensitivity) and misdiagnosed in 2 patients with severe ischemia and considerable (70-80%) redistribution (91% sensitivity). Missed MI's were all inferior, and ECG and ejection fraction (EF) were normal in 4/5. MI score and EF correlated inversely ($R=-.79$, $p<.001$). This improved to $R=-.90$ if the 7 PTS whose posterolateral MI was probably underestimated by single plane angiography were excluded. Only 1/15 patients with an abnormal EF (<55%) had a score < 500 units, and only 2/12 patients with an EF > 55% had a score > 500 units ($p<.001$). Thus, exercise-redistribution TL-201 scintigraphy can diagnose previous MI and quantitate the degree of resulting left ventricular dysfunction.

QUANTITATIVE TL-201 IMAGING BEFORE AND AFTER TRANSLUMINAL CORONARY ANGIOPLASTY (PTCA).

O.Pachinger, H.Sochor, E.Ogris, P.Probst, M.Klicpera, F.Kaindl.
Dept. of Cardiol., Univ. Vienna, AUSTRIA

46 pts having undergone PTCA (39 LAD, 6 RCA, 1 CX) were studied by quantitative TL-201 stress imaging to assess the functional result of this intervention. 38 pts were studied pre, 27 pts pre+post PTCA and 11 only post PTCA, all within 2 weeks after PTCA. 11 pts had follow-up studies after 6 months. Angiographic passage rate was 68%. After circumferential profile analysis the %-CTS in the area of the dilated vessel, a redistribution index (RD=S/R) and %washout (WO=S-R/S) served as quantitative parameters. Comparison with pressure gradient and luminal diameter change showed close correlation for change of RD (r=-.68) and WO (r=-.76). Decrease of RD and increase of %-CTS (pre: 38±19, post: 61±14, p<0.001) and WO indicate positive result. Comparative accuracy of correct prediction of the vessel status was 76% for only post-PTCA, 74% for pre+post-PTCA (qualitative). Quantitative analysis improved prediction to 94% for pre+post-PTCA data. Partial success and recurrent stenosis only can be evaluated with pre + post-PTCA studies. Quantitative evaluation including washout analysis enhances the possibilities of TL-201 scintigraphy in PTCA pts, in whom follow-up studies are essential. TL-201 imaging successfully can evaluate the functional status of the dilated vessel area and can assess the efficacy of PTCA.

INTRACORONARY Tl-201: SHORT ACQUISITION GATED MYOCARDIAL SCINTIGRAPHY. M.E. Siegel, P. Colletti, P. Thom, P.A.N. Chandraratna, and S.H. Rahimtoola. USC School of Medicine, Los Angeles, CA

Visualization of ventricular walls at rest and during exercise with true global motion and myocardial thickening is not possible using present techniques. If Tl-201 is injected intracoronarily, 100% reaches and 85% localizes in myocardium with higher count rates than when given IV, perhaps permitting acceptable acquisition times for gated true wall motion studies. We describe a new technique using intracoronary Tl-201 to acquire high count rate, high contrast, short acquisition time gated wall motion studies.

Thirteen patients were studied. Six/thirteen also had rest/stress IV Tl-201 studies. After coronary angiography, 0.75 mci of Tl-201 was injected into each coronary. Multiple sequential 1 min gated studies were obtained in LAO and RAO projections, followed by sequential 5 min images for 2 hours to determine Tl-201 redistribution kinetics. ROI's over segments of left and right ventricles and background defined temporal and spatial distributions.

Myocardial to background ratios are as high as 13:1, $\bar{x}$ 11:1 compared to 2-3:1 from IV studies. $T_{\frac{1}{2}}$ washout in normal myocardium is 95 ± 5 min. Gated studies are acquired in 3 min with a total count of 1600 K. Perfusion defect size and presence is quite different on diastolic, systolic, nongated and IV studies. Apparent alterations in wall thickness during the cardiac cycle are visualized.

Short acquisition wall motion and high resolution perfusion images obtained by this new technique may be a useful adjunct to the blood pool and coronary anatomy acquired in the cath lab.

3:30-5:00 **Room 275**

CORRELATIVE IMAGING

Moderator: Leonard M. Freeman, M.D.
Co-moderator: Letty G. Lutzker, M.D.

COMPARISON OF SINGLE PHOTON EMISSION COMPUTED TOMOGRAPHY (SPECT) WITH PLANAR SCINTIGRAPHY (PS) AND TRANSMISSION COMPUTED TOMOGRAPHY (CT) IN FOCAL HEPATIC DISEASE (FHD). A.J. Brendel, F. Leccia, J.C. Philippe, F. Lacroix, J.L. Barat, D. Ducassou, Hôpital Univ. Haut Lévêque, Bordeaux, France.

The main purpose of this study was to compare the clinical value of SPECT and PS in FHD. These techniques were also compared with CT.

SPECT and PS were performed in 36 patients and 10 normal volunteers, by using the commercial CGR Gammatome. PS included 5 views. SPECT data were collected during 20 min from 64 projections (360° rotation). Reconstructions of 0.6 cm transverse, sagittal and coronal slices were obtained. CT was performed on the same day in the 36 patients, by using a GE CT/T 8000. Subsequent findings proved that 20 of the patients had FHD. The relative accuracy of SPECT and PS was assessed independently by means of ROC curve analysis performed by 2 "blinded" observers (Obs) using a 1-5 rating scale. In addition, the sensitivity and specificity were calculated by defining a score of 4 or 5 as positive and a score ≤ 3 as negative. CT was interpreted independently and its results analysed in a standard manner.

	PS		SPECT		CT
	Obs1	Obs2	Obs1	Obs2	
Sensitivity (%)	85	80	85	90	90
Specificity	85	96	100	92	100

Statistical analysis (sign test) showed no significant difference between these results. However for both observers, the SPECT ROC curves were displaced upwards and to the left in comparison with PS curves. In addition, SPECT detected more lesions than PS in multiple FHD.

Thus, for detection of FHD, 1) SPECT appears more accurate than PS. 2) SPECT accuracy seems comparable to that of CT.

QUANTITATION OF MYOCARDIAL NECROSIS WITH Tc-99m-MONOCLONAL ANTIMYOSIN Fab AND SINGLE PHOTON EMISSION TOMOGRAPHY. T. Yasuda, B.A. Khaw, H.K. Gold, R.H. Moore, J.T. Fallon, J.S. Zielonka, J.L. Guerrero, R.C. Leinbach, K.A. McKusick, H.W. Strauss, E. Haber. Massachusetts General Hospital, Boston, MA.

To define the extent of infarction when reperfusion is performed requires a marker of myocardial necrosis. This study was undertaken to measure necrosis (N) by Tc-99m-monoclonal antimyosin Fab (Tc-AM) in 6 (20 kg) dogs undergoing a 3 hour ligation of the left anterior decending coronary artery with subsequent reperfusion. Ten minutes after reperfusion, 8 mCi of Tc-AM was given intravenously. Single photon transverse section images (SPT) were recorded 4 to 8 hours later. Data were collected in 3 degree increments for 360 degrees (120 images), at 40 seconds per angle (imaging time = 80 minutes). Images were recorded in a 128x128 matrix with a linear calibration factor of .287 cm per pixel and a rotation radius of 20 cm. Multiple SPT slices of 1.5 cm thickness were reconstructed. The area of N, delineated by Tc-AM was identified by 2 observers. The N was outlined slice by slice and then expressed as total pixel volume. On day 10 the dog was killed and the infarct volume determined by integrating the extent of necrosis from pathology. The results are shown below:

INFARCT VOLUME Dog	1	2	3	4	5	6
Tc-AM pixel No.	559	212	0	0	164	350
Pathology gm	18.2	1.0	0	0	3.8	7.7

Pathology gm = -1.5 + .031 Tc-AM pixel□, r=.94

In conclusion, this study demonstrates a close correlation between infarct volume by pathology and Tc-AM-SPT, and should permit quantification of infarct size.

DETECTION OF MASSES IN THE SUBPHRENIC SPACE. S.D. Johnson, M.K. Loken, J.R. Tennison, D.K. Mielke, and M.P. Frick, University of Minnesota Hospitals, Minneapolis, MN.

The detectability of unit density masses in the subphrenic space of dogs has been studied using techniques of Nuclear Medicine (camera imaging and ECT using a GE 400A system) and Radiology (TCT using a Pfizer 0450). A bifid plastic sack was fabricated and fitted around the triangular ligament in each of three anesthetized dogs. A catheter was attached to each sack and brought to the surface to permit various volumes of water (up to 100 ml) to be instilled during the study. Each animal then received six millicuries each of 99m-Tc sulfur colloid and 99m-Tc MAA by I.V. injection. Standard camera, ECT, and TCT images were obtained for each of several volumes added to the

sack. The dogs breathed normally while standard camera and ECT images were obtained. TCT images were obtained during apnea. Without fluid added, the sacks remained flat along the liver surface and could not be detected as a "mass" by any of the imaging modalities. The smallest added volume detectable by standard camera imaging was 25 ml. The transaxial views of ECT demonstrated volumes as low as 10 ml although the identification of this size "mass" was made somewhat easier when viewing either coronal or sagital reconstructions. Ten ml volumes were also visible on transaxial TCT slices; however, the relatively small density gradient between liver tissue and water made the interpretation of these scans quite difficult. We find that ECT is better than either standard camera imaging or TCT for the detection and the deliniation of small unit density masses in the subphrenic space.

PLANAR VERSUS TOMOGRAPHIC IMAGING WITH Tc-99m PPi FOR DETECTION OF ACUTE MYOCARDIAL INFARCTION IN PATIENTS. MH Lewis, JR Corbett, SE Lewis, TR Simon, EM Stokely, JT Willerson. Univ. Texas Hlth Sci Ctr, Dallas, TX

Technetium-99m pyrophosphate (Tc-99m PPi) scintigraphy is a sensitive indicator of acute myocardial infarction (MI), but superimposed structures can obscure MI in planar scans (PL). Tc-99m PPi tomography (TO) eliminates superimposition; thus, we compared MI detection from PL and TO. Eighty-nine patients (pts) were studied: 47% had transmural MI (Trans), 30% had non-transmural MI (NT), and 23% had no MI, as established by nonimage criteria. TO was done with a rotating gamma camera (32 views, RAO to LPO) after PL. The images were separately coded and randomized for reading by 3 independent observers. Scaled readings indicated confidence that MI was present or absent. Selected pts were read twice; intra-observer correlation ranges were: r=0.96-0.97 for PL (N=11,p<.01), and r=0.94-0.98 for TO (N=13,p<.01). Accuracy (% correct) values for pt subgroups were:

	PLANAR				TOMOGRAPHIC			
	NoMI	Trans	NT	AllPts	NoMI	Trans	NT	AllPts
Obs#1	84%	69%	33%	61%	85%	74%	52%	70%
Obs#2	79	88	74	82	60	93	67	78
Obs#3	40	98	85	81	53	93	82	81

Receiver operating characteristic analysis showed no significant difference between PL and TO for any observer. Blood pool activity and reconstruction noise with TO may contribute to difficulty in distinguishing NT from no MI. TO may also show MI in some pts without other clinical evidence of the event. Further work is needed to refine the TO technique.

CORRELATION OF In-111-LEUKOCYTE (In-WBC) AND GALLIUM-67 (Ga-67) SCINTIGRAPHY WITH TRANSMISSION COMPUTERIZED TOMOGRAPHY (CT), ULTRASONOGRAPHY (US) AND PLANE RADIOGRAPHY (R) IN THE DIAGNOSIS OF FOCAL INFECTION.G.Sfakianakis,W. Al-Sheikh, G. Spoliansky, A. Heal, M. Hourani, F.Ashkar and A. Serafini University of Miami School of Medicine, Miami, FL.

Correlation of imaging modalities in the specific diagnosis of focal sepsis was performed retrospectively. Of 100 patients who had In-WBC and Ga-67 scintigraphy, 51 were studied for an abdominal infection and had either a CT (42), an US (30) or both (21) and 22 patients were studied for a bone infection and had Tc-99m-Methylenediphosphonate bone scintigraphy and plane radiography.

For intraabdominal and abdominal wall infection (24 foci diagnosed) Ga-67 had the greatest sensitivity (S,95%); In-WBC (S,67%) missed subacute or chronic infections and CT (S,58%) and US (S,67%) missed phlegmons and wound infections. In WBC had the highest specificity (Sp,96%); Ga-67 (Sp,54%) showed activity in healing wounds and normal bowel not easily differentiated from infectious foci; CT (Sp,52%) and US (Sp,72%) misdiagnosed loculated aseptic fluid and postoperative or post-traumatic sequellae, but aspiration improved their specificity.

For chronic bone infection (10 cases) with or without previous orthopedic intervention Tc-99m-MDP bone scintigraphy had the highest sensitivity (100%) and worst specificity (17%). Plane radiography showed the highest specificity 75% but rather low sensitivity (70%). In-WBC (S, 80% and Sp, 58%) and Ga-67 (S,80% and Sp, 42%) did not improve the diagnosis adequately.

More selective application of the imaging modalities can improve the diagnosis of focal infection.

RADIONUCLIDE HYSTEROSALPINGOGRAPHY: A PROMISING NEW TECHNIQUE FOR EVALUATION OF FALLOPIAN TUBE PATENCY. R. Egbert, M. McCalley, S.C. Stone, P. Braunstein,Division of Nuclear Medicine and Dept. of OB/GYN, University of California, Irvine, Medical Center, Orange, CA.

More than 12 patients were studied for tubal patency using a radionuclide technique for hysterosalpingography. One mCi of Tc-99m labeled human albumin microspheres was deposited into the posterior fornix of the vagina of each patient-volunteer, followed by placement of a non-absorbing tampon. The patient then dressed and walked to the Nuclear Medicine Department. Gamma camera images using a pinhole collimator with varying degrees of caudal angulation obtained 30 minutes to 4 hours later demonstrate concentration of activity on an ovary if the ipsilateral fallopian tube is patent. The dose to the ovary is estimated to be 18.2 mR. In the initial 12 patients studied with this technique the correlation with anatomic data consisting of either a contrast hysterosalpingogram or intraoperative observation of transit or failure of transit of methylene blue dye from uterus to peritoneum was 96%. This is a relatively non-invasive technique which had ready patient acceptance. While it does not allow for the visualization of tubal anatomy, it may give a more physiologic understanding of tubal capacity to transport material from the vagina to the fallopian tubes and the ovaries.

3:30–5:00 **Room 130**

GASTROINTESTINAL III: BILIARY & ESOPHAGEAL IMAGING

Moderator: Leon S. Malmud, M.D.
Co-moderator: Gary G. Winzelberg, M.D.

THE NORMAL RELATIONSHIP BEWTEEN GASTRIC AND GALLBLADDER EMPTYING TO A SOLID MEAL: J.N.Baxter, J.S.Grime, M.Critchley, and R.Shields. Royal Liverpool Hospital, Liverpool. U.K.

Little is known about the normal relationship between gastric emptying (GE) and gallbladder emptying (GBE). We investigated this relationship in 22 normal adults using a dual isotope technique. 74MBq of Tc-99m-EHIDA were given i.v. following which gallbladder (GB) filling was monitored with a LFOV gamma camera-computer system. After activity in the GB ROI plateaued (52±1min), the subject ate a solid meal containing bran labelled with 9.2MBq of In-113m. GE was then recorded simultaneously with GBE. Window settings were Tc-99m:10% and In-113m:20%. Data were collected on a 64x64 matrix at a rate of one frame/minute.

GE was monoexponential with a T1/2 of 40±3min whereas GBE followed a double exponential function. GBE in 15 subjects started 1.4±0.8min after the commencement of eating then subsequently they emptied 15.2±1.7% of GB contents before GE began. These 15 subjects could also be divided into two subsets based on the T1/2 of the first exponential i.e. Type I (n=9) T1/2=9.6±1.5min, and Type II (n=6) T1/2=44.4±6.5min (P<0.001). The remaining 7 subjects began spontaneously emptying their GB's 33.5±3.7min after the EHIDA injection.

We conclude that (1) GBE occurs in response to a solid test meal according to a double exponential function (2) the results suggest a cephalic phase to GBE exists and (3) there appear to be variations in matching between GBE and GE.

OPTIMIZATION OF CERULETIDE INTRAVENOUS DOSE FOR GALLBLADDER (GB) EMPTYING. G.T. Krishnamurthy, F.E. Turner, D. Mangham, V.R.Bobba, S.A. White, K. Langrell. VA Medical Center and Oregon Health Sciences University, Portland, OR.

The decapeptide ceruletide is approved by FDA for intramuscular use and its intravenous dosage for GB emptying in humans is not known. This project was undertaken to establish reliably the dose response curve for intravenous use. Twenty healthy adult volunteers were divided into 4 groups of 5 each. After an overnight fast each subject received 2 mCi of Tc-99m-DISIDA intravenously (IV) and was positioned 60 minutes (min.) later under a LFOV gamma camera fitted with LEAP collimator. The data was acquired at 1 frame/minute for 30 minutes. Saline placebo at 5 min. and 1, 5, 10 or 15 ng/kg of ceruletide at 10 min. was infused over a 3 minute period. From the net GB curve, the latent period (LP), ejection period (EP), ejection fraction (EF) and ejection rate (ER) were calculated.

The mean, LP, EF and ER were similar for all groups. The EF for 1, 5, 10 and 15 ng/kg groups were 19.4 ± 11.7%, 59.6 ± 26%, 55 ± 23.3%, and 67.8 ± 8.7% respectively. Only 1 of 10 subjects receiving 1 and 5 ng/kg experienced slight nausea, while 5 of 10 subjects receiving 10 and 15 ng/kg dose experienced nausea, abdominal cramps, transent, hypotension and bradycardia. It is concluded that 5 ng/kg of ceruletide produces a mean GB EF of 59.6%, and should be preferred as the optimal intravenous dose.

SIMPLIFIED SCINTIGRAPHIC TECHNIQUE FOR ESTABLISHING DOSE RESPONSE CURVE OF A CHOLECYSTOKINETIC AGENT. F.E. Turner, G.T. Krishnamurthy, V.R. Bobba, K. Langrell. VA Medical Center and Health Sciences University, Portland, OR.

The main objective of this project was to test whether the dose response curve of a cholecystokinetic agent (ceruletide) could be established by administering graded doses sequentially on a single day. The results are compared to individual doses given on separate days. After a 2 hour fast, each of five anesthetized rabbits was given 0.5 mCi of Tc-99m-IDA intravenously (IV). At 60 minutes the animal was positioned under a gamma camera fitted with a LEAP collimator. The data were acquired on a 2.5 times zoomed 64x64 computer matrix at 1 frame/minute for 70 minutes. In a single dose study, 2.5, 5 or 10 ng/kg of ceruletide was infused IV over a 3 minute period on separate days. In the sequential study, the ceruletide doses of 2.5, 5 and 10 ng/kg were infused over 3 minutes sequentially at 5, 20, and 35 minutes on the same day.

The regions of interest were chosen, over the entire GB and the liver as background. The ejection fraction (EF) was calculated from the net GB curve.

	Ejection Fraction (% ± SE)		
Ceruletide Dose	2.5 ng/kg	5 ng/kg	10 ng/kg
Single dose	29 ± 7	57 ± 14	93 ± 3
Sequential dose	22 ± 12	53 ± 13	85 ± 3
P value	NS	NS	0.04

The EF obtained from sequential doses on the same day was very similar to that from the single dose on separate days. It is concluded that the sequential method is as accurate as the single dose method and carries the advantages of simplicity in the establishment of dose-response curve for any future CCK-like agent.

GALLBLADDER (GB) EMPTYING:EFFECT OF SOMATOSTATIN. G.Levin, L.S.Malmud, E.Rock, S. Brody, A.H. Maurer, and R.S. Fisher. Temple University Hospital, Philadelphia, PA.

Quantitative GB scintigraphy with Tc-99m Pipida has been employed previously to measure the response to liquid and solid meals, sham feeding, bethanechol (5mg,subcutaneously) and iv infusion of octopeptide of cholecystokinin (CCK) at rates of 0.1, 0.5,1.0 and 5.0 ng/Kg/min. Significant GB emptying was observed with all the above stimuli. The purpose of this study was to evaluate the effect of somatostatin on GB emptying response to these stimuli. Studies were performed in 40 normal subjects with and without infusion of 0.5 mg/hr of somatostatin. Somatostatin decreased the maximal GB emptying responses to liquid and solid meals from 77.2±3.6 and 71.4±4.2 to 0.2±0.5 (P <.001) and 1.9± 1.0% (P<.001) respectively. In contrast, the gastric emptying of In-111-DTPA labeled liquid meal decreased less markedly from 82±2.1% to 66.3±3.1% (P<.05).

Somatostatin blocked GB emptying responses to bethanechol and sham feeding. CCK at doses greater than 0.1 ng/Kg/hr stimulated the GB emptying response to a meal. The maximal GB emptying response to high dose CCK (5.0 ng/Kg/min) decreased from 84.4±5.5 to 57.1±9.9% (P<.05). The emptying response to CCK at a dose of 0.5 ng/Kg/min was decreased from 81.7±6.4 to 18.4±4.2% (P<.01).

In conclusion, GB emptying is stimulated by solid and liquid meals, cholinergic stimulation (direct or indirect) and infusion of CCK. Somatostatin ablates the responses to liquid and solid meals,sham feeding and bethanechol and decreases significantly the response to CCK. The mechanism for inhibition of GB emptying by somatostatin may be a decreased release of CCK (or related peptide) and suppression of GB muscle response to direct stimuli.

A CHARACTERISTIC PATTERN OF ESOPHAGEAL EMPTYING IN OBSTRUCTIVE LESIONS OF THE ESOPHAGUS. D. Espinola, P. Yang, S. Engin, K. Douglass, D. Loudenslager, H.N. Wagner, Jr. The Johns Hopkins Medical Institutions, Baltimore, MD.

Esophageal scintigraphy is a sensitive indicator of esophageal motor disorders in evaluating patients (pts) with dysphagia. We have studied 93 pts, 28 of whom had radiographically obstructive esophageal lesions. With the pt supine one mCi of Tc-99m-sulfur colloid in 10cc of water was given orally as a bolus. A scintillation camera/computer was positioned to include the entire esophagus and gastric fundus. Images were acquired at 4 msec intervals and time activity curves were obtained for the proximal, mid and distal segments, and entire esophagus. Plateauing of the activity in a specific segment identified the presence and location of an obstructive lesion, the remaining segments being normal. This pattern differed from the incoordinated and adynamic pattern observed with motor disturbances. 25 of 28 (89%) pts had the plateau pattern. Of the remaining 3 pts, 2 had minimal and one had moderate strictures, all easily dilated. 7 non-obstructed pts showed plateauing in a segment; in 4, other segments were abnormal. All had spasm on manometry. Of the 25 pts, 92% of abnormal scans correlated with the region where an obstruction was radiographically found. A ratio of height of the plateau to peak activity indicated severity of obstruction. This correlated with the degree of obstruction determined by barium swallows and with the type of dilator required and extent of dilatation achieved. In view of our new finding of a specific pattern of emptying in pts with obstructive lesions, esophageal scintigraphy can provide an adequate screening test in pts with dysphagia, distinguishing between normal, motor disorders and obstructive lesions.

CORRELATIVE STUDY OF LIQUID PHASE RADIONUCLIDE ESOPHAGEAL TRANSIT SCINTIGRAPHY (RETS) WITH RADIOGRAPHIC, MANOMETRIC AND ENDOSCOPIC PARAMETERS IN PATIENTS (PTS) WITH SUSPECTED ESOPHAGITIS. G. Winzelberg, R. Malik, F. Ismail-Beigi, M. Ennis, S. Bruno, and L. Hershenson. Shadyside Hospital, Pittsburgh, PA.

To determine if liquid phase RETS could detect abnormalities of esophageal function in pts with suspected esophagitis, 16 pts were prospectively studied with Tc-99m sulfur colloid esophageal scintigraphy. Fasting patients swallowed a single homogeneous 10 ml bolus of 300 uC Tc-99m sulfur colloid and water. Images of the esophagus were collected at 0.4/seconds on a large field of view gamma camera interfaced to a dedicated computer. Manually placed regions of interest were then set over the upper, mid and lower portions of the esophagus and stomach and time activity curves generated. The results of RETS were compared to upper GI exams (14 pts), esophageal manometric and acid infusion studies (14 pts) and endoscopy (15 pts). Nine pts had normal RETS (transit time < 8 seconds, normal 3 phase progression of tracer). Of these pts, x-rays were abnormal (ABN) in 4; 2 showed hiatal hernia (HH) and reflux, one showed a HH and one showed reflux. Manometric studies were abnormal in 7 pts. Four pts had reflux and 3 had diminished lower esophageal sphincter pressures. Endoscopy showed esophagitis in 5 pts. In 7 pts with ABN scans, 4 showed dysmotility, 2 had HH with reflux and 2 had prolonged transit. X-rays were abnormal in 5 pts, manometry in 5 pts, endoscopy in 7 pts. RETS can detect both structural and functional esophageal abnormalities in patients with esophagitis. The study is less sensitive than endoscopy and a normal scan does not exclude significant esophageal pathology.

3:30–5:00 **Room 120**

ONCOLOGY II: LYMPHOSCINTIGRAPHY

Moderator: William D. Kaplan, M.D.
Co-moderator: Günes N. Ege, M.D., FRCS, FRCP

THE DUNNING R3327G PROSTATIC ADENOCARCINOMA TUMOR MODEL: TUMOR-LOCALIZATION OF RADIOLABELED THYMIDINE, A POTENTIAL AGENT FOR IMAGING WITH PETT. P.S. Conti, E. Kleinert, B. Schmall, B.M. Sundoro-Wu and W.F. Whitmore, Jr. Memorial Sloan-Kettering Cancer Center, N.Y., N.Y. 10021.

The adult male Copenhagen rat bearing the transplantable, fast-growing (doubling time=2-3 days) Dunning R3327G prostatic adenocarcinoma serves as a good biochemical and histological model for poorly differentiated carcinoma of the prostate in humans. In order to investigate the feasibility of using C-11 labeled thymidine for the visualization of normal and malignant tissue in vivo, the biological tissue distribution of (methyl C-14)-thymidine was studied in normal and tumor-bearing rats. Following intracardiac injection of 2-3 μCi of C-14 thymidine (sp.ac.=53.4mCi/mm), animals bearing the R3327G tumor were sacrificed at 30, 60 and 90 min (5 animals/time point). Five non-tumor-bearing control animals were studied at 60 min. The tissue distribution was determined by calculating the relative concentration (RC) of activity in blood and tissue samples, where RC = dpm found per gm tissue/dpm injected per gm animal weight. The mean RC in tumor tissue at 60 min was 2.69. Tumor/blood, tumor/prostate and tumor/muscle ratios were 3.09, 4.98 and 6.11, respectively. These values suggest that tumor imaging studies of prostatic adenocarcinoma with (methyl C-11)-thymidine could be performed within the time limitations of the C-11 half-life (20.4 min). Carbon-11 labeled thymidine has been prepared in mCi amounts with reaction times of less than 1 hour in our laboratory. Since differences in the relative concentration of radiolabeled thymidine in tumor tissue may reflect variations in tumor growth parameters, comparative studies with slow-growing, well-differentiated R3327 models for prostatic adenocarcinoma are in progress.

QUALITATIVE AND QUANTITATIVE UPPER EXTREMITY RADIONUCLIDE LYMPHOSCINTIGRAPHY. W.D. Kaplan, S.A. Slavin, J.A. Markisz, S.M. Laffin, and H.D. Royal. Joint Program in Nuclear Medicine and Dept of Surgery, Harvard Medical School, Boston, MA.

Changes in lymph drainage of the arm after node dissection or radiation therapy can be a disabling side-effect in the treatment of breast cancer. Lymphatic flow in such pts was studied by qualitative and quantitative analysis of the lymphoscintigrams in 19 women presenting with unilateral lymphedema. Approx. 0.2 ml (1.0 mCi) of Tc-99m Sb_2S_3 was injected (25 g, ½" needle) bilaterally (a) subq. between the 2nd and 3rd fingers and (b) intradermally at the ulnar styloid process. The normal arm served as a control. A 37-PMT gamma camera (LEAP collimator) was used to image injection sites (IS), forearms, upper arms and axillae at 0, 1, 3 and 6 hrs. The percent (%) injected dose (ID) which (a) remained at the IS and (b) reached the axillary nodes was quantitated.

The mean % ID remaining at the normal and abnormal IS differed by no >2% at each time period; egress from the IS stabilized by 3 hrs. Normal %: $\bar{x}$ 84, range 52-98; abnormal %: $\bar{x}$ 86, range 0-100. The % ID in the axillae differed significantly at each of the 3 time periods (Wilcoxon signed rank test). Tracer uptake continued to increase over 6 hrs. At 6 hrs: Normal %: $\bar{x}$ 4, range 0.3-10; abnormal %: $\bar{x}$ 0.6, range 0-3. Qualitative findings included visualization of lymph channels in the normal arm (radial > ulnar), no superficial lymphatics, and prompt axillary nodal uptake. The abnormal arm showed collateral and superficial channels; radial and ulnar lymphatics were poorly seen. Exercise increased forearm flow and axillary uptake in the normal and abnormal arms. Quantitation of lymph flow in the arm offers objective assessment of pts presenting with lymphedema or pre- and post-operatively for lympho-venous anastomosis.

QUANTITATIVE BIPEDAL LYMPHOSCINTIGRAPHY. J. Frühling, B. Massant and A. Verbist. Institut J. Bordet, U.L.B., Brussels, Belgium.

Quantitative bipedal lymphoscintigraphy (LSC) has been carried out in 50 patients with morphologically controlled lymphatic status (23 normal cases and 27 with lymphatic pathology) suffering from histologically proven neoplasic disease, in order to assess by quantification the clinical contribution of this technique and to obtain some quantitative data about lymph clearance under normal and pathological conditions.

3 hours after the subcutaneous injection of 2 x 3 mCi (107 MBq) of Tc-99m-labelled sulfur-microcolloid, a 195 x 65 cm whole body scintigram was realized by a large field scanning-camera connected to a medium size computer.

After BG-substraction and the choice of ROI-s corresponding to liver and spleen, to the main subdiaphragmatic lymphatic groups (lumbar, common iliac, external iliac, inguinal) and to the 2 pedal deposits the activity of each zone was expressed in percent of the total body activity.

Morphologically, all 23 normal cases showed a negative LSC image whereas the true positive ratio was 85 %. From the quantitative point of view : when 20 % extraction of the deposit was chosen as threshold (10 % of the whole body activity) 19 out of 23 normal cases showed higher extraction than this value, whereas 4 cases remained under this level. Among the pathological cases 24 out of 27 presented a lowered (less than 16 %) clearance; especially 4 false negative cases. Total lymph node activity, expressed as cp/sec/mCi injected and measured 3 h after deposit over lymph node areas, allows to characterise differences in the lymph clearance according to age, presence or absence of previous irradiation or of edema.

INTERNAL MAMMARY LYMPHOSCINTIGRAPHY IN BREAST CANCER. D.Casara,C.Polico,A.Bonazza,A.Pluchinotta Padua General Hospital, Padua, Italy.

Internal mammary lymphoscintigraphy(IML)was examined to assess diagnostic value and potential applications in breast cancer treatment planning.

IML with Tc-99m human colloidal albumin was performed on 223 patients staged for breast cancer. 17 patients out of 223 had monolateral subcostal injections.

IML was classified as abnormal in 14% of Stage I, 21.4% of Stage II, 20% of Stage III and 80% of Stage IV. IML was also classified as abnormal in 26.5% of patients with surgically proven axillary involvment. The 15.8% of patients without involvment were also classified as abnormal. 7 out of 17 monolaterally injected patients showed cross-linking between opposite chains. Only a low correlation of IML abnormalities with the site of the tumour was observed. In 29.1% of cases the distance of at least one node from the midline was 4 cm. or more.

The cross-linkage presence and the overrange distance of nodes from the midline require routine IML to personalize radiation fields. Finally, in spite of the relatively high incidence of equivocal results,IML could represent a suggestive diagnostic tool in breast cancer staging.

EFFECTS OF A METASTATIC(13762) AND NON-METASTATIC(R3230AC) MAMMARY ADENOCARCINOMA ON RADIOCOLLOID LOCALIZATION IN REGIONAL LYMPH NODES IN FISCHER 344 RATS. G.N. Ege, J.B. Nold, R.R. Eng, A. Durakovic and J.J. Conklin, The Princess Margaret Hospital, Toronto, Canada and AFRRI, Bethesda, MD.

Effects of a metastatic and non-metastatic tumor on radiocolloid localization in regional lymph nodes in the rat were studied in order to examine further the hypothesis that suppression of radiocolloid uptake results from inhibition of macrophage phagocytic function by tumor products. In the present model using homogenates of autologous spleen and two weakly immunogenic tumors introduced unilaterally into the foot-pad of rats, the primary drainage popliteal lymph nodes of both the experimental and control foot were removed 2.5 hrs after bilateral dorsal pedal injection of Tc-99m antimony sulfide colloid, weighed and

counted, and results expressed as % radiocolloid uptake/mg of lymph node tissue. All nodes were examined histologically. The data show statistically significant increase in lymph node weight with concomittant decrease in radiocolloid uptake, not consistently associated with histologically demonstrable lymphatic metastases. On the basis of this data the proposed "jelly-bean hypothesis" suggests that decreased radiocolloid uptake induced by a regional neoplasm may result from proliferation of non-phagocytic cellular elements within the regional lymph nodes and alterations in the cellular and humoral environment at the site of radiocolloid injection, all of which impede the transport of interstitially administered radiocolloid and its access to the phagocytic macrophages within primary regional lymph nodes.

CLINICAL EVALUATION OF DYNAMIC LYMPHOSCINTIGRAPHY WITH Tc-99m HUMAN SERUM ALBUMIN. E. Ohtake, K. Matsui, Y. Kobayashi, and Y. Ono. Yokohama City University School of Medicine, Yokohama, Japan.

This investigation was undertaken to evaluate the clinical usefulness of dynamic lymphoscintigraphy with Tc-99m human serum albumin (Tc-99m HSA).

Ten cases (11 times) were examined by dynamic lymphoscintigraphy. They were one normal volunteer, 3 with malignant lymphoma, 3 with gynecologic carcinoma and others. Their ages ranged from 34 to 75 years with the average age of 55 yrs. Dynamic lymphoscintigraphy was performed by intradermal injection of 5 – 8 mCi of Tc-99m HSA. The lymphatic system of the upper extremity was examined in 2 cases and that of the lower extremities was examined in 8 cases. Serial images were obtained every 2 min during 30 min. At the same time, the data were collected every 30 sec in computer system and the time activity curves of the lymphatic vessels and/or the lymph nodes were observed. The static image was also obtained 40 min after intradermal injection of Tc-99m HSA. Furthermore, the static lymphoscintigraphic images with Tc-99m HSA were compared with Tc-99m rhenium colloid in 3 cases.

The image of the axillary or inguinal lymph nodes was identified 2 – 4 min after injection in cases with the normal lymphatic flow. The delayed appearance of radionuclide was detected in 4 cases with the disorder of the flow. The collateral pathways of the lymphatic vessels were clearly observed in 3 cases. The static image with Tc-99m HSA was also obtained in excellent quality as observed in radiocolloid lymphoscintigram.

In conclusion, dynamic lymphoscintigraphy with Tc-99m HSA could be a useful procedure for the research of the physiopathologic conditions of the lymphatic system.

3:30–5:00 **Room 132**

BONE/JOINT I: TRAUMA

Moderator: Philip Matin, M.D.
Co-moderator: Naomi P. Alazraki, M.D.

STRESS FRACTURE DIAGNOSIS: CLINICAL OR RADIOLOGICAL. J. Zorba-Rivera, J.P. Canby, P.J. Anderson, R.E. Redd, D.D. Stoddard, L. Morris, and S.A. Conte.

A prospective clinical study in 231 U.S. Army soldiers during basic training was carried out to study stress fractures. Our experience with the diagnostic modalities available in the diagnosis of this condition is reported.

Complaint of pain, medical history and examination, medical impression, ultrasound test, three phase bone scintigraphy and radiography were compared. Sensitivity, specificity and accuracy of these parameters and cost per patient were tabulated.

Our data demonstrates the non-specific nature of musculoskeletal pain and physical signs. Medical impression and ultrasound were not reliable in the diagnosis of stress fracture in our study. Three phase bone scintigraphy was the most sensitive technique. The addition of either bone flow or blood pool images to the standard delayed views proved to be quite useful by allowing us to differentiate areas of accelerated remodeling from stress fractures. Bone scintigraphy increased the cost per patient from $80 to $225. Radiographs taken two weeks after bone scintigrams were 54% as sensitive.

The data supports the following conclusion: (1) Three phase bone scintigraphy is the most reliable technique. It is cost effective in a setting where a certain diagnosis is needed and when dealing with high risk areas like femoral neck; (2) In low risk areas like metatarsal bones, delayed radiographs are sufficient for diagnosis; (3) Radiographs are invaluable since they can rule out other non-traumatic processes; (4) Ultrasound testing is not recommended; (5) Delay bone scan alone over-estimated and radiographs under-estimated the incidence of stress fractures.

SKELETAL SCINTIGRAPHY IN THE DIFFERENTIAL DIAGNOSIS OF LOWER EXTREMITY PAIN IN ATHLETES. P. Matin, R. Carretta. Roseville Community Hospital, Roseville, Ca.

Nuclear medicine techniques are becoming more popular in the investigation of athletic injuries, such as stress fractures. We have investigated the use of bone scintigraphy for the detection of acute soft tissue injury and evaluated the ability to differentiate these abnormalities from skeletal abnormalities such as stress fractures.

Injuries such as skeletal muscle necrosis, tendon insertion injury and joint abnormalities were studied in 40 trained runners, including a group of 15 runners who competed in ultramarathon races of greater than 30 miles. In all cases, the runners complained of lower extremity pain and were studied with 99mTc-phosphate scintigraphy 24 to 72 hours after the race. Whole body images of the lower extremities as well as spot images were obtained. Scintigraphic abnormalities were detected in approximately 70% of the runners, including skeletal muscle rhabdomyolysis in the ultramarathon runners. The other abnormalities identified included true stress fractures, periosteal reaction, joint abnormalities and increased radionuclide concentration at sites of tendon insertion. The tendon insertion injuries were similar in appearance to the small periosteal injuries, but the stress fractures, joint injuries and skeletal muscle abnormalities were easily differentiated from each other in almost all cases.

This leads to the conclusion that nuclear medicine bone scintigraphy can be utilized in the differential diagnosis of lower extremity pain in athletes when performed within a few days after onset.

SINGLE PHOTON EMISSION COMPUTED TOMOGRAPHY IN SUSPECTED INTERNAL DERANGEMENTS OF THE KNEE. B.D. Collier, R.P. Johnson, G.F. Carrera, D.W. Palmer, A.T. Isitman, and R.S. Hellman. Medical College of Wisconsin, Milwaukee, WI.

Eleven adult patients with knee pain were independently evaluated by history and physical, conventional radiography including standing views, planar bone scintigraphy and single photon emission computed tomography (SPECT). For each examination, physicians were asked to localize abnormalities to a particular compartment of the knee. Subsequently, all patients underwent complete arthroscopic knee evaluation. Ten out of 11 patients had complained of severe knee pain for over 6 months with 9 of the patients having a history of significant knee trauma and 2 patients being more than 1 year status post menisectomy. When arthroscopic visualization of cartilage damage in the patellofemoral, lateral, or medial compartments of the knee was used as the standard for comparison, SPECT had a 100% sensitivity for significant derangements of individual compartments of the knee with lower sensitivities for planar bone scintigraphy (79%), conventional radiography (38%), and physical examination (38%).

We conclude that SPECT is a useful non-invasive screening procedure which provides information not available on physical examination, conventional radiographs, and planar bone scintigrams. Based on our initial experience with SPECT bone imaging, orthopedists at our institution no longer consider patients with a normal SPECT examination to be candidates for knee arthroscopy. In addition, abnormal SPECT images are being used as a "roadmap" to direct the arthroscopist to areas within the knee which deserve detailed inspection.

SKELETAL IMAGING IN TEMPOROMANDIBULAR JOINT (TMJ) DISEASE. R.E. O'Mara, R.W. Katzberg, D.A. Weber, G.A. Wilson and R.H. Tallents. University of Rochester School of Medicine and Dentistry, Rochester, NY

TMJ disease is a significant cause of facial pain. The purpose of this preliminary investigation was to compare skeletal imaging with other modalities in 32 patients being worked up for TMJ symptomatology. Scintigraphic evaluation consisted of a perfusion phase, immediate and delayed images in the anterior and lateral projections with mouth opened and closed, and single photon emission computed tomography (SPECT). Skeletal images were compared with routine diagnostic radiologic studies, multidirectional tomography, arthrography, and CT and operative results when performed. The results indicate that open mouth delayed images and SPECT provide the most useful scintigraphic findings. When minimal internal derangements (MDR) were diagnosed by arthrography, abnormal scintigraphic findings were found in 4 of 9 patients (44%), whereas plain tomography was normal in all 9. In 11 patients with more severe internal derangement (MD), the scintigrams were abnormal in 6 (55%), while plain tomography was abnormal in 4 (36%). Osseous degenerative changes were found in the 10 patients with abnormal bone scans.

Skeletal imaging is the most sensitive indicator of arthritic changes in patients with TMJ complaints. It is of great assistance in determining the laterality of findings, especially in patients with bilateral complaints, and as an indicator for choice of therapeutic regimen, i.e. conservative versus more interventional or surgical. SPECT provides a sensitive technique for the detection and quantification of early TMJ disorders and delineation of early arthritic involvement in the fossa or the condyle of the mandible.

COMPARATIVE UPTAKE OF Ga-67 AND Tc-99m MDP IN A BENIGN NON-INFECTED BONE LESION (FRACTURE). J.Bushberg, P.Hoffer, G.Schreiber, A.Lawson, J.Lawson and P.Lord, Yale University, New Haven, CT

Previous investigators have observed that Ga-67 uptake in benign, non-infected lesions is less prominent than uptake of Tc-99m-phosphate. This study was undertaken to determine the concentration of Ga-67 and Tc-99m MDP in healing fractures (a benign non-infected lesion) relative to normal bone as a funcion of time after fracture.

Thirty five rabbits were studied at 11,18,25,32,51 and 78 days following a closed midshaft fracture of the right ulna and radius. The fractured and normal forelimbs were splinted for 3 weeks. Ga-67 was injected followed in 24 hrs by Tc-99m MDP. Dissection of the skin (S), muscle (M) and bone (B) in a 2.5 cm region (ROI) centered over the fracture site and contralateral normal limb was performed to determine fracture/nonfracture specific activity ratios (F/NF SAR). In representative animals, Ga-67 and Tc-99m scintigrams were obtained in conjunction with total dissection of S,M and B in the ROI to compare with the SAR.

The bone F/NF SAR for Tc-99m MDP and Ga-67 at 11 days were 5.91±0.99 and 5.34±1.05 respectively and remained essentially unchanged up to 32 days. The Tc-99m MDP and Ga-67 F/NF SAR continued to parallel each other beyond 32 days; however the SAR decreased to 2.25±0.31 and 2.18±0.19 respectively by 78 days.

The cause of the lower contrast of benign non-infected bone lesions on Ga-67 vs Tc-99m images is thus not due to differences in SAR but due to higher Ga-67 background in soft tissue. This was confirmed by scintigraphy and total ROI dissection of S,M and B.

RADIOCOLLOID HIP SCINTIGRAPHIC PATTERNS IN OSTEONECROSIS: CORRELATION WITH BONE SCINTIGRAPHIC AND RADIOGRAPHIC STAGES. S.H. Yeh, R.S. Liu, Y.K. Chu, and C.Y. Wong. Veterans General Hospital, Taipei, Taiwan.

Management of osteonecrosis (ON) depends on the stages of the disease, and early treatment permits reversibility of the lesion. This study correlated the colloid uptake patterns of the femoral head with the stages of ON.

Scintiphoto of the hip was obtained with a pinhole collimator at one hr after i.v. injection of Tc-99m-sulfur or Tc-99m-antimony colloid. The uptake of the femoral head as compared with that of the adjacent structures was classified into three categories: (A) absent, (B) diffuse low-intensity, or (C) segmental high-intensity. Tc-99m MDP bone scanning and hip radiography were also carried out.

In 36 hips of 32 patients with ON (posttraumatic in 13, nontraumatic in 12, and idiopathic in 7), the correlation of the colloid uptake patterns with the stages as determined by bone scan and radiograph is shown in the table:

Capital colloid uptake	MDP and radiographic stages				
	0	I	II	III	IV
Absent	4	5	0	9	5
Diffuse low-intensity	0	0	1	4	1
Segmental high-intensity	0	0	7	0	0

All hips in Stages 0 and I had no colloid uptake. Segmental uptake occurred in all but one (88%) of the Stage II group, whereas 67% (4/6) of patients with diffuse uptake belonged to the Stage III group. The diagnosis of avascularity and ON was confirmed by core biopsy in 13 cases and histological study of the removed head in 23 cases.

In summary, absent or segmental uptake together with bone scan and radiograph may increase the diagnostic specificity to define osteonecrosis in the reversible phase.

3:30–5:00 **Room 276**

RADIOPHARMACEUTICAL CHEMISTRY IV: RADIOHALOGENATED

Moderator: Furn F. Knapp, Jr., Ph.D.
Co-moderator: H. Donald Burns, Ph.D.

Introduction. Furn F. Knapp, Jr., Ph.D., Oak Ridge National Laboratory, Oak Ridge, TN

RADIOPHARMACEUTICAL DESIGN: ADRENERGIC NERVOUS SYSTEM. M. Inbasekaran, P.S. Sherman, S.J. Fisher, D.M. Wieland. University of Michigan Medical Center, Ann Arbor, MI.

Radiopharmaceutical analogs of norepinephrine (NE) could be used to study adrenergic physiology, especially of the heart. Ideally such an agent would not only map adrenergic nerve density but also serve as a kinetic model for NE. Compounds are screened on the following basis: 1) high affinity for the canine heart and other richly innervated organs; 2) atrium-to-ventricle concentration ratio (A/V) that increases with time (atrium has a 2-3 fold denser innervation); 3) neuronal specificity in the heart approaching that of NE (ie. 85-95%). This latter value is determined in chemically sympathectomized rats using 6-hydroxydopamine.

Eight polar derivatives of the NE storage analog meta-iodobenzylguanidine (MIBG) have been synthesized. The design hypothesis: decreasing the lipophilicity of the aromatic ring of MIBG will decrease the undesirable, non-neuronal component of binding in the heart. One of these compounds, I-125-4-amino-3-iodobenzylguanidine (1) gives a heart-to-blood concentration ratio of 16 at 30 min, an A/V of 2.8 at 24 hours, and a neuronal specificity of 73-82%. Long retention of 1 was observed in the heart, spleen and adrenal medulla. Images of the dog heart were obtained with I-131-1 up to 24 hours after injection. Better heart images were obtained in rhesus monkeys; the walls of both the left V and right V were clearly defined and comparatively low liver radioactivity was observed at 1-2 and 19-20 hours after injection. SPECT analysis is underway to quantitate the regional myocardial concentration of I-123-1.

SYNTHESIS OF NO-CARRIER-ADDED ^{75,77}Br-BENPERIDOL: A POTENTIAL RADIOPHARMACEUTICAL FOR QUANTITATING CEREBRAL DOPAMINE RECEPTORS. S.M.Moerlein and G.L.Stöcklin. Institut für Chemie 1 (Nuklearchemie), Kernforschungsanlage Jülich, Fed.Rep.Germany.

A variety of neuroleptics have recently been radiolabelled for use in mapping cerebral dopamine receptors non-invasively with the PECT method. For preliminary evaluation preceeding use of the positron-emitter ^{75}Br ($t_{1/2}$ = 1.6 hr), we have radiobrominated the butyrophenone neuroleptic benperidol with no-carrier-added (n.c.a.) ^{77}Br. Benperidol was chosen as a bromination substrate due to its high K_i for cerebral dopamine receptor binding (1.4 nM), its relatively low K_i for serotonin (3.7 nM) or α-adrenergic (7.1 nM) binding, and because it is activated toward

electrophilic halogenation at a site on the molecule which is non-essential for receptor recognition. Benperidol was synthesized in 75% overall chemical yield by alkylation of 4-(2-oxo-1 benzimidazolinyl)-piperidine with the ketal of ω-chloro-4-fluorobutyrophenone. Following deketalization and work-up, product benperidol was characterized by ^{1}H-NMR,MS,IR, and melting point. A study of the effects of solvent, dichloramine-T/substrate concentration ratio, reaction time, and reaction temperature on the radiobromination of the oxoimidazolinyl ring was performed. Optimum radiobromination of benperidol resulted in radiochemical yields up to 9o % using n.c.a. $^{77}Br^-$, dichloramine-T, and trifluoracetic acid at elevated temperatures. Separation of brominated benperidol from benperidol was achieved with HPLC (Si-1oo; i-PrOH/$CHCl_3$). Ongoing studies include pharmacokinetic and displacement studies in animals.

★A NEW RAPID, REGIOSPECIFIC SYNTHESIS OF ^{123}I-LABELED 15-(p-IODOPHENYL)PENTADECANOIC ACID. M. M. Goodman and F. F. Knapp, Jr., Nuclear Medicine Group, Oak Ridge National Laboratory (ORNL), Oak Ridge, TN, and P. Richards and L. F. Mausner, Medical Dept., Brookhaven National Laboratory (BNL), Upton, NY

Iodine-123-labeled 15-(iodophenyl)pentadecanoic acid, (15-[^{123}I]IPP) is an agent used to measure myocardial fatty acid metabolism. The triazene decomposition reaction can be used to regiospecifically introduce iodine-123. 15-[^{123}I]IPP can be readily prepared by reaction of H[^{123}I] with 1-[4-(15-oxopentadecanoyl)-phenyl]-3,3-(1,5-pentanediyl)-triazene (VI), prepared by the following transformations: ϕ-$(CH_2)_{14}$-$COOCH_3$ (I) + $Tl(F_3C\text{-}COO)_3$ → $(F_3C\text{-}COO)_2Tl$-ϕ-$(CH_2)_{14}$-$COOCH_3$ (II) + NOCl → p-O=N-ϕ-$(CH_2)_{14}$-CO_2CH_3 (III) + $NaBH_4$ → p-H_2N-ϕ-$(CH_2)_{14}$-$COOCH_3$ (IV) + HONO + piperidine → p-$(C_5H_{10}$-N-N=N)-ϕ-$(CH_2)_{14}$-CO_2CH_3 (V) + OH^- → p-$(C_5H_{10}$-N-N=N)-ϕ-$(CH_2)_{14}$-COOH (VI) + H-I → IPP. 15-[^{123}I]IPP was prepared in <5 min at 0°C with "no-carrier added" ^{123}I in ~30% yield and showed the expected myocardial uptake in rats (% inj. dose/gm; range of 4 rats). This rapid method is attractive for preparation of ^{123}I-labeled 15-IPP for clinical use.

	Heart	Blood	Thyroid
5 min	3.69-6.51	0.83-1.50	11.11-11.44
60 min	2.76-4.22	1.42-1.90	10.75-17.65

Research supported by the Office of Health and Environmental Research, U.S. Department of Energy under contracts W-7405-eng-26 with the Union Carbide Corporation at ORNL and DE-AC02-76CH00016 at BNL.

★RADIOIODINATED (E-1-IODO-1-PENTEN-5-YL)TRIPHENYLPHOSPHONIUM IODIDE: CONVENIENT PREPARATION OF AN ATTRACTIVE MYOCARDIAL PERFUSION AGENT. P. C. Srivastava, A. P. Callahan and F. F. Knapp, Jr., Nuclear Medicine Group, Oak Ridge National Laboratory (ORNL), Oak Ridge, TN.

Recently, high myocardial uptake of tritiated phosphonium bromide derivatives has been reported in rats (D.V. Woo, Circ., Part II, 66, No. 4, II-124, 1982), suggesting that ^{123}I-analogs may be useful perfusion agents. We have developed a procedure to stabilize iodine as a trans(E) vinyl iodide on a phosphonium salt, illustrated by the synthesis of (E-1-iodo-1-penten-5-yl)triphenylphosphonium iodide (II, ϕ=phenyl). Iodination of E-I-$(CH_2)_3$-CH=CHB$(OH)_2$ with NaI-chloramine T gave the E-iodide I (70%) which was condensed with ϕ_3P to yield >90% of II (analyzed: mp 201°C, MS, NMR and % Elements). ^{125}I-II was prepared (200 mCi/mmole) and showed pronounced myocardial uptake (% dose/gm; range of 4 rats), high heart:blood ratios and low liver uptake in rats. The data suggest that the ^{123}I-labeled agent will be attractive for evaluation as a myocardial perfusion agent.

$$\underset{\text{I}}{I\text{-}(CH_2)_3\text{-}CH{=}CH\text{-}I} + \phi_3P \rightarrow \underset{\text{II}}{[\phi_3P^+\text{-}(CH_2)_3\text{-}CH{=}CH\text{-}{*}I]I^-}$$

T, min	Heart	Blood	Liver	Lungs
5	3.78-4.67	0.18-0.21	0.77-1.29	0.96-1.65
30	3.47-5.37	0.09-0.11	0.36-0.45	0.99-1.19
120	3.04-4.50	0.07-0.09	0.14-0.19	0.60-0.85

Research sponsored by the Office of Health and Environmental Research, U.S. Department of Energy, under contract W-7405-eng-26 with the Union Carbide Corporation.

MYOCARDIAL UPTAKE OF RADIOIODINATED P-IODOPHENYLBENZYL-DIMETHYLAMMONIUM BROMIDE: COMPARISON TO Tl-201. D.V. Woo*, H.D. Burnst, R.F. Dannalst, J.G. Emrich*, H.T. Ravertt, and H.N. Wagner, Jrt, *Hahnemann University, Philadelphia, PA; tJohns Hopkins University, Baltimore, MD.

The myocardial uptake of radioiodinated p-iodophenylbenzyldimethylammonium bromide (I-PBDA) was compared to Tl-201 in rats. I-PBDA was synthesized by alkylation of p-iododimethylaniline with benzylbromide. After purification, I-PBDA was characterized using NMR, HPLC, and elemental analysis. Radioiodinated I-PBDA was prepared with I-125 using a Chloramine-T reaction with NaI (no carrier added) and dimethylaniline. After HPLC purification, the radioiodinated intermediate was similarly alkylated to form the labeled product. The I-125, I-PBDA exhibited identical retention times on HPLC as the non-radioactive I-PBDA. Groups of animals received an IV injection of ∿ 10μCi of I-PBDA or Tl-201 and were sacrificed 30 minutes later. Animals receiving I-PBDA demonstrated significantly higher (p=.05) myocardial uptake than Tl-201 (4.6±.8% injected dose/g, I-PBDA; 3.5±.2% injected dose/g, Tl-201; n=5) with significantly better heart/lung (5.0±1.3, I-PBDA; 2.4±.4, Tl-201) and heart/liver ratios (13.3±1.9, I-PBDA; 3.1±.9, Tl-201). The heart/ blood ratios were 42.1±8.0 for I-PBDA and 75±21 for Tl-201. These studies indicate that I-PBDA when labeled with I-123 may offer significant advantages over Tl-201 in the diagnosis of diseases of the myocardium should these results be extrapolated to humans.

APPLICATIONS OF ARYLTRIMETHYLSILANES IN RADIOBROMINATIONS. D.S. Wilbur, Z.V. Svitra, and H.A. O'Brien, Jr. Los Alamos National Laboratory, Los Alamos, NM 87545.

Model compound studies have shown that aryltrimethylsilanes can be used as intermediates in radiobrominations of aromatic rings. Application of this methodology is particularly important in examples where halide exchange reactions will not readily occur. Thus, a study has been carried out using three compounds that contain trimethylsilyl groups on aromatic rings at positions that do not readily undergo exchange. The compounds, p-trimethylsilyl hippuric acid(1), p-trimethylsilyl-N,N-dimethylbenzylamine(2), and 4-trimethylsilyl-N,N,N',N'-tetramethylxylenediamine(3) may have applications in Nuclear Medicine.

Synthesis of 1 was accomplished by the reaction of p-trimethylsilylbenzoic acid(4) with glycine/NaOH. Synthesis of 4 was accomplished by the reaction of p-bromobenzoic acid with n-BuLi/TMSCl. Initial radiobrominations were carried out on 4. Reaction of 4 with no-carrier-added(nca) $Na^{77}Br$/t-BuOCl in MeOH at room temperature for 5 minutes yielded 73% of the p-[^{77}Br]bromobenzoic acid by radioHPLC. Likewise, reaction of 1 with nca $Na^{77}Br$/t-BuOCl in HOAc at 60°C yielded 93% of the desired radiobrominated product by radio-HPLC analysis. Synthesis of 2 was accomplished in four steps from p-bromotoluene, beginning with the reaction of Mg /TMSCl to form the p-trimethylsilyltoluene. Subsequent steps included reaction with NBS to form the benzylbromide, reaction with $HNMe_2$ to form the benzylamine, and reaction with HCl to form the salt. Synthesis of 3 was accomplished similarly, beginning with 4-bromo-m-xylene. Reaction of 2 with nca $Na^{77}Br$/t-BuOCl in HOAc at room temperature yielded 76% of the desired product within 5 minutes. Unfortunately, radiobrominations of the xylylamine,3, were complicated by an apparent instability of the compound.

3:30-5:00 **Room 270**

RADIOASSAY II

Moderator: Arthur Carmen, M.D.
Co-moderator: Benjamin Rothfeld, M.D.

FT4 ESTIMATES IN PATIENTS WITH NONTHYROIDAL ILLNESSES (NTI). L.R. Witherspoon, S.E. Shuler, J. Gonzales, S. Gilbert and F. Husserl. Ochsner Medical Institutions, New Orleans, LA.

The assessment of thyroid function in patients with NTI is difficult. We have examined the Clinical Assays "two-step" (CA2), Clinical Assays "one-step" (CA1), Corning Medical (CM), Damon Diagnostics (D) and Amersham (A) FT4 assays and compared them to equilibrium dialysis (ED) and FTI in the evaluation of 16 patients after coronary artery bypass, 27 patients with chronic renal failure treated by hemodialysis and in 33 other seriously ill patients (NTI). The surgery patients had low-normal total T4s, below normal total T3s and elevated rT3s. The FTI were normal and FT4 by ED low-normal. All FT4 assays produced low-normal or low results except CA2 which produced normal results in all patients. The renal failure patients had low-normal or low total T4s and total T3s and a wide distribution of rT3. The FTI were low-normal or low while FT4s by ED were normal. All FT4 assays produced low-normal or low results. There was a wide range of total T4 results in the NTI patient; 8 were low. The total T3s were low-normal or low while the majority of patients had elevated rT3s. A wide range of FTIs was observed; 7 were low. ED produced mostly normal results. All FT4 assays produced a large number of low-normal or low results except CA2, with which most results were normal. The antibody extraction FT4 assays produce lower than expected results in many euthyroid patients with nonthyroidal diseases. This effect is least with the CA2 assay in which patient serum is removed before the quantitation reaction and most marked in those assays employing a T4 derivative (A,CA1). The very same antibody extraction which produced normal results in the CA2 assay produced patient B/B_0 >100% in 6 patients and low results in others in the CA1 assay. FT4 estimated by antibody extraction assay is not reliable in these groups of patients.

A NEW DERIVATIVE ASSAY (CORNING MEDICAL) FOR ESTIMATION OF FT4. L.R. Witherspoon, S.E. Shuler, J. Gonzales and S. Gilbert. Ochsner Medical Institutions, New Orleans, LA.

We examined the efficacy of a new single-step assay proposed by Corning Medical for estimation of FT4 (CFT4). T4 extracted from serum by a new solid phase (glass bead) antibody is quantitated by competative binding with a labeled T4 derivative. The detection limit is ~0.2 ng/dl and within and between assay precision (C.V.) was 5.6-6.6 and 6.2-7.5%. We estimated CFT4 in 101 eu-, 24 hyper- and 25 hypothyroid patients, in 29 seriously nonthyroidally ill (NTI) patients and in 1 patient with unusual serum T4 binding. We measured total T4, T3 uptake, TBG and FT4 using another derivative assay (Amersham). Other measurements including TSH and T3 were made when appropriate and the clinical findings were reviewed. FT4 by equilibrium dialysis (ED) was measured in the NTI patients. CFT4 was 1.0-2.5 ng/dl in all but 3 euthyroid patients. We observed no TBG dependence. The assay discriminated all hyperthyroid (2.6-6.5 ng/dl) from euthyroid patients. CFT4 was <0.2-1.0 ng/dl in untreated (17) and 0.4-1.3 ng/dl in inadequately treated (8) hypothyroid patients. CFT4 was <0.2-0.9 in 12 and 1.1-1.5 ng/dl in 15 NTI patients (2.1, 3.4 in 2), but normal in most by ED. In 1 euthyroid (normal TRH test) patient with unusual serum T4 binding the FT4 estimate was >6.5 ng/dl. Results with this assay correlate well with those obtained with another derivative FT4 assay in all patients (r=0.98). In patients with significant NTI, an apparently inappropriately low result was obtained in nearly all patients while spuriously elevated results may occur in patients with unusual serum T4 binding because of labeled derivative sequestration. Our experience with dilantin and salicylates is limited. Bearing in mind these limitations, the new Corning FT4 assay provides a simple, reliable FT4 estimate.

CLINICAL CORRELATION OF THE AMERLEX FREE T_4 RADIOIMMUNO - ASSAY IN VARIOUS CLINICAL CONDITIONS. F.S. Ashkar, A.V. Heal, and H. Khan. University of Miami School of Medicine, Miami, FL

Free T_4 should reflect true thyroid function or dysfunction, since it is the active portion of thyroid hormone in contact with the target organs. Most radioassay procedures, however, have failed to perform satisfactorily in certain clinical situations. The purpose of this study was to evaluate the Amerlex free T_4 in various clinical situations especially those which may cause erroneous results.

Over 400 patients separated in various groups were studied and compared to the clinical diagnosis and other thyroid function tests. These patient groups included euthyroid, hypothyroid, hyperthyroid, pregnancy (1st and 3rd trimesters), dilantin treatment, varying levels of triglycerides and cholesterol, and non-thyroidal illness (NTI).

There was good correlation in all patient groups except 3rd trimester pregnancy (33%) and NTI (48%). There was an exponential correlation with triglyceride levels, however it did not affect the clinical correlation significantly.

The intra-assay CV's for 30 samples were 7.0% and 9.2% ($\bar{x}$ = 0.99 and 2.29 ng/dl respectively) and the inter-assay CV's for 30 samples were 13.4%, 4.9% and 8.9% ($\bar{x}$ = 0.25, 1.13, and 2.37 ng/dl respectively).

The Amerlex free T_4 is a simple rapid procedure to perform, with a high specific activity, requiring shorter counting times. Although there were problems in correlation in certain clinical situations, we found it to be a useful screening and confirmation test in our laboratory.

SERUM FREE THYROXINE METHODS, A COMPARATIVE STUDY. C.J. Edeling, B. Foder, H. Funch-Rosenberg and A.M.Hansen, Finsen Institute, Copenhagen, Denmark.

As part of a clinical trial, a new commercial RIA kit for the determination of serum free thyroxine (FT-4)utilizing a labelled T-4 derivative, was compared with our hitherto used Sephadex binding method, with two indirect methods for FT-4 estimation, the total T-4/TBG ratio and free T-4 Index, and with determinations of total T-4, total T-3, and TSH.

The samples were from patients special for a cancer hospital, 50% had a malignant disease, half of them a malignant thyroid disease, and 25% had a non malignant thyroid disease. The patient material consisted of 16 hyperthyroid, 15 hypothyroid, and 184 euthyroid patients, including 61 T-4 treated and 14 T-3 treated patients.

A reasonably good agreement between the four FT-4 methods were found for hyperthyroid and hypothyroid patients, whereas disagreements between the methods were found for a number of euthyroid patients, especially in the group of T-4 treated patients, where 30-60% of the patients had elevated FT-4 values dependent on the FT-4 method used.

From the present series of patients it is concluded, that the new FT-4 RIA is of at least as much diagnostic values as the other three methods. In T-4 treated patients a FT-4 determination should be supplemented with determinations of TSH and T-3.

COMPARISON OF REVERSE T3 AND T3 RESIN UPTAKE. M.D. Harpen, W.N.P. Lee, A.E. Robinson. University of South Alabama Medical Center, Mobile, Alabama.

We have previously described a technique involving the resin uptakes of T3 and T4 which allows the determination of the association constants of the thyroxin binding proteins (TBP) for T3 as well as the distribution of bound hormone among these proteins. The procedure has now been generalized to study the serum binding of reverse T3.

The association constants of the TBP for reverse T3 has been determined as: k(TBGA) = 6.37 E8 (1/M), k(TBGA)= 8.51 E6 (1/M) and k(Alb) = 1.9 E5 (1/M). Reverse T3, T3 and T4 uptake data have been accumulated on a variety of normal and abnormal human sera. Averaged values and ranges of T3 and reverse T3 resin uptake have been determined for the following classification of sera; normal, neonate, hypothyroid, hyperthyroid, low T4 normal FT4 and high T4 normal FT4.

The distribution of bound thyroid hormones (percent) among the TBP in normal sera has been determined:

	TBG	TBPA	Alb
T_4	58.9	31.0	10.1
T_3	52.9	15.1	32.0
rT_3	37.6	15.7	46.7

The differences in the distribution of bound hormone among the TBP allows differences in the resin uptakes of these quantities to be interpreted as variations in the free

binding site concentrations of individual thyroxin binding proteins.

Observed values of resin uptake are explained in terms of the concentration of free TBP. It is also shown that reverse T3 along with T3 and T4 uptake constitutes a more complete description of the thyroid binding properties of human sera.

DOUBLE-ISOTOPE IN VIVO MEASUREMENT OF INTESTINAL CALCIUM ABSORPTION IN PHOSPHATE/VITAMIN D DEFICIENT RATS. C.L. Marsh, A.D. LeBlanc and P.C. Johnson. Technology Incorporated and Medical Sciences Division, NASA/JSC, Houston, TX

A double-isotope technique which requires isotopic analysis of the incisor tooth rather than collection and analysis of plasma, urine and feces has been designed to measure intestinal calcium absorption in the rat. A record of the integrated plasma concentration of two calcium radionuclides administered orally and i.p. will be reflected by the interstitial uptake and retention in the rat tooth. The fractional uptake of the two different calcium isotopes by the tooth should be equal to the calcium transported through the gut mucosa to enter the exchangeable blood pool.

Eleven rats on control or phosphate/vitamin D deficient diets were administered Ca-45 orally and Ca-47 i.p. Intestinal calcium absorption is increased in the phosphate deficient rats (80%) as compared to the control rats (38%). The fractional uptake by the incisor tooth yields an absorption measurement nonsignificantly different from the value obtained from collected excretion data. The urine and fecal collections not only verified the accuracy of the tooth technique but demonstrated an altered pattern of calcium excretion in the phosphate deficient rats. The rats absorb calcium more efficiently and secrete less endogenously resulting in excessive calcium in the urine.

The tooth technique affords one an accurate in vivo measurement of intestinal calcium absorption in the rat without collection of excreta or multiple blood sampling.

THURSDAY, JUNE 9, 1983

10:30–12:00 **Room 123**

CARDIOVASCULAR CLINICAL VI: TI-201 QUANTITATIVE ANALYSIS

Moderator: Ernest V. Garcia, Ph.D.
Co-moderator: James H. Thrall, M.D.

FUNCTIONAL IMAGING OF TL-201 REDISTRIBUTION. D.D. Watson, J.M. Lightner, R.P. Waterfield, J.M. Ryan, R.S. Gibson, G.A. Beller. University of Virginia Hospital, Charlottesville, VA.

Redistribution in delayed thallium myocardial images has been used as a marker of myocardial viability. Studies using quantitative Tl imaging before and after myocardial revascularization often demonstrate important redistribution which is not visually appreciated on conventional sequential images. We have developed a functional redistribution image (FRI) which displays the presence and anatomic regions of redistribution. FRI is proportional to the difference divided by the sum of initial and delayed images. This function can be shown mathematically to indicate correctly the absence of redistribution when all myocardial segments follow similar multicompartmental tracer curves. In magnitude, FRI closely approximates a local logarithmic derivative. The computer program THAL (previously described) is used to subtract background and provide precise spatial alignment of initial and final myocardial images by using a cross correlation technique for automatic image alignment. A mask is also generated to eliminate nonsignificant values from the functional image. The image is intensity scaled so that both positive and negative logarithmic slopes can be represented on a single continuous gray scale with a background gray level representing zero slope for visual reference. A color scale is also provided. These images have been useful in providing a rapid and clear visual indication of redistribution which otherwise requires more cumbersome numerical techniques. In addition, the functional images provide better anatomic delineation of myocardial regions of ischemia in relation to areas of normal myocardium or myocardial scar.

NORMAL LIMITS FOR THE QUANTITATIVE ANALYSIS OF STRESS THALLIUM-201 MYOCARDIAL SCINTIGRAMS: A MULTICENTER VALIDATION. K Van Train, E Garcia, D Berman, J Maddahi, Cedars-Sinai Med Ctr (CSMC), Los Angeles, CA; W Ashburn, Univ of Calif Med Ctr, San Diego, CA; M Freeman, St Michael's Hosp, Toronto, Ontario; H Berger, M Sands, Yale Univ, New Haven, CT; J Friedman, Cardiac & Vascular Diagnostic Ctr, Los Angeles, CA; A Green, New England Nuclear, N Billerica, MA

Which pt population should be used to define normal limits (N/Ls) for quantitative analysis of myocardial Tl-201 (QT) stress distribution and washout and whether these limits developed at CSMC can be applied in other centers are controversial. Thus we compared QT results using N/Ls from 3 different "normal" populations (NP) and the N/Ls with the highest accuracy were validated using pt data from 4 centers independent from CSMC. The 3 NPs consisted of 1) 49 pts having <1% likelihood of CAD based on sequential Bayesian analysis of age, sex, symptoms, and other noninvasive tests; 2) 25 pts having <10% likelihood of CAD, and 3) 30 pts with normal coronary arteries (NCA). N/Ls for each group were derived as the mean minus a variable number of standard deviations. Fifty-one CSMC CAD pts were used to evaluate the accuracy of each set of N/Ls. ROC analysis indicated that the <1% N/Ls calculated as the mean -2.5 SD provided the highest accuracy. These <1% N/Ls were then used to evaluate the multicenter pts consisting of 114 pts undergoing coronary angiography (25 NCAs) and 25 pts with low likelihood of CAD. The sensitivity for CAD detection was similar to that of CSMC for single (74%), double (81%), and triple (94%) vessel disease and overall (83%). The true negative rate was also similar to that of CSMC for the <1% pts (88%) and NCA pts (48%). Thus the <1% pts at the mean -2.5 SD level offer the best N/Ls, and these CSMC limits can be applied at other centers to accurately assess CAD.

SOURCES OF VARIABILITY IN THALLIUM CIRCUMFERENTIAL PROFILE CURVE ANALYSIS. P.T. Makler, Jr., D.M. McCarthy, C. Colvin, and A. Alavi. Hospital of the University of Pennsylvania, Philadelphia, PA.

Detecting the presence and extent of coronary artery disease by circumferential profile (CP) analysis of thallium perfusion images has been shown to be more accurate than simple visual scan interpretation. A fundamental assumption of this objective approach is that regional thallium distribution is accurately reflected in CP curves. Potential sources of error include variability in patient positioning and variability in data analysis. We investigated these effects on the CP curves in 19 patients who had two redistribution (4 hour) 40° LAO images separated by at least one other view. The technologist was instructed to reproduce the views as closely as possible. Following an interpolated background subtraction, 60 point CP curves were generated independently from both 40° LAO images by two experienced observers, one of whom repeated the analysis one week later. The two curves were analyzed by adding the absolute difference of the two curves at each of the 60 points and dividing by 60. The variance was expressed as a percent of the average value of the curve from the first image.

Results were (1) intraobserver variation (one image, one observer, analyzed twice) was 4.9±2.5% (mean±standard deviation); (2) interobserver variation (one image, two observers) was 5.4±2.8%; and (3) repositioning variation (two images, one observer) was 12.9±6.4%.

The data indicate that intra and interobserver variability in generating thallium CP curves is quite good, but that the major potential source of error is in the positioning of the patient. This should be considered when interpreting CP curves.

EARLY CHANGES IN THALLIUM DISTRIBUTION: EFFECT ON SCAN QUANTITATION. P.T. Makler, Jr., D.M. McCarthy, H.A. Goldstein, and A. Alavi. Hospital of the University of Pennsylvania, Philadelphia, PA.

Methods of quantitative analysis (QA) of thallium (Tl) scans presume that the post-stress images in several views reflect the initial distribution of Tl in the heart. We have reported that, by visual analysis, 15% of defects may resolve within 30 minutes. We investigated the effect of this rapid resolution on QA.

The study population comprised 32 patients (pts) with coronary artery disease and an abnormal anterior stress Tl scan. The anterior view (A1) began within 8 minutes of exercise. A second anterior view (A2) was collected 30 minutes later. Redistribution images (RD) were collected at 4 hours. Following a modified Goris background subtraction, Tl concentration was determined at 60 points on the myocardial circumference. A defect was defined as a 36° sector having a Tl concentration averaging <75% of the maximum.

In 13 pts, the defect on the A2 scan was smaller than on the A1 scan (in 6 of these the A2 scan was normal). In 11 pts, the defect on the A2 scan was equal to the defect on A1 scan. In 8 pts, the defect on the A2 scan was larger than on the A1 scan. The QA diagnosis (e.g., scar vs ischemia) by A1/RD or A2/RD comparison was altered in 10 of the 32 pts.

The results demonstrate that rapid changes in the distribution of Tl occur which may significantly affect QA. This observation may also be important in single photon emission tomography, if the reconstruction algorithm is sensitive to changes in Tl distribution during image acquisition.

THALLIUM-201 KINETICS SHORTLY AFTER TERMINATION OF EXERCISE: IMPLICATIONS FOR QUANTITATIVE ANALYSIS. M. Heitzman, R.C. Fetterman, J.A. Mattera, J.P. Clements, F.J. Wackers. University of Vermont, Burlington, VT.

The concept behind quantitative analysis of Tl-201 washout (WO) assumes activity in normal myocardium to peak immediately post exercise (EX) and then to decrease steadily. However, if peak activity is delayed, the first Tl-201 image acquires submaximal counts and WO is erroneously low. On the other hand,if Tl-201 WO occurs at a steady rate, delayed imaging conceivably can be performed early post EX, which logistically is advantageous.Hence, we studied Tl-201 kinetics shortly after EX in 42 random patients (pts) by serial LAO imaging: #1 immediately post EX, #2 30 min post EX,#3 2 hr post EX. After interpolative background subtraction, circumferential count, WO profiles, and Tl-201 time activity curves were generated. Tl-201 kinetics showed 3 patterns: A,B,C. A: In 15 of 42 pts (36%), activity peaked in study 1 and then decreased (normal WO).One of 15 pts had prior infarct (PI). B: In 12 pts (28%), activity peaked in study 2. In 5/12 WO was normal in study 3 compared to 1. Five of 12 had PI. C: In 15 pts (36%) activity did not change from study 1 to 2.In 12/15 WO was normal in study 3, compared to 1. Ex performance was comparable in 3 groups. Overall, seventeen pts with normal uniform WO in study 3 had segmental differences in WO rate in study 2. If study 2 was used to post EX study to calculate WO, interpretation changed in 8 pts (19%): 3 abnormal studies into normal, in 5 the extent of abnormal WO would be reduced. Thus: 1. Tl-201 kinetics post EX is variable. Delayed peaking or no change of activity (in particular in PI or defects), may effect calculated WO. 2. Initial serial imaging is essential to recognize a variant pattern. 3. Therefore, it is not prudent to advance delayed imaging in time.

NONUNIFORM WASHOUT OF THALLIUM-201 (WITHIN NORMAL RANGE): CRITERION FOR IMPROVED DETECTION OF SINGLE VESSEL CORONARY ARTERY DISEASE. F.J. Wackers, D. Bales, R.C. Fetterman, W. Gundel, J.P. Clements. Univ. of Vermont, Burlington, VT.

Quantitative analysis Tl-201 myocardial washout after exercise has significantly improved the noninvasive detection of significant coronary artery disease(CAD). Abnormal washout generally is defined by absolute values:more than 2 standard deviations(SD) below the mean of normal. In normal subjects(n=20),we noted Tl-201 washout to be uniform on circumferential profiles after interpolative background subtraction in all myocardial segments. Relative to the 10° angle with maximal washout,mean(±SD) variability of washout/angle is minimal:18±7%. We observed that in some patients(pts) with CAD, although overall absolute percent washout was within normal range,segmentally variations occurred exceeding the mean+2SD of variability in normals. These pts display nonuniform washout (NUWO). To further evaluate the significance of NUWO, we analyzed Tl-201 stress studies of 74 pts(9 normals,65 with CAD:36 1-vessel (V)disease(D),29 multi(M)-VD) who also had coronary angiograms. NUWO was noted in none of 9 normals,but in 16 of 65 pts with CAD. Of 16 pts,13 had 1-VD,3 had M-VD. In 14/16, the anatomic area of NUWO correlated well with angiographic CAD. In 15/16 pts NUWO was the only abnormality. Using NUWO as new additional diagnostic criterion,overall sensitivity improved from 80% to 91%,for 1-VD from 69% to 86% and for M-VD from 93% to 96%. One pt with NUWO and 1-VD underwent successful coronary angioplasty. Repeat Tl-201 stress scintigraphy subsequently showed uniform normal washout. Thus, 1)isolated NUWO is an abnormal TL-201 washout pattern; 2) isolated NUWO is highly suggestive for 1-VD;3)in addition to absolute criteria for myocardial washout, relative criteria should also be applied for improved detection of CAD.

10:30-12:00 **Room 130**

NUCLEAR MAGNETIC RESONANCE: CLINICAL

Moderator: Lawrence R. Muroff, M.D.
Co-moderator: Thomas J. Brady, M.D.

CARDIAC NUCLEAR MAGNETIC RESONANCE IMAGING CORRELATED WITH THALLIUM-201 SPECT FOR VISUALIZATION OF HEART CHAMBERS, VENTRICULAR WALL MOTION AND MYOCARDIAL INFARCTION. RT Go, WJ MacIntyre, JK O'Donnell, M Geisinger, W Chilcote, C Napoli, B Sufka and TF Meaney. Department of Nuclear Medicine, Cleveland Clinic Foundation, Cleveland, Ohio.

Cardiac Nuclear Magnetic Resonance (NMR) Imaging has been performed at our institution utilizing a resistive magnet of 0.15 Tesla. Through the use of volume (three-dimensional) data acquisition, the cardiac chambers and great vessels were visualized in the transverse, coronal, and sagittal planes. Measurements were made with a gating pulse synchronizing the position of the heart at various times during diastole-systole and both saturation recovery and inversion recovery techniques were compared. The chambers visualized by the NMR techniques were compared with tomographic sections recorded by Thallium-201 transaxial single photon emission computed tomography (SPECT), also in transverse, coronal, and sagittal planes.

Ten patients with previous myocardial infarction confirmed by cardiac angiography were compared at rest with the NMR and SPECT systems. Identification of myocardial infarction was noted in both procedures with greater spatial resolution obtained in the NMR technique and increased contrast resolution noted in the Thallium-201 SPECT studies. Within the NMR techniques, inversion recovery gave greater contrast differentiation between normal and infarcted tissue. For lesions involving the inferior, posterior, or diaphragmatic wall, the availability of visualizing the coronal and sagittal planes in both techniques has been found to be extremely valuable.

The complementary effect of the two techniques has yielded an improved detection and delineation of myocardial infarction.

NMR IMAGING OF THE THYROID. V.M. Runge and F.W. Smith. Vanderbilt Hospital, Nashville, TN and the Aberdeen Royal Infirmary, Aberdeen, Scotland.

The thyroid gland of 22 patients was evaluated by NMR imaging. Correlation was made with the results of hormone assays and radionuclide thyroid scans.

The Aberdeen 0.04 tesla resistive magnet system was used for NMR imaging. The spin-warp method was employed allowing display of the transverse images obtained by proton density or calculated Tl. Imaging time was four minutes per section.

The Tl of normal thyroid tissue in the 4 control patients studied varied from 150 to 195msec (170±20,mean±

SEM). This differed significantly from the T1 of thyroid tissue from 3 patients with Graves disease (196-265 range). One patient studied with Hashimoto's thyroiditis had a T1 within the range of that of Graves disease. The range of T1 of abnormal thyroid tissue in 2 patients with benign adenomas was 190-350msec. Adenomatous tissue could not be distinguished by T1 values from neoplastic tissue in 2 patients with thyroid carcinoma and 1 patient with lymphoma. Colloid cysts in 4 patients, multinodular goiters in 4 patients, and a retrosternal goiter in 1 patient could all be readily diagnosed by NMR imaging on the basis of their anatomical appearance (on proton and T1 images).

As demonstrated in this short clinical series, thyroid scanning by NMR can readily identify gross anatomical lesions (like CT and ultrasound). In addition, because of the T1 parameter, NMR imaging has superior soft tissue resolution and one can identify Graves disease of the thyroid as distinct from normal. The value of NMR imaging in the diagnosis of benign versus malignant thyroid disease awaits further clinical trials.

COMPARISON OF NMR IMAGING AND X-RAY CT IN DETECTING BRAIN TUMORS. T.J. Brady, F.S. Buonanno, I.L. Pykett, P.F.J. New, and J.P. Kistler. Massachusetts General Hospital, Boston, MA.

Thirty-two patients with histologically proven tumors (n=12) or with a clinical diagnosis of neoplasm (n=20) of the central nervous system were studied at the Massachusetts General Hospital using a prototype resistive Technicare NMR imaging system (1.5 kGauss). True three-dimensional (3D) volumetric NMR data were acquired using one or more RF pulse sequences including inversion-recovery (IR), saturation-recovery (SR) and Carr-Purcell-Meiboom-Gill spin echo (SE). NMR images were matched to appropriate CT levels by post processing of the 3D NMR data. Tumor involvement on IR and SR images appears as either regions of decreased signal intensity suggesting prolonged T_1, or as areas of increased signal intensity suggesting shortened T_1 values; tumor involvement on SE images appears as regions of increased signal intensity suggesting prolonged T_2 values. Using one or more of these RF sequences, NMR imaging demonstrated lesions in all 32 patients including three patients in whom contrast enhanced CT studies did not demonstrate the lesion. Tumors were demonstrated on 31 of 32 IR studies, 10 of 15 SR studies and 18 of 18 SE studies. From these preliminary data, it appears that NMR imaging using IR and SE pulse sequences has an excellent sensitivity in detecting brain tumors, when compared to CT.

PHOSPHORUS-31 NUCLEAR MAGNETIC RESONANCE (P-31 NMR) SPECTROSCOPY IN PEDIATRIC NEUROMUSCULAR DISORDERS. H. T. Harcke, H.G. Marks, C.R. Hartzell, B. Chance, R.A. Warnell. Alfred I duPont Institute, Wilmington, DE, Johnson Research Foundation, University of Pennsylvania, Philadelphia, PA.

P-31 NMR, a non-invasive technique now available for the study of muscle bioenergetics, offers a method for in-vivo screening of energy pathways. A protocol for P-31 NMR examination of children was developed using a surface coil contained in a 1.9T superconducting magnet with 25 cm. bore. The gastrocnemius muscles were studied at rest and after exercise. Four normal children were evaluated under the protocol to serve as controls.

Five patients with Friedreich's ataxia (FA), an inherited disorder characterized by progressive spinocerebellar degeneration, were studied. Selection of this group of patients was based on reports linking spinocerebellar degeneration with abnormalities of pyruvate dehydrogenase complex, an enzyme group in the pathway of oxidative glucose utilization in muscle.

Resting P-31 spectra were analyzed for relative concentrations of phosphocreatine (PCr), inorganic phosphorus (Pi) and ATP. Mean Pi/PCr = .11 $\pm$ .03 vs .13 $\pm$ .03 for controls suggested that FA patients possess a normal bioenergetic potential. Post-exercise scans showed no delay in return to resting values of PCr and Pi for FA patients. This preliminary study indicated that under limited exercise conditions, there were no detectable alterations of muscle bioenergetics in FA and demonstrated the feasibility of using P-31 NMR spectroscopy for studying some pediatric neuromuscular disorders.

TECHNIQUES EMPLOYED IN DEVELOPMENT OF IV NMR CONTRAST AGENTS. S.E. Schmittle, V.M. Runge, J.A. Clanton, A Beth, A.E. James, and C.L. Partain. Vanderbilt University Medical Center, Division of Nuclear Medicine, Nashville, TN.

Two nitroxide stable free radicals (NSFR) complexes were evaluated *in vitro* and *in vivo* as potential IV NMR contrast agents, and compared with a (non-toxic) paramagnetic chelate.

The *in vitro* samples were prepared in serial dilutions of NSFR's in saline and serum. The paramagnetic chelate was an aqueous solution (50mg/ml).

In vivo NSFR samples were prepared after serum and homogenated liver and kidneys were obtained from sacrificed mice at various time points. Ascorbic acid oxidase was added to the samples because ascorbic acid is presumed to reduce NSFR's *in vivo*. Following IV injection of paramagnetic chelate in dogs, contrast enhanced NMR images were obtained using a Technicare 3KG superconducting NMR imaging system.

T_1 measurements were made by the inversion-recovery technique, utilizing a JEOL FX-90Q NMR spectrometer. Inversion-recovery is a technique in which the nuclei in the sample are irradiated with a pulse of radiofrequency (RF) radiation. This action creates a resonant effect and some of the nuclei move to a higher energy state. The nuclei will relax to their original ground state. The time it takes these nuclei to relax is T_1.

NSFR's and paramagnetic chelates both serve as effective intravenous NMR contrast agents in experimental animals, allowing assessment of tissue vascularity and renal function. High cost, relative short *in vivo* half-life and possible carcinogenesis are disadvantages of NSFR's when compared to paramagnetic chelates.

P-31 NUCLEAR MAGNETIC RESONANCE SPECTROSCOPY IN THE EVALUATION OF BIOCHEMICAL PARAMETERS OF RED BLOOD CELL STORAGE. D.R. Ambruso, D.L. Johnson, B. Hawkins, A.R. Fritzberg, E. McCabe, and W.C. Klingensmith III. U. of Colorado Health Sciences Center, Bonfils Memorial Blood Center, Denver, CO. and the Colorado State University Regional NMR Center, Ft. Collins, CO.

Maintaining intracellular levels of ATP and 2,3-diphosphoglycerate (DPG) is important for assuring adequate *in vivo* survival of and oxygen transport by stored red blood cells (RBCs). Recent advances in NMR instrumentation have allowed application of this technique to biological systems. In this study levels of DPG and ATP were measured by P-31 NMR spectroscopy on a Nicolet NT-150 spectrometer and by standard biochemical techniques. Five units of blood, anticoagulated with CPD-A, were obtained from normal adults according to standard blood banking procedures and processed as packed RBCs. Serial samples were obtained and levels of DPG and ATP were expressed as µmol/gm of hemoglobin. Results below are mean values.

Storage	DPG		ATP	
day	NMR	Biochemical	NMR	Biochemical
1	11.60	12.37	2.68	3.28
15	6.24	6.16	2.78	3.86
29	1.50	0.73	2.52	2.57

There were no significant differences between techniques in the results for DPG or ATP although there was a tendency for NMR to give lower results for ATP. Both techniques demonstrated a significant ($p<0.05$) decrease in DPG with time and no significant change in ATP with time. NMR spectroscopy may provide an accurate, non-invasive method of quality assurance of stored packed RBCs.

10:30-12:00 **Room 132**

GASTROINTESTINAL IV: LIVER/GI BLEEDING

Moderator: Robert C. Stadalnik, M.D.
Co-moderator: Aldo N. Serafini, M.D.

QUANTITATION OF PORTAL BLOOD FLOW FOLLOWING PORTACAVAL SHUNTING USING Tc-99m MAA. M. Fardi, K.P. Lyons, R. Conroy, I.J. Sarfeh, and E.B. Rypins. Nuclear Medicine, Radiology, and Surgery, VAMC, Long Beach, and UC Irvine, CA.

Side to side portacaval shunts provide intravenous access to the portal circulation. A method for quantitating shunt flow after portacaval anastomosis is described using Tc-99m MAA. The shunts were canulated transvenously and the direction of portal flow was assessed angiographically. Then the catheter was positioned in the superior mesentric vein (SMV) and 2-5 mCi of Tc-99m MAA was slowly infused in 10 cc of saline. Images of chest and abdomen were obtained with a large field of view camera interfaced to a computer. The catheter was then repositioned into the portal vein (PV) and a second dose of Tc-99m MAA was injected. The percent activity in both lung fields and the liver was calculated from the SMV and also from the PV study after computer subtraction of residual activity from the first injection. Ten patients were studied, 5 with angiographically proven prograde and 5 with retrograde portal flow. In 5 patients with reversed portal flow 1.04±0.58% of the dose injected in the SMV and 1.2±1.0% of the PV dose appeared in the liver. In 5 patients with forward flow, the corresponding percentages were 23.5±12% for SMV and 73.6±32.5% for PV injections. Radionuclide studies correlated significantly with angiograms (P<.001, Mann-Whitney V-Test). Conclusion: Tc-99m MAA infusion study reliably distinguishes between patients with prograde and retrograde flow and quantitates porto-systemic flow ratios. Heretofore, only qualitative assessment by angiography was possible.

EVALUATION OF "PORTAL SCINTIGRAPHY" BY INTESTINAL ADMINISTRATION OF Tc-99m USING ENDOSCOPY IN LIVER CIRRHOSIS. M.Kudo,Y.Ibuki,K.Fujimi,S.Tomita, H.Komori,Y.Okimoto,A.Todo,Y.Kitaura and K.Ikekubo Kobe General Hospital,Kobe,Japan; N.Tamaki and K.Torizuka. Kyoto University,School of Medicine, Kyoto,Japan.

The purpose of this study was to evaluate "Portal scintigraphy(PS)" in liver cirrhosis(LC).

"PS" was performed in 36 patients with LC by intestinal administration of Tc-99m(10mCi) using endoscopy. We used endoscopy in order to put RI into the intestine accurately and to avoid physiological shunts in the rectum. We obtained time-activity curve upto 20 min and heart/liver uptake ratio(H/L ratio) at 4 min after administration. We classified the curves into 3 types. We investigated the relationship between H/L ratio and liver and spleen volume in each type. These volumes were obtained by utilizing SPECT.

The results were as follows:(A) In the type of preceding liver uptake but finally dominant heart uptake, we found negative correlation of H/L ratio with liver volume(r=-0.64) and positive correlation of H/L ratio with spleen volume(r=0.61). (B)H/L ratio in moderate esophageal varices showed higher value than that in mild varices. (C)Using "PS",the collateral veins branching from the portal trunk were visualized in 9 out of 15 cases(60 %) with moderate or severe esophageal varices.

In conclusion, "PS" is an excellent method to analyze the various pathological states of liver cirrhosis from the viewpoint of portal circulation.

SCINTIPHOTOSPLENOPORTOGRAPHY: THE METHOD FOR SCANNING THE PORTAL CIRCULATION AND ESTIMATING THE REGIONAL HEPATIC BLOOD FLOW. T. Kashiwagi. Department of Medicine, Osaka Kosei-Nenkin Hospital, Osaka, Japan

We have already reported the technique of scintiphotosplenoportography(SSP), which permits a visualization of portal venous system by injecting Tc-99m sodium pertechnetate into the spleen and following its course by scintillation camera(1). Recent advent of high resolution scintillation camera facilitated to investigate the abnormalities of portal venous system in more detail. Various types of collaterals were clearly visualized. SSP was performed in 161 patients and no significant complications were encountered. Flow patterns of SSP were classified into nine groups according to the direction of collateral flow. Hepatopetal collateral flow was frequently observed in pancreatic cancer. In portal hypertension, cephalic collateral flow was more frequently observed than caudal flow.

In the case of injecting Xe-133 in saline solution into the spleen, the functional image of the liver representing topographically the intrahepatic distribution of regional hepatic blood flow(r-HBF), was obtained using the Xe-133 tissue clearance method and a scintillation camera with a computer system. Heterogeneous intrahepatic distribution of r-HBF was clearly demonstrated by this method. Greater flow regions were frequently observed in the right lobe and r-HBF was decreased in liver cirrhosis.

Therefore, SSP appears to be a clinically useful technique, as it provides, easily and safely, useful information about the functional state of portal circulation and hepatic blood flow.

1) T. Kashiwagi, et al: Gastroenterology 67:668-673, 1974.

99mTc-RBC SCANNING IN THE DIFFERENTIAL DIAGNOSIS OF FOCAL LIVER LESIONS. S.A. Rabinowitz, K.A. McKusick, H.W. Strauss. Massachusetts General Hospital, Boston, MA.

Hepatic hemangiomas are the most common benign liver tumor. Their appearance on colloid liver-spleen scans and ultrasound is non-specific and cannot be differentiated from metastases. On 99mTc-RBC scans, hemangiomas have been reported to have decreased flow but uptake more than normal liver on delayed images. To determine the specificity of this finding 28 patients (pts) underwent hepatic Tc-RBC imaging after liver-spleen scan or ultrasound indicated single or multiple liver lesions.

Red cell labeling was performed with 740MBq of $^{99m}TcO_4^-$ using a modified in vitro technique. Flow images as well as early (1, 5, 10, 15 min) and delayed (1-2 hr) 200OK static images were obtained. Diagnosis was made by needle biopsy,surgery or angiography. These diagnoses included 7 pts with hemangiomas, 3 hepatomas, 15 metastases (13 adenoCa of the colon, 1 oat cell, 1 gastric carcinoma), 1 abscess and 2 pts with liver cysts.

Six of the 7 hemangiomas demonstrated uptake greater than normal liver on the static images. The time this increased uptake was first seen varied from 1 to 10 minutes post injection but was always most apparent on the 1-2 hr delayed view. There was decreased flow in all cases except for one large hemangioma that displayed increased flow. The remaining hemangioma had no uptake on static images and open biopsy showed cavernous hemangioma with fibrosis.

Two of the 3 hepatomas demonstrated uptake greater than normal liver. One of these had been previously treated by chemotherapy. However, in contrast to the hemangiomas these showed no further increase in uptake relative to normal liver on the delayed scan. The 3rd hepatoma showed no uptake on static imaging. All hepatomas had increased flow.

None of the metastases, cysts or abscess had increased uptake on static imaging.

Tc-RBC scanning was able to differentiate hemangiomas from metastases and other benign focal liver lesions. A false negative scan occurs in hemangiomas with thrombosis or fibrosis. Hepatomas may be difficult to differentiate from hemangiomas on the basis of this technique.

COMPARISON OF TECHNETIUM-99m RED BLOOD CELLS AND TECHNETIUM 99m SULFUR COLLOID IN THE DETECTION OF GASTROINTESTINAL HEMORRHAGE. D Tanasescu, J Rigby, M Brachman, L Ramanna, A Waxman, Cedars-Sinai Medical Center, Los Angeles, Calif.

The purpose of this study is to compare the sensitivity of Tc-99m red blood cells (RBC) with Tc-99m sulfur colloid (SC) in detecting gastrointestinal hemorrhage (GIB) and in establishing the site of bleeding.

29 studies were performed in 26 patients (pts). The i.v. injection of 10 mCi of TcSC was followed by sequential one minute (min) anterior abdominal views (AAV) for 20-30- min. Immediately afterwards, 15 mCi of in vitro labelled TcRBC were injected i.v. and 1 min AAV were obtained every 15 min for 40 min. A high resolution Anger camera was used. All views had 1,000.000 counts and were acquired by computer. Delayed images were done at 2-4 hours and 24 hours. Correlation with endoscopic, arteriographic, surgical and clinical findings was made.

Of the 29 studies using TcRBC, 18 were positive (+) and 11 negative (-). There were 16 true positive (TP) and 9 true negative. The results show that the sensitivity of Tc RBC is 89% with a specificity of 82% for detection of bleeding. Of 16 TP cases using RBC, none were + with TcSC.

Ten positive studies were evaluated for the site of bleeding. 9 sites were correctly determined and 1 was wrong. Early views (0-40 min) were positive in 6 of 10 studies. Delayed views (4-24 hours) resulted in 4 additional positive cases.

We conclude that the TcRBC is the current test of choice for diagnosis and localization of GIB. The TcSC study yielded no TP studies and is considered of little value in evaluating cases of GIB. Localization of bleeding sites is enhanced using delayed views, especially if the early studies are negative.

FURTHER VALIDATION OF SUPERIORITY OF 99mTc RED BLOOD CELL METHOD OVER 99mTc SULFUR COLLOID IN THE DETECTION AND LOCALIZATION OF GASTROINTESTINAL BLEEDING. T. K. Chaudhuri, R. W. Ware, W. H. Beal, and J. D. Straw, VA Medical Center and Univ. of Texas Health Science Center, San Antonio, TX.

Acute gastrointestinal bleeding was simulated in anesthetized, open-abdomen dogs at various times post injection of 5 mCi of either 99mTc labeled red blood cells (RBC) or 99mTc sulfur colloid (SC). Approximately 20 ml of venous blood were withdrawn from dog A1 at 1 min and 5 min, from A2 at 2 and 6 min, from A3 at 3 and 7 min, and from A4 at 5 and 10 min post injection of RBCs. Similarly, 20 ml of blood were withdrawn from each of dogs B1, 2, 3, and 4 at the same respective time intervals post injection of SC. As quickly as possible, from the first 20 ml sample, several measured aliquots (1, 2, 5, and 10 ml) were prepared and injected into gut lumen of each respective dog at 4 widely separated sites. Gamma scintigraphy of the abdomen was then performed for subsequent image evaluation. After withdrawal of the second 20 ml of blood, intraluminal deposits of 1, 2, 5, and 10 ml were made into each of 4 additional easily distinguishable sites in the gut and imaging was repeated. Results demonstrate that SC "bleeding" was detected with greater sensitivity than that of the tagged RBCs when time between injection of radiolabel and simulated bleeding was 2 min or less; however, for all GI bleeding simulated at 3 min or more after label injection, the tagged RBC method was clearly superior. A second experimental series was performed following the administration of SC in 5 dogs and RBC in another 5 dogs. In a similar way, measured volumes of timed blood samples were held in rubber finger-cots placed in the abdominal cavity for imaging and interpretation. These resulted in the same conclusion.

10:30–12:00 **Room 275**

DOSIMETRY/RADIOBIOLOGY

Moderator: Edward G. Bell, M.D., Ph.D.
Co-moderator: Harold L. Atkins, M.D.

THE DOSIMETRY OF N-ISOPROPYL I-123 P-IODOAMPHETAMINE. R. E. Zimmerman, J. R. Shapiro, B. L. Holman, A. G. Jones, M. L. Kaplan, T. C. Hill. Dept. of Radiology, Harvard Medical School, Boston, MA.

The human dosimetry of N-isopropyl I-123 p-iodoamphetamine (IMP) has been calculated based on the biodistribution of IMP in 11 Macaca fascicularis monkeys. Biodistribution was determined by dissection and organ counting at 15 min., 1 hour, 4 hours, 24 hours and 48 hours after injection. Absorbed doses for major organs were determined using MIRD tabulated S factors for I-123, I-124 and I-125 labelled IMP. Absorbed doses for the eye, retina and lens were calculated for activity distributed in the retina chorid, pigmented epithelium and iris using the scaled absorbed dose distribution of Berger for non-penetrating radiation and the specific absorbed fraction for point isotopic sources of Berger for penetrating radiation together with an eye model consisting of concentric spherical shells and integrated appropriately for source and target geometry. The results indicate that for biodistribution similar to the monkey the critical organ is the eye with a dose of 0.59 rads/mCi for pure I-123 IMP increasing to 1.83 rads/mCi with 4% contamination of I-124 IMP and to 1.23 rads/mCi with 0.4% contamination of I-125 IMP. However, eye uptake in humans has not been observed. Other significant doses include the liver and thyroid doses of 0.129 rads/mCi and 0.127 rads/mCi, respectively for pure I-123 and increasing by a factor of 2-4 with I-124 impurity and increasing less for I-125 contamination. For clinical studies the thyroid dose can be reduced to very low levels by blocking the thyroid gland. The results indicate that doses of several mCi are acceptable for clinical cerebral blood flow images.

DOSIMETRY OF ANTI-COLON CARCINOMA MONOCLONAL ANTIBODY $F(ab')_2$ FRAGMENTS IN HUMANS. N.D. Hammond, P.J. Moldofsky, M.A. Beardsley, C.B. Mulhern, Fox Chase Cancer Center/ Jeanes Hospital, Philadelphia, Pa.

We are radiolabelling the antigen-associated $F(ab')_2$ fragments of mouse monoclonal antibody 1083-17-1A and adminstering the product to patients with colon carcinoma for imaging and to quantitate biologic distribution of antibody fragments in the human. $F(ab')_2$ fragments are radiolabelled with Iodine-131(iodogen technique) and tested for sterility, pyrogenicity, labelling efficiency and relative immunoreactivity. Images of known tumor deposits are obtained daily for seven days on a gamma camera with data stored and processed by computer techniques. Blood samples are obtained to determine the effective half-life of total and protein-bound I-131. Iodine-131 in the tumor deposits and surrounding tissues is evaluated quantitatively with a methodology utilizing counts from diametrically opposing views of tumor deposits and surrounding normal tissue which eliminates correction factors for lesion depth. Corrections are made for patient attenuation, lesion size and surrounding tissue activity. The total I-131 activity in blood and the protein-bound I-131 in plasma were found to follow a two-compartment model with an average initial fast half-life of 4.3 and 3.6 hours, respectively, followed by a slow half-life of 29.0 and 19.3 hours, respectively. A typical tumor uptake in a 7 cm diameter hepatic metastasis was found to be approximately 0.5% of the administered dose at 48 and 72 hours. Typical liver activity (including metastasis was 8.4%, 5.1% and 0.5% of administered dose at 24, 48 and 72 hours, respectively. This quantitative evaluation of blood half-lives and tissue localization forms the basis of our calculations of whole body and tumor dosimetry.

THE DOSIMETRY OF I-131 LABELED METAIODOBENZYLGUANIDINE IN THE TREATMENT OF MALIGNANT PHEOCHROMOCYTOMAS. J.E. Carey, Jr., D. Swanson, J.C. Sisson, B. Shapiro, L.J. Meyers, W.H. Beierwaltes. University of Michigan Medical Center, Ann Arbor, MI.

I-131 labeled metaiodobenzylguanidine (MIBG) is being used to treat patients with metastatic pheochromocytomas with resultant reduction in tumor size and function.

A conjugate view imaging technique was evolved to estimate tumor absorbed dose. Tumor I-131 MIBG activity was measured as a function of time with a calibrated gamma camera/minicomputer combination. Transmission computed tomography was used to estimate tumor volume. From these measurement I-131 MIBG tumor concentrations and effective half-lifes were obtained and absorbed doses estimated. Absorbed doses of 80-90 rad per mCi administered were calculated for some tumors. Absorbed doses for whole body, thyroid, liver, adrenals, and bladder were calculated using the conjugate view technique or in vitro animal and human data.

The widely distributed nature of pheochromocytomas required modification of the technique for tumors in various body locations including head, lung, and liver. Problems due to collimator septal penetration, varying background activities, and tumor sizing are addressed.

The need to estimate human pheochromocytoma tumor dosimetry using conventionally available imaging instrumentation and I-131 required the development of the conjugate view technique within our laboratory. Using this technique a total accumulated absorbed dose to tumor of 20,000 rads was calculated. The technique evolved is applicable to dosimetry estimation using other I-131 labeled pharmaceuticals for cancer therapy.

THE PROPERTIES OF I-125 LABELED 11-β-METHOXY-17-α-IODOVINYL ESTRADIOL (IMOX). R.E. Gibson, B.E. Francis, E.L. Jagoda, H. Goodgold, N. Ferreira, R.C. Reba, W.C. Eckelman. The George Washington University Medical Center, Washington, DC

Radiohalogenated derivatives of estradiol have been shown to localize in estrogen receptor containing tissues and provide images of estrogen-(+) tumors. The sensitivity of receptor detection is determined by receptor affinity, metabolic clearance and the extent of non-receptor binding. Moxestrol exhibits these desired properties and H-3 moxestrol provides the highest target to blood ratios for estrogen derivatives. We have prepared an I-125 labeled

compound, IMOX, as a closely related compound to moxestrol bearing radioiodine and determined its in vivo and in vitro properties.

The I-125 IMOX (specific activity 1800 Ci/mmole, 95% radiochemical purity) exhibits an affinity 3-fold less than H-3 estradiol (H-3 E-2). In vivo, 19% dose/g localized in uterus of weanling rat at 2 hrs. By 6 hrs, this reduced to 6%/g (4%/g is non-specific). By contrast, peak levels of H-3 E-2 (5%/g) were obtained in 1 hr and 2%/g at 6 hrs (0.5%/g non-specific). These results are consistent with in vitro kinetic studies for E-2 and moxestrol. The on rate of moxestrol is slower than estradiol and therefore the delay in peak activity is to be expected. An injection of E-2 (25-50 µg) at 1 hr after injection of I-125 IMOX effects 75% washout of IMOX in 30 min. The uterus to blood (U/B) ratio of 95 is the largest observed for an E-2 analogue (U/B for H-3 E-2 is 12 at 1 hr). I-123 labeled IMOX should provide images of estrogen receptor positive tumors.

VERIFICATION OF ABSORBED FRACTION VALUES WITH CHEMICAL DOSIMETRY. W.T. Oravez, K.A. Lathrop, P.V. Harper. University of Chicago. Chicago, IL.

Little effort has been made to verify experimentally the radiation absorbed dose estimates calculated with the mathematically derived values for the fraction of energy absorbed in organs of the MIRD mathematical model of the 70-kg adult. The coefficient of variation attached to many of the tabulated values are as high as 50%. Such inaccuracies become unacceptable as the amount of ionizing radiation used for diagnosis increases. In the present study we are making use of the fairly energy independent Fricke (ferrous -ferric) dosimeter for measuring absorbed doses in organs constructed of plastic to the dimensions of the MIRD mathematical model. A chemical dosimeter was used since it measures the average dose over a volume of tissue, an approach which appears preferable to averaging values obtained from point measurements. The sensitivity was increased by using 10 cm cuvettes and the auto-oxidation (drift) was greatly reduced by lowering the ferrous ion concentration from .001M to .0001M. The 224 nm absorption peak gave erratic results at low ferric ion concentrations so that the 304 nm absorption peak, although less sensitive, gave more stable results. With these modifications reliable ±10% readings were obtained with doses of 50 rads. Preliminary measurements with F-18 in a 100 ml spherical vessel agreed within ±13% of calculated values. Meaningful measurements on a number of source-target organ pairs thus appear to be feasible. This approach is being extended by using the terephthalic acid dosimeter which is reported to be effective down to 1 rad. The fact that this dosimeter is somewhat energy dependent will be evaluated by comparison with the Fricke dosimeter under identical geometry.

QUANTITATIVE MEASUREMENT OF LONG TERM IN VIVO THALLIUM DISTRIBUTION IN THE HUMAN. C.T. Chen, K.A. Lathrop, P.V. Harper, R.D. Bartlett, V.J. Stark, K.R. Fultz and P.F. Faulhaber. University of Chicago. Chicago, IL.

Extrapolation of animal distribution data to human for intravenously administered thallium-201 (73h half-life) predicted from our previous work prompted the present study to confirm data at long time intervals. Thallium-202 produced by (p,n) reaction on mercury-202, used because of its 12.2d half-life, was shown to have a distribution in mice identical with commercial thallium-201. With a conjugate whole-body scanning system, quantitative measurement of in vivo thallium distribution was performed at various times for eight weeks. Whole-body retention was further followed for more than four months with a set of uncollimated detectors. Blood samples were collected at intervals for two weeks. Fecal and urinary excretion was recovered quantitatively for six weeks. Kidney activity was about 6% of that retained in the body at all times. Redistribution of activity was minimal except for a gradual progression into the brain for the first two days. Variable intestinal and bladder contents were clearly observed from time to time. Measurement of cumulative excretion correlated closely with the retained activity calculated from the whole-body image. Experimental blood and whole-body retention curves were in good agreement with those predicted from previous animal extrapolation studies. The whole-body retention curve was fitted with a two-exponential function with half-times equal to 7d for 63% of the injected activity, and 28d for 37%. The detailed analysis of results provided improved information for the absorbed dose calculation.

10:30-12:00 **Room 120**

ONCOLOGY III: GALLIUM-MAA

Moderator: Carlos Beckerman, M.D.
Co-moderator: Richard S. Benua, M.D.

!IGH DOSE GALLIUM IMAGING IN THE EVALUATION OF LYMPHOMA. W.D. Kaplan, K.C. Anderson, R.C.F. Leonard, Divisions of Nuclear Medicine and Medical Oncology, Sidney Farber Cancer Institute, Harvard Medical School, Boston, MA.

Recent general and nuclear medicine articles suggest a limited role for Ga-67 in evaluating lymphoma pts. Analyses of these studies reveal persistent use of rectilinear scanners and tracer doses of 35-50 µCi/Kg. We assessed the role of Ga-67 scans using larger administered tracer doses and a triple peak gamma camera; scan interpretations were retrospectively compared with other radiologic studies and clinical follow-up. Between 1977-1981, 52 consecutive patients [21 Hodgkin's (H), 31 non-Hodgkin's] were imaged for staging and follow-up. They received 7-10 mCi IV and were studied between 48 and 72 h using 20% (94, 184 KeV) & 30% (296 KeV) windows and a 5200 parallel hole ME collimator. Clinical data and/or at least one other radiologic procedure (median=2, range=1-6) were obtained within 3 weeks of scan. Analysis of 99 scan results by site showed a sensitivity of 0.97 (H) and 0.92 (NH); specificity was 1.0 for both and the combined accuracy was 0.96. No false positive scans were encountered. When Ga-67 scans were compared to 169 contemporaneous radiologic studies (abdominal and chest CT, CXR, LAG, US, liver and bone scans) the tests agreed, i.e. both positive or both negative in 147 cases (87%). In 22 instances of disagreement, the Ga-67 was correct in 18 (82%). There were 6 cases of chest or abdominal CT identifying "bulk" disease which was Ga-67 negative in pts who have not evidence disease over 12-60 months. Of 4 sites (4 pts) in which the Ga-67 scan was false negative, other sites of disease were identified in 2 pts. Ga-67 imaging is sensitive, specific, and accurate in the evaluation of lymphoma pts. A negative Ga-67 scan, even with a positive abdominal or thoracic US or CT scan, strongly suggests inactive disease.

INADVERTENT ADMINISTRATION OF ANTINEOPLASTIC AGENTS TO PATIENTS PRIOR TO GA-67 INJECTION: RECOGNITION OF A SPECIFIC RADIONUCLIDE DISTRIBUTION PATTERN AND ITS DIAGNOSTIC SIGNIFICANCE. C. Bekerman, D.G. Pavel, J. Bitran, S. Pinsky and U.Y. Ryo. Michael Reese Hospital and Medical Center, and University of Illinois at the Medical Center, Chicago, IL

Alteration of Gallium-67 (Ga-67) distribution, in normal and tumor-bearing animals, following administration of chemotherapeutic agents has been demonstrated. Such an experiment may be impossible to reproduce in a clinical environment, however, accidental administration of antineoplastic agents prior to Ga-67 injection may occur. Eight patients (pts) had a Ga-67 scan that fit the description of the animal experiments: marked increased uptake in bone with suppressed uptake in liver, muscle and tumor. Five pts had hematologic neoplasms, and 3 pts had solid tumors. None had evidence of parenchymal liver disease. Review of the charts revealed a strikingly similar sequence of events in the 8 pts; they all had received an injection of one or multiple chemotherapy agents in the 24 hrs prior to Ga-67 administration. Follow-up Ga-67 scan in 4 pts while off antineoplastic medication showed a revert to the classical Ga-67 distribution pattern. Inhibition of protein synthesis or of a serum binder for Ga-67 or competitive blockage of specific Ga-67 organ receptors by the antineoplastic agents may result in the altered Ga-67 distribution. Recognition of this specific pattern of distribution and its cause should be considered when interpreting a Ga-67 scan with increased deposition in bone and decreased liver, muscle and tumor uptake.

THE CLINICAL SIGNIFICANCE OF PULMONARY Tc-99m MAA FOLLOWING RADIONUCLIDE HEPATIC ARTERY (HA) PERFUSION. W.D. Kaplan, S.E. Come, S.M. Laffin, R.W. Takvorian. Divisions of Nuclear Medicine and Medical Oncology, Sidney Farber Cancer Institute, Harvard Medical School, Boston, MA.

HA infusion of 5-FUdR provides high hepatic drug levels but little systemic toxicity since 5-FUdR is effectively detoxified by hepatocytes. We previously demonstrated that slow infusion Tc-99m MAA via HA aids in catheter placement, predicts response to therapy, and identifies extrahepatic flow in the gastroduodenal (GDA) or splenic (SA) arteries as a correlate of toxicity. Marked pulmonary uptake (>20% of total tracer dose) in 4 pts who showed major GI toxicity prompted us to retrospectively investigate lung activity as a predictor of systemic toxicity. 14 consecutive pts treated over 17 mos. were studied. None had perfusion of the GDA or SA during therapy. All received baseline and follow-up(7-27 d) slow infusion studies (4.0 mCi, Tc-99m MAA at 10-21 ml/hr). The % injected dose in the lung was determined: $\bar{x}$ number of cts/cell in lung + $\bar{x}$ number of cts/cell in lung + $\bar{x}$ number of cts/cell in liver. (This method had previously been validated in another set of pts where the $\bar{x}$ number of cts/cell vs the total number of cts/cell using 20% lung uptake as predictive of toxicity correctly classified 100% of pts.) We found that pts with baseline lung uptake of >20% had significantly more severe GI toxicity than pts with baseline values of <20% (1/11 vs 3/3 pts; p=0.01). No pts showed >12% change in lung uptake on follow-up and there did not appear to be a relationship between changes in lung activity during therapy and the development of GI toxicity. Our findings support the existence of hepatic A-V communications in some patients, suggests these are present pre-therapy and that pulmonary activity of $\geq$ 20% is predictive of impending GI toxicity.

MODEL FOR EVALUATION OF TUMOR LOCALIZATION OF LABELED CHEMOTHERAPEUTIC AGENTS. M. Webber, R. Verma. UCLA School of Medicine, Los Angeles, CA.

The distribution of Ga-67 as a tumor scanning agent is well known. Comparing potential agents to Gallium appears reasonable. This paper describes a comparison study of H-3 labeled 5 Fluorouracil, (5FU) Methotrexate (MTX), and Adriamycin (ADR), to GA-67.

Sprague-Dawley rats bearing solid Walker 256 carcinosarcoma were used. Four rats were studied for each agent and the results averaged. The mean i.v. doses injected were 30, 25 4.3, & 100 µCi of 5FU, MTX, ADR, & Ga. The rats were sacrified at 2 hrs. 4 rats were studied at 48 hrs with Ga. Tissue samples were obtained, weighed, solubilized and counted. The tracer concentrations are expressed as RPD (relative % dose/gm i.e. cpm/gm of sample divided by the sum of cpm/gm of all tissues studied).

RPD of therapeutic agents was low (1-4%) in blood and skeletel muscle. For tumor it was 2.2-8.6% and in the viscera, 2.2-14%. Liver was 11-20% and spleen, 1-14%. For Gallium RPD was 24% at 2 hrs and 2.1% at 2 hrs for blood and for skeletal muscle it was 4.6% at 2 hrs and 2% at 48 hrs. Ga RPD for tumor was 14% at 2 hrs and 18% at 48 hrs, and the level for viscera was 11% at 2 hrs and 7.1% at 48 hrs.

Tumor/tissue ratios for the chemotherapeutic agents are significantly lower than those for Gallium. This comparison to a widely used reference allows us to anticipate that the scans with the agents studied would not be better than Gallium, in the tumor and host studied. Further studies are suggested to determine if such results can be generalized.

MICROCIRCULATION OF HEPATIC TUMORS STUDIED BY SPECT AND INTRA-ARTERIAL Tc-99m MAA. H.A. Ziessman, J.W. Gyves, J.H. Thrall, W.H. Ensminger, J.W.Keyes, Jr., M. Tuscan, University of Michigan Medical Center, Ann Arbor, MI.

Tumor neovascularity provides nutritional blood supply essential to continued growth. Tc-99m MAA hepatic art. perfusion scintigraphy (HAPS) and single photon emission tomography (SPECT) offer a means of quantitating differences between tumor and normal tissue since the no. of microspheres entrapped in the first arteriolar-capillary bed is proportional to blood flow. 24 pts underwent SPECT with a GE 400T after receiving TC-99m MAA via a hepatic artery catheter. Tumor size was measured and ct density ratios of tumor to uninvolved liver were calculated. 26 colo-rectal tumor nodules (18 pts) were analyzed. Nodules >=9.6 cm had a central core of no activity surrounded by a hypervascular rim. The size of the core varied but the rim size varied less, median of 3.15 (range 1.8-4.2). Nodules <=8.4 cm did not have a hypovascular core and appeared solid. The largest rim thickness was 4.2 cm. The greatest radius of the small nodules was 4.2 cm suggesting the maximum depth to which tumor neovascularity can be generated. The tumor/normal liver activity ratio was always >1 (median 2.7) and unrelated to size. 14 carcinoid tumors (5 pts) were studied. Large nodules (>=9cm) had a central core lacking activity and a rim of increased activity. The largest rim measured 3.9 cm which approximated the radius of the largest solid nodule. Small nodules (=8.0 were solid with no central core. Tumor/liver ratio was >1 (median 4.4). In a pt with hepatoma, 3 small nodules (4.2 - 6.6 cm) all had a solid pattern. The tumor/normal tissue activity ratio was >20. Conclusion: HAPS and SPECT can define the vascularity of liver tumors. Potentially exploitable differences between tumors and normal liver microcirculation exist.

CLINICAL EXPERIENCE WITH Tc-99m MAA HEPATIC ARTERY PERFUSION SCINTIGRAPHY (HAPS) H.A. Ziessman, J.H. Thrall, P.J. Yang, W.D. Ensminger, J.E. Gyves, J.E. Niederhuber, M. Tuscan, University of Michigan Medical Center, Ann Arbor, MI 48109

In the past 2 years, we have performed 449 HAPS studies on 207 pts being treated for primary and metastatic liver cancer. These pts receive chemotherapy through an indwelling hepatic art catheter attached to a subcut. implanted Infusaid pump. The success of this approach depends on the complete perfusion of the liver tumor and lack of extrahepatic perfusion. In the initial 126 studies (61 pts), 90% of the pts with normal and 75% with variant anatomy at the time of catheter placement had complete perfusion of both lobes. Extrahepatic GI uptake was seen on 20 studies (11 pts) and significant lung uptake was seen in 27 studies (22 pts). Focal uptake at the catheter tip was seen in 72 studies (39 pts) due to small non-obstructing thrombi.

The pattern of distribution within the tumors was frequently characteristic. Carcinoid tumors were uniformly hypervascular while colo-rectal cancer nodules were frequently found to have a hypervascular rim that was not seen on contrast angiography and hypovascular centers corresponding to necrotic tumor cores seen pathologically.

A subset of 42 consecutive studies had quantification of the percent A-V shunting to the lung. Percent shunt = lung cts/(lung cts + abdominal and liver cts). This ranged from 1.8 to 20% (mean 7.0, SD 4.6).

HAPS has proven valuable and necessary for evaluation of catheter placement, blood flow distribution to the tumor and liver, as well as in the detection of extra-hepatic flow and A-V shunting which are associated with systemic toxicity.

STARCH MICROSPHERES AND QUANTITATIVE HEPATIC ARTERIAL PERFUSION SCINTIGRAPHY IN CANCER CHEMOTHERAPY. H.A. Ziessman, J.H. Thrall, W.E. Ensminger, J.E. Gyves, J.E. Niederhuber, M. Tuscan, University of Michigan Med. Ctr, Ann Arbor, MI

Hepatic art. infusion chemotherapy results in a higher concentration of drug delivered to the tumor with less systemic exposure than possible by IV therapy. However, extrahepatic blood flow and lung shunting can be a limitation. This study describes a quantitative method for calculating the extrahepatic component and changes in it due to a new adjunctive therapy, degradable starch microspheres (DSM). DSM temporarily occlude the hepatic art. circulation, thereby increasing the uptake of chemotherapeutic agents.

20 pts with metastatic liver cancer underwent baseline HAPS using Tc-99m MAA to determine blood flow distribution, and to quantitate extrahepatic uptake. The percent shunt index (PSI) was determined: PSI = (Total field cts-liver cts)/Total field cts. Patients then received incremental doses of DSM and the PSI was calculated after each dose. The PSI range was 6-26% (mean 12.3±5.8 SD). The mean PSI increased progressively after each injection of DSM/Tc-MAA suspension. After injection #1: 12.5%, #2: 15.3%, #3: 17%, #4: 21%, #5: 26.8%.

2 patterns of change in shunting were seen: a progressive increase in PSI from baseline, a decrease to a value lower than baseline after 1 of the injections, ususally fol-

lowed by a rise to its highest level. All 3 pts with more than one study had consistent patterns, however the PSI's were higher for each subsequent study.

Conclusion: 1) Since increased shunting can result in increased systemic toxicity, quantitative HAPS provides a means to measure the extrahepatic component, warn of potential side effects, and help guide chemotherapy decisions. 2) Extrahepatic shunting increases in response to DSM.

10:30–12:00 **Room 276**

RADIOPHARMACEUTICAL CHEMISTRY V: SHORT-LIVED RADIOPHARMACEUTICALS

Moderator: Joanna S. Fowler, Ph.D.
Co-moderator: Michael R. Kilbourn, Ph.D.

Introduction. Joanna S. Fowler, Ph.D., Brookhaven National Laboratory, Upton, NY

NO-CARRIER-ADDED (NCA) ^{18}F-SPIROPERIDOL. A.P. Wolf, M. Watanabe, C.-Y. Shiue, P. Salvadori, and J.S. Fowler. Chemistry Department, Brookhaven National Lab., Upton, NY

NCA p-[^{18}F]fluorobenzonitrile (2) has been synthesized from Rb^{18}F in 50% radiochemical yield and converted to ^{18}F-labeled spiroperidol (5) in a 3-step synthesis with an overall radiochemical yield of ~ 8–10% (based on

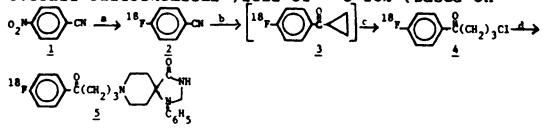

a. Rb^{18}F/DMSO; b. cyclopropyl lithium; c. HCl; d. 1-phenyl-1,3,8-triazaspiro[4.5]decan-4-one/Na_2CO_3/KI/DMF.

^{18}F$^-$). The Rb^{18}F used in the initial nucleophilic displacement step is prepared by evaporating aqueous ^{18}F$^-$ from a $H_2{}^{18}O$ target with Rb_2CO_3. No special drying of the Rb^{18}F is required and $H_2{}^{18}O$ is recovered for reuse. Intermediate 3 is not isolated but converted *in situ* in a single reaction vessel to give 4[a] which is condensed to form 5. Flash chromatography gives 5 in 94% radiochemical purity as determined by HPLC in a synthesis time of 90 minutes. Since this new method provides 4 in a radiochemical yield of ~ 30% it should provide access into a series of NCA ^{18}F-labeled receptor ligands of the p-F-C_6H_4-CO-$(CH_2)_3$-Y structure by varying the amino group (Y).

[a] 4 has also been prepared from NCA p-[^{18}F]fluoronitrobenzene (via nucleophilic aromatic substitution) by reduction, reductive deamination to [^{18}F]fluorobenzene and acylation with 4-chlorobutyryl chloride in an overall yield of 15%.

SYNTHESIS OF 16α-FLUOROESTRADIOL USING FLUORIDE ION AS A SOURCE OF FLUORINE. T.J. Tewson, THe University of Texas Medical School, Houston, TX.

Although several estrogen derivatives containing radiohalogens have been prepared with the objective of external detection and quantification of the estrogen receptor none has proved totally satisfactory. The fluorine-18 fluorinated derivatives have all been at too low a specific activity to show satisfactory receptor binding and the combination of nuclear and chemical properties of the bromo and iodo derivatives are less than ideal for 'in vivo' studies. The 16α-position of estradiol can be substituted without major effect on its estrogenic activity as shown by the 16α-iodo, bromo and hydroxy compounds. Thus fluorine-18 16α-fluoro estradiol should bind effectively to the estrogen receptor, retain the radiolabel 'in vivo', be available at very high specific activity and be imageable with a positron tomograph. However, most synthetic routes to this compound using fluoride ion would be expected to give mixtures of product and slow reactions.

The 16β, 17β-cyclic sulfate of epiestriol-3-acetate reacts rapidly (10 mins at reflux) with tetramethylammonium fluoride to give after acid hydrolysis, two products in the ratio of 10:1. The major product is 16α-fluoro-17β-hydroxy estradiol and the minor product is probably 17α-fluoro-16β-hydroxy estradiol, although this compound is not yet fully characterized. When the reaction is performed with a deficiency of fluoride the unlabelled by-products are well separated on HPLC from the fluorinated materials and so separation of a high specific activity product should be straighforward. The synthesis will be performed with 'no carrier' added fluroine-18 fluoride in the near future.

1-[F-18]-FLUOROPENTESTROL: SYNTHESIS AND PRELIMINARY TISSUE UPTAKE STUDIES OF A POSITRON-EMITTING ESTROGEN IN RATS. S. W. Landvatter, K. D. McElvany,* M. R. Kilbourn,* J. A. Katzenellenbogen, and M. J. Welch.* University of Illinois, Urbana, IL, and *Washington University School of Medicine, St. Louis, MO.

1-Fluoropentestrol, a compound with high binding affinity for the estrogen receptor (RBA = 135%), can be prepared by the simple fluoride displacement reaction shown below. In model reactions, using 0.3 μmol of the fluoride ion, yields of fluoropentestrol of up to 50% can be obtained (based on fluoride ion). The displacement proceeds rapidly at room temperature, and the product is well-separated from other UV-absorbing byproducts by HPLC on silica gel.

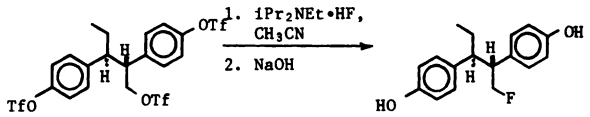

Using [F-18]-fluoride prepared in a water target by the O-18(p,n)F-18 reaction, 1-[F-18]-fluoropentestrol could be prepared in low yield. In a preliminary tissue uptake study in immature rats, this compound showed a uterus to non-target tissue ratio of 11.8 ± 0.7 (n = 5) at 1 hr; this ratio was reduced to 3.71 ± 1.29 (n = 3) when the animals were treated simultaneously with an excess of unlabeled estradiol to block receptor-mediated uptake. This investigation illustrates that an F-18 labeled estrogen can be prepared with sufficiently high specific activity to achieve receptor-mediated uptake in target tissues in animals.

VALIDATION OF F-18-3-DEOXY-3-FLUORO-D-GLUCOSE (3FDG) AS AN AGENT FOR MEASUREMENT OF GLUCOSE TRANSPORT BY POSITRON EMISSION TOMOGRAPHY. J.R. Halama, J.E. Holden, S.J. Gatley, D. Bernstein, K.T. O'Hora, C.K. Ng, T.P. DeGrado, Dept. of Medical Physics, Univ. of Wisconsin, Madison, Wisconsin 53706.

Regulation of glucose metabolism begins with entry into cells. Assessment of glucose transport may be useful in diabetes and congestive heart disease. Three aspects of the behavior of the glucose analog 3FDG in rat heart and brain were studied extending our preliminary work with this agent (J Nucl Med 23:79, 1982). The inhibition of glucose consumption in isolated hearts was measured after addition of stable 3FDG to the perfusion medium. Using the Michaelis-Menton model for competition of two substrates for the same carrier molecules, the half-maximal inhibition constant (Ki) was determined to be 11.5 ± 2.5 mM. Extracts of heart and brain obtained one hour after injection of 3FDG or F18-2-deoxy-2-fluoro-D-glucose (2FDG) into intact rats were analyzed by high pressure liquid chromatography for phosphate and free glucose analog fractions. For 2-FDG essentially all the F-18 in brain could be attributed to the phosphate. For 3-FDG 10% of the F-18 had the expected retention time for the 6-phosphate; the rest was unchanged 3-FDG. Time-activity curves were measured after bolus injections of D- and L-3FDG and 2FDG. Comparison clearly indicated D-3FDG transport into and out of space denied to the unnatural L-3FDG. Increased glucose in the perfusion medium inhibited 3FDG entry. Metabolically trapped 3FDG was < 5% that of 2FDG. Our data indicate that 3FDG is transported, but poorly phosphorylated. These properties allow regional quantitation of glucose transport rates by positron emission tomography.

SPECIFIC LABELING IN VIVO OF MURINE NEUROLEPTIC BINDING SITES USING ^{18}F-HALOPERIDOL, A POTENTIAL NON-INVASIVE PROBE FOR PSYCHIATRIC DISEASE, P.B. Zanzonico, R.E. Bigler, and B. Schmall, Memorial Sloan-Kettering Cancer Center, NY, NY 10021.

^{18}F ($T_{½}$: 110 min; β^+: 97%) labeled haloperidol (0.4 Ci/mmol), prepared by the Balz-Schiemann reaction, was evaluated in a murine model as a potential radiotracer for the non-invasive determination of regional concentrations of brain dopamine (DA) receptors using PET. As the haloperidol dose was increased from 0.01 to 1000 µg/kg, the relative concentration (µCi found per gm tissue specimen/µCi injected per gm body mass) of ^{18}F-haloperidol 1 hr after iv injection decreased from 30 to 1.0 in the striatum and from 8.6 to 1.0 in the cerebellum. The sigmoidal decrease in the striatum (relative concentration vs log dose) presumably reflects competition between labeled and unlabeled haloperidol for a single class of accessible binding sites. Because the cerebellum is deficient in DA receptors, the decrease in cerebellar ^{18}F may reflect a saturable component of haloperidol transport into brain (Tewson, et al, Brain Res 192:291, 1982). In contrast, commercially available ^{3}H(G)-haloperidol, evaluated as a "model" radioligand for receptor studies in vivo, yielded a constant striatum-to-cerebellum ^{3}H ratio of only 1.0. Even at doses as low as 1 µg/kg, where demonstrable specific binding is expected to occur, selective striatal localization of ^{3}H was not observed, suggesting (together with TLC) that de-tritiation occurred in vivo. Nevertheless, the high brain concentrations and the unexpectedly high striatum-to-cerebellum concentration ratios (>4 at doses ≤ 1 µg/kg) for ^{18}F-haloperidol suggest that it warrants further investigation as a potential DA receptor-binding radiotracer.

A NEW SYNTHESIS OF C-11-ARALKYL AMINO ACIDS: [3-(C-11)]PHENYLALANINE. D.D. Dischino, M.R. Kilbourn, and M.J. Welch. Washington University School of Medicine, St. Louis, MO.

A new synthesis of carbon-11 labeled phenylalanine has been developed, in which the label is placed in the benzylic position. Carbon-11 labeled benzyl chloride was prepared in three steps by carboxylation (C-11 CO_2) of phenylmagnesium bromide (3 min, 95%), reduction of the C-11 benzoic acid to the alcohol ($LiAlH_4$, 2 min, 100%) and chlorination (CCl_4, $(n\text{-octyl})_3P$, 10 min, 52-84%). The C-11 benzyl chloride was then used to alkylate N-diphenylmethylene glycine ethyl ester using phase-transfer catalysis (H_2O/CH_2Cl_2, KOH, $(n\text{-butyl})_4NBr$, 10 min, 50-94%), and the resultant N-diphenylmethylene phenylalanine ethyl ester hydrolyzed (6N HCl, 10 min, 100%) to d,l-[3-(C-11)]phenylalanine. For example, from 132 mCi of $^{11}CO_2$ was prepared 3.7 mCi of [3-(C-11)]phenylalanine in a synthesis time of 66 min (not optimized), a decay- corrected yield of 23% for a 5 step synthesis. This reaction sequence should be applicable to syntheses of C-11 labeled tyrosine and 3,4-dihydroxyphenylalanine (DOPA). Production of C-11-DOPA labeled in the benzylic position would allow study of in vivo distribution of C-11-dopamine following C-11-DOPA decarboxylation. The application of this synthetic approach to other aralkyl amino acids, as well as the resolution of d,l-isomer mixtures by HPLC using chiral support ligand exchange chromatography, will be discussed.

1:30–3:00 **Room 123**

CARDIOVASCULAR CLINICAL VII: EXERCISE RADIONUCLIDE VENTRICULOGRAPHY

Moderator: Robert H. Jones, M.D.
Co-moderator: Alan Rozanski, M.D.

IMPROVED INTERPRETATION OF TECHNETIUM 99M GATED SEQUENTIALLY GRADED EXERCISE ANGIOGRAPHIC(EGNA) DATA USING MULTIVARIATE ANALYSIS(MVA). J.H. Paldi, Y. L. Wu, J. Milanes, M.L. Goris and D.A. Goodwin. Stanford University School of Medicine and Veterans Administration Medical Center, Palo Alto, CA.

Our integrated method for analyzing EGNA data takes into account the effects of age, sex and duration and intensity of exercise on the ejection fraction(EF) response to exertion. An interpretive framework was developed by establishing tables of age, sex, and effort dependent expected EF responses. EF's were determined 4 times in 12 normal men ages 45-55(mean 50) over 10 min periods of sequentially increasing effort levels from resting to maximum predicted pulse rates and/or exhaustion. A mean EF curve(+/- 7% SD) vs mean % maximal effort achieved was defined as the expected EF response to exertion for 50 y.o. men. The EF response curve and cumulative effort/10 min test were normalized for adults of both sexes using factors derived from published data defining age and sex depentent variation in cardiac response to graded effort stimuli. Each new patient was exercised until exhaustion or objective endpoint was achieved. The observed EF response curve vs cumulative effort expressed as % maximum age and sex depnedent predicted effort/10 min graded test was compared with age and sex dependent predicted normal values. The ratio observed/predicted values is a normalized measure of cardiac reserve(ECR).

EGNA data from 36 consecutive patients refered for evaluation for ischemic coronary artery disease(ICAD) was analyzed by traditional end-point methods(EPA) and by MVA and the results compared to the findings at contrast coronary arteriography.

	EPA(falling)	EPA(falling or flat)	MVA
Sens.	.65	.96	.92
Spec.	.90	.08	.83
Acc.	.72	.67	.89

For detecting ICAD in a clinical practice MVA yielded superior accuracy compared to end-point analysis.

THE TIME OF ONSET OF STRESS-INDUCED LEFT VENTRICULAR WALL MOTION ABNORMALITIES AIDS IN THE PREDICTION OF THE PRESENCE AND SEVERITY OF CORONARY ARTERY DISEASE. A. Kimchi, A. Rozanski, C. Fletcher, J. Maddahi, A. Waxman, H.J.C. Swan, D.S. Berman, Cedars-Sinai Medical Center, Los Angeles, CA.

Similar to ischemic ST segment depression, the development of stress-induced left ventricular (LV) wall motion abnormality (WMA) is a commonly utilized marker for the detection of coronary artery disease (CAD). However, the relationship between the time of onset of WMA during exercise (EX) and the presence and the severity of CAD is not known. Therefore, the time of onset of both ST depression (+) and WMA, expressed as % of maximal predicted heart rate (MPHR) at which these abnormalities first occurred during graded EX, were assessed in 89 patients (pts) without infarction who underwent both coronary angiography and two-view (45° LAO and anterior) EX equilibrium radionuclide ventriculography (Tc-99m). Segmental WM was scored with a 5-point system (3=normal, -1=dyskinesis) with a decrease of 1 score, defining onset of WMA. CAD=≥50% stenosis and was "critical" if ≥90% stenosis present. Results: (n=# of pts.)

Onset of	ST +			WMA		
Abnormality	n	CAD	"Critical"	n	CAD	"Critical"
<70% MPHR	13	100%	77%	25	100%	92%
71-84% MPHR	16	75%	69%	18	78%	56%
>85% MPHR	15	73%	53%	18	67%	39%
None	45	73%	40%	28	64%	25%

Thus: The early onset of an EX WMA, occurring ≤70% of the MPHR: 1) is highly specific for CAD; 2) is a more sensitive indicator for CAD than the electrocardiographic response; and 3) identifies CAD patients likely to have severe coronary stenosis, more accurately than the ST segment response.

CLINICAL VALIDATION OF A TOTALLY AUTOMATED METHOD FOR ASSESSING REGIONAL LEFT VENTRICULAR FUNCTION FROM REST/EXERCISE RADIONUCLIDE VENTRICULOGRAPHY. E Garcia, J Areeda, A Rozanski, K Van Train, F Prigent, T Weiss, A Waxman, D Berman, Cedars-Sinai Medical Center, Los Angeles, CA

Although objective methods for the assessment of regional wall motion (RWM) and regional ejection fraction (REF) have been described, their combined assessment during exercise (Ex) has not been reported. Thus, we developed a quantitative (Qt) method for the totally automated assessment of regional function during Ex and validated it against visual assessment (V) and angiography in 20 normals (nls) and 20 CAD pts (≥50% stenosis) undergoing 45° LAO Ex radionuclide ventriculography. Pattern recognition techniques were used to define automatically the LV edge, and RWM (% change in radial distance) and REF (% change in cts) were then expressed as circumferential profiles and compared to normal limits. The REF is divided into an inner and outer half of the end-diastolic region of interest corresponding to the function of the walls moving perpendicular and parallel to the detector. Qt and V assessment was divided into 3 LV regions per pt. Frequencies of abnormality in the 42 "jeopardized" regions (i.e., subtended by CAD) are:

	Septum (17)	Posterior (12)	Apex (13)	Total (42)
Qt Analysis	15	8	13	36
RWM Visual	12	11	12	35

Of the 11 nonjeopardized regions in the CAD pts, 4 were abnormal by V and 5 by combined QT analysis. The remaining 7 regions were apical and could not be ascribed to a specific coronary artery. Among the 20 nls, all 60 regions were nl by V as were 56 by Qt analysis. Thus, this totally automated comprehensive analysis of regional function during Ex correlates highly with the visual prediction of CAD.

A COMPARISON OF SUPINE BICYCLE AND DOBUTAMINE RADIONUCLIDE CARDIAC STRESS TESTING: TECHNICAL CONSIDERATIONS. M. Freeman, R. Palac, S. Virupannavar, J. Mason, W.E. Barnes, G. Eastman, H. Loeb, E. Kaplan. Hines VA Hospital, Hines, IL.

In an attempt to expand the number of pts. benefitting from stress testing and to increase acquisition times, we have been evaluating a pharmacologic alternative to exercise. The agent chosen, dobutamine, has the following favorable properties: 1) ability to be given safely in a peripheral vein, 2) rapid onset, 3) short duration of action. Each pt underwent supine bicycle progressive resistance testing of 2 minutes per stage, followed 30 minutes later by dobutamine administration. Beginning at 5 ug/kg/min and after a 5 minute wait, a 3 million count density gated image was obtained. The dose was increased in 5 ug increments and terminated at 20 ug or at the onset of chest pain, significant arrythmias, hypo- or hypertension. Either a decrease in ejection fraction of >5% or the development of new wall motion abnormalities was judged to be an abnormal test. RESULTS: In 29 pts (11 with angiographically proven normal coronary arteries) the ability to separate normals from abnormals was:

	BICYCLE	DOBUTAMINE
ACCURACY	0.93	0.93
SENSITIVITY	0.94	0.89

Mean count density was 3 million for dobutamine versus 1.84 million for bicycle. All observers concluded that the higher density images were technically better and easier to evaluate. CONCLUSION: Incremental infusions of dobutamine appear to be as accurate and sensitive as supine bicycle testing. While not designed to replace bicycle testing, it does provide better technical studies and may prove to be a satisfactory radionuclide method for previously excluded patients.

THE ROLE OF PRELOAD RESERVE DURING DYNAMIC EXERCISE IN PATIENTS WITH MYOCARDIAL INFARCTION. BH.Kim, M.Inoue, M.Matsumoto, M.Fukushima, Y.Ishida, T.Tsuneoka, K.Kimura and H.Abe. 1st Dept. of Med. Osaka Univ. Med. Sch. Japan.

To evaluate the role of preload reserve during exercise (EX) under limited reserve of myocardial contractility, multi-gated radionuclide angiography was performed at rest and during maximal EX in 10 normals(G-NL) and 19 patients (pts) with myocardial infarction(MI). Nineteen pts with MI consisted of 2 groups, 5 pts(G-MI+EA) with and 14 pts(G-MI) without effort angina. Myocardial contractility was estimated from P/V index, peak systolic pressure/end-systolic volume index. There was no significant difference in increases in cardiac index(CI), blood pressure(BP) and heart rate(HR) during EX between G-NL and G-MI, but the increases in these parameters in G-MI+EA were less than in G-NL. In G-NL, P/V index significantly increased(4.6±1.4 to 7.8±1.4 mmHg/ml/m^2, p<0.001) without significant increase in end-diastolic volume index(EDVI)(78±12 to 85±17 ml/m^2, NS). In G-MI, P/V index moderately increased from 2.8±1.0 to 3.7±2.2 mmHg/ml/m^2 with significant increase in EDVI(100±28 to 117±42 ml/m^2, p<0.01). In G-MI+EA, P/V index significantly decreased from 6.0±0.8 to 4.5±1.0 mmHg/ml/m^2 with substantial increase in EDVI during anginal attack(72±10 to 92±19 ml/m^2, p<0.05). There was inverse correlation between percent changes in EDVI and P/V index during EX.

These results indicate that in pts with limited augmentation of myocardial contractility(P/V index), increases in cardiac output required during EX is obtained by increases in preload(EDVI).

MAINTAINED LV EXERCISE RESPONSE AND REGIONAL WALL MOTION ABNORMALITIES (WMA) IN PATIENTS ON DOXORUBICIN. J.H. Bae, M. Schwaiger, E. Henze, H.R. Schelbert, UCLA School of Medicine, Los Angeles, California

A dose-dependent decrease in resting LV ejection fraction (EF) during doxorubicin therapy has been demonstrated with radionuclide angiography previously. This study was to examine if the LVEF exercise response is sensitive for detecting doxorubicin toxicity and if regional LV dysfunction is related to doxorubicin. Two patient groups were studied with radionuclide angiography. In Group I, 48 pts (24 males) were studied once during doxorubicin (mean total dose of 429.5 mg/m^2; range 200 - 850 mg/m^2). Resting EF averaged 48.2±6.7%. With supine exercise, performed in 24 pts, EF increased from 48.8±6.9% at rest to 52.8±9.0% (p<0.03). In Group II with 17 pts, serial studies were performed at various times before, during and after doxorubicin. Rest EF's initially averaged 54.1±3.3% and declined to 45.3±5.2% with therapy (p<0.001). With supine exercise in 9 pts, EF increased by 4.7% with exercise before and by 5.3% (NS) during treatment indicating that rest LV function had deteriorated but not the exercise response. Of the 17 pts, 11 were studied before and again after doxorubicin therapy. The initial rest EF in these pts averaged 56.1±3.1% and 45.1±5.5% during therapy (p<0.001). In 8 of 11 (72.7%) pts, new WMA (mild apical hypokinesis) were observed after therapy. WMA were also present in 28 (58.3%) of the 48 pts in Group I. In the 17 Group I pts, WMA were noted in 2 pts (11.8%) before and in 14 (82.4%) after therapy. The results indicate development of mild resting WMA during doxorubicin. Also, despite a decline in resting LV function, EF response to exercise remains normal. Thus, exercise radionuclide angiography does not improve detection of doxorubicin induced LV dysfunction.

1:30–3:00 **Room 120**

ENDOCRINE I

Moderator: I. Ross McDougall, M.D.
Co-moderator: James C. Sisson, M.D.

SENSITIVITY AND SPECIFICITY OF m-IODOBENZYLGUANIDINE (MIBG) SCINTIGRAPHY FOR THE DETECTION OF PHEOCHROMOCYTOMA (PHEO). R.S. Hattner, J.P. Huberty, B.L. Engelstad, M.D. Roizen. University of California, San Francisco, CA.

Workers from the University of Michigan have reported the ability of MIBG to detect PHEO. However, the sensitivity and specificity of MIBG scintigraphy for detection of PHEO is not discernable from their publications. For this reason we have investigated this problem. Twenty-seven patients were studied who had typical signs and symptoms of PHEO and at least two abnormal determinations of plasma or urinary catecholamines or their metabolites, or had multiple endocrine neoplasia, types IIa or IIb. Twenty-four patients had high quality information concerning the presence or absence of disease. The total number of patients with PHEO was twelve. Seven were surgically proven, and five had either positive CT or unequivocal biochemical evidence of PHEO, or both. Three patients with PHEO had negative CT scans (25%), one of which was surgically proven, and all three had positive MIBG scans. Twelve patients were judged to be free of disease by surgery, one, or by failure to corroborate the biochemical abnormalities, or by negative CT, or both, in eleven. Four false negative MIBG scans were incurred (sensitivity = 0.67). No false positive MIBG scans were incurred (specificity = 1.00). We conclude that MIBG scintigraphy is relatively insensitive for detection of PHEO, but highly specific. We recommend that in the presence of typical signs and symptoms, and biochemical evidence, of PHEO that MIBG be employed when CT fails to localize the lesion.

INTRATHORACIC PHEOCHROMOCYTOMAS CONCENTRATE THALLIUM-201 CHLORIDE AND I-131-METAIODOBENZYLGUANIDINE. J. Glowniak, B. Shapiro, J. Thrall, J. Sisson and W.H. Beierwaltes. University of Michigan Medical Center, Ann Arbor, MI.

The diagnosis of pheochromocytoma (PC) is made by characteristic clinical symptoms and elevated catecholamines or their metabolites in blood and urine. Finding the tumors is often difficult. Primary intra-thoracic PC in particular has presented an exceptionally challenging prob-

lem. With the advent of I-131-metaiodobenzylguanidine (MIBG), an agent that is specifically concentrated in catecholamine-secreting tissue, a method has been developed that detects PC with high sensitivity and specificity.

In 4 patients extensive investigations including CT, arteriography and venous sampling failed to locate the PC. MIBG scintigraphy demonstrated intrathoracic concentrations of I-131 that indicated a PC in each. In order to more precisely locate the PC, thallium-201 chloride was administered and images of the heart were superimposed on the MIBG images. In 3 cases, the MIBG uptake was contiguous with or partly superimposed on the cardiac thallium image. In the fourth case, MIBG concentrated in a rib metastasis. In all four cases, thallium-201 concentrated in the areas of abnormal MIBG uptake, strongly in the 3 juxta-cardiac lesions (JCL) and weakly in the rib metastasis. Dynamic CT scanning following bolus intravenous contrast showed intense enhancement by the JCL suggesting a blood flow effect as the cause for thallium uptake. In two patients with JCL, the PC were surgically removed and all biochemical abnormalities returned to normal.

In conclusion, PC are often highly vascular tumors and thus may concentrate thallium. Thallium-201 scintigraphy can aid in defining the location of thoracic PC, especially when guided by MIBG images.

I-131-METAIODOBENZYLGUANIDINE (MIBG) UPTAKE REFLECTS INTEGRITY OF SYMPATHETIC INNERVATION. M. Nakajo, B. Shapiro, J.C. Sisson, D.P. Swanson, V. Kalff and W.H. Beierwaltes, University of Michigan Medical Center, Ann Arbor, MI.

The uptake and excretion of I-131-MIBG by the salivary glands was studied to elucidate its relationship to sympathetic innervation. Review of I-131-MIBG images from 151 patients screened for pheochromocytoma revealed a discrepancy in the frequency of visualization of the salivary glands (100% at 24 h, 95% at 48 h) and stomach (0% at 24 and 48 h) both of which concentrate free I-131. In dogs, a high tissue concentration (kg % dose/g) was observed in the submandibular gland (0.50 $\pm$ 0.06, mean $\pm$ SE, n=6) and the parotid gland (0.48 $\pm$ 0.12, n=6) 2 h after injection. In dogs only the submandibular gland concentrates iodide. Left stellate ganglion sympathectomy decreased submandibular uptake 17% (range: 9-26%, n=3). In a patient with Horner's syndrome, only the contralateral gland was visualized with I-131-MIBG. In a patient with severe adrenergic autonomic neuropathy, no salivary gland activity was seen. Imipramine, an inhibitor of norepinephrine uptake in neurons, prevented salivary gland uptake of 131-I-MIBG in 2 patients. In 9 patients without salivary gland disease, saliva/plasma I-131 ratios as high as 13.1 were observed 4 h after injection. The chemical forms of radioactivity determined by thin-layer chromatography were 98% 131-I and 2% I-131-MIBG. We conclude that: the salivary glands take up I-131-MIBG; the uptake is dependent on intact adrenergic nerves; after initial uptake I-131-MIBG is in part deiodinated and excreted as I-131 in saliva; and salivary gland imaging with labeled MIBG may permit evaluation of sympathetic neuronal integrity in adrenergic disorders.

THE SCINTIGRAPHIC LOCALIZATION OF THE ABNORMAL ADRENALS IN PRIMARY ALDOSTERONISM (PA). M.D. Gross, B. Shapiro, R.J. Grekin, J.E. Freitas, D.P. Swanson, W.H. Beierwaltes. The University of Michigan and VA Medical Centers, Ann Arbor, MI

The localization of aldosteronomas (A) and their differentiation from bilateral hyperplasia (BH) is critical to the successful management of PA. Dexamethasone suppression (DS) adrenal scintigraphy has been shown to be an efficacious method to locate and quantitate abnormal adrenal function in PA. Previously, unilateral or bilateral adrenal imaging < 5 days after ^{131}I-6β-iodomethylnorcholesterol (NP-59) would suggest A or BH, respectively. The present study was conducted to assess whether quantitation of adrenal gland NP-59 uptake would improve the interpretation of DS scans in PA.

Percent uptake calculations were made on DS scans from 50 patients with PA (30 with A and 20 with BH). DS scanning was performed using 1 mCi of NP-59 given after 7 days of 4mg DS daily and throughout a 5 day imaging interval. A computer algorithm was used to calculate % dose uptake from each adrenal gland at 5 days post NP-59.

Unilateral early imaging (< 5 days) was seen in all patients with A. Mean uptake in A was 0.2 $\pm$ .02% (range .03 to 0.72). A contralateral "normal" (N) adrenal was identified in 8 of 30 on day 5 (% uptake 0.04 $\pm$ .01) and in 4 of the 8 NP-59 adrenal N to A ratios were $\geq$ .5. In BH mean % uptake was 0.28 $\pm$ .04% and marked asymmetric activity (ratio $\leq$ 0.5) was seen in 3 of 20. Based upon uptakes alone, 4 patients with A and 3 patients with BH would have been incorrectly labeled if single imaging and uptake procedures were performed only at 5 days post NP-59.

Thus, the correct interpretation of DS-NP-59 scans in PA is dependent upon the time course of imaging and not on the levels of NP-59 uptake achieved.

ADRENAL SCINTIGRAPHY WITH I-131-6-BETA-IODOMETHYL-19-NOR-CHOLESTEROL (NP-59) IN PRIMARY ALDOSTERONISM. B.G. Anderson and J.C. Melby, Boston University Medical Center, Boston, MA.

Adrenal scintigraphy was performed with NP-59 in 46 patients with primary aldosteronism to distinguish adrenal cortical adenomas from hyperplasia. Posterior views of the adrenals were evaluated as showing symmetrical or asymmetrical adrenal uptake. Asymmetrical uptake was graded as slight (1+), moderate (2+), or marked (3+).

In 26 patients adrenal uptake was symmetrical. Of these 2 were subjected to surgery and were found to have an aldosteronoma. The other 24 patients were presumed to have adrenal cortical hyperplasia on the basis of chemical and other findings. Of 9 patients with 1+ asymmetry, 6 had hyperplasia, 2 of which were verified at surgery; of 3 others operated on, one had an aldosteronoma, one had an enlarged adrenal and one had a normal adrenal. Of 8 patients with 2+ asymmetry, 6 had pathologically verified aldosteronomas and 2 were not subjected to surgery. All 3 patients with 3+ asymmetry had pathologically verified aldosteronomas. Dexamethasone suppression was used in 23 patients; 2 had false positive scintigrams with 1+ asymmetry. In 23 patients not given dexamethasone there were 4 false positive scintigrams with 1+ asymmetry and 2 false negative scintigrams with symmetrical uptake.

Adrenal scintigraphy with NP-59 is a sensitive method for distinguishing adenoma from hyperplasia in patients with primary aldosteronism. Grading the degree of asymmetrical uptake of NP-59 improves the specificity of the procedure. The use of dexamethasone suppression may be a helpful adjunct.

DIAGNOSIS OF EARLY PANCREAS TRANSPLANT REJECTION WITH INDIUM-111 OXINE LABELED PLATELETS. L.M. Lieberman, H.W. Sollinger, K.S. Cook, D.L. Kamps, T.F. Warner. The University of Wisconsin Center for Health Sciences, Madison, WI.

A test that would indicate pancreas rejection at an early and potentially reversible stage would be especially important in pancreas transplantation where elevations of blood sugar (BS) and abnormal blood glucose tolerance tests (GTT) occur at a late and irreversible stage of rejection. We have investigated the early diagnosis of pancreas rejection in dogs with Indium-111 oxine labeled platelets (ILP).

Ten mongrel dogs were pancreatectomized and allowed to become diabetic. One week later segmental pancreas transplantation was done. All animals received either prednisone and Imuran, or prednisone and cyclosporin for anti-rejection therapy. Rejection was monitored by blood sugar (BS) assays and glucose tolerance tests (GTT). Platelets from 40 ml of whole blood were labeled with In-111 oxine by a modified method of Thakur. Eighty to 280 μCi of ILP were injected IV and the animals scanned daily or every other day. Ratios of pancreas to background radioactivity were determined with a gamma camera and PDP/11 computer. A ratio of over 1.5:1 was found to correlate with rejection as judged by open biopsies of the transplant done on the same day.

The scan was positive in five dogs when BS was normal. In two dogs the scan was positive with normal BS and GTT. Five dogs had open pancreas biopsies correlating with the scans. Our preliminary findings suggest that ILP can identify rejection 24-48 hrs before BS or GTT become abnormal. Further work is planned to confirm the efficacy of the test to diagnose early pancreas rejection in patients.

1:30-3:00 **Room 132**

GASTROINTESTINAL V: GASTRIC EMPTYING/SMALL BOWEL TRANSIT

Moderator: Brahm Shapiro, M.D.
Co-moderator: Harold A. Goldstein, M.D.

THE EFFECT OF GASTROPLASTY FOR MORBID OBESITY ON GASTRIC EMPTYING FUNCTION MEASURED BY RADIONUCLIDE-LABELED TEST MEALS. B. Shapiro, F. Eckhauser, M. Nakajo, W.E. Strodel and D. Swanson, University of Michigan, Ann Arbor, MI.

Morbid obesity is a potentially life-threatening disorder which is highly resistant to dietary therapy. Surgical intervention in the form of gastroplasty has been shown to result in significant weight loss with little morbidity. Despite the frequency with which it is employed, little is known of the mechanism by which gastroplasty induces satiety or of its functional effect on kinetics of gastric emptying. A total of 31 patients with Gomez gastroplasties and 21 patients with Mason gastroplasties were studied by means of a Tc-99m DTPA in water liquid test meal and/or Tc-99m Chelex 100 Resin in oatmeal semi-solid test meal. Studies were performed preoperatively, within 6 weeks of surgery, and between 6 weeks and 52 weeks of surgery. These studies showed that the small (< 50 ml volume) proximal compartment emptied rapidly; t 1/2 for liquid 2.06 ± 0.34 min. (mean ± SE, n=27); t 1/2 for semi-solid 15.11 ± 4.83 min. (n=20). The remaining distal stomach (and hence overall) gastric emptying times for liquid and solid test meals were not significantly delayed from the preoperative values in either the early or late postoperative period. Late postoperative solid emptying was more rapid ($p<0.05$).

	Preoperative	Early Postoperative	Late Postoperative
Liquid	32.0±11.7(26)	51.7±17.5(27)	21.1±6.0(14)
Solid	77.2±13.0(22)	54.3±17.3(18)	44.8±3.2(20)

(t 1/2 in minutes, Mean ± SE,n)

Thus, gastroplasty does not appear to induce satiety by delaying gastric emptying. Rapid transient distension of the proximal compartment of the partitioned stomach may mediate a neural or hormonal signal for satiety.

DEFINITION OF THE SPECTRUM OF GASTRIC EMPTYING IN PATIENTS WITH BULIMIA. B.B.Grill, D.Greenfield, E.Glass, R.Lange, and R.W.McCallum, Yale University, New Haven, CT

We have reported that gastric emptying of the solid component of a meal was delayed in 80% of patients with anorexia nervosa. Patients with bulimia (binge eating, self-induced emesis) may have significant morbidity and also complain of symptoms suggesting gastric retention. We investigated gastric emptying of solid and liquid meal components in 13 females of mean age 22.3 (range 13-40 yrs) with bulimic eating disorder of mean duration 4.7 yrs and whose % ideal body weight (IBW) was 81.4% (range 61-115%). A dual isotope method of measuring gastric emptying used Tc-99m-S-colloid labeled chicken liver as the solid phase and In-111 labeled water as the liquid phase. The percent of each iotope retained in the stomach over 2 hrs (mean ± 1 SEM) was compared to the results of 10 similarly aged females of normal weight (#=$p<0.05$).

	Solids			Liquids	
Group	60	90	120	30	60	120
Bulimia	84±6.0	78±7.0	70±8.0#	39±3.0	21±2.0	7±1.0
Normals	83±4.0	67±3.0	51±3.0	40±4.0	22±2	5±1.0

42% of bulimics had normal emptying of solids while 58% were slow (>2D from normal). There was no correction of % IBW and gastric emptying. We conclude that in patients with an eating disorder and bulimia: 1)gastric emptying of the solid component of a meal is delayed in approximately half; 2)liquid emptying is always normal; 3)these results suggest impaired antral motility in some bulimics either as a primary event or an epiphenomenon; 4)recognition that delayed gastric emptying may occur with bulimia has therapeutic application because of the possible role of gastric prokinetic agents.

ALTERED GASTRIC EMPTYING DURING RADIATION-INDUCED VOMITING. A. Dubois, J. Jacobus, M. Grissom, R. Eng, J.J. Conklin. USUHS and AFRRI, Bethesda, MD.

The relation between radiation-induced vomiting and gastric emptying is unclear and the treatment of this condition is not established. Therefore, we explored (1) the effect of cobalt-60 irradiation on gastric emptying of solids and liquids and (2) the possibility of preventing radiation-induced vomiting with the dopamine antagonist, domperidone (D). Twenty dogs were studied on 2 separate days, blindly and in random order, following IV injection of either a placebo (P) or 0.06 mg/kg D. On a third day, they received 800 rad whole body irradiation after either P (n=10) or D (n=10). Before each study, each dog was fed chicken liver tagged in vivo with 1 mCi Tc-99m sulfur colloid (solid marker), and 1 mCi In-111 DTPA in water (liquid marker). Dogs were placed in a Pavlov sling for the subsequent 3 hours and radionuclide imaging was performed at 10 min intervals. The slope of the exponential decline of intragastric contents (%/hour) of Tc-99m (K solids) and In-111 (K liquids) was determined for each study. Irradiation produced vomiting in 9 of 10 dogs given P but only in 1 of 10 dogs pretreated with D ($p < 0.01$). As shown below, gastric emptying of both liquids and solids was significantly suppressed by irradiation ($p < 0.01$) both after P and D.

	Placebo		Domperidone	
	Basal	Irradiation	Basal	Irradiation
K liquids (In)	22.2±5.4	4.5±2.0*	18.6±3.0	4.2±1.2*
K solids (Tc)	9.0±3.0	1.0±0.8*	7.2±1.2	1.8±0.6

* $p < 0.05$ compared to Basal

These results demonstrate that radiation-induced vomiting is accompanied by suppression of gastric emptying. Furthermore, prevention of vomiting with D does not alter the delay of gastric emptying produced by ionizing radiations.

DELAYED GASTRIC EMPTYING IN PEDIATRIC PATIENTS WITH CROHN'S DISEASE AND GROWTH FAILURE. B.B.Grill, A.C.Hillemeier, R. C.Lange, R.W.McCallum, J.D.Gryboski and M.W.Plankey, Yale University, New Haven, CT

Malnutrition due to reduced oral intake has been implicated in the growth failure (GF) associated with Crohn's disease (CD). Since many of these patients have anorexia and symptoms suggesting gastric retention, we evaluated gastric emptying of both solids and liquids. 13 children with CD of various sites (1 colonic; 4 small bowel and/or ileal; 8 small intestinal plus colonic) were studied. GF was defined as height < 95% for age or weight < 90% ideal body weight. Gastric emptying of solids (S) and liquids (L) was determined using a dual isotope technique using Tc-99m-S-colloid-labeled chicken liver, and In-111-labeled water. The percent of each isotope remaining ($\bar{x}$±1 SEM) in the stomach was measured over 120 minutes, and compared in patients with and without (s) GF and 13 normal controls.

Group	N	60 min		90 min		120 min	
		S	L	S	L	S	L
CD + GF	6	91±5	31±3	82±7	21±6	77±7	12±4
CD s GF	7	77±5	25±4	64±6	17±4	54±7	11±3
Normals	13	76±4	20±2	59±5	10±2	41±5	4±1

Gastric emptying for solids at 90 and 120 min was significantly ($p<0.05$) slower in patients with CD and GF, compared to both CD without GF and controls. Gastric emptying of liquids was similar among the 3 groups. Duodenal CD was present in only 3 of the 6 patients with GF and in one patient without GF. We conclude: 1)gastric emptying of solids but not liquids was significantly delayed in CD with GF; 2) delayed gastric emptying occurred with or without evidence of duodenal CD; 3)these data are consistent with an antral motility disturbance accompanying CD.

SMALL BOWEL TRANSIT TIMES STUDIED WITH RADIOACTIVE MARKERS: METHODOLOGY. J.S. Robertson, M.L. Brown, J.A. Duenes, G.M. Thomforde, M.M. Remington, J.-R. Malagelada. Mayo Clinic and Foundation, Rochester, MN.

Intestinal transit times were measured for non-digestible solids using I-131 labeled cellulose as a solid tracer. Relative activities were determined by computerized gamma counting in regions of interest marked with a light pen. Quantification of the small intestinal transit time from direct measurement of activity in the small intestinal area proved to be

impractical. An alternative approach treated the rate of appearance of activity in the colon as a convolution of the rate of stomach emptying and the small bowel transit times. This method involves fitting third to fifth degree polynomials to the colon and stomach radioactivity curves and numerically deconvoluting the derivatives of the fitted functions to yield a spectrum of small bowel transit times. That is, for each individual the small intestinal transit time is not a single value, but is a range of times spent in the intestine that can be characterized by minimum, median and maximum values. In 6 normal subjects the mean + SD values for the minimum, median and maximum were 107 + 63, 164 + 49 and 278 + 81 min. In 8 patients with surgically shortened bowels the corresponding values were 35 + 21, 92 + 42 and 217 + 87 min. The results are consistent with the hypothesis that a bolus entering the small bowel would be spread out over an appreciable distance during its transit through the small intestine.

THE EFFECT OF METOCLOPRAMIDE AND MORPHINE ON SMALL INTESTINAL TRANSIT TIME IN NORMAL SUBJECTS. E.K. Prokop, V.J. Caride, K. Winchenbach, F.T. Troncale, R.W. Mc Callum. Hospital of St. Raphael and Yale University, New Haven, CT.

We have previously reported (JNM 23:P51, 1982) a scintigraphic method to determine small intestinal transit time (SITT) in man. Subjects received an isosmotic lactulose solution and 1mCi of 99m-Tc-DTPA (Sn) orally and were studied supine under a 15 inch gamma camera. Data were collected and stored in a computer at one frame per minute for 120 minutes. The study was viewed in a movie format. Regions of interest were selected over the cecum and ascending colon. The time of first appearance of radioactivity in the region of the cecum was taken as the small intestinal transit time. For 20 determinations the normal SITT was 73.0 + 6.5 min. (mean + SEM). In order to further validate this method, we studied 10 male volunteers in a baseline state and again separately after receiving 10mg of metoclopramide and 8mg of morphine intravenously 5 minutes after drinking the test meal. For the baseline study, the SITT was 81.2 + 10.6 min. After metoclopramide, the SITT was significantly decreased to 49.9 + 6.0 min. ($p < 0.001$) and increased to 161 + 15 min. ($n=8$; $p < 0.001$) with morphine. Gastric emptying was unaffected by metoclopramide, but significantly delayed by morphine, but this did not explain morphine's effect on SITT. Thus, the scintigraphic method for determination of SITT can accurately detect pharmacologically induced changes in small intestinal motility. In addition, the scintigraphic method has the advantage that gastric emptying, regional small intestinal transit, and potentially large bowel transit times can be simultaneously measured.

1:30–3:00 **Room 130**

BONE/JOINT II: ONCOLOGY/NEWER CONCEPTS

Moderator: R.E. O'Mara, M.D.
Co-moderator: William D. Kaplan, M.D.

PALLIATION OF METASTATIC CANCER TO BONE WITH STRONTIUM-89. R.G. Robinson, J.A. Spicer, A.V. Wegst, A.H. Gobuty, D.F. Preston, N.L. Martin, M.B. Sheridan. University of Kansas College of Health Sciences and Hospital, Kansas City, KS.

Our objective was to evaluate the potential use of systemically administered Sr-89 to treat metastatic cancer in bone for relief of bone pain.

Seventy-two patients with multiple bony metastases, primarily from prostate or breast, have been treated prospectively with the beta emitter Sr-89 over the past 4 years. The first 20 received a dose of 30 uCi/kg, the remainder received 40 uCi/kg. Response to treatment was evaluated by daily diary entries, change in pain medication requirements, laboratory values and periodic bone images. Some patients received additional 30 uCi/kg doses at 3-month intervals.

Thirty-one patients did not survive at least 3 months following the administration of Sr-89 or were lost to follow-up. The remaining 41 patients form the basis for this report. Three patients noted no improvement following Sr-89 administration. Thirty-eight showed mild to marked improvement in their clinical status with a measurable decrease in pain, including 7 who became pain free for a significant period of time following Sr-89 treatment. No patients in the treatment group noted a worsening of symptoms following Sr-89. Bone marrow depression attributable to Sr-89 was not observed.

This prospective study suggests that Sr-89 may be a valuable adjuvant therapy for palliation of pain from metastatic cancer to the skeleton. Ninety-two percent of our patients showed improvement in their level of pain. As Sr-89 is distributed differently from P-32, Sr-89 may prove superior as a systemic radioisotopic treatment for metastatic cancer to bone.

EFFECT OF DIETHYLSTILBESTROL THERAPY ON RADIOISOTOPIC BONE SCAN FINDINGS IN PATIENTS WITH METASTATIC CARCINOMA OF THE PROSTATE. M.A. Antar and R.A. Rembish. Univ. of Conn. Sch of Med., Farmington, CT & V.A. Medical Ctr., Newington, CT

Diethylstilbestrol (DES) has been extensively used in the treatment of prostatic carcinoma with metastases. Several tests have been utilized in order to gauge the effects of therapy and to assess the progress of the disease. One hundred and twenty-four Tc-99m phosphate bone scans in 36 patients with prostatic carcinoma were examined to document the response of prostatic bony metastases to DES during a one to three year period. When other modalities of therapy with DES were administered, such combined effects were excluded. The average DES dose was 1 mg daily. Serum acid and alkaline phosphatases were also obtained. In patients who responded well to therapy, bone scans showed dramatic improvement (near normal) in uptake corresponding with improvement in clinical status. On the other hand, changes in serum phosphatases did not correspond well to changes in scan findings. Of the 24 patients on DES, 16 patients showed positive bone scans, 6 negative scans and 2 equivocal. Of the 16 patients on DES with positive scans, 7 patients (44%) showed dramatic improvement as shown by decreased uptake of the metastasis. Seven patients experienced progression and 2 patients showed no change in bone scans. Serum acid and alkaline phosphatases were within normal limits respectively in 8 and 10 patients out of 16 patients with positive scans. The findings suggest that serial bone scans are more sensitive than serum enzyme levels for evaluating the response of prostatic bony metastases to DES.

SCINTIGRAPHY OF PRIMARY BONE NEOPLASIA. H.M. Goodgold, D.C.P. Chen, M. Majd, N.G. Nolan. Washington Hospital Center and Children's Hospital National Medical Center, Washington, DC.

We reviewed bone scans obtained in 78 cases (44 male, 34 female) of suspected primary skeletal neoplasia (age range 2 months to 70 years). Final diagnoses were biopsy proven in 61 or based on x-ray findings and 1-2 year clinical follow-up in 17. The most common diagnosis was exostoses in 14; also included in this series were osteogenic sarcoma in 10, giant cell tumor (GCT) in 9, osteoid osteoma in 5, reticuloses in 4, non-ossifying fibroma in 4, fibrous dysplasia in 3, bone cyst in 3, solitary metastasis in 3, enchondroma in 3, sarcoma in 3, and 17 others. Twenty-one cases were malignant conditions and 57 were benign (7 non-neoplastic).

Although malignant conditions could not be differentiated from benign ones on the basis of intensity of uptake alone, incorporation of a variety of characteristic features including shape, size, and pattern of uptake enabled malignant conditions to be correctly identified in 16/18 cases (positive predictive value = 0.89) and benign conditions in 54/59 (negative predictive value = 0.92). Of the exostoses, there were no instances of sarcomatous degeneration despite markedly increased uptake in 4 cases. A characteristic scan appearance was identified in GCT (8/9 cases) easily discernible from unicameral or aneurysmal bone cyst (ABC).

We conclude that bone scanning (1) may be quite helpful in differentiating benign from malignant neoplastic processes, (2) may be used to differentiate GCT from ABC, but (3) is of limited value in screening for sarcomatous degeneration in multiple hereditary exostoses.

BONE MASS ASSESSMENT AT DIFFERING SKELETAL SITES BY MULTIPLE DIAGNOSTIC PARAMETERS. C.H. Chesnut, J.A. Hanson, R.F. Kilcoyne, R. Murano, T.K. Lewellen, W.B. Nelp, L. Mack, M.M. Graham, B. Hu. University of Washington, Seattle, WA.

A number of techniques have been recently developed for determination of peripheral and spinal bone mass: single photon absorptiometry (SPA) for radial bone mineral content (85% cortical bone: CB, 15% trabecular bone: TB), and dual photon absorptiometry (DPA) and computed tomography (CT) for vertebral (T12-L4) bone mineral content (90% TB, 10% CB). We have compared bone mass measurements by these different modalities to the established technique of total body calcium (TBC) by neutron activation analysis (a measurement of total skeletal bone mass: 80% CB, 20% TB); such a comparison assesses not only technique variability but also the variability between the amount of bone present at different skeletal sites, both cortical and trabecular. Current data assessment in 26 postmenopausal osteoporotic females reveals:

y	vs	x	r	p value	n
CT (spine)	TBC(total)	.44	<.05	18
SPA (radius)	TBC(total)	.57	<.05	26
DPA (spine)	TBC(total)	.95	<.001	5
CT (spine)	SPA(radius)	.41	NS	20

Preliminary data suggest modest correlations between various parameters, and between sites of cortical and trabecular bone mass, with the strongest correlation (n=5) between total bone mass (TBC), and vertebral bone mass as measured by the dual photon technique. The currently available data would indicate the necessity of obtaining bone mass measurements at multiple sites in assessing the overall status of skeletal bone mass.

COMPARISON OF RADIOGRAPHIC AND RADIONUCLIDE HIP ARTHROGRAPHY IN DETERMINATION OF FEMORAL COMPONENT LOOSENING OF CONVENTIONAL TOTAL HIP ARTHROPLASTIES. B.G. Uri, H.N. Wellman, W.N. Capello, J.A. Robb and G.F. Greenman. Indiana University Medical Center, Indianapolis, IN.

With standard radiographic arthrograms (XA), it is difficult to detect femoral component (FC) loosening of total hip prostheses because the metal prosthesis and surrounding radiopaque cement obscure radiographic contrast agents. Radionuclide Arthrogram (RA), is useful because the Tc-99m photons are not shielded by the prosthesis and cement nor is the radionuclide distribution confused with the cement.

Ten ml of Hypaque 60% injected intraarticularly were followed by 0.5 mCi of non-absorbable Tc-99m sulfur colloid in 1 ml via same needle. After XA, RA images were obtained in ant.,lat. and frog leg positions with an LFOV gamma camera and parallel hole collimator, also with companion Co-57 transmission images, comparing XA contrast and RA distributions.

Eighteen patients were studied for a total of 19 matched XA and RA (1 bilat). In 5, the RA and the XA both showed loosening of the FC (2/5 surgical proof), however, the RA showed a greater extent of FC loosening and more obviously than the XA in all. In 8, the RA and the XA were both neg. (2/8 surgical proof). In 6, the RA was pos. and the XA neg. Four of the 6 loosened prostheses were surgically verified. In no patient was the XA pos. and RA neg. 11 had MDP scans.

RA is a desirable, easily-performed adjunct in determining loosening of conventional femoral metallic prostheses, due to the difficulties in interpretation of XA. Further development is underway to better relate radionuclide distribution to the prosthesis using a combination of intra-articular In-111 non-absorbable radiopharmaceutical and simultaneous Tc-99m MDP bone imaging.

COMPARISON OF PLANAR BONE SCINTIGRAPHY AND SINGLE PHOTON EMISSION COMPUTED TOMOGRAPHY (SPECT) IN EVALUATION OF PATIENTS WITH PARANASAL SINUS DISEASE. R.J. Mitnick, J.E. Postley, P.D. Esser, F.V. Mignogna, P.O. Alderson. Columbia University, New York, NY.

The capability of planar bone imaging (PI) and SPECT to detect and localize bony involvement in paranasal sinusitis was compared in 15 patients (age range 23-76 yrs); 12 had active sinusitis, 10 also had asthma and 3 were asymptomatic at the time of imaging. Each patient (pt) received 20 mCi of Tc-99m diphosphonate and 4-view (anterior, Water's, both laterals) PI of the head was obtained 2.5 hrs later. SPECT was then performed with imaging through 360° of rotation, using either 64 (n=7) or 90 (n=8) views and an acquisition time of 20 sec/view. Transaxial, sagittal and coronal reconstructions were made and displayed at 2 pixels (1.24 cm) per slice. The PI and SPECT images were reviewed independently by an examiner who had no knowledge of the pts' symptoms or other test results. Each sinus was scored separately as normal or as showing 1+ to 3+ increased activity. Of the 75 sinuses examined, 27 (36%) showed increased activity on SPECT vs 7 (9.3%) on PI ($p < .001$). Only one abnormal sinus showed more than 1+ PI intensity, whereas 12 had 2-3+ intensity by SPECT. SPECT showed sphenoid sinus abnormalities in 12 pts vs 3 by PI. In one pt with 1+PI and 3+SPECT sphenoid abnormalities, surgery revealed active sphenoid necrosis. In 3 other sinuses with proven infection, SPECT was 1+ positive and planar studies were negative. Only 2 sinuses were positive by PI and not by SPECT, but there was no confirmation of disease. The findings suggest that SPECT of the sinuses is more sensitive than PI, and that further study of SPECT in the evaluation of sinus disease is warranted.

1:30–3:00 **Room 275**

INSTRUMENTATION III: PHANTOMS AND QUALITY ASSURANCE

Moderator: L. Stephen Graham, Ph.D.
Co-moderator: Guy H. Simmons, Ph.D.

Quality Assurance - How Much is Enough?
John W. Keyes, Jr., M.D., University of Michigan Medical Center, Ann Arbor, MI

IMPROVED METHODS FOR CHARACTERIZING AND MONITORING SYSTEM PERFORMANCE OF ROTATIONAL GAMMA CAMERAS. J Areeda, D Chapman, K Van Train, J Bietendorf, J Friedman, D Berman, A Waxman, E Garcia, Cedars-Sinai Med Ctr, Los Angeles, CA

Acceptance testing and quality assurance procedures for rotational gamma camera SPECT systems have not yet been standardized. Thus we developed acquisition methods and processing algorithms for measuring gantry stability and alignment, field uniformity, and spatial and contrast resolution to evaluate both the Siemens Orbiter and the dual-detector Rota SPECT systems interfaced to MDS computers. Point sources are acquired weekly in 32 projections over 360 and are analyzed by an algorithm which tracks the center of mass of the point source in the x and y directions from the projection images. Ideally, there is no motion in the y direction while the x coordinate describes a perfect sine wave. Variations from these findings indicate problems in detector alignment, gantry stability or positioning. Another algorithm aligns the electrical axis of both detectors of the Rota, using a simultaneously acquired flood for gross adjustment and three equidistant Co-57 line sources for fine adjustment. No movement of the lines during flip-flop cine display indicates a perfectly aligned system. Thirty-million-count Co-57 flood images are acquired weekly to develop uniformity correction matrices. Uniformity appears to change significantly only after service is performed on the system. The Jaszczak and Iowa phantoms are used to measure spatial and contrast resolution and to assess attenuation correction and counting statistics. With tomograms of 100 million cts, the 7.9 mm rods and 12.7 mm diameter spheres of the Jaszczak phantom are resolved. Conclusion: The methods developed provide a comprehensive standard for characterizing and monitoring the performance of rotational gamma camera systems.

EVALUATION OF SPECT SYSTEM PERFORMANCE USING A SPECT PHANTOM. R. L. Haerten, J. A. Bieszk, E. G. Hawman, and R. E. Malmin. Siemens Gammasonics, Inc., Des Plaines, IL.

For SPECT system evaluation a physical phantom has distinct advantages over the use of clinical images alone. A phantom offers accurate knowledge of the true activity distribution, freedom from motion blurring, and the potential for low image noise through very high count data acquisition. A commercially available, high resolution SPECT phantom has been used to evaluate a SPECT camera/computer

system with respect to performance criteria such as spatial resolution, uniformity, and the existence of artifacts.

The phantom has three sections: a uniform cylinder, cold spheres and cold rods. It was filled with 35 mCi Tc-99m. A total of 90M counts per study were acquired in 180 views over 360°. Co-57 flood images of 90M counts were acquired for flood correction. Center-of-rotation correction data were obtained using an array of five Co-57 point sources. Various convolution filters were used for reconstruction and attenuation was corrected by post-processing. Both high resolution and ultra high resolution collimators were used and studies were done with 64, 128, and 256 linear sampling of the 40 cm projection profiles.

It has been found that 90M counts in a study with 128 sampling is appropriate for the evaluation of SPECT resolution. Using flood correction based on 90M count flood images and attenuation correction, highly uniform, artifact-free images are obtained. A comparison of 64, 128, and 256 sampling indicates that 128 is required to preserve camera system resolution and to avoid aliasing. This study shows that with a high quality system and careful attention to the correction of system errors SPECT images with resolution approaching the theoretical detector/collimator limit can be obtained.

AN IMPROVED FLOOD FIELD PHANTOM FOR SINGLE PHOTON EMISSION COMPUTED TOMOGRAPHY (SPECT). P.D. Esser, R. Angels, D.W. Seldin, P.O. Alderson. Columbia University, New York, NY.

Reconstructed SPECT images are sensitive to artifacts produced by minor variations in the uniformity of the flood source used to calibrate the imaging field. With current thin fluid-filled flood sources, hydrostatic pressure can cause small bulges in the surface that result in such nonuniformities. We have designed a water-filled flood source that minimizes these problems. The design was based on the premise that an acceptable variation would create no more than 1% change in count rate (CR) per 0.5 mm change in fluid level in the source. Using the attenuation coefficient of Tc-99m in water, we calculated that a depth of approximately 4 cm would be required. Thus, a thick flood source was designed from readily available materials. It consisted of a 10 cm deep, 17 in. diameter hexagonal plastic tub (weight=17 lbs, with 4 cm water=31 lbs). Easy access to the tub is provided by top ports and fluid is drained from a valve positioned low on one side of the tank. Handles are attached to facilitate movement. Measurements (n=17) of actual changes in Tc-99m CR with changes in depth were made at 0.5 cm steps from 0-10 cm of water using a 15% window. Digital data were recorded and %CR changes caused by a 0.5 mm change in water depth were calculated. The data reveal that a 1.5% CR change was caused by a 0.5 mm change in water at a depth of 2.8 cm, and that a 1% CR change occurred at a depth of 3.9 cm. The results suggest that a thick water-filled flood source can minimize problems with SPECT field uniformity determinations.

USE OF A CARDIAC PHANTOM FOR QC CHECKS OF CAMERA/COMPUTER SYSTEMS. E. Busemann-Sokole and T.D.Cradduck, Victoria Hospital and University of Western Ontario, London, Ontario

Quality control procedures for a camera/computer system require that the dynamic as well as static imaging parameters be simulated if a complete check of the hardware and software is to be made. Although a number of different phantoms have been described that attempt to simulate the conditions during collection of gated blood pool studies of the heart only one has become available commercially. This phantom is known as the Vanderbilt cardiac phantom and consists of two rotating chambers that have the form of prolated spheroids. These chambers are intended to simulate the left ventricle and left atrium so their major axes are orthogonal and the projections they present to the detector are therefore in anti-phase. A background chamber can be mounted behind the rotating chambers to simulate right heart and large vessels. Three attenuators can be used to simulate three different ejection fractions. Experience with this phantom has demonstrated that the design leaves much to be desired. The positioning of the background chambers and the use of an attenuator to simulate an ejection fraction precludes the use of this phantom to compare software algorithms, or even to determine the efficacy of an algorithm, because the "background" in and adjacent to the projection of the left ventricle does not remain constant. Despite its simplicity, this phantom cannot be recommended as a suitable tool for routine quality control of the total system.

QUALITY ASSURANCE TESTS AND PHANTOMS FOR NMR IMAGING. F.H. DeLand, S. Smith, P. Wang, C. Coffey, G. Bellis, University of Kentucky Medical Center, Lexington, KY and Technicare Corporation, Cleveland, OH.

With the introduction of NMR as a new clinical imaging modality, there is need for quality assurance testing and associated test phantoms. We report image test data collected on a Technicare 0.15 Tesla resistive magnet NMR unit operating at 6.25 MHertz. The following NMR image parmeters have been determined: signal-to-noise ratio, resolution (high and low contrast), linearity, homogeneity, uniformity, slice thickness, edge contrast, T_1 contrast, and T_2 contrast. The NMR image parameters were further investigated as a function of pulse sequencing (saturation recovery, inversion recover, and spin-echo). The image parameters were investigated for both head and body radiofrequency coils. Conventional phantom materials utilized for image parameter testing were: (1) aqueous mixtures with the addition of varying concentrations of paramagnetic ions; (2) nonaqueous materials such as mineral oil containing nonprotonated solvents for signal-to-noise studies and mixtures of such materials to obtain varying T_1 and T_2 values; and (3) semisolid materials such as waxes, gelatins, and plastics which have T_1 relaxation times relative to those found in biological tissues. Quality assurance testing and the selection tissue equivalent NMR phantom materials have provided the means to routinely evaluate instrument performance and to correlate NMR parameters with in vivo results.

1:30–3:00 **Exhibit Hall**

POSTER SESSION II

More than 200 poster presentations of scientific papers will be on display Tuesday through Friday and approximately half of the authors will be present to answer questions during this time period. For a complete listing of posters, authors, and times, see POSTER PRESENTATIONS, which immediately follow the Scientific Papers on Friday.

3:30–5:00 **Room 123**

CARDIOVASCULAR CLINICAL VIII: PLATELET IMAGING

Moderator: Harvey J. Berger, M.D.
Co-moderator: Philip O. Alderson, M.D.

THE DETECTION OF ACUTE CORONARY THROMBOSIS IN PATIENTS WITH THE USE OF IN-111 LABELED PLATELETS. K.A.A. Fox, S.R. Bergmann, C.J. Mathias, K.T. Hopkins, A.S. Jaffe, W.J. Powers, B.A. Siegel, B.E. Sobel, M.J. Welch. Washington University School of Medicine, St. Louis, MO

The high incidence of coronary artery thrombosis early in the course of infarction and advances in thrombolytic therapy have intensified interest in the role of platelets. With the use of a vascular marker to correct for circulating radioactivity, we have previously shown in animal preparations and in man that incorporation of platelets into thrombi can be detected non-invasively with In-111 platelets. To

determine whether this approach can detect coronary thrombosis in patients, 500uCi of In-111 labeled autologous platelets and 2-6 mCi of Tc-99 RBC (a vascular marker) were administered within 9 hours of the onset of symptoms. Scintigraphy was performed 1-8 hours and 18-24 hours after the administration of labeled cells. Based on a reference region (right carotid artery) where blood pool activity is high and active platelet deposition unlikely, the ratio of In-111 to Tc-99m was calculated and digitized images were corrected for radioactivity associated with circulating In-111 platelets. In each patient with acute infarction (n=6), coronary artery thrombus was visualized in processed scintigrams as a localized focus of indium excess relative to blood pool [10.8 (3.0-27.3)% (mean and range) at 1-8 hrs. and 19.1 (9.5-27.5)% at 18-24 hrs.]. Seven of 8 patients evaluated for cerebrovascular disorder (without evidence of cardiac disease) exhibited no myocardial platelet accumulation. The technique should permit improved characterization of platelet contributions to the pathogenesis of coronary artery disease and its response to antiplatelet therapy.

EVALUATION OF PLATELET DEPOSITION AT THE SITE OF CORONARY ANGIOPLASTY USING INDIUM-111 LABELED PLATELETS. R.J. Callahan, R.W. Bunting, P.C. Block, C.A. Boucher, K.A. McKusick and H.W. Strauss. Massachusetts General Hospital, Boston, MA.

To determine if significant platelet deposition occurs at the dilatation site following percutaneous transluminal coronary angioplasty 6 patients undergoing this procedure were studied with In-111 labeled autologous platelets. Platelets were labeled with In-111 oxine using an albumin density gradient separation technique to isolate the cells. Two hundred and fifty microcuries of In-111 platelets were injected intravenously on the day before PTCA. Anterior images of the chest, abdomen and groin were obtained 4 hours after injection and 8 to 24 hours following PTCA. Systemic heparinization was used during PTCA and patients were maintained on intravenous dextran post-PTCA.

Four out of six patients had successful dilation of coronary artery lesions.

In 4 out of 6 patients, platelet deposition was seen on images of the femoral arteriotomy site. Subclavian and occasionally carotid arteries and abdominal aorta also showed platelet deposition. No coronary artery deposition of platelets was observed in any of the six patients studied.

Platelet deposition in coronary arteries could not be visualized using this technique. These results suggest that platelet deposition at the site of PTCA is minimal or absent. Visualization of other sites of accumulation indicate that functional platelets were within the circulation at the time of PTCA despite anticoagulation.

INHIBITION OF THROMBOTIC AORTOCORONARY BYPASS GRAFT OCCLUSION WITH VERAPAMIL AND PAPAVERINE IN DOGS. M.K. Dewanjee, P. Gloviczki, D. Kluge, M.P. Kaye, Mayo Clinic and Mayo Foundation, Rochester, MN.

The effect of a vasodilator papaverine (PPV) and a Ca^{2+} channel blocker verapamil (VP) on vein graft preservation was evaluated in aortocoronary bypass graft (ACBG) model in mongrel dogs. Nineteen dogs in three groups underwent ACBG surgery. Femoral vein grafts were incubated with papaverine (100 µg/ml) and verapamil (22 µg/ml) in ACD-plasma for 60 minutes at 25°. 200-300 µCi of autologous In-111-labeled platelets were administered post-cardiopulmonary bypass procedure and the dogs were killed three hours post-administration. From the platelet count in EDTA blood and In-111-radioactivity in sections of proximal (PX), middle (MD), distal (DT), proximal and distal anastomoses (PA, DA), and blood measured with a gamma counter, (mean ± SD) values of platelets deposited per unit area of graft (Pl/cm^2) x 10^6 were calculated and tabulated below:

	Control (n=6)	Papaverine (n=6)	Verapamil (n=7)
PA	82 ± 47	35 ± 34	57 ± 57
PX	9 ± 7	7 ± 7	8 ± 5
MD	11 ± 9	7 ± 5	5 ± 4
DT	18 ± 17	7 ± 5	7 ± 7
DA	108 ± 67	49 ± 35	67 ± 63

Previous studies suggest that both drugs maintain more endothelial cells on graft intima by relaxation of medial smooth muscle cells. Our results confirm reduction of platelet adhesion and aggregation ($p < 0.05$) in PA and DA of treated graft. Graft incubation in VP and PPV before implantation tends to reduce platelet depositions and therefore may reduce early thrombotic graft occlusion.

USE OF INDIUM LABELED PLATELETS TO MONITOR PLATELET DEPOSITION ON VASCULAR GRAFTS. B.T. Allen, C.J. Mathias, R.E. Clark, K.T. Hopkins, and M.J. Welch. Washington University School of Medicine, St. Louis, MO.

Vascular graft thrombosis is the limiting factor in successful peripheral vascular reconstruction. To define the platelets role in graft failure, we employed In-111-platelet scans to serially monitor in vivo platelet deposition on canine implanted vascular grafts. Autologous jugular vein, PTFE (Goretex), and two dacron (Meadox and USCI) grafts were implanted into the femoral arteries of 17 dogs. Autologous In-111-platelets and Tc-99m labeled red cells were used to quantitate platelet deposition on each graft serially to one month post implant. For all types of grafts, platelet deposition [% Indium Excess (%IE)] was highest immediately post implant and decreased over time. %IE on the synthetic grafts was greater than on vein grafts throughout the study period but difference was significant only during the first two weeks. Goretex grafts accumulated fewer platelets than the dacron grafts during the first 24 hours. To determine if the degree of platelet deposition affected graft function, grafts patent or thrombosed at one month were compared in terms of their post implant %IE. Grafts which thrombosed during the first month accumulated significantly more platelets during the initial 24 hrs post implant than did the grafts which remained patent. We conclude that 1) platelet deposition on all grafts peaks soon after graft placement; 2) vein grafts have a significantly lower platelet affinity than synthetic grafts during the first 2 weeks, a trend which continues for one month; 3) Goretex grafts accumulate fewer platelets than dacron grafts during the first 24 hrs; and 4) excessive early platelet deposition promotes eventual graft failure.

SCINTIGRAPHIC DEMONSTRATION IN PATIENTS OF THE EFFECT OF ASPIRIN ON PLATELET DEPOSITION AT SITES OF TRANSLUMINAL ANGIOPLASTY. D.A. Cunningham, B. Kumar, B.A. Siegel, L.A. Gilula, W.G. Totty, K.T. Hopkins, C.J. Mathias, J.L. Wilson, and M.J. Welch. Mallinckrodt Institute of Radiology, St. Louis, MO.

This prospective study was undertaken to evaluate the effects of prior therapy with aspirin on the accumulation of platelets at sites of peripheral arterial injury secondary to transluminal angioplasty. We have studied 15 male patients undergoing angioplasty for iliac and femoral arteriosclerosis. In-111 labeled autologous platelets were administered 2-18 hours before angioplasty and images were obtained immediately before and within 1 hour after angioplasty. All patients received intra-arterial heparin immediately prior to angioplasty and subcutaneous heparin and oral aspirin after angioplasty. Aspirin therapy before angioplasty was not randomised; however, 8 patients were not pretreated with aspirin based on the preference of the referring physician. A blinded observer evaluated the pre- and post-angioplasty images for changes in activity distribution. Among the 8 patients not pretreated with aspirin, the scintigrams showed unequivocally increased activity at the angioplasty site in 6 and equivocal uptake or no change in 2. In contrast, among 7 patients pretreated with aspirin (300 to 1200 mg/day), the scintigrams were equivocal or negative in all (P=0.006). The arteriotomy site was positive in all patients. These preliminary results suggest that aspirin therapy before transluminal angioplasty limits the early platelet deposition at peripheral angioplasty sites in men.

THE DIAGNOSTIC ACCURACY OF INDIUM-111 PLATELET SCINTIGRAPHY IN THE DIAGNOSIS OF ACUTE DEEP VEIN THROMBOSIS. C.F. Pope, M.D. Ezekowitz, D. Sostman, E.O. Smith, M. Glickman, S. Rapoport, C. Balint, D. Galloway, R. Pelker, G. Friedlaender, B.L. Zaret. Departments of Medicine and Radiology, Universities of Oklahoma, OK City, OK & Yale, New Haven, CT.

Indium-111 platelet scintigraphy (PS) may be used to detect deep vein thrombosis (DVT). The purpose of this paper was to define the diagnostic accuracy of the technique against contrast venography (CV). Two groups of patients

were studied; group I (N=11) had a major lower limb orthopedic procedure. Group II (N=9) had a clinically suspected DVT. Autologous platelets were separated from 43 ml blood, labelled in ACD:NS (1:7) with Indium-111 8-OH quinoline and injected IV 0.9 ± 0.5 days after surgery and 6.9 ± 2.1 days before CV in group I and 3.2 ± 2.6 days after CV in group II. In 25/27 limbs studied, images of the pelvis, thigh and calf were obtained within 24 hours of the injection of the platelet suspension. In 2 limbs the earliest image was at 48 and 72 hrs. Subsequent images were obtained up to 144 hrs. All 27 limbs had CV. A positive scintiphoto was defined as an area of increased activity, not related to the wound, occurring during the imaging period. Doubtful images were considered negative. The sensitivity and specificity of PS was 40 and 88%. Excluding patients on continuous IV heparin (activated partial thromboplastin time (APTT) range 1.5 - 3 X control) the sensitivity increased to 100% while specificity remained unchanged. One patient on continuous IV heparin (1,000 IU/hr, APTT 2.0 X control) was positive by PS and CV. All patients positive by PS and CV were positive within 24 hrs of injection of labelled platelets. We conclude that PS may be used for accurate and early diagnosis of DVT. Continuous infusion of heparin inhibits uptake of platelets on venous thrombi. PS may be used to monitor the adequacy of therapy.

3:30–5:00 **Room 132**

CARDIOVASCULAR BASIC III: IMAGING

Moderator: Philip O. Alderson, M.D.
Co-moderator: Ernest V. Garcia, Ph.D.

DYNAMIC CARDIAC STUDIES WITH SUPER PETT I. M.M. Ter-Pogossian, E.M. Geltman, B.E. Sobel, and D.C. Ficke, Washington University School of Medicine, St. Louis, MO.

Super PETT I is a positron emission tomograph which utilizes photon time-of-flight information in its image reconstruction process. Three features have been incorporated into the design of Super PETT I to optimize its suitability for fast dynamic studies particularly for cardiac imaging. 1) A short coincidence resolving time (2.3 nsec for body studies; 1.6 nsec for head studies); 2) The utilization of time-of-flight information in the image reconstruction process; and 3) Data acquisition in the list mode. The short coincidence resolving time allows data acquisition at high counting rates with minimal interference from random coincidences. The utilization of time-of-flight information improves the signal to noise ratio in the reconstructed images. This gain can be utilized in improving either the spatial contrast, or temporal resolution of the examination. The data acquisition in list mode facilities dynamic studies by allowing the reconstruction of images for any temporal window after completion of the examination and this feature permits retrospective cardiac gating. The above features of Super PETT I have been applied in a series of studies including 1) dynamic visualization of the beating heart; 2) assessment of cardiac wall motion in the tomographic mode in normal subjects and in patients suffering from MI; and 3) dynamic studies of the metablic utilization of palmitate in different portions of the myocardium. The rapid data acquisition capabilities of Super PETT I have also been found to be useful in the myocardial imaging with rubidium-82.

MULTIGATED RADIONUCLIDE STUDIES OF THE ARTIFICIAL HEART. P.E. Christian, W.L. Hastings, W.C. DeVries, F.L. Datz, A.T. Taylor. University of Utah School of Medicine, Salt Lake City, UT

Multi-interval gated cardiac studies of the Jarvik 7 artificial heart have been performed on a mock circulation device using a scintillation camera interfaced to a computer. The Jarvik 7 has ventricles made of polyurethane supported on an aluminum base. Each ventricular chamber contains a rubber diaphragm which expands with pressurized air to act as a pump for the ventricle. The heart driver allows the control of the pumping parameters. Failure of the heart in animals most commonly results from diaphragmatic calcification. Baseline functional performance data for the artificial heart have been obtained for both the mock circulation device and an implanted patient.

Radionuclide count changes correlated well (r=.99) with known ventricular volume changes. Increasing the duration of end systole did not affect the ejection fraction but diminished the time for ventricular filling. When pumping pressure was increased from 60 to 80 mm of mercury, there was an increase of 8 EF units. An increase in pumping rate primarily shortens end diastolic filling. An understanding of the physiologic effect of changes in driving parameters is critical in determining the proper setting for patient use. Functional images including stroke volume, recovery, time to maximum amplitude, fractional amplitude and cardiac phase analysis were also obtained to evaluate regional diaphragmatic motion. The normal Jarvik 7 heart showed excellent diaphragmatic excursion and uniform diaphragmatic motion.

In summary, baseline data have been obtained by applying multi-interval cardiac analysis and functional imaging to studies of the artificial heart.

ECT OF THE HEART USING THE ROTATING-SLANT-HOLE COLLIMATOR AND TWO ORTHOGONAL CAMERA POSITIONS. K.F. Koral, C. Nolder, G. Ciliax, W. L. Rogers and J.W. Keyes, Jr., University of Michigan Medical Center, Ann Arbor, MI.

It is well known that limited-angular-range tomography leads to an elongating distortion of the true object in the direction perpendicular to the camera (along the z axis). One possible remedy is to append to the usual data set another set of projections taken after the camera is rotated 90° about an axis perpendicular to the z axis. We call such a method 2-view tomography. Possible advantages of the method over transverse-section tomography are the requirement of only a basically standard camera, the availability of bedside imaging and the need for accurate camera calibration in only two, rather than many, orientations. Although 2-view tomography is applicable to any limited-angular-range tomographic collimator, we have restricted the present investigation to the rotating-slant-hole collimator with 12 projections per view. The SMART iterative algorithm with impedance estimate is employed for reconstruction.

Simulation results have been obtained for a half-ellipsoid shell with noise and attenuation effects included. Reconstructions have also been obtained for the Au-195 ring phantom in air and for a ventricle phantom situated within a water bath to approximate body attenuation. Results show that 1) the method is not especially sensitive to noise, 2) for a shell with uniform strength plus a defect the image does not exactly reproduce the object especially with attenuation, 3) for simulations and phantoms a normal result can be established and the defect detected by variations from that normal, 4) for simulations, the results are not particularly sensitive to the orientation of the long axis of the ventricle model. In conclusion, 2-view tomography has promise for thallium-type heart imaging.

GATED CARDIAC BLOOD POOL EMISSION COMPUTED TOMOGRAPHY FROM ONLY TWO CODED VIEWS. J.Fonroget, D.Lefkopoulos, and J.C.Roucayrol . Hôpital Cochin, Paris Cedex 14.

Cardiac blood pool investigation using SPECT has proved to be of great interest to evaluate ventricular function. A new tomographic method is proposed. It permits to obtain a series of transaxial slices of the beating heart without a rotating camera, but with two stationnary cameras fitted with two multiple-pinhole coded collimators, at an angle of 60° to each other.

Each collimator is constituted by several adjacent unidimensional two-pinhole codes divided by lead septa in order to avoid interference of coded informations coming from different slices. The radioactive dose of Tc-99m labelled serum albumin injected and the acquisition time are the same as in conventional methods. The recording of the coded data are synchronised with ECG, the cardiac cycle being divided into sixteen frames of equal times. Then for each slice eight images have to be reconstructed from coded data.The tomographic system is characterized by a coding matrix which is determined so that it takes into account gamma ray attenuation and shift variance. The reconstruction problem is the ill-conditionned problem of solving a first

kind Fredholm integral equation. Each slice is reconstructed separately by a matricial regularizing method involving the determination of the coding matrix SVD pseudo-inverse .

This method provides accurate high resolution images of the heart blood pool at each time interval of the cycle and then is particularly well adapted to cardiac dynamic studies.

NON-ORTHOGONAL FACTOR ANALYSIS IN GATED CARDIAC STUDIES. F. Cavailloles*, J.P. Bazin**, R. Di Paola**. *Dept. of nuclear medicine, 94 Kremlin-Bicêtre/**INSERM U66, 94800 Villejuif - France.

Factor Analysis of Dynamic Structures (FADS) has been applied to 45 gated studies. This method which was introduced by Di Paola (1975), Bazin (1979) and Barber (1980), automatically provides "physiological" factors. They are related to anatomical structures which have different temporal behaviours. The results provided by FADS include the "physiological" factors with their associated spatial factor images and their relative contribution to the total information. Trichromatic display was used to show the superposition of the factors. In normal patients, two factors are extracted. A third factor can be obtained when additional dynamic structures exist, even in case of overlapping. In this case, the pathological significance results from the shape of the factor and its relative position on the factor image.

Among the 45 patients, 4 were normal, 11 had a congestive cardiomyopathy, 29 had a coronary artery disease (26 with a previous infarct) and 1 had a pace-maker. 11/45 had a bundle branch block (BBB). Results obtained by FADS were compared to the amplitude and the phase of the first harmonic of Fourier Analysis (FA). Their common results were compared to the final diagnosis based on 2-D echocardiography and/or ventriculography, using a scale from 0 (no agreement) to 3 (total agreement) Globally, FADS is significantly better than FA in RAO view ($p < 5\%$). This superiority appears clearly in BBB (LAO $p < 5\%$; RAO $p < 1\%$). No significant difference were obtained in regional wall motion abnormalities (RWMA). Conclusion : FADS gives satisfactory results in RWMA and in BBB, specially in case of overlapping. Furthermore, FADS is a versatile method and a powerful tool for data compression.

POSTEXTRASYSTOLIC POTENTIATION IN THE DOG VENTRICLE USING RADIONUCLIDE VENTRICULOGRAPHY. J.F. Polak, P.J. Podrid, B. Lown and B.L. Holman. Harvard Medical School and Brigham and Women's Hospital, Boston, MA.

We studied the effects of induced ventricular premature beats in five dogs using list-mode radionuclide ventriculography. Plunge electrodes inserted at five sites in the myocardium were used to induce ectopic beats with a coupling interval of 150 msecs at every 5th sinus beat. The control sinus beat, interrupted sinus beat, and first and second postextrasystolic sinus beats (PESB) were analyzed separately. The left ventricular ejection fraction (EF), end-diastolic counts/volume (EDV), end-systolic counts/volume (ESV) and ejection counts/stroke volume (SV) were the same for control and interrupted beats. EF, SV and EDV were markedly increased during the first PESB. There was a mild increase in EF during the second PESB despite a lower EDV.

	Control Beat	Interrupted Beat	First PESB	Second PESB
Number	19	19	19	11
% EF	41.5 ± 4.0	40.6 ± 4.9†	56.8 ± 3.9**	43.6 ± 4.2*
Δ EDV°	-	+0.5 ± 2.9†	+11.7 ± 4.9**	-2.8 ± 2.5*
Δ ESV°	-	+1.9 ± 5.3†	-16.2 ± 5.2**	-5.4 ± 4.3*
Δ SV°	-	-1.4 ± 4.4†	+51.6±16.8**	+1.2 ± 3.2†

† p:NS * p < .05 ** p < .001
° values expressed as % change

We conclude that list-mode radionuclide ventriculography can be used to determine changes in cardiac function associated with induced ventricular ectopic beats. An increase in contractility is seen primarily during the first post-extrasystolic beat and is associated with an increased EDV.

3:30–5:00 **Room 130**

NEUROLOGY III: BASIC SCIENCE PETT

Moderator: Michael E. Phelps, Ph.D.
Co-moderator: Henry Huang, D.Sc.

MYELIN IMAGING WITH PET. D.D. Dischino, M.J. Welch, M.R. Kilbourn, P. Herscovitch, J. Trotter, and M.E. Raichle. Washington University School of Medicine, St. Louis, MO.

Over the past several years there has been interest in the development of radiopharmaceuticals to image myelin in demyelinating diseases such as multiple sclerosis (Frey KA et al, Ann Neurol 10:212, 1982). An agent for this purpose should be highly lipophilic, freely permeable across the blood brain barrier and either be unmetabolized during the imaging time or metabolized in such a way that the products of metabolism will not re-enter the brain. A series of ethers and alcohols with octanol water partition coefficients between 0.2 and 25,000 were labeled with the 20.4 min half-lived positron-emitting radionuclide carbon-11. The single pass extraction of these compounds was evaluated in a primate model (Raichle ME et al, Am J Physiol 230:543, 1976) and it was determined that the compounds with partition coefficients <1,000 were extracted with an efficiency of >95% at blood flows of 60 ml/min/hg. Metabolism studies have been carried out on several potential candidates for myelin imaging, including 1-hexanol, benzyl methyl ether, and diphenylmethanol. It has been determined that C-11-diphenylmethanol has the desirable characteristics of a myelin imaging agent and imaging studies utilizing PETT VI with this compound in baboons confirmed this fact. Tissue distribution studies in rats using C-11-diphenylmethanol have shown that, following a 30 mCi administration to a human, the critical organ would be the small intestine which would receive a radiation dose of 2.5 rads. Preliminary studies carried out in humans show an initial distribution of the compound proportional to blood flow followed by a redistribution over ~ 15 min with the distribution at this time reflecting the local lipid content of the brain.

ABSOLUTE QUANTITATION OF LOCAL CEREBRAL BLOOD FLOW AND PARTITION COEFFICIENT WITHOUT ARTERIAL SAMPLING. R.A. Koeppe and J.E. Holden, Medical Physics Department, University of Wisconsin, Madison WI 53706.

A new technique that requires neither arterial blood sampling nor knowledge of the tracer's tissue:blood partition coefficient has been developed for absolute quantitation of local cerebral blood flow. This technique is an extension of an existing method using F-18 methyl fluoride administered by 2 minute rebreathing from a dry spirometer, and positron computed tomography. In the method, the shape and scale of the arterial blood curve, $C_a(t)$, are determined from the concentration of tracer in the subject's expired gas, $C_{exp}(t)$, and venous blood, $C_v(t)$. The expired air radioactivity is measured in a flow-through plastic scintillator. The arterial blood concentration is assumed to be proportional to the expired air curve interpolated between end-tidal values ($C_a(t) = h \cdot C_{exp}(t)$). The venous samples are counted in a NaI well-counter and scaled to units identical to those of the positron images. The arterial scaling factor, h, is determined by fitting the venous concentration curve, C (t), to a multi-compartment model:

$$C_v(t) = \sum_i A_i C_{exp}(t) * e^{-k_i t} \quad ; \quad h = \sum_i A_i / k_i$$

where the asterisk denotes convolution.

Results show gray and white matter flow values of 60-75 and 25-35 ml/100 ml min, and methyl fluoride partition coefficients of 1.3 and 1.1 respectively. The method provides the quantitation necessary for inter-study comparisons while avoiding the trauma of arterial puncture.

THE AUTORADIOGRAPHIC MEASUREMENT OF REGIONAL CEREBRAL BLOOD FLOW (CBF) WITH POSITRON EMISSION TOMOGRAPHY: VALIDATION STUDIES. P. Herscovitch, W.R.W. Martin, and M.E. Raichle. Washington University School of Medicine, St. Louis, MO.

We have adapted the classic tissue autoradiographic method (Kety, Methods Med Res 8:228) for the measurement of local CBF with positron emission tomography (PET) and intravenously administered O-15 water. We here report direct validation of this technique. CBF was measured with PET, in anesthetized baboons, and was compared to flow measured with a standard tracer technique employing residue detection of a bolus of O-15 water injected into the internal carotid artery.

The correlation between CBF measured with PET, using a 40 sec scan length, and the true CBF for the same hemisphere was excellent. Over the flow range of 10-63 ml/min/hg, CBF(PET) = 0.90 CBF(true) + .40, (n=23, r=0.96, p<0.001). At higher flows, especially greater than 80 ml/min/hg, CBF was progressively underestimated due to the known permeability limitation of water (Eichling et al, Circ Res 35:358). This will not be important in practice, as such flows are infrequently encountered.

However, increasing scan lengths from 40 sec to 80 and 120 sec, resulted in measured flows decreasing by up to 31%. Such declines also occurred with the highly permeable tracer, C-11 butanol, and have previously been observed with the tissue autoradiographic method (Eklof et al, Acta Physiol Scand 91:1). As these declines occurred with a freely diffusible tracer, other assumptions in the Kety model may be involved.

Thus, provided scan measurements are brief (e.g. 40 sec), the PET autoradiographic method provides a reliable measurement of CBF.

OXYGEN UTILIZATION MEASURED BY O-15 RADIOTRACERS AND PET. M.A. Mintun, M.E. Raichle, W.R.W. Martin, and P. Herscovitch. Washington University School of Medicine, St. Louis, MO.

We have developed, implemented, and validated a method for the measurement of the local cerebral metabolic rate for oxygen ($CMRO_2$) with emission tomography (PET). We use data from a single breath inhalation of O-15 CO for cerebral blood volume (CBV), an injection of O-15 H_2O for cerebral blood flow (CBF) and a single breath inhalation of O-15 O_2 for the final calculation of $CMRO_2$ and the extraction of oxygen (E). Our mathematical model consists of two compartments and accounts for production and egress of water of metabolism in the tissue, recirculating water of metabolism, and the brain arterial, venous, and capillary content of O-15 O_2. We validated our technique in baboons by comparing the PET measured E with E measured using an intracarotid injection of O-15 O_2, a technique previously described (J Clin Invest 49:381, 1970) and validated (J Appl Physiol 40:638, 1976). The correlation between these two techniques was excellent [E(PET) = 1.035 E(true) - 0.018, R squared = 0.9578, N=22] over an E range of 0.08 to 0.58. Mathematical simulations were done to examine the effect of errors in the CBV, CBF, and recirculating water of metabolism. At a $CMRO_2$ of 4 ml/min/100 g a 5% error in CBF results in a 5.3% error in $CMRO_2$ and a 0.6% error in E. A 5% error in CBV results in a 1.5% error in $CMRO_2$, and a 5% error in the recirculating water measurement results in a 0.3% error in $CMRO_2$. Importantly, a 10 to 20% error results if recirculating water is ignored. The technique was implemented on normal human subjects. In five normal subjects the global $CMRO_2$ was 2.93 ± .37(SD) ml/min/100 g and a E was 0.38 ± .05.

THEORETICAL EVALUATION OF A TOMOGRAPHIC TECHNIQUE FOR SIMULTANEOUS MEASUREMENT OF CBF AND OXYGEN UTILIZATION (MRO) WITH O-15 OXYGEN. S.C. Huang, R.E. Carson, M.E. Phelps, UCLA School of Medicine, Los Angeles, CA.

We have investigated a tomographic technique for simultaneous measurement of local CBF and MRO using single breath inhalation of O-15 oxygen. After inhalation of O-15 oxygen, the initial uptake of radioactivity in brain tissue is related to CBF times the extration fraction(E) of oxygen. The uptake and clearance of the recirculated activity in form of O-15 water provides information about CBF. Thus, by utilizing the full dynamics of O-15 radioactivity in tissue, both CBF and MRO can be determined. This simultaneous measurement technique eliminates physiological changes that may occur between the separate measurement times of CBF and MRO using O-15 water and O-15 oxygen that are required by existing techniques. Computer simulations were used to evaluate the feasibility and error sensitivity of the technique. Initial results indicate that the error sensitivity is very dependent on the values of E, CBF, and on the shapes and relative concentrations of the input functions of O-15 oxygen and water. That is, accuracy of the estimates is related to these parameters. For CBF=0.6 ml/min/g, E=0.5, and reasonable input functions, accuracies of ±15% and ±10% for the estimated CBF and MRO, respectively, are achievable with a positron CT scan of 5 million counts in 8 min. For larger(smaller) CBF and E, the estimation errors are smaller(larger). While the advantages and practical limitations of the simultaneous measurement technique as compared to alternative methods still need to be better assessed, the present study indicates that simultaneous determination of CBF and MRO is feasible.

MEASUREMENT OF CEREBRAL BLOOD FLOW WITH C-11 BUTANOL AND POSITRON EMISSION TOMOGRAPHY. M.E. Raichle, W.R.W. Martin, P. Herscovitch, M.R. Kilbourn, and M.J. Welch. Washington Univerity School of Medicine, St. Louis, MO.

We have previously described (J Cereb Blood Flow Metab 1:S19, 1981) a method for the measurement of local cerebral blood flow (CBF) using an adaptation of the classic Kety, tissue autoradiographic technique; oxygen-15 labeled water as the diffusible tracer; and positron emission tomography (PET). Despite the immense convenience of oxygen-15 water as a tracer for this work, it suffers from the fact that brain is not freely permeable to water (Circ Res 35:358-364, 1974). As a result, CBF may be underestimated in areas of high flow. Thus, we have investigated the use of C-11 butanol as an alternative tracer. Previous work in our laboratory indicated that alcohols of increasing chain length become progressively more permeable (Am J Physiol 230:543-552, 1976). Based on this work we have, first, measured the brain permeability of C-11 butanol in baboons using a single injection, external detection technique developed in our laboratory (Am J Physiol 230:543-552, 1976). These data indicate that C-11 butanol is freely permeable up to a CBF of at least 180 ml/(min·100 g) and should accurately measure CBF when used with PET. Second, to establish the validity of this assumption, we measured CBF with PET and C-11 butanol in adult baboons and compared it to CBF measured with a standard, intracarotid injection, residue-detection technique (Circ Res 35:358-364, 1974). The correlation was excellent [CBF(PET/butanol)=0.91 CBF(true) + 0.83, r=0.97, n=9]. These data establish C-11 butanol as a standard against which to test the behavior of other tracers such as O-15 water with PET in humans. Such a comparison is currently under way in our laboratory.

3:30-5:00 **Room 276**

INFECTIOUS DISEASE

Moderator: George N. Sfakianakis, M.D.
Co-moderator: Andrew T. Taylor, M.D.

INDIUM-111 LEUKOCYTE SCINTIGRAPHY FOR DETECTION OF PERITONEAL CATHETER TUNNEL INFECTIONS. S. Kipper, R. Steiner, R. Basarab, M. Kipper, K. Witztum, S. Halpern, W. Ashburn. University of California and VA Medical Centers, San Diego, CA

Peritoneal catheter (PC) tunnel infections (TI), a frequent cause of relapsing peritonitis (RP) in the continuous ambulatory peritoneal dialysis patient, are difficult to diagnose short of PC removal. We searched for TI with In-111-labeled leukocytes (In-111-WBC) in 11 patients (18 scans) with chronic indwelling PC. A cobalt-57 marker was used to locate the PC exit site on a separate film overlay. The 18 scans were divided into 4 groups according to clinical presentation: Group I (n=2),asymptomatic patients; Group 2 (n=4), exit site infections (ESI) without peritonitis; Group 3 (n=8), uncomplicated peritonitis without ESI; Group 4 (n=4), RP. Each scan was retrospectively interpreted by 5 physicians (double blinded) and compared to original readings and

clinical course. There was 100% interobserver agreement in 8/9 (89%) negative scans and in 9/9 (100%) positive scans. Only 2 scan readings were retrospectively changed from negative to positive. Group 1 scans were negative. Group 2 and Group 3 scans, positive only for ESI in 5/12, correlated well with the clinical course and were not associated with TI; 7/12 were negative. Group 4 scans (3 patients) all showed uptake in the PC tunnel or internal cuff. TI was documented by culture at surgical PC removal in 2 patients and by pericatheter leaking in the third patient. Conclusion: In-111-WBC appear to be reliable in detecting and localizing peritoneal catheter associated infections (tunnel and exit site infections) in this increasingly popular form of dialysis.

COMPARISON OF In-111 ACETYLACETONE LABELED GRANULOCYTES, Ga-67 CITRATE, AND 3-PHASE MDP SKELETAL IMAGING IN COMPLICATED OSTEOMYELITIS. D.S. Schauwecker, B.H. Mock, H.N. Wellman, H.M. Park, and R.W. Burt. VAMC, Indiana University School of Medicine, Indianapolis, IN.

Evaluation of osteomyelitis (OM) superimposed upon other diseases with rapid bone turnover (DWRBT) may be difficult. DWRBT may cause both 3-phase MDP skeletal imaging (3P) and gallium-67 citrate (Ga-67) abnormalities, with or without superimposed OM. Indium-111 acetylacetone labeled granulocytes (IAAG) are unaffected by DWRBT and are a logical choice for evaluating OM superimposed on neurotropic osteopathy, loose prostheses, fracture, bone surgery, etc.

Thus far we have evaluated 20 patients for OM, 5 uncomplicated cases and 15 superimposed on DWRBT. The 3P and Ga-67 images were 100% accurate in the diagnoses of OM in the uncomplicated patients. IAAG was correct in 18/20 cases where the diagnoses were established by surgery or discharge diagnoses and follow-up. The 2 false negatives were on long-term antibiotics; 1 was an uncomplicated OM, the other had DWRBT. There were no false positives with IAAG. In all cases with DWRBT, the 3P showed intense activity in all phases, and thus was not specific for OM. Ga-67 was correct in about 60% of the cases with DWRBT. There was 1 false negative Ga-67 in a patient on long-term antibiotics; this was the false negative with IAAG mentioned previously. Positive Ga-67 localization, in those cases where IAAG was negative and agreed with the established diagnoses, was attributed to DWRBT alone.

3P has high sensitivity and is a logical first step in evaluating OM. It is very accurate singly in uncomplicated cases. IAAG should be used to increase specificity in cases complicated by DWRBT.

INDIUM-111 CHLORIDE IMAGING IN PATIENTS WITH SUSPECTED ABSCESSES. B. Sayle, S. Balachandran, and C. Rogers, Division of Nuclear Medicine, University of Texas Medical Branch, Galveston, TX.

Two hundred and fifty-eight patients referred with a diagnosis of possible abscess were imaged with Indium-111 Chloride. Imaging was performed between four and seventy-two hours following the injection of 3mCi. Gastrointestinal activity was not a problem; bowel preparation was only rarely required. Results: There were seventy-two true-positive scans. Thirty-six were proven by surgery, biopsy or autopsy. Twenty-four patients had subcutaneous lesions, e.g. fistulas and wound infections. Fourteen were confirmed by ultrasound, CT or radiography. Three patients had palpable masses that improved with antibiotic therapy. There were nine false-positive scans: three due to neoplasms and two to a recent colostomy. Two patients had increased activity in the splenic bed following splenectomy, and two had increased activity in the kidney bed following nephrectomy. There were 211 negative studies: twenty-four were confirmed by tissue examination, and thirteen patients had normal ultrasound examinations. There were six false-negative studies showing walled-off abscesses found either at surgery or biopsy. Conclusion: The sensitivity was 92%, the specificity 95%, and the accuracy was 94%. The positive predictive value was 89% and the negative predictive value was 97% at a 30% prevalence. This study indicates that Indium-111 chloride is more accurate than Gallium-67 in detecting inflammatory disease.

EARLY In-111 LEUKOCYTE IMAGING HAS A LOW SENSITIVITY FOR DETECTING OCCULT INFECTION. F. Datz, J. Jacobs, N.Alazraki, W. Baker, W. Landrum, A. Taylor. University of Utah Medical Center and VA Medical Center, Salt Lake City, UT

In-111 leukocyte imaging has been shown to be a sensitive modality for the detection of occult infection. Imaging is commonly performed 24 hours post-injection. A prospective study was undertaken to determine if images performed 1-4 hours post-injection would allow an earlier diagnosis of septic foci.

Forty studies were performed in 35 patients with possible occult infection. Autologously labeled leukocyte imaging was performed 1-4 hours post-injection and repeated at 24 hours. The studies were reviewed by two experienced observers. Diagnosis was confirmed by clinical course, x-ray studies, surgery and necropsy findings.

In 21 of 40 (53%) patient studies, a clinically positive site of infection was present. The early images had a sensitivity of only 33% (7 of 21) compared to the 24 hour images which had a sensitivity of 95% (24 of 25). None of the studies which were positive early became negative on delayed imaging. Of the 7 studies positive on both early and delayed images 71% (5 of 7) had more intense uptake at 24 hours. In no case was the earlier image more intense than the delayed image. Furthermore, there were no false positive scans on either early or delayed imaging.

The falsely negative early imaging studies included: 4 abdominal abscesses, 1 abdominal wall abscess, 1 dental abscess, 3 infected grafts, 2 pneumonias, 1 case of pyelonephritis, and 1 case of osteomyelitis.

We conclude that early imaging with In-111 leukocytes has a low sensitivity for detecting sites of occult infection. However, a positive early scan is specific for the presence of an inflammatory focus.

THE DIAGNOSTIC VALUE OF GALLIUM-67 IN DETECTION OF POST-OPERATIVE STERNAL OSTEOMYELITIS. D.H. Feiglin, A. Detsky, A.E. Simor, C.M. Minuk, R.D. Weisel, I.E. Salit. Toronto General Hospital, Toronto, ONT.

Sternal osteomyelitis is a serious complication often requiring prolonged hospitalization, intravenous antibiotics, surgical drainage and is associated with a high mortality.

As diagnosis of this disease is potentially difficult a prospective blinded and randomized study of Gallium-67 scanning in the early post cardiac surgery period was performed.

Twenty seven patients were scanned on the 7th post-operative day, two days after administration of 148 MBq of Ga-67. Simultaneous independent clinical assessment by two infectious disease consultants and a cardiovascular surgeon was performed with the aid of laboratory results but without knowledge of scan results.

Scans were graded, by three nuclear medicine specialists into 3 categories and blindly assessed with 10 other scans, 5 proven normal; 5 proven sternal osteomyelitis.

Clinical assessment suggested no patients with high probability, 2 with medium and 25 clinically uninfected. At six months, no patient showed evidence of disease. One scan was interpreted as being high probability giving a specificity and negative predictive value of 96%. Interobserver reading was concordant in 90% and in only 2 readings (2%) did assessment differ by 2 grades.

Additionally, 6 patients with clinical sternal osteomyelitis had scans blindly but retrospectively analysed; 5 were positive, giving a sensitivity and positive predictive value of 83%

Gallium scanning in the early postoperative phase appears to be useful in detecting/excluding osteomyelitis.

TYPE SPECIFIC RADIOIMMUNOIMAGING OF EXPERIMENTAL TYPE-B HEMOPHILUS INFLUENZAE OSTEOMYELITIS. G.N. Sfakianakis and P. Scoles. University of Miami, Florida and Case Western Reserve University, Cleveland, Ohio.

In rabbits experimental osteomyelitis of the proximal metaphysis of the tibia was induced by a percutaneous injection of 0.1 ml concentrated culture of hemophilus influenzae (type B) and 0.1 ml 5% sodium morrhuate, an irritant facilitating the infectious process. The other

tibia served as control injected with the irritant alone. Osteomyelitis was developed in 8 out of the 10 rabbits injected, as indicated by Tc-99m-diphosphonate scintigraphy and documented at sacrifice later.

Rabbit produced type-specific antihemophilus antibody was separated from the serum by salt precipitation and labeled with I-131 by the lactoperoxidase method. The animals were injected intravenously with 150 μCi of the I-131 antibody and 3 days later with 500 μCi of Tc-99m-human-serum-albumin (HSA) for blood pool imaging. Scintigraphy was performed sequentially and without moving the animal on the 364 and 140 keV peaks of the radioisotopes with computer acquisition of the data.

The scintigrams showed increased radioantibody activity in the osteomyelitic foci. After subtraction of the blood pool activity (140 keV Tc-99m-HSA images) from the radioantibody activity (364 keV I-131 antibody images) the infected lesions were enhanced whereas the activity of the control sides disappeared.

At autopsy pus was found only within the metaphysis of the infected sites, which produced the positive radioantibody images.

The results of this experiment indicate the feasibility of studying bone infection with organism specific radioantibody.

3:30-5:00 **Room 120**

ENDOCRINE II: THYROID

Moderator: Harry R. Maxon, III, M.D.
Co-moderator: I. Ross McDougall, M.D.

THYROID FUNCTION IN HEMODIALYSIS PATIENTS. R.B. Shafer, A. Mooradian, J.E. Morley, K.W. Ma and W. Korchik. VA Medical Center, Minneapolis, MN.

Chronic hemodialysis has been reported as a cause of hypothyroxinemia (T4) and elevated thyrotrophin (TSH). Iodine deficiency due to abnormal uptake (trapping or organification) or loss of iodine during dialysis has been proposed to explain this chemical hypothyroidism. To identify a potential defect in trapping or organification, we performed perchlorate discharge tests in 8 chronic dialysis patients. In addition, salivary/plasma ratios of I-131 were measured to demonstrate any defect in iodine absorption. Thyroid function (T4, T3, T3U and TSH) was quantitated in an additional 29 hemodialysis patients. Our results confirm the previously described low T4 (5.8± .4 vs 8.6±.3 μg%) and low T3 (84±.9 vs 124±5 μg%). An inverse correlation between serum T4 and chronicity of hemodialysis was found ($p < 0.05$). TSH levels were not significantly different. There was a decrease in 60' uptake of I-131 in dialysis patients (2.8±.4 vs 3.6±.4%). Following perchlorate there was a continued uptake of I-131 in dialysis patients unlike normal controls (0.6±.14 vs 0.06±.04% $p < 0.05$). Salivary/plasma ratios were increased in dialysis patients (70±10 vs 42±4:1 $p < 0.025$). We conclude that there is abnormal iodine trapping by the thyroid in dialysis patients. This defect appears to be specific for the thyroid gland and does not involve salivary glands. This defect is not related to iodine absorption. In addition, we confirm that multiple alterations in the pituitary/thyroid axis occur in hemodialysis patients. The low T4 and T3 levels may be due to diminished binding to TBG, altered peripheral deiodination of T4 or intrinsic impairment of T4 release by the thyroid gland.

SERUM 3,3'-DIIODOTHYRONINE(3,3'-T2), 3',5'-T2 AND 3,5-T2 LEVELS IN NORMAL AND ALTERED THYROID STATES. M.Nishikawa, M.Inada, K.Naito, H.Ishii, K.Tanaka, Y.Mashio and H.Imura. Kansai Medical Univ., Osaka and Kyoto Univ., Kyoto, JAPAN.

To investigate the effects of aging and thyroid function state on T4 metabolism, six kinds of iodothyronine (T4, T3, rT3, 3,3'-diiodothyronine(3,3'-T2), 3',5'-T2 and 3,5-T2) concentrations in serum were determined by specific radioimmunoassays(RIAs) in normal controls and in hyper- and hypothyroid patients. RIAs for 3,3'-T2, 3',5'-T2 and 3,5-T2 were originally developed in our laboratory. Each antiserum was prepared by immunizing rabbits with the protein conjugate of each T2. [I-125]3,3'-T2, [I-125]3',5'-T2 and [I-125] 3,5-T2 were prepared from 3-T1, 3'-T1 and monoiodotyrosine, respectively. They were specific, sensitive and reproducible enough to measure serum T2s.

In 81 normal subjects, although no significant correlation existed between T4 levels and age, serum T3, 3,3'-T2, 3',5'-T2 and 3,5-T2 values had significant inverse correlation with age, the correlation coefficients being -0.28, -0.38, -0.58 and -0.47, respectively. Serum levels of 3,3'-T2 and 3',5'-T2 in hyper- and hypothyroid patients before and during methimazole or T4 treatment well reflect the thyroid function states. Serum 3,5-T2 levels, however, did not show the significant changes in altered thyroid function states. Serum 3,5-T2, as well as 3,3'-T2 levels rose significantly with a marked rise of serum T3 following T3 administration, 75μg/day for 7 days.

These data indicate that sequential monodeiodinating activities in T4 metabolism decrease with increasing age, and that serum levels of 3,5-T2, unlike 3,3'-T2 and 3',5'-T2 do not well reflect the thyroid function state, although it is monodeiodinated from T3 in vivo.

COMPETITION FOR PROTEIN BINDING RAISES FREE TRIIODOTHYRONINE LEVELS IN PATIENTS UNDER THYROXINE MEDICATION. R. Schmitz, L.-A. Hotze, H. Bongers, K. Joseph. University of Marburg, Marburg, FRG

In order to clear the function of FT3 in suppressive thyroxine treatment T4, FT4, T3 and FT3 were determined in the serum of 35 eumetabolic patients with endemic goiter before and after a 14 day period of oral medication with 200 μg/die LT4. Apart from a significant increase in the total and free thyroxine there was only a slight increase in the total T3 concentration from 143± 26 ng/dl to 158±29 ng/dl ($p < 0.01$).

In contrast to this there is a clear increase of FT3 from 497±73 pg/dl to 809±171 pg/dl (normal range from 280 to 560 pg/dl, $p < 0.0001$).

To resolve these findings a protein binding analysis was conducted as a model calculation following the method suggested by Princé and Ramsden (1). The computer model shows that the percentage of T3 combined with TBG is reduced from 79.60% to 70.53% and is not completely compensated by the binding on TBPA (9.38 to 13.55%) and on albumine (10.72 to 15.49%). There is a release of an additional 0.13% of total T3, which means an increase in free T3 by 59%. Compared with the increase in total T3, the FT3 increases 5.8 times more in the calculation model and 6.3 times more in the experiment.

It is concluded, that FT3 gives a clear contribution to the suppressive effect of thyroxine medication.

1. H.P. Princé and D.B. Ramsden, Clin. Endocrinol. 7: 307-324, 1979

PRIMARY HYPOTHYROIDISM CAUSED BY TSH-RECEPTOR ANTIBODIES: DIAGNOSIS BY THYROID UPTAKE AND RADIORECEPTOR ASSAY OF TSH. K. Endo, J. Konishi, Y. Iida, K. Kasagi, T. Misaki, T. Nakajima, and K. Torizuka. Kyoto University Medical School, Kyoto, Japan.

It is generally agreed that hyperthyroidism in Graves' disease is caused by thyroid-stimulating IgG. These IgG are thought to be antibodies (Ab) against TSH receptors and are detectable by using the radioreceptor assay of TSH. Previous reports from our laboratory revealed that TSH-receptor Ab were detectable not only in Graves' patients but also in some untreated hypothyroid patients (N.Eng.J.Med. 303:738,1980). Up to now 6 hypothyroid patients were found to have TSH-receptor Ab. These patients have common clinical and laboratory characteristics; 1) primary hypothyroidism developing at ages ranging from 15 to 38, 2) no palpable goiter, and 3) very low or no Tc-99m pertechnetate and/or I-131 thyroidal uptake. These are findings compatible with so called primary myxedema.

In the radioreceptor assay of TSH, serum IgG fraction from these 6 hypothyroid patients almost completely inhibited the binding of I-125-labelled TSH to the human thyroid membranes. These Ab had no thyroid-stimulating activity

and caused inhibition of the thyroid-stimulation induced by TSH, both in vitro and in vivo. Further transient hypothyroidism was noted in 3 babies born from 2 of these patients due to the transplacental passage of TSH-receptor Ab. The etiology of primary myxedema is still unknown, however, a small part of primary myxedema (approximately 10%) would be caused by the presence of the blocking type of TSH-receptor Ab. Therefore, in primary hypothyroid patients with no palpable goiter, both thyroid uptake studies and measurement of TSH-receptor Ab, using the radioreceptor assay of TSH, should be performed.

ACCUMULATION OF Tc(V)-99m DIMERCAPTOSUCCINIC ACID IN THE MEDULLARY THYROID CARCINOMA. K. Endo, H. Ohta, D. Hamanaka, A. Shimazu, K. Ikekubo, K. Makimoto, Y. Iida, J. Konishi, R. Morita, N. Hata, A. Yokoyama, and K. Torizuka. Kyoto University, Faculty of Medicine and Pharmaceutical Sciences, Kyoto, Japan.

We have previously reported that Tc(V)-99m dimercaptosuccinic acid (Tc-DMS), which was labelled under optimal pH 8 and very low $SnCl_2$ concentrations, had different characteristics from that used for the renal scanning agent. An equilibrium betweem a stable form and a dissociated form of anion TcO_4^{3-}, structually analogous to PO_4^{3-}, was postulated from in vitro and in vivo studies. Structual similarity of Tc-DMS with PO_4^{3-} led us to the scintigraphic studies in patients with medullary thyroid carcinoma (MTC), which were known to secret calcitonin and, in some cases, accumulate Tc-99m phosphate compounds and Tl-201.

Studies were performed in 3 patients with MTC and high calcitonin values. All patients showed intense accumulation of Tc-DMS in the tumors of MTC and its cervical or lung metastatic sites and, in one postoperative case, Tc-DMS clearly revealed nonpalpable residual tumors. On the other hand, no significant accumulation was observed in other thyroid malignancies, including 10 patients with papillary - and follicular adenocarcinoma, one patient with undifferentiated carcinoma and one patient with thyroid lymphoma. More than 80% of Tc-DMS in the blood was bound to plasma protein and neither was there any significant uptake in the normal thyroid glands, salivary glands, stomach or bone of adults. Images were better than those obtained by using Tl-201. Although the exact mechanism of Tc-DMS accumulation in MTC remains to be elucidated, these data indicated that Tc-DMS scintigraphy would be useful in the diagnosis and follow up of MTC.

"IMAGING" OF INSULIN INTERACTION WITH ITS RECEPTORS IN NORMAL RATS AND HUMANS. F. Sodoyez-Goffaux, J.C. Sodoyez, S. Treves, and C.R. Kahn. Depts of Pediatrics and Int. Med., Liege, Belgium, Children's Hospital Medical Center and Joslin Diabetes Center, Boston, Mass.

In order to investigate the metabolic fate of circulating insulin, the biodistribution and kinetics of ^{123}I-labeled hormone was studied in experimental animals and normal humans. Insulin was labeled with carrier-free Na ^{123}I and ^{123}I Tyr A14-Insulin (^{123}I-Ins) rapidly purified by reverse phase HPLC and sterilized by ultrafiltration. ^{123}I-Ins (50 µCi) was IV injected to anesthetized rats lying on the collimator of a γ camera. Frames were recorded at a rate of 1 per 5 sec for the lst 5 min and 1 per 30 sec for the next 25 min. At the end of the experiment, the rats were sacrificed, actual radioactivity of selected organs was measured and used to calibrate the time-activity curves of regions of interest over the liver and kidneys. After ^{123}I-Ins alone, the hormone was concentrated by the liver and the kidneys (respectively 30 and 15 % of injected dose at 3 min). Past this maximum, radioactivity rapidly decreased in both organs as bound ^{123}I-Ins was degraded and free $^{123}I^-$ was released into the plasma. Injection of an excess of unlabeled insulin or of antiinsulin receptor serum blocked the uptake of ^{123}I-Ins by the liver and conversely enhanced that by the kidneys. In man, the biodistribution and kinetics of ^{123}I-Ins (1 to 2 mCi) was very similar to that observed in control rats. It is concluded that liver binding of ^{123}I-Ins is rapid, quantitatively important, saturable and mediated by insulin receptors whereas kidney uptake of insulin is non saturable. In both organs the half life of ^{123}I-Ins is very short. In view of ^{123}I low radiotoxicity, this procedure might be employed to investigate disorders of insulin metabolism in man.

3:30–5:00 **Room 275**

COMPUTERS III: DIGITAL PROCESSING

Moderator: A. Bertrand Brill, M.D., Ph.D.
Co-moderator: Bruce R. Line, M.D.

EFFECT OF TEXTURE ON DETECTABILITY OF ABNORMALITIES IN MEDICAL IMAGING. K.J.Voss, H.H.Barrett, M.C.Borgstrom, D.D.Patton, G.W.Seeley. Optical Sciences Center, University of Arizona, Tucson, AZ.

Imaging modalities in nuclear medicine are often characterized by the signal-to-noise ratio obtained in the resulting images. However, different imaging systems may yield images with equal mean and variance but different correlation properties. For example, the post-processing filter in a pinhole imaging system is generally a low-pass filter, whereas ECT images are processed by a high-pass filter. The difference in filter characteristics produces images with different second order statistics, or correlation properties, which is perceived as different textures by the human eye. We have simulated images by computer with equal mean and variance but different correlation properties to isolate the effect of texture on an observer's ability to detect abnormalities in a medical image. Two separate imaging systems were modeled, one with a high-pass filter and one with a low-pass filter. Each system had the same overall point spread function. The images were shown to ten observers, who rated their level of certainty as to whether a disk object was present in the image on a standard six-point scale. ROC curves were generated from the observer data. We conclude from the data that an observer's ability to detect abnormalities is significantly higher when the texture is low-pass rather than high-pass in nature. This is a clear indication that signal-to-noise ratio alone is an inadequate measure of image quality when images of different texture type are involved.

COMPARISION OF INTERPOLATING METHODS FOR IMAGE RESAMPLING. J.A. Parker, R.V. Kenyon, Beth Israel Hospital and Massachusetts Institute of Technology, Boston, MA.

When resampling an image to a new set of coordinates (for example when rotating an image), there is often a noticable loss in image quality. The interpolating function used for the resampling should be an ideal low pass filter. To determine which limited extent convolving functions would provide the best interpolation, 5 functions were compared--A. nearest neighbor, B. bilinear interpolation, C. cubic convolution, D. cubic spline (a=-.5), and E. cubic spline with edge enhancement (a=-1). The functions which extend over 4 pixels (C,D,E) were shown to have a better frequency response than those which extend over 1 (A) or 2 (B) pixels. The nearest neighbor function shifted the image up to 1/2 a pixel. Bilinear interpolation and cubic convolution tended to smooth the image. The best response was obtained from the cubic spline functions.

$$(a+2)x^3-(a+3)x^2+1 \qquad (0,1)$$

$$ax^3-5ax^2+8ax-4a \qquad (1,2)$$

For any resampled point, the sum of the four values of this function corresponding to the initial coordinate points is 1. The location of the resampled points with respect to the initial coordinate system has a dramatic effect on the response of the sampled interpolating function--the data is exactly reproduced when the points are aligned, and the response has the most smoothing when the resampled points are equidistant from the original coordinate points. Thus, at the expense of some increase in computing time, image quality can be improved by resampled using the cubic spline interpolation as compared to the nearest neighbor, bilinear, or cubic convolution.

RAPID DIGITAL FILTERING. T.R. Miller, K.S. Sampathkumaran, and M.A. King. Mallinckrodt Institute of Radiology, St. Louis, MO and University of Massachusetts, Worcester, MA.

Small digital filters are widely used in nuclear medicine. Larger filters can be designed with special properties tailored to

match the characteristics of the imaging equipment or to enhance certain features of the image. Here, rapid methods of digital filtering are evaluated to determine if large filters can be applied quickly to images, thus making practical their routine use in the clinical setting.

A 64x64- pixel image was filtered in the spatial domain using a convolution mask (FIR filter) and in the frequency domain using the fast Fourier transform (FFT). For FIR filtering, the standard, direct convolution (DIRECT) is compared to a recently published method using the Chebyshev recursion relation (CHEBY) in which a 3x3 mask is passed repeatedly over the image. All filtering was performed on a 16-bit minicomputer, while the DIRECT and FFT algorithms were also computed on an array processor (AP). The computation time in seconds, excluding disk I/O, is shown for FIR filtering with masks of size 3x3 to 23x23 and for FFT filtering.

	3x3	13x13	23x23		FFT
DIRECT	3.7	35	71	NO AP	34
CHEBY	1.4	5.9	9.3	AP	0.12
AP	0.19	0.36	0.54		

These results demonstrate the dramatic reduction in processing time achievable, even without an array processor, using the new Chebyshev algorithm. Thus, the larger, and potentially most valuable, digital filters can be computed rapidly on conventional minicomputers, thereby making feasible their routine clinical use.

DIGITAL METHODS FOR CHANGE DETECTION IN SCINTIGRAPHIC IMAGES. A. Venot, J.F. Lebruchec, J.L. Golmard, and J.C. Roucayrol. Hopital Cochin and INSERM U194, Paris, France.

The purpose of this paper is to present original methods for the computerized comparison of two scintigraphic images of an organ explored under varying conditions (time phased studies, different tracers, various physiological or pharmacological stimulations..).

The alignment and normalisation of the images were first considered. Both problems were solved simultaneously by maximising iteratively a similarity criterion R with respect to the alignment and normalisation parameters. R was the number of sign changes in a window area of the subtraction image scanned line by line. This method was successfully applied to radioactive phantom and patient images (lungs, liver, heart). It appeared to be highly insensitive to structural modifications in the images and provided better results than the correlation techniques.

Secondly, in order to compare the registered images point by point, a maximum likelihood ratio test was devised (assuming a Poisson distribution for the count fluctuations in each pixel). Using this test at various significance levels as a decision rule, images of the positive and negative changes were generated.

Studies on phantom and patient images in controlled conditions, demonstrated that this procedure made possible the detection of changes which could not be recognized from a visual inspection either of the two initial images or of the classical subtraction image. These methods have lead to the development of a software which can be proposed for routine use in a nuclear medicine department if the data processing system is linked to an array processor.

A COMPREHENSIVE METHOD FOR FAST QUANTIATIVE ANALYSIS OF GAMMA CAMERAS DISTORTIONS AND THEIR CORRECTIONS. Y. Bizais, R.W. Rowe, I.G. Zubal, G.W. Bennett, and A.B. Brill. Brookhaven National Laboratory, Upton, NY.

A flood field is imaged through a multihole plate as an array of about 500 PSF located on a distorted square grid. Location of each PSF depends both on gamma camera global tunings (centering and gains) and on local distortions. The optimal set of global tuning parameters is given by a 2D least-squares fit. The distance between the measured location and the non distorted location derived from the optimal parameter set defines a distortion vector in each PSF. This corresponds to the more compact sampling allowed by the detector resolution because of the multihole plate design. Maps of displacement along axes and of distorted pixel areas are obtained from the distortion vector set through a 2D spline interpolation, and can include a registration step (standardization of global tuning parameters). When photon energy can be digitized, energy distortion is characterized by the centroid and the width of the photopeak in each pixel.

The related correction procedure involves two successive steps: a pointwise multiplication of the image to be corrected by the distorted pixel area matrix, followed by a non linearity distortion correction using displacement maps. This approach avoids the generation of artifacts likely to occur because sampling paths in the distorted and corrected images are approximately equal.

Improvements of image quality in terms of field uniformity and ability to use asymetric energy windows are exemplified, and are equivalent to or better than can be achieved with hardware correctors used in new cameras.

OPTIMAL MYOCARDIAL SPECT IMAGING PARAMETERS. U. Raff, V.M. Spitzer, W.C. Klingensmith and W.R. Hendee, U. of Colorado Health Sciences Center, Denver, CO 80262

Three papers concerned with specific aspects of 180^0 vs 360^0 SPECT data collection have recently been published. A teaching editorial (JNM 1982; 23:655) emphasizes the need for further investigation in this area for optimun clinical usefulness. Other data collection parameters for SPECT imaging are equally controversial. A phantom was loaded to produce a 3:1 viable myocardium to background ratio for a planar view. The infarct area (90^0 or 45) was loaded with a radioisotope concentration equal to 50% of the viable myocardium. Additional 4^0 lesions with no activity are also present as chamber separations. Three collection parameters have been investigated: 1) The reconstruction starting angle relative to an asymmetric lesion for 180^0 data collection, 2) 180^0 vs 360^0 data collection for both Tl-201 and Tc-99m statistics and 3) 64x64 vs 128x128 matrix resolution data collection. Quantification of the reconstructed data was obtained from a "circle" analysis. 360^0 variation in the reconstruction starting angle relative to the lesion produces variations in the 180^0 reconstruction slice lesion depth of + 18%. Imaging statistics similar to clinical Tl-201 studies were utilized. The 360^0 reconstructed lesion depth of the same data was 15% less than the deepest lesion (50%) reconstruction from the starting angle data above. The choice of matrix size for data collection have been demonstrated to be clearly in favor of 64x64 matrices (6mm pixels) for the low count statistics of Tl-201. 128x128 data collection has introduced statistical variations larger than the depth of the smallest phantom lesion. For imaging situations with much higher count rates (x10) the situation is reversed.

FRIDAY, JUNE 10, 1983

10:30–12:00 **Room 123**

CARDIOVASCULAR CLINICAL IX: ACUTE MYOCARDIAL INFARCTION

Moderator: Samuel E. Lewis, M.D.
Co-moderator: Sherman Sorenson, M.D.

DETAILED ASSESSMENT OF REGIONAL WALL MOTION IN ACUTE TRANSMURAL MYOCARDIAL INFARCTION: FREQUENT SPONTANEOUS IMPROVEMENT AND DISCORDANCE FROM GLOBAL LEFT VENTRICULAR FUNCTION. Jay L. Meizlish, Barry L. Zaret, Michael Plankey, Harvey J. Berger. Yale University, New Haven, CT.

Regional wall motion (RWM) and left ventricular ejection fraction (LVEF) were assessed in 53 patients (pts) with initial acute transmural myocardial infarction (MI) using 4-view high resolution multigated cardiac blood pool imaging within 24-48 hours of chest pain (#1) and prior to hospital discharge (#2). By ECG, 24 pts had anterior (A) MI, and 29 inferior (I) MI. All pts received routine coronary care unit (CCU) management. The LV was divided into 11 segments, and each was scored by 2 blinded observers on a 5-point scale from dyskinetic (dys,-1) to normal (nl,+3). Total LV score (nl=33) correlated well with LVEF (r=0.83). All pts had ≥ 1 abnl LV segment at study #1. Improvement was defined as normalization of an

abnl segment or any improvement in a dys or akinetic segment. Of 215 abnl segments identified on study #1, 82 (38%) improved spontaneously at study #2, 105 (49%) remained unchanged, while only 28 (13%) worsened. Furthermore, RWM improved in 18 pts (33%), only 11 of whom also improved LVEF significantly. Similarly, RWM was unchanged in 26 pts (49%), 13 of whom had significant changes in LVEF. In total, there was major discordance between changes in RWM and changes in LVEF in 49% of pts (26/53).

Thus, RWM improves frequently following acute MI in the absence of major therapy to limit MI size. This must be considered in the design and interpretation of therapeutic intervention trials. The discordance between changes in global and regional LV function justify the need for detailed assessment of RWM in acute MI.

CRITICAL IMPORTANCE OF LEFT LATERAL AND LEFT POSTERIOR OBLIQUE VIEWS FOR EVALUATING REGIONAL WALL MOTION WITH MULTIGATED CARDIAC BLOOD POOL IMAGING IN ACUTE MYOCARDIAL INFARCTION. Jay L Meizlish, Michael Plankey, William Levy, Barry L Zaret, Harvey J Berger. Yale University, New Haven, CT.

While accurate radionuclide assessment of regional wall motion (RWM) in myocardial infarction (MI) requires characterization of the inferior (I) and posterior (P) regions of the left ventricle (LV), these segments are imaged poorly on routine 2-view gated equilibrium studies (anterior (A) and L anterior oblique (LAO)). Therefore, RWM was assessed using 4-view high resolution bedside multigated cardiac blood pool imaging at 24-48 hrs after chest pain in 54 consecutive patients (pts) with initial transmural MI. Left lateral (LL) and L posterior oblique (LPO) views were obtained in the decubitus position. The LV was divided into 11 segments (5 A, 4 I, and 2 apical (Ap)), and each was scored by 2 blinded observers on a 5-point scale from dyskinetic (dys,-1) to normal (nl,+3). By ECG, 26 pts had IMI and 28 AMI. 22/26 IMI pts had abnl posterobasal (PB) RWM on the LL and/or LPO; 11 of these pts also had additional abnl I segments. The A view was nondiagnostic in 22/26 IMI pts, with the I segments obscured in 10/26 pts and nl in the remaining 12 pts. The LAO was abnl only in 6/26 IMI pts. If only the routine 2-views had been obtained, RWM would have been judged incorrectly as nl in 48% of IMI pts and abnl only in 24%. In contrast, the lateral views correlated closely with ECG findings of IMI, as well as providing complimentary data on the anterior wall and apex.

Thus, the LL and LPO views are essential for accurate evaluation of RWM in acute IMI and demonstrate the consistent involvement of the PB segment.

RIGHT BUNDLE BRANCH BLOCK IN ACUTE TRANSMURAL ANTERIOR MYOCARDIAL INFARCTION: RELATIONSHIP OF PROGNOSIS TO DEGREE OF VENTRICULAR DYSFUNCTION. S Reisman, PK Shah, FG Shellock, D Berman, HJC Swan, Cedars-Sinai Med Ctr, Los Angeles, CA

Although right bundle branch block (RBBB) is associated with an ominous prognosis in acute anterior myocardial infarction (MI), whether this risk is due to the conduction abnormality or the underlying degree of ventricular dysfunction has not been evaluated. Thus we assessed the results of equilibrium radionuclide ventriculography (RNV) performed within 20±17 hrs of onset of symptoms in 54 patients with first anterior MI, including 17 patients with (GrA), and 37 without (Gr B) RBBB. All patients were followed-up for 1 year. Results are shown below:

			%	Mortality		
	LVEF	RVEF	AKS	Overall	LVEF<.30	LVEF>.30
Gr A	.25±.10	.36±.12	55%	47% (8/17)	57% (8/14)	0% (0/3)
	p<.01	p=.02		p=.005	p=NS	p=NS
Gr B	.37±.11	.44±.09	39%	11% (4/37)	36% (4/11)	0% (0/26)

(EF=ejection fraction, LV=left ventricular, RV=right ventricular, AKS=akinetic/dyskinetic LV segments). These results confirm the presence of greater LV and RV dysfunction in pts with anterior MI and RBBB and the associated high mortality. However, when severe LV dysfunction (LVEF≤0.30) is considered, the mortality is high regardless of the presence or absence of RBBB. Thus, we conclude that 1) the high mortality in pts with anterior MI and RBBB is attributable to greater prevalence of severe LV dysfunction and not to RBBB per se, and 2) radionuclide ventriculography is a useful technique for defining high and low-risk subgroups of these patients.

INCIDENCE, SEVERITY, AND CLINICAL COURSE OF RIGHT VENTRICULAR INVOLVEMENT AFTER INFERIOR MYOCARDIAL INFARCTION; ASSESSMENT BY SEQUENTIAL ^{99m}Tc-PYROPHOSPHATE SCANS AND GATED BLOOD POOL SCANS. T. Nishimura, T. Yasuda, H.K. Gold, R.C. Leinbach, C.A. Boucher, K.A. McKusick, H.W. Strauss. Massachusetts General Hospital, Boston, MA.

To evaluate incidence, severity, and clinical course of right ventricular (RV) involvement after acute inferior myocardial infarction, 78 patients (pts) with IMI were investigated by ^{99m}Tc-pyrophosphate scan (PYP scan) and gated blood pool scan (GBPS). GBPS was performed at admission (<18hr) and at 10 days whereas PYP scan was performed at 3 days to 6 days. RV uptake of ^{99m}Tc-PYP was demonstrated in 25 (32%) pts on initial PYP scan and remaining 53 did not. RV akinesis or severe hypokinesis by GBPS was observed in 39 (50%) pts on the acute scan; 25 pts (group A) had positive RV uptake of PYP and 14 pts (group B) of no RV uptake. In remaining 39 pts, 10 pts (group C) showed mild RV hypokinesis and 29 pts (group D) showed normal RV wall motion. The results of serial measurements of RVEF in each group were shown as follows. (Data=Mean±SD, AD=admission, D10=10 days, SH=shock/hypotension, D=death during hospital course)

Group	n	AD	RVEF(%) D10	SH	D
A	25	30.8±12.3	40.9±6.7	9	1
B	14	35.6±8.2	45.4±10.5	5	0
C	10	42.8±7.6	48.4±11.6	0	0
D	29	48.0±10.5	52.7±10.8	0	0

The RVEF improved nearly 10 points at 10 days in group A and B, however, the recovery of RV function was much less in group A. In group A and B, 14 pts of 39 who had developed shock/hypotension improved strikingly after volume-loading except 1 death in group A during hospital course.

Our data demonstrated; 1) many patients with RV dysfunction in IMI do not have necrosis; 2) those with RV (+) PYP and depressed RV function have less recovery of function than those with RV(-)PYP; 3) the combination of PYP scan and GBPS offers prognostic information in IMI with RV dysfunction.

HIGH RISK SUBGROUP OF INFERIOR MYOCARDIAL INFARCTION: IMPORTANCE OF ANTERIOR WALL MOTION AND RIGHT VENTRICULAR FUNCTION. T. Nishimura, T. Yasuda, H.K. Gold, R.C. Leinbach, K.A. McKusick, H.W. Strauss. Massachusetts General Hospital, Boston, MA.

To identify high risk subgroups in inferior myocardial infarction (IMI), 75 patients with IMI were investigated by sequential gated blood pool scan (GBPS). The patients (pts) were divided into 4 groups on the presence of RV dysfunction (RVD) and abnormal anterior wall motion (AAW) of the left ventricle by GBPS at admission (AD). Repeated GBPS was also performed at 10 days (D10). Thirty eight pts also had cardiac catheterization before discharge and all pts were followed up for one year to determine their clinical outcomes. The results of serial measurements of LVEF(%) and RVEF(%), LAD involvements, and one-year mortality in each group were shown as follows (Data: Mean±SD, LAD-S:>75% LAD stenosis by angiogram, *p<0.01):

GROUP		AD	D10	LAD-S	Death
A (n=27)	LVEF	45.5± 9.6	46.3±10.4	13/17	5/27
RVD,AAW	RVEF	*34.0± 8.3	*42.6± 9.8		
B (n=19)	LVEF	59.8± 8.0	61.9±12.6	4/8	0/19
RVD	RVEF	*31.1± 9.9	*45.9± 9.8		
C (n=11)	LVEF	45.4±15.4	46.3±15.0	5/6	1/11
AAW	RVEF	48.2± 3.3	53.0± 7.4		
D (n=18)	LVEF	61.0± 9.0	60.0±15.0	2/7	0/18
	RVEF	52.1±10.7	55.1±13.7		

These data clearly identify Group A as a high risk group compared to other groups because of lower biventricular function, high incidence of LAD stenosis, in addition to RCA disease, highest mean CPK (762, 519, 540, 314 in A, B, C, D) and high mortality. In conclusion, IMI associated with RVD and AAW predicts severe coronary artery disease and poor biventricular function, therefore, this group should be identified at AD and if necessary, coronary angiogram may be indicated to investigate coronary anatomy which significantly alter the patient prognosis and appropriate treatment would be indicated.

THE PATTERN OF MYOCARDIAL PERFUSION AT REST IN PATIENTS WITH UNSTABLE ANGINA PECTORIS. A.S. Iskandrian and A.H. Hakki. Hahnemann University, Philadelphia, PA.

The purpose of this study was to examine the rest thallium-201 perfusion pattern during the angina-free periods in patients (pts) with unstable angina pectoris. None of the 40 pts studied evolved acute infarction by enzymes or electrocardiograms, but 17 pts had had Q wave in 1 or more locations >6 months before the study. One vessel disease (≥70% diameter narrowing) was present in 8,

and multivessel disease in 32 pts. The perfusion defects (PD) were considered fixed or reversible, depending on the absence or presence of redistribution in the 4-hour delayed images. There were 40 PD (26 fixed and 14 reversible) in 27 pts whereas 13 pts had normal scans. Reversible PD were present in 10 pts (25%). Of the 26 fixed PD, 17 did not have corresponding Q waves. The PD were more frequent in the distribution of diseased left anterior descending (18 of 34; 53%) and right coronary arteries (16 of 28; 57%) than the left circumflex artery (6 of 26; 21%)(P<0.02). Occluded vessels (29 of 46; 63%) had more PD than vessels with subtotal occlusion (13 of 44; 30%)(P<0.01). The PD size measured by perimetery was larger in pts with ejection fraction <30% than in pts with higher ejection fraction (P=0.0006).

We conclude: 1) rest PD are common in pts with unstable angina pectoris even during the angina-free periods; 2) the PD are reversible in 25% of the pts indicating that at least in these pts, the regional coronary blood flow is reduced at rest; 3) the degree and site of stenosis affect the presence of PD; 4) fixed defects may be present even in the absence of corresponding Q waves; and 5) the global left ventricular function is related to the size of the PD.

10:30–12:00 **Room 120**

NEUROLOGY IV: MISCELLANEOUS

Moderator: John Mazziotta, M.D., Ph.D.
Co-moderator: Stephen C. Jones, Ph.D.

DIRECT EVALUATION OF THE INTERRELATIONSHIPS OF LOCAL CEREBRAL BLOOD FLOW (LCBF), GLUCOSE METABOLISM (LCRGM), AND PROTEIN SYNTHESIS (LCRPS) USING SIMULTANEOUS MULTIPLE RADIONUCLIDE AUTORADIOGRAPHY (SMRA). *J.L. Lear, R.A. Ackermann, M. Kameyama, R. Carson, S.C. Huang, D.E. Kuhl, and M.E. Phelps. *Stanford University/VA Medical Center, Palo Alto,CA, and UCLA Medical Center, LA, CA.

Using double radionuclide autoradiography, we directly explored the coupling of LCBF and LCRGM in normal rats and rats with pathological conditions simulating human cerebral disease using I-123-isopropyliodoamphetamine (IMP) and F-18-fluorodeoxyglucose (FDG). Decoupling of LCBF and LCRGM was found consistently in rats undergoing seizures or following chronic cortical lesioning. The hippocampos proved most vulnerable to flow-metabolism imbalance where markedly low (less than ¼ normal) LCBF/LCRGM ratios occurred. This imbalance may be a cause of progressive injury, such as mesio-temporal sclerosis, seen in human epilepsy.

Surprisingly, and in contradiction to previous reports, significant deviations (>50%) from normal LCBF/LCRGM ratios were found in several areas in normal animals. Triple radionuclide autoradiography with FDG, IMP, and C-14-leucine was developed and used for further investigation. The higher than normal LCBF/LCRGM ratios were found in structures with very high rates of LCRPS such as cell body lines. It is possible that increased LCBF is necessary to deliver substrates for protein synthesis.

SMRA allows rapid, quantitative assessment of interrelationships of various parameters of cerebral function with high spacial detail. It greatly expands basic animal autoradiographic studies, and thus can be used to plan protocol and pharmaceutical selection in human emission tomographic studies.

FUNCTIONAL RESPONSE OF THE HUMAN BRAIN TO INDIVIDUAL AND COMBINED VISUAL AND AUDITORY INPUTS. M.E. Phelps, J.C. Mazziotta, E. Halgren, S.C. Huang, R. Carson, J. Bayer. UCLA School of Medicine, Los Angeles, CA

Previously we used a lower resolution positron CT (ECAT II) with F-18 fluorodeoxyglucose (FDG) to examine cerebral metabolic responses to visual and auditory inputs. Results demonstrated 1) increasing metabolic activity of visual cortex to increasing visual scene complexity, 2) 50% crossing of visual system and 3) hemispheric specialization to auditory language/musical inputs. In the present studies we used high resolution (NeuroECAT) FDG and $H_2{}^{15}O$ cerebral blood flow (CBF) studies to examine selective cortical responses to a) visual stimuli, binocular full field, non verbal, N=5; binocular central field (< 2°), verbal, N=3; ears plugged, b) auditory stimuli, verbal, N=3 and eyes patched, and c) triple studies (N=3) using identical word lists with 1) central visual field (< 2°), ears plugged, 2) auditory, eyes patched, and 3) simultaneous audiovisual presentations. Results show modality specific activations of primary cortical receptive zones. Transverse temporal cortex increased LCMRGlc during both auditory (21.7±11.2%) and audiovisual (30.0±18.3%) stimulation. Similarly, visual cortex activations of 41.0±13.1% and 50.5±6.4% occurred during visual and audiovisual stimulation, respectively. Full visual field activated entire visual cortex whereas central field stimulation activated only occipital poles (macula), both for LCMRGlc and CBF. Studies demonstrate 1) selective tomographic mapping of visual and auditory cortex to selective input, 2) increased magnitude of response and submit cortical delineation with higher spatial resolution, 3) combined audiovisual input produced an anatomical cortical response equal to sum of individual inputs but magnitude of activation when inputs were combined (i.e. increases in LCMRGlc of the auditory cortex were larger from audiovisual stim than auditory alone. True also for visual system).

ALTERNATIVE APPROACH TO SINGLE-SCAN DETERMINATION OF CEREBRAL GLUCOSE METABOLIC RATE USING 2-FLUORODEOXYGLUCOSE (2-FDG) WITH PARTICULAR APPLICATION TO ISCHEMIA. G.D. Hutchins, J.E. Holden, R.A. Koeppe, J.R. Halama, S.J. Gatley, and R.J. Nickles, Dept. of Medical Physics, University of Wisconsin, Madison, WI 53706.

In the 2-FDG method, time courses of tissue and plasma radioactivity are measured, and analyzed in terms of first order exchange of label between plasma 2-FDG, tissue 2-FDG, and tissue 2-FDG-6-phosphate. The rate of phosphorylation is calculated from a simple combination of the fitted rate constants. Because the measurement of the rate constants requires many hours of dynamic data acquisition, estimations of the rate from a single scan have been developed (1,2). The measured tissue concentration C is approximated as C=aR+b, where R is the reaction rate, and a and b are calculated from the arterial 2-FDG time course and a set of average population kinetic rate constants. The previously reported linearizations R=(C-b)/a differ in their sensitivity to differences between current and population kinetic rate constants and thus in their accuracy. We have developed a method that is insensitive to the presumed value of the blood flow/capillary wall transport parameter k_1. Our method performed comparably to that of Ref. 2 in the refitting of the 13 normal cases in Ref. 1. In the analysis of the 6 ischemic cases in Ref. 3, and in ischemic cases studied in our own laboratory, our method consistently performed better than any previous method.

1. SC Huang, ME Phelps, EJ Hoffman, et al, Am J Physiol 238: E69 (1980).
2. RA Brooks, J Nucl Med 23: 538 (1982).
3. RA Hawkins, ME Phelps, SC Huang, et al, J Cerebral Blood Flow and Met 1: 37 (1981).

REGIONAL CEREBRAL GLUCOSE METABOLISM DURING ELECTRIC SHOCK INDUCED PAIN. R.A. Margolin, M.S. Buchsbaum, R.M. Kessler, and R.G. Manning. National Institutes of Health, Bethesda, MD and University of California, Irvine, CA.

This study was undertaken to investigate whether the pattern of regional cerebral glucose metabolism (rCMRglu) differs during acute pain from that seen in a resting state. Regional cerebral glucose metabolic rate (rCMRglu) was determined by positron emission tomography (PET) with (F-18)-2-Fluoro-2-deoxy-D-glucose (FDG) in response to electric shock stimulation of the right forearm and at rest. Seven slices were obtained for each subject. Of these, three which represented superior, middle and inferior levels respectively were chosen for analysis. An outer "peel" of pixels, corresponding to cerebral cerebral cortex, was obtained and divided into 8 sections, four for each hemisphere. These were standardized to the mean of the entire peel and correlated.

Significant differences (p=.05) were found in the pattern of rCMRglu between shocked subjects (n=14) and resting controls (n=7). Many regions were highly correlated in

shocked patients but not in resting controls, especially in superior slices.

These results suggest that pain associated with electric shock stimulation of an extremity may induce metabolic coupling in functionally related brain regions. The results have implications for the study of normal neurophysiology and diverse disorders involving pain perception.

MEASUREMENT OF DOPAMINE RECEPTOR DENSITIES. O.T. DeJesus, J. Revenaugh, R. Dinerstein, and A.M. Friedman. University of Chicago and Argonne National Laboratory, IL

The specific binding of H-3-Spiroperidol (Sp), Br-75 and Br-77-Bromospiroperidol (BrSp) was measured in the brain of rats, mice and cats. In addition, receptor densities at saturation (in mice) were measured by using drug loadings of over 200-1000 micrograms per kg. The kinetics of uptake of the drugs are such that equilibrium was reached in 1-2 hours.

We have developed a computer simulation which solves the equilibrium binding equation used by Triggle, for the case of a single receptor and two competing ligands. When the parameters of the model are adjusted to fit the data on specific binding, we find that the endogenous dopamine appears to have a marked effect on the binding. It is also found that the value of receptor density needed to fit, with the equations, the measured values of specific binding is 75+/-15 picomoles/gram of tissue. The experiments at higher drug loadings is 100+/-10 picomoles/gram of saturated receptor densities. That measurement is model independent and is in general agreement with the model predictions.

The results of these eperiments indicate that either specific binding ratios or saturation levels can be used for measurements of receptor densities, in vivo. It also appears that the two ligand, equilibrium binding equations provide an adequate model of receptor binding.

L-[1-C-11]PHENYLALANINE FOR THE DETERMINATION OF CEREBRAL PROTEIN SYNTHESIS RATES IN MAN WITH POSITRON EMISSION TOMOGRAPHY. J.R. Barrio, R. Keen, H Chugani, R. Ackerman, D.C. Chugani and M.E. Phelps. UCLA School of Medicine, Los Angeles, CA

Phenylalanine, labeled at C-1, seems to be an especially interesting amino acid for studying brain protein incorporation using rat autoradiography and, potentially, for PET studies in animals and man. Even though phenylalanine hydroxylase seems to be absent in brain tissue, the phenylalanine hydroxylating activity of tyrosine hydroxylase makes it highly likely that phenylalanine could serve as an important precursor of catecholamines in vivo, a prediction that has in fact been verified. Using phenylalanine labeled at C-1, this process is clearly traceable because DOPA decarboxylase will release the label as CO_2. This is supported by our initial autoradiographic experiments with L-[1-C-14]phenylalanine which showed virtually no difference in radioactivity distribution in the brain when compared with L-[1-C-14]-leucine, and no increased radioactivity in areas of the brain in which catecholamine synthesis is known to occur. HPLC analysis (O-phthaldehyde precolumn fluorescence derivatization) of the arterial input function revealed that up to 20 minutes only radiolabeled phenylalanine is found in the acid soluble fraction, and a considerable build-up of proteins, probably synthesized in the liver, was observed with time. In order to test the validity of this approach for quantitative studies of cerebral protein synthesis rates in man using PET we have prepared L-[1-C-11]phenylalanine with good radiochemical yields (20-25%) and activities (30-40 mCi) using the Bucherer-Stecker reaction in combination with D-amino acid oxidase.

10:30–12:00 **Room 132**

PULMONARY II

Moderator: Philip O. Alderson, M.D.
Co-moderator: Daniel R. Biello, M.D.

EVALUATION OF ACUTE PULMONARY OXYGEN TOXICITY BY In-111 LEUKOCYTES. P.O. Alderson, T.S.T Wang, C. Iga, N. Kuromoto, S. Oluwole, M. Olesnicky, C. Pirani. Columbia University, New York, NY.

Leukocytes (LK) are thought to play a major role in the development of hyperoxic lung injury. LK kinetics and the potential role of labeled LKs in diagnosis of pulmonary oxygen toxicity were investigated in Lewis rats by injecting 15 uCi of In-111 LKs i.v., then exposing the rats to 90%O_2 for varying times (1-72 hrs) in a closed tent. The animals (n=3/group) were sacrificed at frequent intervals and the tissues were counted. Blood was drained from the lungs prior to counting. Other animals exposed to O_2 were injected with Ga-67 citrate or Tc-99m DTPA, and rats kept in room air also were evaluated with In-111 LKs. Histology of the lungs was obtained in 14 animals exposed to O_2 and in 15 kept in room air. In the first 6 hrs of O_2 exposure there was perivascular and peribronchial infiltration of lymphocytes; later polymorphonuclear LK infiltration was more prominent. There was significantly greater LK activity in the lungs and blood of animals exposed to O_2 than in controls. After 1 hr of hyperoxia, whole lungs contained 12.8%ID/g of LKs vs. 3.6%ID/g in controls ($p < .001$). There was a modest increase in LK blood activity/g in hyperoxic animals (4.5% vs 3.8% control) and a 2:1 lung/blood ratio (%ID/g) after 1 hr of hyperoxia. Whole lung activity fell to 6.4%ID after 6 hrs of exposure and to control levels after 36 hrs. The %ID/g of Ga-67 and Tc-99m DTPA in lung remained low throughout the study. The findings demonstrate that marked changes occur in LK pulmonary accumulation after acute exposure to O_2 and suggest that further investigation of In-111 LKs as an agent for diagnosis of pulmonary oxygen toxicity is warranted.

EARLY DIAGNOSIS OF ADULT RESPIRATORY DISTRESS SYNDROME BY Tc-99m HUMAN SERUM ALBUMIN AND PORTABLE PROBE. K.M. Spicer, H.D. Reines, and B.W. Garvin. Medical University of South Carolina. Charleston, SC 29425

As early diagnosis of Adult Respiratory Distress Syndrome (ARDS) is critical to successful therapeutic intervention, we studied the ability of Tc-99m Human Serum Albumin (Tc-HSA) to measure the pulmonary capillary leakage of protein rich exudate. Ten millicuries Tc-HSA was injected into 10 normal volunteers (Nl), and 15 patients (Pts) with ARDS. Initially, a small field portable gamma camera and digital computer acquired seven 256 byte, 500K images every 15 minutes. Upon recovery (> 10 days), scans were repeated on 5 ARDS Pts. Average counts were obtained in left and right lung and left ventricular regions of interest. Average lung counts were divided by heart counts (L/H) at each time. Nl L/H started at .6 or less, stayed the same or decreased with time. All ARDS Pts had values of .6 or greater, which increased with time to .8 or more. Five Pts recovered from ARDS had flat leakage curves with L/H of .6 or less.

Next, a portable 2" probe with 0.1" hex-hole collimator and scaler was built and evaluated. Two minute counts from 3 lung regions (L) were averaged and divided by 2 minute counts from mid sternum (heart,H). L/H were obtained simultaneously on probe and gamma camera for 10 controls and 7 ARDS. Close correlation between gamma camera and probe was obtained. For the probe, Nl L/H started at .4 and decreased with time, while ARDS started at .5 and increased to .8 or more. Two Pts with congestive heart failure (CHF) had initial L/H of .5 which decreased slightly with time. The L/H of 3 Pts with pneumonia started at .6 and remained unchanged. In conclusion, we feel that a simplified portable monitor and Tc-HSA may be utilized to identify Pts with ARDS and distinguish them from nls, CHF, and pneumonia Pts.

DIAGNOSIS OF PULMONARY EDEMA BY In-111 CHLORIDE LUNG-HEART IMAGING. W-J Shih, G. Simmons, L-Y Lee, F.H. DeLand, J.J. Coupal and P.A. Domstad. Veterans Administration and University of Kentucky Medical Centers, Lexington, KY.

To detect pulmonary edema (PE) a radionuclide method that demonstrates increased capillary permeability was performed in five mongrel dogs. The anesthetized dog was positioned under a scintillation camera interfaced to a computer. Through a femoral artery cannula arterial blood samples were obtained before and after induced PE with

oleic acid. Dynamic data were recorded at one frame/min for 40 mins after injection of 1.5 mCi In-111 chloride. At the mid point of the study 0.3 ml/kg of oleic acid were injected. After oleic acid administration the cardiac blood pool activity rapidly decreased and pulmonary activity increased. The computer generated curves of lung/heart (L/H) ratios ranged from 0.6 at baseline to 1.5 in the end stage of PE. The dramatic increase in pulmonary activity correlated well histologically with marked congestion and alveoli filled with edematous fluid. The blood pH and pO_2 decreased from 7.28 to 6.97 and 63 to 34 mmHg, respectively and pCO_2 increased from 30 to 44 mmHg. It is believed that oleic acid induces alveolar capillary membrane damage. Since the In-111 chloride instantly binds to plasma transferrin - an excellent intravascular imaging agent - leakage of this tracer into the aveoli reflects loss of wall competency. Pulmonary edema as in acute respiratory distress syndrome is difficult to diagnose radiographically and this radionuclide method with In-111 chloride may be potentially useful.

REGIONAL EXTRAVASCULAR LUNG WATER (rELW) DETERMINATION IN EDEMATOUS DOGS BY POSITRON EMISSION TOMOGRAPHY (PET).
O. Schober, G.-J. Meyer, C. Bossaller, P. Lobenhoffer, H. Creutzig, J. Sturm, and H. Hundeshagen
Medizinische Hochschule Hannover, Hannover, F.R. Germany

The purpose of this study was the evaluation of PET as a tool for the determination of rELW during the formation of regional pulmonary edema in the laboratory and possibly in clinical situations.
Pulmonary edema was induced in anesthetized horizontally suspended dogs (n=5; 37±6 kg) by injection of oleic acid (0.06 ml/kg). Total lung water (TLW), blood volume (BV), and extravascular lung water (ELW:=TLW-BV) were measured in absolute quantities with a positron camera system (M 4200; Cyclotron Corp.). Constant infusion of O-15 labeled H_2O was used as a water tracer and C-11 labeled CO as a blood labeling agent. An uniform Cu-64 field source was used to operate the tomograph in the transmission mode in order to examine lung areas and attenuation correction parameters. Reference values of ELW were obtained by a double indicator dilution method (thermo-dye-dilution TDD). At the end of the experimence the dogs were sacrificed, the lungs were weighed, and the wet/dry ratio was determined.
The mean ELW measured by PET increased from 0.21±0.02 g/cm³ to 0.37±0.04 g/cm³. This correlates with the data obtained from the TDD method which rose from 7.1±1.3 ml/kg to 13.3± 1.9 ml/kg (r=0.94). The data of the edematous states were confirmed by the gravimetric method which yielded 14±3 ml/kg Analysis of the rELW in at least 11 regions in each dog revealed a range of 0.10-0.29 g/cm³ in normal states and 0.24-0.70 g/cm³ in edematous states. The rELW increased from apex to base zones. Development and degree of edematous states was found to be inhomogenous with significant regional differences.

PULMONARY EXTRACTION OF N-ISOPROPYL-P-I123-AMPHETAMINE (IMP) MEASURED BY MULTIPLE INDICATOR DILUTION TECHNIQUE.
J.J. Touya, H.F. Corbus, D. Grubbs, D. Hudson, J.Rahimian, E. Glass and L.R. Bennett. UCSF, Fresno Medical Education Program, CSU, Fresno and UCLA.

In previous publications we demonstrated the feasibility of the metabolic lung scan using I123-IMP, and measured the extraction ratio by pulmonary endothelial cells. The objectives of this study were to confirm previous findings using a different vascular tracer (Tc99m dextran) and to evaluate a new animal model (West African dwarf goat).

Tc99m DTPA was the extracellular tracer and ketamine the competitive agent. I123 IMP was injected as a bolus in the jugular vein, followed 10 minutes later by the reference tracer. From dynamic images time/activity curves for reference and test tracers constructed over the right heart and over the lung were gamma fitted and deconvoluted to give the pulmonary impulse response function of each tracer, $H_R(t)$ and $H_T(t)$. Impulse response functions were normalized to the peak values and the extraction fraction [E(t)] computed as: $E(t)=H_T(t)-H_R(t)/1-H_R(t)$.

Based on 15 animal experiments E(t) for I123 IMP was 0.96±0.02 before ketamine and 0.73±0.12 after ketamine. For Tc99m DTPA the value was 0.15. The goat model was superior to the dog in cost, availability, ease of acquisition and care, optimal size for imaging, accessibility of the jugular vein, tolerance for experimental manipulation and respiratory physiological parameters.

The E(t) values are consistent with the previous findings in dogs and confirm the value of I123 IMP as a metabolic lung imaging agent. The West African dwarf goat offers an attractive alternative to the dog as an experimental model.

LUNG DISTRIBUTION AND KINETICS OF I-123 HIPDM: A POTENTIAL AGENT FOR EARLY DETECTION OF LUNG CELLULAR INJURY.
M. Pistolesi, F. Fazio, G. Marini, P. Gerundini, M.C.Gilardi, F. Colombo, M. Miniati, G. Taddei, P. Fazzi, C. Giuntini. University of Milan, H. San Raffaele, Milano, and CNR Institute of Clinical Physiology, Pisa, Italy.

Pulmonary metabolism of several amines has been experimentally demonstrated. We studied the lung regional distribution and kinetics of the brain imaging agent N,N,N'-trimethyl-N'-(2-hydroxyl-3-methyl-5-iodobenzyl)-1,3-propanediamine (I-123 HIPDM) in 12 normal volunteers. Tomographic views and time activity curves over the lung fields were obtained up to 4 hours from injection by a rotating gamma camera. Venous blood activity fell to a stable (10% of the peak) value within 30 min. A fairly homogeneous distribution of I-123 HIPDM was observed in transaxial, frontal and sagittal lung tomographic slices. Liver and spleen uptake was negligible until 3 hours from injection. Exponential analysis of externally detected time activity curves showed that I-123 HIPDM lung kinetics is adequately described by three compartments. The first two compartments may reflect early redistribution and appear to end up by 30-40 min. The third compartment is characterized by a shallow downslope with a long half time (8.45 ± 2.40 hours) and may be interpreted as essentially stable cellular binding. Hence, I-123 HIPDM stands as a non particulate agent suitable for lung imaging and kinetics studies. Alterations in regional distribution and/or changes in pulmonary kinetics of I-123 HIPDM may be expected in early stages of lung cellular damage.

10:30-12:00 **Room 130**

BONE/JOINT III: OSTEO/PROSTHESIS

Moderator: Hirsch Handmaker, M.D.
Co-moderator: Paul B. Hoffer, M.D.

SKELETAL IMAGING IN OSTEOMYELITIS.
R.E. O'Mara, G.A. Wilson and A.M. Burke. University of Rochester School of Medicine and Dentistry, Rochester, NY

A prospective study was carried out over a two-year period (1980-81), in which all patients entering this institution with the clinical diagnosis of suspected osteomyelitis were studied utilizing skeletal imaging and diagnostic radiographic procedures including magnification radiographs and tomography where indicated. Two-hundred and ten patients were studied. The final diagnosis was 18 with osteomyelitis, 32 with osteomyelitis and cellulitis, 10 with cellulitis and 150 without osteomyelitis or cellulitis. Diagnosis was achieved by surgery, clinical course of disease and follow up after a one-year interval. Skeletal imaging was performed using a three-phase technique including a perfusion study following bolus, I.V. administration of Tc-99m MDP, early immediate imaging post perfusion, and delayed imaging 2 hours after injection. In 28 patients, Ga-67 citrate studies were also obtained.

Skeletal imaging achieved a sensitivity of .76 and a specificity of .99, and overall accuracy of .93. Standard radiographic techniques demonstrated a sensitivity of .24, specificity of .96 and an accuracy of .79. The delayed gallium scan had high sensitivity and specificity (1.0 each) in distinguishing osteomyelitis from cellulitis and septic arthritis. However, routine skeletal imaging after minimum

and 8 hour delay in 8 patients also demonstrated similar results. The perfusion and early images were of great help in separating out inflammatory from noninflammatory conditions and in allowing one to distinguish between cellulitis and osteomyelitis.

We conclude that skeletal imaging is a procedure of high value in cases where osteomyelitis is suspected and will present a decision tree based on these results.

PROSPECTIVE In-111 WBC SCAN VS Tc-99m-MDP-Ga-67 SCAN FOR LOW-GRADE OSTEOMYELITIS. FINAL REPORT. K.D. Merkel, M.L. Brown, R.H. Fitzgerald, M.K. Dewanjee, and M.F. Hauser, Mayo Clinic and Mayo Foundation, Rochester, MN.

We had previously reported our methodology and early results in comparing the standard sequential Tc-99m-MDP-Ga-67 scan (BS-GA) with In-111 WBC scan [JNM 23(5):P65]. 50 patients were entered into the protocol; 6 patients did not receive one of the 3 scans, and 2 patients had insufficient follow-up for diagnosis. Of the remaining 42 patients there were 53 sites evaluated, 40 with surgical confirmation by histology and culture. BS-GA was considered + if incongruent or very intense GA, indeterminate if moderate congruent GA and - if mild congruent or no GA. There were 11 indeterminate sites of which 8/11(73%) were infected and 3/11(27%) not infected.

	In WBC		BS-GA (Excluding Indeterminate)	
	+	-	+	-
Infected	27	6	18	6
Not Infected	2	18	1	17
Sensitivity	82%		75%	
Specificity	90%		94%	
Accuracy	85%		83%	

All three observers performed better on ROC analysis with the In-111 WBC scans. Although easier to read and with a slight improvement in sensitivity with In WBC scans, the technical complexities of cell labeling may outweigh these advantages in daily practice.

CAN THE THREE-PHASE BONE SCAN DIFFERENTIATE OSTEOMYELITIS FROM METABOLIC OR METASTATIC BONE DISEASE? G.F. Edeburn and R.B. Shafer. VA Medical Center, Minneapolis, MN.

The three-phase bone scan has been reported of value in the diagnosis of osteomyelitis. The use of a radionuclide angiogram, an immediate post-injection "blood pool" image, and 2-3 hour delayed image has been useful in separating non-osseous inflammatory disease from osteomyelitis. Dependence on increased blood flow and focal hyperemia for this diagnosis may limit the use of the study if other processes are shown to produce similar results. To identify limitations of the 3-phase bone scan we studied 13 patients with metastatic bone disease (8 with CAP, 3 lung cancer, and 2 breast cancer), and 6 patients with Paget's disease. Each patient received 18 mCi of MDP by bolus injection with the area of interest centered under an LFOV camera. Serial 3 second images, an immediate 300K "blood pool" image and 2-3 hour delayed images of the region of interest were obtained. The flow study was quantitated as to no increase, intermediate increase (1-2+) or intense (3-4+) increase. Flow results showed no increase in 2/12 patients with metastases, intermediate increase in 7/12 patients with metastases and 1/7 patients with Paget's, and intense increase in 4/12 patients with metastases and 5/6 patients with Paget's. The immediate blood pool study showed increased activity in all patients, except one with metastases. All 19 patients showed marked focal activity on delayed images. We conclude that because of increased flow, Paget's disease may be difficult to separate from osteomyelitis on the 3-phase bone scan. Metastatic disease can usually be differentiated on the basis of quantitatively reduced focal hyperemia. The 3-phase bone scan remains of value in the diagnosis of osteomyelitis, but other diseases of bone must be included in the differential diagnosis.

INDIUM-111 CHLORIDE IMAGING IN THE DETECTION OF OSTEOMYELITIS. B. Sayle, G. Cierny, III, and J. Mader, University of Texas Medical Branch, Galveston, TX.

Imaging with Indium-111 Chloride in our laboratory has been shown to be both sensitive and specific for the detection of inflammatory disease. A prospective study has been undertaken to determine the ability to detect osteomyelitis. Twenty-six patients with suspected osteomyelitis were studied. Twenty-five had osteomyelitis following trauma from one month to forty-three years prior to imaging, and the inflammatory process followed a deep groin infection in one patient. All received a bone scintigram and were injected with 3mCi of Indium-111 Chloride immediately thereafter: imaging was performed 48-72 hours later. Correlation was made with radiographs and bacteriologic cultures in all patients. Twenty-four patients underwent surgery and two had biopsies. Four patients also received Gallium-67 Citrate imaging one week following the Indium-111 Chloride. Results: Bone and Gallium-67 scintigrams showed extensive bony involvement, whereas the Indium-111 studies demonstrated involvement limited to the inflammatory process. There were two false-positive studies in patients who had received cancellous bone grafts eight and nine months prior to imaging. In both, tracer concentration was very minimal; no inflammation was found on bone biopsy. One patient had a normal Indium study and no infection was demonstrated. Conclusion: Indium-111 scintigraphy has proven to be useful to detect osteomyelitis. Technetium bone scintigrams and Gallium-67 studies were found to be sensitive but overestimated the amount of bone involved. A negative Indium scintigram excludes the possibility of osteomyelitis.

EVALUATING THE PAINFUL PROSTHETIC JOINT WITH SEQUENTIAL Tc-99m-MDP-Ga-67. K.D. Merkel, M.L. Brown, and R.H. Fitzgerald, Mayo Clinic and Foundation, Rochester, MN.

Tc-99m-MDP bone scan (BS) combined with Gallium-67 imaging (GA) (BS-GA) has been reported to be highly accurate in differentiating infected prosthesis from other pathological processes. We retrospectively reviewed the results of patients who had sequential BS-GA between 1976 and 1981 for evaluation of painful prosthesis. Studies were classified as + for infection if there was incongruent or very intense GA localization; indeterminate if there was moderate congruent GA activity and - if there was mild congruent or no GA activity. One hundred and one patients had 103 scans (89 hips, 11 knees, 1 shoulder, 1 ankle, and 1 elbow); 52 scans had surgical confirmation with culture and histology and 51 scans had clinical evaluation. As a group these patients represented suspected indolent low-grade infections in that none had systemic manifestations of infection, only 6 had sinus tracts, and laboratory and X-rays were generally nondiagnostic. There were 32 infections, 29 aseptic loosening and 42 other non-infected prostheses. The indeterminate group had 4/11 (36%) infection and 7/11 (64%) non-infected. The results of the positive and negative scans are given in the table:

	BS-GA +	BS-GA -
Infected	19	9
Not infected	13	51

This yielded a sensitivity of 68%, specificity of 80%, accuracy of 76%, predictive value of (+) test 59% and predictive value of (-) test 85%. We conclude that in patients with suspected low-grade infection of a prosthetic joint a (-) BS-GA suggests an aseptic process but a (+) BS-GA does not reliably predict infection.

THE VARIABILITY OF FOLLOW-UP BONE SCANS AFTER ASYMPTOMATIC TOTAL HIP PROSTHESES. J.A. Utz, R.J. Lull, and E.G. Galvin Walter Reed Army Medical Center, Washington, D.C., and Letterman Army Medical Center, San Francisco, Ca.

A four point grading system for evaluation of bone scans after total hip replacement which compares activity about the prosthesis to normal femur (grade 0) or with iliac crest or sacro-iliac joint (grade 2) has been utilized to grade bone scans in 59 asymptomatic patients with total hip prostheses. All patients had serial scans using Tc-99m MDP starting within one year after surgery. One hundred thirty four follow-up scan pairs were analyzed for change in activity between any two sequential images. Twenty six patients showed minimal increase in activity on at least one scan pair in at least one of the five regions analyzed (acetabulum, greater trochanter, lesser trochanter, shaft, tip) for a total of 46 areas out of 670 areas analyzed (7%). Twenty five of these episodes occurred at a time greater than one year after surgery. Additional follow-up scans

were available on 24 of the 46 areas and 23 of them showed stabilization or subsequent decrease in activity. No follow-up is yet available on the remaining 22. Only one patient showed a progressive increase in activity on three sequential scans and that patient was subsequently shown to have a loosened prosthesis. Only two patients had a serial increase in activity of more than one grade. One of these patients had loosening of the prosthesis while the other had an extended pattern on bone scan but is asymptomatic.

In conclusion, minor changes in bone scan activity on serial bone scans must be interpreted with caution. Marked changes more than one grade in activity are unusual and raise the question of prosthesis loosening.

10:30–12:00 **Room 276**

HEMATOLOGY II

Moderator: Mathews B. Fish, M.D.
Co-moderator: Howard G. Parker, M.D., Ph.D.

THE NATURAL HISTORY OF PLATELET DEPOSITION ON DACRON AORTIC BIFURCATION GRAFTS IN THE FIRST YEAR FOLLOWING IMPLANTATION IN MAN. J.R. Stratton, and J.L. Ritchie. VA Medical Center and Univ. of Washington, Seattle, WA.

To define the dynamics of platelet deposition on Dacron aortic bifurcation grafts in the first year following implantation, we performed serial indium-III platelet imaging with quantitative analysis of platelet uptake. Eight men were studied 1-2 wks following implantation and 5 were restudied at a mean of 31 and 55 wks. No subject received anticoagulant or platelet inhibitory drugs. Imaging was performed 24 to 96 hrs after platelet injection. Quantitative analysis was by a graft/blood ratio which compared background-corrected indium-III platelet activity in the graft region to well-counted whole blood at each imaging time. In addition, blinded visual analysis compared graft area activity to adjacent native arteries. A reduction in deposition by visual analysis was defined as conversion of a positive study to negative or equivocal.

The mean of all graft/blood ratios (24, 48, 72 and 96 hours) decreased from 4.4 ± 2.1 (± 1 SD) at 1-2 wks to 3.0 ± 1.8 at 31 wks ($p = 0.002$). There was no further significant decrease at 55 wks (2.8 ± 2.0). For comparison, 12 normals without grafts had a mean aortofemoral blood pool/whole blood ratio of 1.8 ± 0.7. The ratio in graft pts was greater than in normals at all time periods. Visual analysis detected deposition in 7 of 8 grafts at 1-2 wks; 1 was negative. All 5 pts with followup studies had an initially positive study. Deposition decreased qualitatively at late study in 2 of 5 pts (1 became negative, 1 equivocal).

We conclude that there is consistent, early deposition on Dacron grafts in man which decreases over 31 wks. However, platelet accumulation remains readily detectable by both quantitative and qualitative analysis in most patients at 1 year, which implies absent or incomplete endothelialization of the graft.

TICLOPIDINE FAILS TO INHIBIT PLATELET DEPOSITION ON DACRON PROSTHETIC SURFACES IN MAN. J.R. Stratton, J.B. Martin, K.W. McFadden, and J.L. Ritchie. VA Medical Center and University of Washington, Seattle, WA.

To determine if the experimental platelet inhibitory drug ticlopidine (250 mg bid) decreases platelet deposition on Dacron grafts, we conducted a randomized placebo-controlled double-blind trial in 10 males with chronic (> 1 yr) aortic bifurcation grafts. Placebo (or drug) was given for 14 days followed by a 7 day washout and then the alternate therapy. Platelet deposition was assessed by imaging indium-III platelets 24-72 hrs after injection. Quantitative analysis was by a graft/blood ratio which compared background-corrected indium-III platelet image activity in the graft to well-counted whole blood. In addition, blinded visual analysis compared graft activity to adjacent native arteries.

Injected indium-III dose did not differ between placebo (372 ± 7 μCi, ± SEM) and drug (377 ± 6). The bleeding time increased from 5.3 ± 0.5 to 17.1 ± 3.1 min on drug ($p < 0.01$). By quantitative analysis, the graft/blood ratio was unchanged. For comparison, results in 12 normals without grafts are presented.

	Mean Graft/Blood Ratios		
	24 Hr	48 Hr	72 Hr
Placebo	2.6±0.3	3.2±0.4	4.0±0.6
Ticlopidine	2.3±0.4	3.1±0.5	3.9±0.7
Normals (n=12)	2.0±0.2	1.8±0.2	1.7±0.2

Independent visual interpretation revealed that 9 of 10 patients had positive studies on both placebo and ticlopidine. One patient was equivocal on placebo and negative on ticlopidine. No normal subject had platelet deposition. Similar negative results were previously reported for sulfinpyrazone (200 mg qid).

We conclude that ticlopidine in a dose of 250 mg bid prolongs the bleeding time but does not significantly inhibit platelet deposition on chronically implanted Dacron grafts in man.

QUANTITATIVE MEASUREMENT OF INTRAVASCULAR THROMBUS SIZE WITH INDIUM-111 PLATELET SCINTIGRAPHY. W.J. Powers, K.T. Hopkins, and M.J. Welch. Washington University School of Medicine, St. Louis, MO.

We have developed and validated a technique that permits accurate scintigraphic measurement of intravascular thrombus size using In-111 platelets and Tc-99m labeled red blood cells as a second radiotracer for the blood pool. Following the injection of both In-111 platelets and Tc-99m red blood cells, thrombi were induced in rabbits by passing an electrical current through a wire in the abdominal aorta. Animals were then given 1000 units of heparin and killed to insure that the thrombus size remained constant. Separate scintigraphic images for Tc and In were collected. These were used to calculate a percent injected dose (% ID) index based on the In and Tc counts in the thrombus relative to those in uninvolved aorta and on the % ID of In in 1 ml of blood. This was compared with the % ID of In in the thrombus determined in vitro in a well counter. The relationship between the two was linear with a high correlation coefficient ($r=.931$, $n=6$, $p<0.01$). Other techniques of scintigraphic quantitation proved to be less accurate. There was no significant correlation between the % ID of In determined in vitro and scintigraphic measurements of In cpm, In cpm/ID, In cpm/pixel or In cpm/pixel/ID (all $p>0.10$). The scintigraphic ratio of In cpm/pixel thrombus to In cpm/pixel uninvolved aorta also correlated poorly with in vitro measurements of % ID or thrombus to blood ratio ($p>0.10$). This is a simple non-invasive technique for providing a quantitatively accurate measurement of local platelet deposition and should be useful for studying the effect of anti-thrombotic drugs in both animals and man.

ACCUMULATION OF In^{111} LABELLED THROMBOCYTES IN LEFT VENTRICULAR AND AORTIC ANEURYSMS. E.A. van Royen, M.D.Trip, C.Visser, M.R.Hardeman, J.B. van der Schoot. Dept. of Nuclear Medicine and Cardiology, University Hospital Wilhelmina Gasthuis, Amsterdam.

Labelling of thrombocytes with In^{111} oxinate has proved a reliable and useful method to study platelet deposition in thrombotic processes. We studied 33 patients with left ventricular aneurysm.

Platelets were isolated and labelled with 200-300 μCi In^{111} oxinate as described previously. Gamma camera images were obtained 48 and 96 hrs after injection. Blood pool subtraction was performed after 96 hrs employing Tc^{99m} labelled RBC. In 12 patients clear focal In^{111} activity was found in or near the aneurysms, whereas scans were negative in 21 patients. 2D echocardiography agreed well with the scan in the positive patients: 11 positive and 1 negative. In the 21 negative patients echocardiography detected 5 further thrombi.

Nearly all patients of both groups were on oral anticogulant drug therapy which clearly demonstrates that these agents are not able to prevent platelet accumulation in cardiac aneurysms. Patients with In^{111} positive cardiac thrombi tended to be somewhat younger, to have a more recent aneurysm and showed spontaneous platelet aggregation in a larger proportion of cases.

We found the incidence of In^{111} positive thrombi in cardiac aneurysms (36%) to be lower than found in a group of 15 patients with aortic aneurysms (73%).

BIODISTRIBUTION AND SURVIVAL OF HUMAN PLATELETS LABELED IN BUFFERED MEDIA AND PLASMA. J.S. Robertson, M.K. Dewanjee, W.L. Dunn and H.W. Wahner, Mayo Clinic and Foundation, Rochester, MN.

Human platelet (PL) biodistribution and survival were studied in 28 normal subjects using PL labeled with In-111 oxine in 4 ml of ACD saline and in five normal volunteers

using PL labeled with In-111 tropolone in 0.5 ml ACD plasma. The advantage of the oxine method is that oxine can be used directly as obtained from commercial suppliers, whereas tropolone must be prepared fresh for each study. The advantage of tropolone is that labeling is performed more physiologically in plasma. A Ficoll-Hypaque gradient technique was used to separate five layers from the labeled cell preparation: plasma, PL, PMN cells, gradients and red cells. Radioactivity in each fraction was determined by gamma-ray counting. Labeling efficiency with the oxine method was 64 ± 13%, with tropolone 83 ± 9%. By either method initial recoveries were 70-90%. PL survival times in normal subjects were determined from 5 ml blood samples at 10 min, 2hr, 24hr, then daily to 10 days. Organ distributions were determined from regions of interest by computerized gamma camera methods. The mean survival time (exponential function) by the oxine method was 5.8 ± 1.2 d and for the tropolone cases was 5.6 ± 0.6d (mean ± SD). By either method at 20 to 30 hrs 35 ± 10% of the activity was in the spleen and 6 ± 3% in the liver. Activity in the spleen rose slowly to 40 ± 13% at 7 d, at which time there was 25 ± 8% in the liver. The results indicate that the more convenient saline method yields values that are equal to those from the plasma method. The use of the plasma labeling environment does not increase platelet survival.

In-111-PLATELET CLEARANCE, SCINTIGRAPHY AND DISTRIBUTION STUDIES IN EXPERIMENTAL AND CLINICAL IMMUNE THROMBOCYTOPENIA. G.N. Sfakianakis, A. Heal, R. Myvaganam, P.G. Sprinz, R.P. Junghans, Y.S. Ahn, W.J. Harrington and A. Serafini. University of Miami School of Medicine, Miami, FL

Animal and human platelets were separated by centrifugation and labeled with In-111-Oxine by incubation for 15 min in 1 ml normal-saline-phosphate-buffer pH 7.5 at 37°C. Labeling efficiency was between 60-90% and aggregation studies showed preservation of platelet function.

Alloimmune thrombocytopenia was studied in an animal model developed using inbred Brown Norway (BN) and Lewis (L) rats. BN rats were immunized with L platelets and anti-L-plateled-antibodies were induced. The antibodies were detected by immunofluorescent microscopy and they were found in the serum of all animals by the 7th week of immunization.In the immunized BN rats In-111-labeled-L platelets had a survival at 10 min of 17% of the injected activity, as compared with 71% in the non-immunized control BN rats. Scintigraphy showed that the fast disappearance of the L-platelets from the circulation of the immunized BN rats was due to prompt hepatic localization. Liver to spleen (L/S) and heart to spleen (H/S) ratio by computer analysis of scintigraphic data at 30 min post injection was, for the immunized animals, L/S = 14:1 and H/S = 0.31:1 and, for controls, L/S = 2:1 and H/S = 2:1.

Studies in patients with alloimmune thrombocytopenia (AT) and idiopathic thrombocytopenic purpura (ITP) were performed using homologous (for AT) or autologous (for ITP) In-111-labeled platelets. Prompt hepatic platelet sequestration was noticed in AT but mainly splenic sequestration was found in ITP.

In-111-platelet distribution studies are essential for the evaluation of immune thrombocytopenia, experimental or clinical.

FUNCTIONAL ASPLENIA AND PATIENTS WITH CHRONIC GRAFT-VERSUS-HOST DISEASE. M. Al-Eid, P. Tutshka, G. W. Santos, H.N. Wagner, Jr. and Min-Fu Tsan, The Johns Hopkins Medical Institutions, Baltimore, Maryland

Bone marrow transplantation has been increasingly used for the treatment of patients with hematologic malignancies or aplastic anemia. Infections continue to be a major cause of morbidity and mortality in these patients especially those who develop chronic graft-versus-host disease (GVHD). Spleen plays an important role in the host defense against microbial infections. In this study, we analyzed 53 bone marrow transplant patients who had Tc-99m sulfur colloid liver-spleen scans performed between 1 and 12 months after transplantation. Absent splenic uptake was noted in 5 of the 10 patients who developed chronic GVHD, but in none of the 7 patients who developed acute GVHD, or 36 patients who had no GVHD complications. None of these 5 patients with absent splenic function had prior history of splenectomy. Two of these 5 patients had nuclear scans. Thus, these five patients most likely had functional asplenia. The difference in the methods treating the patients before transplantation or the duration between transplantation and liver-spleen scan could not account for the observed effect among these three groups of transplant patients. We conclude that 1) there is a high association between chronic GVHD and functional asplenia, and 2) functional asplenia may contribute to the increased susceptibility of bacterial infections in patients with chronic GVHD.

10:30–12:00 **Room 275**

INSTRUMENTATION IV: SINGLE-PHOTON TOMOGRAPHY

Moderator: Barbara Y. Croft, Ph.D.
Co-moderator: Ernest V. Garcia, Ph.D.

SPECT RESOLUTION AND UNIFORMITY IMPROVEMENTS BY NON-CIRCULAR ORBIT. S. Gottschalk, D. Salem, C.B. Lim, R.H. Wake. Technicare Corporation, Solon, OH

Non-Circular orbit Single Photon Emission CT that brings the camera head close to an object at each angle by a combination of rotational and translational motions significantly improves SPECT image resolution and uniformity. The latter is achieved by suppression of ring artifacts due to the relative motion between the detector and object centers. This has been experimentally demonstrated by comparing the SPECT imaging performance from an Omega 500 system equipped with a HR collimator between an elliptical orbit of 40cm x 30cm axes and an equivalent circular orbit of 40cm diameter. The measured FWHM spatial resolution improvements near the image center were 2.4mm from 14.4mm to 12.0mm. Lesion contrasts were measured from circular cold rods of 6 to 14mm diameter located at various positions immersed in Tc-99m water-filled uniform activity cylinder of 21cm diameter. The values measured at 7.5cm off-center on the minor axis are as follows:

ROD DIA.	CONTRAST MEASURED		REL. CONTRAST
(mm)	ELLIPTICAL	CIRCULAR	INCREASE
6	.20	.07	2.8
8	.35	.27	1.3
10	.40	.33	1.2
12	.55	.42	1.3
14	.52	.52	1.0

The contrast values measured at other locations showed similar improvements. Visual inspection of cold rods and other phantom images showed better lesion shape definition, sharper edge response, and clearly distinguishable detectability improvements in the elliptical orbit over the circular orbit. Translation motion reduced ring artifacts by an order of magnitude, particularly near the image center.

A SIMPLE SYSTEM FOR GENERATING NON-CIRCULAR ORBITS IN SPECT IN ORDER TO REDUCE THE IMPORTANCE OF UNIFORMITY ARTEFACTS. A. Todd-Pokropek Dept. of Medical Physics, University College London, London, U.K.

Many rotating gamma camera SPECT systems have their image quality considerably reduced by the presence of artefacts resulting from non-uniformity of the detector. Such non-uniformity can be amplified by a factor of upto 20 at the centre of rotation. The use of non-circular orbits can reduce this amplification by about an order. A simple method is proposed for achieving such orbits by altering bed-height in synchrony with detector rotation such that various non-circular orbits may be generated, which could in principle be fitted even with older rotating gamma camera systems. Essentially, for each angular rotation of the camera, the bed-height is altered by a constant increment of the order of 1-3mm. The direction (and if possible the amplitude) of the displacement needs to be under computer control. A wide range of orbits can thus be generated. A trivial modification is required for the reconstruction algorithm.

The benefit of such a system has been tested by simulation, and on phantoms. The results show a dramatic reduction in the presence of artefacts, which can be further reduced using a circular artefact filter. This

means essentially that the uniformity requirements for a SPECT system need no longer be at the (impossible?) level of 2%, but that systems with 5% uniformity can produce acceptable SPECT images.

APPLICATION OF THE BUDINGER EQUATION TO EVALUATE SIGNAL TO NOISE RATIOS OF SINGLE PHOTON EMISSION TOMOGRAPHIC SYSTEMS. WJ MacIntyre, TS Houser, B Sufka, RT Go, and JK O'Donnell. Department of Nuclear Medicine, Cleveland Clinic Foundation, Cleveland, Ohio.

It has been proposed by Budinger, et al, that the fractional standard deviation (FSD) of a target resolution cell as reconstructed by emission tomography may be expressed by the equation:

$$FSD = K\ (Me)^{3/4}\ (N)^{-\frac{1}{2}}$$

where K is a constant depending on the reconstruction method, Me is the effective number of target cells and N is the total number of counts. The effective number of resolution cells equals the sum of the number of cells in the target plus the number of cells in the background divided by the target-to-background contrast ratio.

This relationship has been tested experimentally by reconstruction of an ellipsoidal phantom filled with a radioactive solution by both the GE 400 T rotating transaxial camera and the Siemens Rota Camera. Both systems used 64 projections for 360° rotation and reconstruction for both were obtained on the Simis IV Informatek. The total counts recorded through the midpoint of the ellipsoid ranged from 120K to 6 million counts per slice. Good agreement was obtained between the theoretical equation and the experimental results. In the slice with 120K total counts, the FSD was predicted at 39% and recorded experimentally at 25%. In the 256K slice, the prediction was 9.5% and the measured value 11%. Between one million and ten million total counts, however, the measured FSD decreased only from 11% to 7% suggesting that the asymptotic noise value is that due to the tomographic system and cannot be improved by additional count collection.

COLLIMATOR CHOICE FOR DIFFERENTIAL UPTAKE MEASUREMENTS USING SPECT IMAGING WITH I-123. L.P. Clarke, S. Vaughan, M. Hourani and A. Serafini. University of Miami School of Medicine, Miami, Florida.

SPECT imaging has been proposed as a means of performing differential uptake or absolute measurements in-vivo. Important factors in this type of measurement are the choice of collimator and detector shielding, in particular for imaging moderate to high energy photons, because of the integrated effects of photon penetration across the crystal face. For example, I-123 (159 KeV, $T_{\frac{1}{2}}$ = 13.3 hrs) has been proposed for quantitative SPECT imaging. However the cyclotron production method (^{124}Te (p, 2n)^{123}I) results in I-124 ($T_{\frac{1}{2}}$ = 4.5 days) contamination, whose relative abundance although small emits high energy photons. This paper is therefore a quantitative evaluation of the effects of photon penetration and scatter in SPECT and planer imaging using I-123. A Picker SPECT system, with high energy detector shielding (500 KeV) and two parallel hole collimators were evaluated. Phantom measurements using a volume source containing I-123 (28 hrs EOB) were performed in air and scattering medium to differentiate penetration and scattering effects. Measurements were repeated with Tc-99m (140 KeV) where photon penetration is not significant. Specific parameters investigated included the relationship between ROI area and integrated counts obtained. In addition, the influence of reconstruction filter was investigated. Results demonstrated that penetration effects are significant for both imaging modes and hence at least a medium energy collimator is required. The filter choice also influenced the quantitative results of differential uptake measurements. These results are also important for absolute measurements.

ANGULAR SINGLE PHOTON EMISSION COMPUTED TOMOGRAPHY (SPECT): AN IMPROVED METHOD FOR CRANIAL TOMOGRAPHIC IMAGING. P.D. Esser, R.J. Mitnick, J. Arliss, P.O. Alderson. Columbia University, New York, NY.

In standard SPECT the minimum diameter of the camera's rotation arc is specified by the width of the patient's (pt) shoulders. This leads to an air gap between the pt's head and the camera face that decreases image resolution. However, by slanting the camera head caudally it can be rotated in close apposition to the pt's head using circular gantry movement and standard software. A rotation angle of 30° to horizontal was chosen on the basis of the head to shoulder angle in 50 pts ($\bar{x}$ angle = 26° ± 2° SD). To compensate for this angulation, a collimator with .055 in. hexagonal holes slanted at 30° to the camera's vertical axis was utilized. The capabilities of this angulated system (AS) were compared with those of a system using a .055 in. parallel hole collimator and standard rotation (SR) by imaging line sources, a cylindrical phantom and 15 pts referred for SPECT of the paranasal sinuses. The FWHM of the line source was 1.4 cm for AS vs. 2.0 cm for SR. Images (100K) of the cylindrical phantom with AS resolved defects as small as 7 mm vs. only 14 mm for SR. The AS images in pts consistently revealed excellent anatomic detail of the paranasal sinuses. A physician then evaluated 3 unidentified sets of SPECT images obtained sequentially with the AS and SR methods in pts with sinus disease. In each case the AS images were correctly identified by virtue of their improved detail. The findings suggest that AS will improve resolution without loss of sensitivity in SPECT imaging of the cranium and its contents.

POTENTIALITY OF D7PHT FOR DYNAMIC TOMOGRAPHY. Y. Bizais, I.G. Zubal, R.W. Rowe, G.W. Bennett, A.B. Brill. Brookhaven National Laboratory, Upton, NY.

In numerous physiological processes, temporal information is as important as spatial information. To perform dynamic tomography, a stationary, high sensitivity detector with a fast reconstruction algorithm is ideal. For this purpose a new tomographic modality (dual seven pinhole tomography: D7PHT) has been investigated; the detectors of a dual camera system are oriented orthogonally and mounted with seven pinhole collimators.

The reconstruction algorithm has been broken into two parts: the first one, distribution-independent, computes the projection matrix from the system geometry; the second one iteratively builds a 3D radioactivity distribution from its projections using the projection matrix. Importantly, this algorithm can reconstruct large volumes.

Physical performances of this system have been characterized. Sensitivity is 8 Kcps/(μCi/cc) for a 22 cm diameter phantom. The overall resolution is isotropic and FWHM of the impulse response varies from 9 mm for a point source at 230 mm from each detector to 15 mm at 480 mm.

The limiting factor in dynamic studies is the count rate acceptable with regard to patient dose, and detector dead time. For the present sensitivity and for injected activities between 1 and 10 mCi, 1 million events can be detected in 1 to 5 minutes. This acquisition time is compatible with the study of dynamic and cyclic processes, particularly cerebral and myocardial uptake and gated blood pool imaging. Potentiality of D7PHT for dynamic tomography will be demonstrated with phantoms and in vivo experiments, including the study of myocardial uptake of thallium in dogs and cerebral sequestration of amphetamine analogs.

1:30–3:00 **Room 123**

CARDIOVASCULAR CLINICAL X: NEW DIRECTIONS

Moderator: H. William Strauss, M.D.
Co-moderator: William L. Ashburn, M.D.

MEASUREMENT OF MYOCARDIAL BLOOD FLOW IN MAN WITH XENON-133 DURING DYPRIDAMOLE INDUCED CORONARY VASODILATION. S.Port, T.A.Lassar, S.Patel, G.Ray and D.H.Schmidt. Univ. Wisconsin Medical School, Mount Sinai Medical Center, Milwaukee, WI.

Regional heterogeneity of myocardial blood flow (MBF) not apparent at rest can be induced with the coronary vasodilator, dipyridamole (D), in patients with coronary

artery disease (CAD). In this study, we examined both the ability of the Xenon-133 washout method to measure the markedly elevated MBF seen after D and the reproducibility of such measurements. MBF was measured in nine patients by selective left coronary injection of Xenon-133 and external counting with a multicrystal gamma camera. Flows were measured once at rest (R), twice (D1 and D2) after 0.15 mg/Kg/min for four minutes of D intravenously and once after 250 mg IV aminophylline (A) which reverses the vasodilator effect of D.

	MBF (ml/100gm/min)			
	R	D1	D2	A
Left Coronary	64±18	162±40	178±40*	74±16
LAD	68±21	174±55	186±47**	75±20
Circumflex	64±15	161±37	183±50*	71±16

*p <0.05 or **P=NS compared to D1

These data show that D increases MBF in humans 1.7 to 4.5 fold and flow returns to near baseline following A. Furthermore, the Xenon-133 method can reproducibly measure the high MBF seen with D. Although small differences between D2 and D1 are apparent, those differences may be due to the higher systolic blood pressures seen during D2 compared to D1 (135±20 vs. 130±13, p <0.05).

This application of the Xenon-133 technique offers an exciting new approach to the physiologic assessment of the coronary circulation.

DETECTION OF CORONARY ARTERY DISEASE AT REST USING PEAK SYSTOLIC PRESSURE-END SYSTOLIC VOLUME INDICES. A.H.Maurer, J.A.Siegel,B.A.Denenberg, P.S.Robbins, K.M.Blasius, J.F. Spann, and L.S. Malmud. Temple University Hospital, Philadelphia, PA.

Resting ejection fraction (EF) is insensitive for the detection of coronary artery disease (CAD). We have attempted to better characterize abnormal LV function by measuring peak-systolic pressure/end-systolic volume (PSP/ESV) indices in patients with CAD. Twenty-three consecutive patients with suspected CAD had cardiac gated blood pool (GBP) studies performed within 24 hours of cardiac cathetherization. Four minute GBP images were obtained in the LAO 40° projection at rest (R), during isometric handgrip (ISO), and after sublingual nitroglycerin (NTG). ESV was calculated using a previously described count based technique which uses a venous blood sample and an esophageal point source to correct for attenuation. Average PSP was obtained using an arm cuff averaging pressures obtained after each minute of GBP acquisition. A resting PSP/ESV ratio was calculated as well as the slope of the line determined by three PSP/ESV points (R,ISO,NTG). The mean values ± 1 standard deviation (SD) obtained were:

	PSP/ESV(R)	Slope	EF (R)
Normals (n=4)	4.8 ± .27	4.2 ± .36	68 ± 6
CAD patients (n=19)	2.2 ± .92	1.1 ± .61	58 ± 9

Of 19 patients with CAD only 4 had abnormal resting GBP studies and EF's. Using the PSP/ESV (R) ratio alone 18/19 were abnormal (outside ± 2 SD) while 19/19 were abnormal using the slope calculations. We conclude that PSP/ESV indices can detect abnormal LV function in patients with CAD who have normal resting wall motion and EF's.

A MERCURIC IODIDE DETECTOR FOR CONTINUOUS MONITORING OF LEFT VENTRICULAR FUNCTION. A. Lahiri, J.C.W. Crawley and E.B. Raftery, Dept. of Cardiology & Radioisotope Division, Northwick Park Hospital & Clinical Research Centre, Harrow, Middx. U.K.

Mercuric Iodide (HgI2) has two main theoretical advantages over Cadmium Telluride (CdTe) for monitoring left ventricular function. The greater stopping power of HgI2 should give a higher sensitivity for the same size whilst the superior energy resolution should reduce the scatter fraction. Tests on a HgI2 detector have shown an energy resolution of 8.5 kev (FWHM) at the 140 kev photopeak of Tc-99m. A 60 mm sq. x 0.5 mm thick HgI2 crystal was connected via a pre-amplifier in such a way that it could be rapidly interchanged with the NaI probe of the Nuclear Stethoscope which has been validated against a gamma camera for ejection fraction (EF) (r=0.92, P < 0.001; n=30). Eighteen patients undergoing routine investigation with radionuclide angiography for suspected coronary heart disease were studied with the two detectors in rapid succession. There was good correlation between EF, ejection rate and peak filling rate: r=0.92, P < 0.001; r=0.78, P < 0.01; r=0.94, P < 0.001 respectively. The count rate from the HgI2 detector was 55% of that from the NaI detector of the Nuclear Stethoscope. We suggest that HgI2 may be superior to CdTe and a suitable detector for continuous cardiac monitoring.

RAPIDLY ALTERNATING GATED CARDIAC BLOOD POOL AND MYOCARDIAL PERFUSION IMAGING USING GOLD-195m AND THALLIUM-201. F. J. Wackers, R. Giles, P. Hoffer, R. Lange, M. Plankey, H. J. Berger, B. L. Zaret. Yale Univ., New Haven, CT and Univ. of Vermont, Burlington, VT.

Although rapidly alternating assessment of left ventricular (LV) function and perfusion would be of value in evaluating acute interventions, the physical characteristics of Tc-99m and Tl-201 preclude this approach. However, by continuous intravenous(iv)infusion of Au-195m ($t_{1/2}$:30.5sec) equilibrium gated cardiac blood pool imaging (GBPI) can be achieved using the Hg-195m/Au-195m generator. Initially, in 3 dogs after iv Tl-201, intermittent discontinuation of Au-195m infusion permitted technically excellent GBPI and myocardial perfusion imaging (MPI) over a 3 hour period. Fifteen patients (pts) had GBPI with continuous iv infusion of Au-195m at 7ml/min. This elution rate achieved maximal steady state Au-195m activity in BP and minimal radiation dose to the critical organ due to Hg-195m breakthrough. Au-195m GBPI resulted in 18869±8933 (mean±SD) counts/end-diastolic region in 4.5 min acquisitions using a single crystal camera and medium energy collimator. The right ventricle had more activity than the left ventricle (LV), and there was minimal subdiaphragmatic activity. LV ejection fraction by Au-195m GBPI correlated well with Tc-99m GBPI (r=.87). Regional wall motion analysis in Au-195m studies agreed closely with that in Tc-99m studies. In 5 pts, rapidly alternating Au-195m GBPI and Tl-201 MPI resulted in excellent images. Thus, GBPI with Au-195m is feasible using continuous generator elution and a conventional single crystal gamma camera. Intermittent discontinuation of infusion allows concomitant serial Tl-201 imaging. The properities of Au-195m make alternating assessment of both LV function and perfusion possible.

ULTRA-SHORT LIVED GOLD-195m: USE IN THE SIMULTANEOUS EVALUATION OF LEFT VENTRICULAR FUNCTION AND MYOCARDIAL PERFUSION WITH THALLIUM-201. I. Mena, K.A. Narahara, J. Maublant, M. Brizendine, J. Darcourt. Division of Nuclear Medicine and Cardiology, Harbor-UCLA Medical Center, Torrance, CA.

We evaluated the feasability of simultaneous first pass ventriculography (FPV) with Gold-195m (Au-195m) and myocardial perfusion imaging with thallium-201 (Tl-201). Background-free FPV can be obtained every 3 min with Au-195m ($T_{1/2}$ = 30.5 sec). Tl-201 was injected at maximal exercise (MAX EX). Immediately thereafter 20-30 mCi of Au-195m were injected for FPV in the 30° RAO projection. Tl-201 images were obtained 5 min and 3 hrs later on the same single crystal digital camera. Sequential rest FPV were performed after the 3 hr Tl-201 reperfusion images were obtained. Left ventricular (LV) ejection fraction (EF) was analysed. Our normal MAX EX EF response is an increase of 5 EF units. Wall motion (WM) was evaluated using phase analysis. Thirty patients including 20 with a prior infarct and 10 with coronary disease and no infarct were studied (70% were receiving beta blocker therapy). Nine normal subjects were also studied. The abnormalities (AB) in patients with coronary disease included:

Abnormal stress Tl-201	25/30	(83%)
Abnormal stress LVEF	27/30	(90%)
Abnormal stress WM	19/30	(63%)

There was at least 1 AB in 27/30 (90%);2 AB in 25/30 (83%), and 3 AB in 13/30 (43%). Nine normal individuals showed normal Tl-201 myocardial perfusion and normal WM at MAX EX: 8 had a normal increase in LVEF. The short $T_{1/2}$ of Au-195m allows the simultaneous acquisition of complementary cardiac data at rest or during maximal exercise. Sequential low radiation FPV can be obtained reliably every 3 min.

MYOCARDIAL IMAGING WITH 75 SECOND RUBIDIUM-82 ADMINISTERED INTRAVENOUSLY. J.W. Ryan, P.V. Harper, V. Stark, G.Gustafson and L. Resnekov. The University of Chicago, Chicago, IL

The 75 second generator produced positron emitter Rb-82 appears admirably suited for sequential myocardial imaging studies. Because of the short half life, large amounts of activity must be administered intravenously in order to collect satisfactory images. Imaging of positrons in the single photon mode with conventional instrumentation will permit use of Rb-82 in clinical nuclear medicine facilities which do not possess positron emission tomographic imaging systems. We used an Anger camera equipped with a special tungsten collimator(JNM 16:517,1975) in exploratory studies in order to determine the parameters required for routine imaging studies with intravenously administered Rb-82. Intracoronary administration of Rb-82 previously has been shown to be very effective (JNM 23:P69,1982). Nine male patients without uptake defects on stress thallium scans were studied. Results indicate that 30-60 seconds should elapse after the end of injection for blood pool clearance prior to initiation of myocardial imaging; 40-60 mCi yield good left ventricular images with heart-lung contrast of 1.7-2.4 to 1. Liver activity is minimal and does not interfere with visualization of the inferior-apical myocardial regions. Only one view per injection is obtainable with this technique. The radiation absorbed dose has been demonstrated not to be a significant limiting factor. These findings indicate that serial myocardial imaging studies at short intervals are feasible in patients undergoing diagnostic or therapeutic intervention procedures, particularly in acutely ill patients with demonstrable perfusion defects.

1:30–3:00 **Room 130**

ONCOLOGY IV: ANTIBODY IMAGING

Moderator: R. Edward Coleman, M.D.
Co-moderator: Sally J. DeNardo, M.D.

LIMITATIONS IN IMAGING OF HUMAN TUMOR XENOGRAFTS IN NUDE MICE WITH RADIOLABELED MONOCLONAL ANTIBODIES, B.D. Mann, M.B. Cohen, R.E. Saxton, L.S. Graham, L. Spolter, C.C. Chang, W.F. Benedict, and M.W. Burk, VAMC, Sepulveda, CA., University of California, Los Angeles, CA.

Two monoclonal antibodies (Mab) were selected for imaging of human tumor xenografts in nude mice to determine if in vitro binding specificities (Sp) of Mab to tumor nodules would reflect in vitro antibody Sp as determined by radioimmunoassay (RIA). Mab #436 binds over 50 times more to the M20 melanoma, than to the P3 carcinoma by RIA. Mab #44 binds to P3 over 50 times more than to M20. Nude mice bearing a M20 melanoma in one flank and a P3 carcinoma in the other were injected IV with 5-25 ug of each Mab labeled with either I-125 or I-131; in separate animals the labels were reversed. Animals were imaged daily with a camera equipped with a pinhole collimator. Animals were sacrificed on day 6 and binding of the Mabs to tumors and normal tissue were measured. Similar studies were performed with a non-immune IgG_1. Biopsies of selected tumors were returned to tissue culture and repeat RIAs were performed.

Mab #436 had about a two-fold in vivo binding advantage for the melanoma, whereas Mab #44 had up to a two-fold binding advantage for the carcinoma, thus confirming the in vitro Sp of each. However, in vitro assays of biopsied tumors again revealed greater than a 50-fold advantage for the specific Mab. Imaging on day 4 and computer analysis of percent radioactivity in the tumors showed that tumor images were related directly to tumor size and relatively uninfluenced by Mab Sp. All large tumors could be imaged with both Mab and with non-immune IgG_1. Thus, even though Mab Sp can be demonstrated by differential tissue counting, imaging of tumor deposits appears to involve a non-specific phenomenon largely dependent upon tumor weight.

F(ab')2 FRAGMENTS OF MONOCLONAL ANTIBODIES IN TUMOR BEARING MICE. J. Powe, A. Alavi, D. Herlyn, Z. Steplewski, and H. Koprowski. Wistar Institute and the University of Pennsylvania, Philadelphia, PA.

A monoclonal antibody (MoAb) 1083-17-1A against a human colorectal carcinoma (CRC) tumor-associated antigen was evaluated for it's in-vivo localization in immunosuppressed CBA mice bearing 7-10 day old human CRC tumor xenografts. MoAb was labeled with I-131 using the iodogen method to a specific activity of approximately 2-5 uCi/ug and 15 uCi injected simultaneously with I-125 labeled non-specific MoAb as a control. Organ biodistribution was obtained by sacrificing mice from 2-14 days after injection and counting removed organs in a dual channel well counter. F(ab')2 fragments of 1083-17-1A prepared by pepsin digestion were similarly labeled and injected and biodistribution obtained from 2-6 days later.

Higher tumor to normal tissue ratios were obtained using the F(ab')2 fragments (tumor to blood 19:1 vs. 11:1 and tumor to muscle 67:1 vs. 11:1) and optimum values were reached earlier (3-4 days vs. 8-14 days). This was due largely to the much shorter biological half-life of the fragments ($T_{\frac{1}{2}}$ 14 hrs. vs. 72 hrs.). Using F(ab')2 fragments of four other MoAbs against human CRC or melanoma associated antigens, specific localization was demonstrated only in those tumors that bound antibody in-vitro and not in unrelated tumors used as negative controls. Excellent images of tumor grafts (75-150mg.) could be obtained starting 48 hrs. after the injection of 100 uCi I-131 labeled F(ab')2 fragments of these MoAbs without background subtraction.

The use of F(ab')2 fragments of some MoAbs can improve tumor localization and enable imaging within a shorter time after injection.

COMPARISON OF In-111 LABELED FAB AND WHOLE 111 In ANTI-CEA MONOCLONAL ANTIBODY (MoAb) IN NORMAL MOUSE - HUMAN COLON TUMOR MODELS. P.L. Hagan, S.E. Halpern, and A. Chen, University of California and VA Medical Center, San Diego; and J.M. Frincke, R.M. Bartholomew, G.S. David, and D.J. Carlo, Hybritech, Inc., San Diego, CA.

I-131 Fab antibodies have been reported to offer advantages over the intact molecule for tumor (T) imaging. 111 In labeled MoAbs have been shown to be more stable than 131 I MoAbs. Accordingly, this study was undertaken to compare the distribution (D) and T incorporation of 111 In-Fab anti carcinoembryonic antigen (CEA) with whole 111 anti CEA MoAb.

Anti-CEA Fabs were prepared from two IgG1 MoAbs (CEJ-326 and CET-149). The Fabs and whole anti-CEA MoAb (CEJ-326) were labeled with 111 In and remained 70 percent (%) immunoreactive. Normal mice were administered (Ad) CET-149 Fab and sacrificed (sac) at 4, 24, and 48 hrs. Whole CEJ-326 and Fab CEJ-326 were Ad to nude mice bearing CEA producing T and sac at 4, 24, 48, 72 (Fab) and 24 and 72 hrs (whole MoAb). Tissue D and T uptake were assessed.

Fifty (CET-149) and 65 (CEJ-326) % of the Fab was removed by the kidneys (K) in 4 hours. Peak Fab T concentrations (conc) occurred at 4 hrs (4.2% dose/g) and decreased with time. Peak T levels of whole MoAb occurred at 72 hrs (37%/g). T/blood (B) and muscle (M) values for Fab and whole MoAb at 72 hrs were respectively 100:1, 18:1, 7.2:1, and 51:1. The whole MoAb values for most tissues (except K) were about an order of magnitude higher than for Fab.

We conclude that In-111 Fab is less well conc by T tissue than whole MoAb. The T/B ratios are higher for Fab than whole MoAb, but lower for T/M. The rapid K clearance of Fab precludes high conc in the T and could deliver high rad doses to the K.

EFFECT OF TUMOR SIZE, CARCINOEMBRYONIC ANTIGEN (CEA) PRODUCTION AND SECRETION ON THE DISTRIBUTION OF 111 In AND 125 I MONOCLONAL ANTITUMOR ANTIBODIES (MoAb) IN ANIMAL MODELS. P.L. Hagan, S.E. Halpern, A. Chen, L. Krishnen, VA Medical Center, and University of California; and J.M. Frincke, R.M. Bartholomew, G.S. David, D.J. Carlo, Hybritech, Inc., San Diego, CA.

Heterogenous antibodies and MoAbs are being used to image human tumors (T). Controversy has arisen regarding the effect of T size, CEA production and serum (S) CEA values on T uptake and distribution of these radiopharmaceuticals. The purpose of this study was to observe the distribution of 111 In and 125 I labeled MoAbs in T models which varied in these characteristics.

Four human T differing in their concentrations (conc) of CEA, CEA secretory rates (SR) and S conc of CEA were grown in nude mice. The mice were administered 111 In and 125 I

anti-CEA MoAb in double tracer (Tr) experiments, sacrificed and their T and other organs counted against standards.

Tumor uptake of 111 In always exceeded 125 I. The T conc of Tr decreased as the T enlarged. In general, S CEA and the uptake of 111 In in the liver rose with increasing T size. For each of the T types, the SR/g remained the same as the T grew. Acquisition of Tr by the T varied with each of the models. The T and S CEA conc and SR of CEA ranged widely in the different types of T, yet T with the highest antigen conc or lowest CEA secretion (and S conc) did not necessarily show the greatest uptake of Tr.

We conclude that as T enlarge and S CEA rises the Tr uptake by the T decreases and Tr uptake by the liver increases. While antigen on the T is necessary for Tr specificity, given adequate antigen conc, differences may be seen in T accumulation of Tr. In all cases, however, the conc of 111 In MoAb by the T exceeded 125 I MoAb.

IN VIVO BINDING OF In-111 LABELED MONOCLONAL ANTIBODY (MoAb) TO A HUMAN HIGH MOLECULAR WEIGHT MELANOMA-ASSOCIATED ANTIGEN (HMW-MAA). R.A. Fawwaz, T. S.T. Wang, S.C. Scrivastava, A. Esterbrook, P. Giacomini, P. Richards, S. Ferrone, M.A. Hardy, P.O. Alderson. Columbia University, New York, NY and Brookhaven National Laboratory, Upton, NY.

The in vivo binding of In-111 anti-HMW-MAA MoAb was investigated in nude mice bearing either human melanoma, other tumors or abscesses. Anti-HMW-MAA MoAb was labeled with In-111 using DTPA as a bifunctional chelate (labeling efficiency=25%). Three groups of mice (n=12) received 5 uCi of In-111 anti-HMW-MAA MoAb i.v.; the first had 2 week old subcutaneous (SQ) melanoma tumors ($\bar{x}$ weight=0.05 g); the second had similar implants of human prostate carcinoma; the third had a chronic SQ infection induced by cholesterol pellets. In separate experiments, mice (n=8) bearing SQ melanoma received either In-111 chloride, In-111DTPA or In-111 labeled MoAb to a murine breast tumor (BT). All animals were sacrificed 4 days post-injection and %ID/g in the lesion and other tissues was determined. The highest %ID/g in melanoma was achieved by In-111 anti-HMW-MAA MoAb (16.1±4.1%) but In-111 chloride (5.2±1.4%) and In-111 BT MoAb (2.9±0.4%) also showed uptake. The mean tumor:blood ratio for In-111 anti-HMW-MAA MoAb was 3.9:1 (SD±0.3). In-111 anti-HMW-MAA MoAb also showed small degrees of localization in human prostate tumor (2.3±0.2) and in infection (2.8±0.3). In-111 DTPA was rapidly eliminated from the body and did not concentrate in any lesion. These results indicate that In-111 anti-HMW-MAA MoAb does not localize significantly in non-melanoma lesions and may be useful for imaging melanoma in patients.

Pd-109 LABELED MONOCLONAL ANTIBODY (MoAb) TO HUMAN HIGH MOLECULAR WEIGHT MELANOMA ASSOCIATED ANTIGEN (HMW-MAA): A POTENTIAL AGENT FOR RADIOTHERAPY OF HUMAN MELANOMA. R.A. Fawwaz, S.C. Srivastava, T.S.T. Wang, A. Esterbrook, P. Giacomini, P. Richards, S. Ferrone, M.A. Hardy, P.O. Alderson. Columbia University, New York, NY and Brookhaven National Laboratory, Upton, NY.

In the past, tumor therapy with radiolabeled antibodies has been limited to I-131 compounds. Bifunctional chelate labeling may allow other beta emitters, e.g., Pd-109 (Pd) and Zn-69 (Zn) to be attached to antibodies and used for in vivo therapy. To investigate this possibility, the tissue distribution of Pd and Zn labeled anti-HMW-MAA MoAb was evaluated in nude mice bearing human melanoma and compared to that of radioiodinated anti-HMW-MAA MoAb. Iodination was performed using the iodogen technique (labeling efficiency=30%) and DTPA was used as a bifunctional chelate for attachment of Pd and Zn (labeling efficiency=10% and 3%, respectively). In control experiments, Pd and Zn were also given in ionic forms, e.g., as the chloride. All labeled compounds (1 to 5 uCi) were given iv. Animals (n=18) were sacrificed 4 days later and the %ID/g tissue determined. Pd anti-HMW-MAA MoAb showed good tumor uptake (10.0±1.6%) and high renal activity (17.7±2.1%). Tumor uptak of Zn anti-HMW-MAA MoAb (3.0± 0.9%) and iodinated anti-HMW-MAA MoAb (2.3±0.1%) were significantly lower ($p<0.001$) than Pd anti-HMW-MAA MoAb. These results suggest that Pd anti-HMW-MAA MoAb may be a potentially useful agent for iv therapy of human melanoma and that the need exists for improved binding of Pd to MoAb to reduce renal excretion and irradiation.

TUMOR LOCALIZATION IN RODENTS USING RADIOLABELED MONOCLONAL ANTIBODIES TO ISOFERRITIN (FEV-212). M. Blend, H. Mermall and S. Pinsky. Michael Reese Hospital and Medical Center, Chicago, IL

Radiolabeled antiferritin IgG polyclonal antibodies have been used to image hepatomas, lung cancers, and neuroblastomas. Implanted tumor xenografts were imaged with a labeled monoclonal antibody to a tumor-produced isoferritin. This antibody (FEV-212) was labeled with In-111-DTPA. Twelve Buffalo strain rodents were used; 8 with implanted Morris Hepatoma tumors and 4 normal controls. Two of the controls were injected with In-111-DTPA-FEV-212 and two were injected with In-111-DTPA. Four of the tumor-bearing rodents were injected with labeled antibody and 4 with In-111-DTPA. Animals were imaged at 24, 48, 72, and 96 hours and percent organ uptake was also determined. Images at 24 hours showed antibody injected animals with greater hepatic uptake (14:1), whereas DTPA showed high kidney uptake (56:1). After 24 hours, liver uptake in the antibody injected animals was twice that of kidney but the reverse was true after 96 hours; presumably due to hepatic metabolism of the antibody molecule with subsequent renal uptake of the In-111 moiety. Visualization of the transplanted tumor was best at 96 hours. AK-4 lymphoma implants in a murine model injected with 111-Indium-FEV-212 did not visualize as well as hepatoma implants. This study indicates the usefulness of radiolabeled monoclonal antibodies as a specific method for tumor imaging.

1:30–3:00 **Room 132**

GASTROINTESTINAL VI: MISCELLANEOUS

Moderator: Kenneth A. McKusick, M.D.
Co-moderator: John E. Freitas, M.D.

TAGGED ULCER-AVID MATERIAL IMAGING (TUMI): A POTENT NEW METHOD FOR THE EVALUATION OF PEPTIC ULCER DISEASE. P. Braunstein, T.E. Vasquez, R.L. Bridges, A.-L. Jansholt, and H. Meshkinpour. University of California, Irvine, Medical Center, Orange, CA.

The therapeutic agent sucralfate, when administered orally, selectively binds to peptic ulcers. A technique for labeling this drug with Tc-99m has been developed. Tc-99m sucralfate retains the essential properties of sucralfate. We have performed distribution studies in rabbits and evaluated its efficacy for the detection of peptic ulcers in 1) rabbits with induced gastric ulcers and 2) more than 12 patients. Following oral administration of Tc-99m sucralfate, serial gamma camera imaging was performed for the next 2-3 hours. Eight gastric ulcers produced in rabbits varying in size from 0.5 to 2 mm were all readily detected by imaging. In patients, all but one peptic ulcer was detected. Proof in patients was always by endoscopy. The smallest lesion detected in patients was about 2 mm and was produced by the endoscopist taking a bite biopsy prior to the TUMI scan. The patient with a false negative study had a 3 cm ulcer filled with fresh blood clot. No false positive "lesions" were found. The ulcers were in the stomach, pylorus and duodenal bulb. Areas of gastritis were also detected both in rabbits and humans. The TUMI study is associated with a lower radiation dose than upper GI barium series. It has none of the risks associated with endoscopy and appears to be more sensitive than either upper GI series or endoscopy. The TUMI examination can also be performed at the bedside on patients in ICU's where the possibility of stress ulcers is frequently a problem.

COMPARISON OF IN VITRO AND IN VIVO LABELED CHICKEN LIVER FOR EVALUATION OF GASTRIC EMPTYING. B.S. Greenspan, F.E. Mayer, J. H. Meyer, L.S. Graham, J. Thompson, VAMC, Sepulveda, CA.

To compare chicken liver labeled in vitro with in vivo labeling of chicken liver, ten normal subjects ate a standard meal of 213g of beef stew, 32g of chicken liver and 200 ml of water. The liver was labeled in vivo with In-113m colloid; it was then excised and injected directly with Tc-99m sulfur colloid prior to cooking. Anterior counts were obtained on peak and scatter settings with posterior counts on peak settings on a Technicare S410 gamma camera equipped with a 400 keV parallel hole collimator and interfaced to a DEC computer.

Corrections were made for errors in septal penetration and scatter. Corrections for changes in depth were achieved by (1) modified geometric means of anterior and posterior counts and (2) peak-to-scatter ratios of anterior counts, which are potentially simpler to use.

Gastric emptying curves were the same for the in vitro (Tc-99m) and the in vivo (In-113m) labeled chicken liver. The half-emptying times for the geometric mean method were: 110.2min. (in vitro) and 112.4min. (in vivo). For the peak-to-scatter method, the half-emptying times were: 114.8min. (in vitro) and 108.1min. (in vivo).

We conclude: (1) The peak-to-scatter method is equivalent to the modified geometric mean method for correction of depth-related errors. (2) Gastric emptying curves are identical for in vitro and in vivo labeled chicken liver.

CLINICAL EXPERIENCE WITH Tc-99m-GALACTOSYL-NEOGLYCOALBUMIN (Tc-NGA): A HEPATIC RECEPTOR-BINDING RADIOPHARMACEUTICAL R.C. Stadalnik, D.R. Vera, L.F. O'Grady, K.A. Krohn, and P.O. Scheibe. University of California, Davis Medical Center, Sacramento CA.

Receptor-binding radiopharmaceuticals provide an opportunity to study the functional state of a specific biochemical process, as well as the hemodynamic status of the target tissue. The physiologic role of hepatic binding protein (HBP), a receptor found only in the liver, is the endocytosis and catabolism of plasma glycoproteins. We have developed a synthetic HBP ligand, Tc-NGA, which exhibits the receptor properties of high tissue specificity, and, affinity and dose-dependent uptake. As a result, Tc-NGA kinetics is sensitive to hepatic blood flow and hepatocellular function.

To evaluate the clinical usefulness of this hepatocyte specific agent patients with known primary and secondary tumors were studied: hepatoma with severe hepatitis, metastases. Tc-NGA was compared to Tc-sulfur colloid (Tc-SC) studies. Kinetic analysis of Tc-NGA was performed.

Tc-NGA and Tc-SC both demonstrated the hepatic lesions. Visualization of the kidneys and gastrointestinal tract, due to metabolic products, was present on the Tc-NGA study, but did not interfere with interpretation. Only a small amount of bone marrow activity was seen with the receptor agent which was a distinct contradiction to the reticuloendothelial agent. Tc-NGA images were equal or superior to Tc-SC. Kinetic analysis of Tc-NGA demonstrated decreased function with increased tumor involement.

Tc-NGA, a hepatic receptor-binding radiopharmaceutical, produces excellent images of the liver and has the potential of measuring the pharmacokinetic parameters (both blood flow and receptor concentration) of liver disease.

THE USE OF In-111-LABELLED WHITE BLOOD CELLS IN THE INVESTIGATION OF ACUTE PANCREATITIS. **J.D. Laird, W.R. Ferguson, J.R. Anderson & R.A.J. Spence, The Royal Victoria Hospital, BELFAST, Northern Ireland, U.K.**

Three patients with complications of acute pancreatitis showed increased In-111 uptake in the region of the pancreas. This finding prompted a prospective study to assess its significance. All patients presenting with acute pancreatitis had full clinical and biochemical examination and In-111 scans as soon as possible after admission. Most patients also had ultrasound examination, and several had C.T. scans.

To date, 13 fully-documented cases have been studied. Using accepted clinical and biochemical criteria, only three patients showed features of severe pancreatitis, and had positive white cell scans. There was a fourth positive scan with biochemical evidence of mild pancreatitis only. However, this patient developed a pseudocyst, indicating severe disease. The remaining nine patients with negative scans all had mild disease, and all settled without complications.

Of the seven positive scans (three initial and four in the survey), at least three showed evidence of white cell accumulation in extensive areas of fat necrosis (identified on C.T. scan or at surgery).

The initial finding of this series suggests that an In-111 white cell scan, performed on admission, may separate mild from severe acute pancreatitis. Fat necrosis can also be identified.

III-INDIUM GRANULOCYTE SCANNING AND QUANTITATIVE FAECAL EXCRETION IN THE ASSESSMENT OF INFLAMMATORY BOWEL DISEASE S. Saverymuttu, A.M. Peters, H.J.F. Hodgson, V.S. Chadwick and J.P. Lavender. Hammersmith Hospital, London, UK.

III-Indium tropolonate labelled granulocytes have been used in 140 studies (60 Crohn's disease, 40 ulcerative colitis and 40 non-inflammatory disorders, eg. the irritable bowel syndrome) to assess disease distribution and disease activity in inflammatory bowel disease (IBD). Abdominal scans were performed between 40 min and 3 hrs after reinjection of the labelled cells. Faecal indium-III granulocyte excretion was measured in a four day faecal collection and expressed as a percentage of the injected dose. All patients with active IBD had abnormal scans with localisation corresponding to the known distribution of disease. Serial studies demonstrated improvement in the scans with clinical response to treatment. Faecal indium-III granulocyte excretion was less than 2% of the injected dose in all patients with non-inflammatory bowel diarrhoea. In patients with active disease, indium-III excretion ranged from 2.4% to 52% of the injected dose and showed significant correlations with established assessments of disease activity - Crohn's disease activity index, $r = 0.73$, $p < 0.001$, erythrocyte sedimentation rate $r = 0.68$, $p < 0.001$, c-reactive protein, $r = 0.72$, $p < 0.001$. Serial studies showed significant decreases in faecal granulocyte excretion with response to treatment. These studies demonstrate that indium-III granulocyte scanning is an effective technique for assessing disease distribution and quantitative granulocyte excretion is a specific method of assessing disease activity in IBD.

COMPARISON OF RADIONUCLIDE ESOPHAGEAL TRANSIT AND ESOPHAGEAL MANOMETRY IN GASTRO ESOPHAGEAL REFLUX DISEASE. D.H.I. Feiglin, R. Ilves, L. Choiniere. Toronto General Hospital, Toronto, ONT.

Fifteen patients who had clinical symptoms of gastro-esophageal reflux were studied by esophageal manometry using a direct pressure transducer catheter. Thirteen patients had endoscopy and ten had prolonged pH monitoring.

Radionuclide esophograms using 4MBq Technetium-99m sulphur colloid were performed on all fifteen patients using both solid and liquid swallows in the upright and supine positions. As previously reported by us, "normal" solid transit in the esophagus is extremely variable and was not used as a differential marker in this study.

Comparison of the radionuclide transit, from cricoid to gastric entry, was made using the liquid supine mode of the nuclear esophogram. Five patients had abnormal esophageal manometry characterized by decreased amplitude of peristaltic waves and increased low amplitude simultaneous (3^{0}) waves. Three of these patients had abnormal nuclear transit, one was borderline and one had normal transit. In ten patients both esophageal manometry and the total transit time were normal. However local transit in the lower third of the esophagus was substantially slower than normal in six of these patients.

The pH scores were positive in 14 of the 15 patients and endoscopy results ranged from normal to grade III esophagitis.

It appears the radionuclide esophogram is capable of matching esophageal manometry in picking up subtle motor abnormalities (4/5) and possibly more sensitive in showing further transit abnormalities in patients with reflux disease.

1:30-3:00 **Room 120**

RENAL/ELECTROLYTE/HYPERTENSION III

Moderator: Peter T. Kirchner, M.D.
Co-moderator: Gary F. Gates, M.D.

CLINICAL EVALUATION OF Tc-99m-N,N'-BIS(MERCAPTOACETYL)-2,3-DIAMINOPROPANOATE (COMPONENT A) (Tc-99m-CO_2-DADS-A) AS A REPLACEMENT FOR I-131-HIPPURAN. W.C. Klingensmith III, A.R. Fritzberg, V.M. Spitzer, D.L. Johnson, C.C. Kuni, M.R. Williamson, G. Washer and R. Weil III. University of Colorado Health Sciences Center, Denver, CO.

Tc-99m-CO_2-DADS-A is an analog of the previously reported Tc-99m-DADS (JNM 1982; 23:377) and appears superior to Tc-99m-DADS in animals (JNM 1982; 23:592). We have conducted a clinical comparison between Tc-99m-CO_2-DADS-A and I-131-hippuran in a seriies of five normal volunteers and eighteen patients. Each subject was studied in one session with Tc-99m-CO_2-DADS-A and I-131-hippuran; digital and analog images were recorded for 30 minutes and after voiding for both agents. In digital images in the normal volunteers Tc-99m-CO_2-DADS-A demonstrated a kidney to background ratio at 3 minutes that was 150 ± 37% (mean ± SD) of I-131-hippuran, a leading edge parenchymal transit time that was 108 ± 18% of I-131-hippuran, and a percent of injected dose excreted in the urine in 30 minutes that was 81 ± 4% of I-131-hippuran ($p<0.05$). In patients (serum creatinine = 1.0 to 14.3 mg/dl) decreasing renal function had a greater effect on Tc-99m-CO_2-DADS-A than on I-131-hippuran in the percent of injected dose in the urine($p<0.01$); decreasing renal function had a similar effect on Tc-99m-CO_2-DADS-A and I-131-hippuran with respect to kidney to background ratio and leading edge transit time. In analog images Tc-99m-CO_2-DADS-A always gave superior spatial resolution; neither radiopharmaceutical showed evidence of hepatobiliary excretion. We conclude that Tc-99m-CO_2-DADS-A and similar compounds should be pursued as possible replacements for I-131-hippuran.

AN EVALUATION OF 16 NEW Tc-99m COMPOUNDS FOR RENAL TUBULAR EXCRETION STUDIES. G. Subramanian, R.F. Schneider, J.G. McAfee, T. Feld, C. Zapf-Longo, E. Palladino, G.M. Gagne and F.D. Thomas. Upstate Medical Center, Syracuse, NY.

Based on the original work of Davison & Jones (JNM 23:801/82), N,N'-bis (mercaptoacetamido) ethylenediamine (DADS)I, its carboxyl derivative and two new parent compounds N,N'-bis (mercaptoacetamido) propylenediamine II, N,N'-bis (mercaptoacetamido)-o-phenylenediamine III were synthesized as their thioesters. Fourteen new derivatives of I, II & III were also prepared containing methyl, hydroxyl, oxo, phenyl, carboxyl, hydroxyphenyl and sulfo substituents by a new synthetic method using succiminidyl-S-benzoyl mercaptoacetate (active ester). After the identity of the compounds was verified, they were labeled with Tc-99m at alkaline pH using $SnCl_2$ as the reductant. Labeling yields determined by HPLC were > 98%. (Spherisorb S5 ODS-2, C_{18} Reverse phase column 35% ACN with 65% 0.005 M Bu_4NOH in water).

With all 16 compounds, sequential posterior images of rabbits were obtained up to 60' post injection using a gamma camera. Only II and its asymmetric carbonyl derivative, [N-[N'-mercaptoacetyl -β alanyl]-2 mercapto ethylamine] IV, showed excellent blood clearance and urinary excretion with negligible accumulation in the liver and GI tract. Images with II in dogs demonstrated considerable localization in the liver but this was not so in the monkey. Compounds II & IV both had a blood clearance and urinary excretion similar to that of I-131 Hippuran (urinary excretion ratio 0.94 for II and 0.97 for IV at 1 hr.). They merit further evaluation as Hippuran substitutes because they can be prepared as an instant kit without further purification.

SPLIT RENAL FUNCTION TESTING USING 99mTc-DTPA: A RAPID TECHNIQUE FOR DETERMINING DIFFERENTIAL GLOMERULAR FILTRATION. G.F. Gates, Good Samaritan Hospital, Portland, OR

Tc-99m DTPA is cleared by glomerular filtration but until now estimation of the glomerular filtration rate (GFR) required the obtaining of serial blood samples over intervals of several hours in order to perform the necessary calculations. This lengthy procedure can now be circumvented by direct scintigraphic analysis of renal uptake of DTPA which requires only 6 minutes of patient time in order to accurately estimate GFR.

This technique was developed by determining the fractional renal uptake of injected DTPA in 47 patients who were studied 51 times. This uptake value was compared to the patients' 24 hour creatinine clearance determinations (Range: 1-116 ml/min). Several variables were tested including: appropriateness of different time intervals used for computational purposes, variations in configuration of areas used for background correction and the use of renal depth correction factors. A linear regression analysis comparing fractional DTPA uptake (using appropriate time intervals, background areas and depth correction) with creatinine clearance had a correlation coefficient of 0.97. The reproducibility of GFR estimates by the subsequent derived formula was determined by studying a group of patients on successive days. Linear regression analysis of paired GFR computations for each kidney yielded a correlation coefficient of 0.99, thus documenting the technique's excellent reproducibility.

This study has resulted in a formula by which total, as well as individual kidney, GFR may be easily and accurately estimated. The procedure requires only 6 minutes of patient time and does not require any blood samples.

COMPUTER-QUANTITATED RENAL UPTAKE VS. PLASMA CLEARANCE OF Tc-99m DTPA IN RATS WITH AND WITHOUT GLOMERULAR DAMAGE. F.D. Thomas, J.G. McAfee, B. Lyons, G.M. Gagne, and C. Ritter

To assess the validity of predicting the plasma clearance of Tc-99m-DTPA from early in vivo measurements of renal uptake, groups of 12 Sprague-Dawley rats (200-250g) were given puromycin aminonucleoside in single intravenous doses of 2.5, 5 or 10 mg/100g body weight. Nine days later, anesthesized animals (including a control group) were injected with 1.2-1.5 mCi of Tc-99m DTPA. From 7 tail-vein plasma samples from 10 to 120 minutes, plasma clearance in ml/min/100g was quantitated by double exponential analysis. Simultaneously, 15-second images were obtained on a dedicated minicomputer system with sufficient amplification to produce a 64 x 64 pixel image of a three-inch field of view. Regions of interest for each kidney and local background were quantitated for the 0.5-1.5 min. interval after injection and compared to a one-minute image of the injected dose. The total % uptake from both kidneys was compared to the plasma clearance.

Linear regression analysis of renal uptake versus plasma clearance revealed a significant correlation ($p<.001$, $R = .88$, estimating equation: clearance = [.0774 X uptake] -.3292). Glomerular damage induced by 5 and 10 mg/100g doses of puromycin depressed both renal uptake and clearance. However, no significant depression was observed with the 2.5 mg/100g dose.

Renal uptake measurements of Tc-99m DTPA in small animals can predict glomerular clearance, with results comparable to those in humans, (Gates, AJR 138:565-570, 1982) with a standard nuclear medicine computer, given adequate amplification of the scintillation camera signals. Supported by NIH Grant CA 32848.

DIRECT DETERMINATION OF RELATIVE RENAL BLOOD FLOW USING THE TECHNETIUM-99m DTPA RENOGRAM. K.K. Ford, C.C. Harris, and R.E. Coleman. Duke University Medical Center, Durham, NC.

To determine the accuracy of relative renal blood flow estimates made directly from renal activity curves, renal dynamic imaging studies using Tc-99m DTPA were performed on dogs with renal artery stenosis. Stenoses were created by ligature or balloon catheter. Relative renal blood flow was expressed as the right-to-left ratio of the slopes of the intital phase of the renal activity-vs-time curves which, dimensionally, should be proportional to actual blood flow ratio. Relative blood flow was measured using a flowmeter or radiolabelled microspheres. Radionuclide estimated were compared with measured flow ratios with good correlation ($r = 0.89$, slope = 1.05, $N = 13$).

Several operational problems were noted; difficulty of

assignment of regions-of-interest (ROI) on statistically impaired images, uncertainty of proper background ROI assignment and lack of reproducibility of ROI assignment due to different display contrast scales. The best correlation occurred with maximum-renal-outline ROI, with no background correction. Any smaller ROI correlated less well and were irreproducible, even with a single operator. Excessively large background ROI (e.g. semicircular perirenal ring) resulted in over-correction and worse correlation with measured flow ratios. ROI assignment reproducibility was improved by use of special display translation tables and adjustable display contrast, and by analysis of raw images using ROI assigned on filtered image counterparts.

We conclude that estimation of relative renal blood flow from the ratio of the slopes of Tc-99m DTPA activity-vs-time curves can be both practical and accurate.

MONOCLONAL ANTIBODY RADIOIMMUNODETECTION OF TRANSPLANT REJECTION. R.L. Wahl, C.W. Parker. Mallinckrodt Institute & Howard Hughes Medical Institute, St. Louis, MO.

The diagnosis of transplant rejection is difficult. Since T-lymphocytes (T)are important mediators of rejection (R), radiolabelled monoclonal antibodies (MAB) directed against cytotoxic T (Lyt 2,3 surface +) potentially could be used in the radioimmunodetection of rejection.

To investigate this possibility we adapted the sponge matrix allograft technique originally described by Roberts and Hayry. Sponges implanted in donor animals become populated with cells expressing the donor's major histocompatibility locus determinants (H2 in mice), major determinants of rejection. The sponge is then transplanted to an allogeneic (A) recipient and R occurs with maximal cellular infiltration at about 14 days post transplant.

Four BALB/c mice (H2d) and four C57/BL6 mice (H2b) received sterile intraperitoneal urethane sponges. Seven days later the sponges were sterilely removed and one of each type transplanted s.q. into four new BALB/c mice. Thus each mouse received a syngeneic (S) and an A sponge matrix graft. Ten days later each recipient recieved i.v. 10uCi of I-125 monoclonal anti Lyt 2.2 (espressed on BALB/c cytotoxic lymphocytes). Animals were sacrificed 11 days later. Organs and sponges were weighed and counted. The A sponge had significantly more anti Lyt 2.2 ($p<.005$) than the S control (1.37= $\bar{x}$, range 1.26-1.49) on a counts/gram basis. Mean A sponge/blood ratio was 1.93 (r=1.72-2.04) and mean A sponge/liver ratio was 4.62 (r=3.98-5.43).

Although the localization is moderate, this study clearly demonstrates preferential localization of I-125MAB to sponge A near the time of maximal R. MAB to T may become useful in diagnosing immunologically mediated disorders.

1:30–3:00 **Room 275**

COMPUTER IV: EMISSION COMPUTED TOMOGRAPHY

Moderator: Gerd Muehllehner, Ph.D.
Co-moderator: John J. Erickson, Ph.D.

True Three-Dimensional Reconstruction in Single Photon Emission Computed Tomography. G.T. Gullberg. General Electric Medical Systems Operation, Milwaukee, WI.

Originally three-dimensional single photon emission computed tomography using a rotating gamma camera was performed by reconstructing a single transaxial slice and stacking the slices to give the three-dimensional image. The transaxial slices were reconstructed using a back projection of filtered projection algorithm where the Fourier transform of the filter function equaled the product of a window function with a ramp function. With the recent development of oblique tomography for such applications as imaging the short axis of the heart, it became evident that preferential smoothing transaxially gave streak artifacts in oblique planes. This observation led to algorithms which correspondingly performed a separate smoothing in the axial direction on the planar projection data. However, one can show that application of separable smoothing filters in the axial and transaxial directions does not give an isotropic three-dimensional impulse response.

A true three-dimensional reconstruction algorithm, that is, an algorithm which has an isotropic three-dimensional impulse response, can be implemented which takes the 2D FFT of each planar projection and applies a window function which is a function only of the frequency space spherical coordinate. After application of a spherically symmetric window function a ramp function is applied in the transaxial direction. Then the 2D inverse FFT is applied and each filtered planar projection is back projected to give each transaxial slice. The impulse response of the algorithm is invariant under rotation. Therefore the point response in any oblique plane will remain isotropic. This means that texture variations or noise spikes will not correlate along any preferred direction.

APPLICATION OF THE EM RECONSTRUCTION ALGORITHM TO POSITRON EMISSION TOMOGRAPHY. M.E. Carson, K. Lange, S.C. Huang, E.J. Hoffman, M.E. Phelps, UCLA School of Medicine, Los Angeles, CA

A new iterative CT reconstruction algorithm has been developed and applied to positron emission tomography. The technique is based upon the maximum likelihood approach and uses the EM algorithm of statistical estimation theory to iteratively compute the reconstruction. A stochastic model of Poisson counting statistics and a physical model describing the projection measurements is included directly into the iteration formulas. The physical model can include such factors as detector spatial resolution, redundant projection sampling, attenuation, and random coincidences. All pixel values in the final reconstructed image are guaranteed to be non-negative. The algorithm also provides a measure of the goodness of the reconstruction, the log likelihood function, which determines when iterations can cease.

The EM algorithm has been applied to data from low count phantom and brain FDG studies performed on the NeuroECAT. As compared to reconstructions of the same data with the filtered backprojection method, the EM images have less noise (~16%) and the noise is less correlated. There is particular improvement in the definition of the edge of the head and phantom and in the complete removal of noise outside the object. The log likelihood function converges rapidly within 6-10 iterations (~5 minutes per iteration). These initial studies suggest that the EM reconstruction algorithm is a highly promising technique to improve PET images, particularly for low count scans.

FAST WIENER DIGITAL POST-PROCESSING OF SPECT IMAGES. M.A. King, R.B. Schwinger, and P.W. Doherty. University of Massachusetts Medical Center, Worcester, MA.

Reconstruction of SPECT images usually requires a soft preprocessing filter to counteract the amplification of Poisson noise by the backprojection process. An alternative approach is to use a sharp preprocessing filter, and "optimally" filter the reconstructed image for noise suppression and resolution recovery. Such filtering can be performed by the Wiener filter which uses as its "optimality" criterion the minimization of the mean square error between filtered image and the original undergraded object image. Its form in the frequency domain is:

$$W(f) = MTF(f)/[MTF^2(f) + P_n(f)/P_0(f)]$$

where f is spatial frequency, MTF is the modulation transfer function, P_n is the noise power spectrum, and P_0 is the object power spectrum. For our implementation, the MTF is derived as the Fourier transform of a Gaussian fit by a non-linear least-squares routine to the SPECT reconstruction of a point source. P_n and P_0 are obtained from the image power spectrum in the following manner. The general shape of P_n for a given preprocessing filter was obtained from noise simulation studies. This form is fit to the end of the image power spectrum, and P_0 obtained as the difference. One of the disadvantages of Wiener filtering has been the execution time of the programs on the minicomputer systems of nuclear medicine. By using an array processor (AP 400) the time to reconstruct and filter a 64 by 64 pixel study has been decreased to under four seconds. In

both phantom and clinical images this method has provided pronounced noise suppression and detail enhancement compared to images filtered by standard methods.

THE SUBTRACTION OF SCATTERED EVENTS FROM SPECT PHOTOPEAK EVENTS. R.J. Jaszczak, R.E. Coleman, and K.L. Greer. Duke University Medical Center, Durham, NC.

SPECT images are qualitatively and quantitatively degraded as a result of the inclusion of Compton scattered photons detected within the photopeak energy window of the NaI(Tl) detector. Phantom and patient liver scans were used to evaluate a technique that consists of subtracting a fraction (equal to 0.5) of the image reconstructed using events recorded within a secondary energy window from the image reconstructed using events recorded within the primary photopeak (127-153 keV). The pulse height analyzer used for this secondary window was adjusted to accept Compton scattered events with an energy between 100 and 120 keV for the phantom studies, and between 92 and 124 keV for the patient data. The primary photopeak and secondary Compton events were acquired simultaneously during the rotational SPECT scan. The phantom consisted of 6 acrylic spheres (diameters equal to 10, 13, 16, 19, 25, 32mm) placed within a cylindrical (22cm dia.) distribution of Tc-99m. The patient data consisted of a liver scan containing a 2cm diameter filling defect. The average magnitude of the image contrasts for the spheres increased by 16% between the original and processed images. The signal-to-noise ratios remained nearly constant (to within ± 5%). For the 2cm defect within the liver the magnitude of the image contrast for the lesion increased by 35% (0.17 to 0.23), while the signal-to-noise ratio decreased by 6% (3.3 to 3.1). This technique offers the potential for qualitative and quantitative improvements in the image contrasts of lesions with little change in signal-to-noise ratios.

A "FIGURE-OF-MERIT" APPROACH TO THE EVALUATION OF ALGORITHMS FOR ECT. B.E. Oppenheim and C.R. Appledorn, Indiana University School of Medicine, Indianapolis, IN.

Different reconstruction algorithms applied to the same set of projection data can produce images that differ greatly in terms of spatial resolution and noise content and texture. The appropriate algorithm for a particular application is dependent upon the contrast and spatial frequency content of the object to be detected, the sensitivity and spatial resolution of the detector, and the noise amplification and spatial resolution of the reconstruction algorithm. It can be shown that for detection of Gaussian-shaped objects superimposed upon a noisy background with uniform expected values, the relative performance of algorithms is represented by the figure-of-merit expression

$$F=[\sigma_O^2/(\sigma_O^2+\sigma_S^2+\sigma_Y^2)]/FSDM$$

where σ_O^2, σ_S^2 and σ_Y^2 represent the variances of the Gaussian point spread functions for the object, the imaging system, and the reconstruction algorithms, respectively, and FSDM is the fractional standard deviation of the noise in the reconstruction of a uniform object from projections containing 1 million total counts. The values of σ_O^2 and σ_S^2 are determined by the experimental situation, and σ_Y^2 and FSDM are evaluated through computer simulation.

We compared a modified form of ART2, a new ART that uses variably weighted backprojection (ARTW), and three convolution kernels using three types of interpolation, by evaluating F and generating images for each algorithm. For a typical ECT imaging situation we found the best algorithm to be ARTW using 18 projections and one cycle of iterations, followed by ART2, and then by the low pass convolution kernel using 36 or 72 projections and linear interpolation.

COMPUTER-AIDED DATA ANALYSIS OF ECT DATA. R. Dann, G. Muehllehner, A. Rosenquist, University of Pennsylvania, Philadelphia, PA.

Quantitative data analysis of functional images obtained in brain metabolism studies using positron emission tomography requires placement of multiple regions of interest (ROI) on transverse section images. To facilitate reproducible placement of ROI's on images, a program was developed which allows previously stored regions to be overlayed on section images. Each set of ROI's as a whole can be translated, rotated, and expanded or contracted independently in the x and y directions. This permits adjustments for gross anatomical variations between subjects. In addition, each ROI may be moved individually to compensate for anatomic or functional variations of individual areas.

To determine the average location of structures in the brain, eight normal fixed half brains were cut and photographed at an angle corresponding to the section images in 4-mm increments. Forty anatomical areas were outlined in the photographs; rectangular or elliptical ROI's were inscribed and transferred to computer files. After adjustments for overall size and shape differences, each ROI was averaged for all brain sections.

It was found that the location of many regions varied by less than ± 3 mm after adjusting for size and shape of the brain as a whole. The method described is convenient, rapid, reproducible and less subject to bias than the unaided placement of ROI's based only on the appearance of the section image. The accuracy of the data thus obtained requires further investigation.